

**TOPICAL REPORT
REFERENCES
VOLUME I**

**References for
Topical Report
Entitled
Credit for 90% of the ¹⁰B in BORAL**

**Submitted by:
AAR Manufacturing
12633 Inkster Road
Livonia, Michigan 48150
Tel: 734-522-2000
Fax: 734-522-2240**

AAR Report 1829, Revision 0

January 18, 2005

Standard Review Plan for Dry Cask Storage Systems

Final Report

**Manuscript Completed: January 1997
Date Published: January 1997**

**Spent Fuel Project Office
Office of Nuclear Material Safety and Safeguards
U.S. Nuclear Regulatory Commission
Washington, DC 20555-0001**



6.0 CRITICALITY EVALUATION

I. Review Objective

The criticality review ensures that spent fuel remains subcritical under normal, off-normal, and accident conditions involving handling, packaging, transfer, and storage.

II. Areas of Review

This portion of the dry cask storage system (DCSS) review evaluates the criticality design and analysis related to spent fuel handling, packaging, transfer, and storage procedures for normal, off-normal, and accident conditions. Consequently, this chapter of the DCSS Standard Review Plan (SRP) provides guidance for use in conducting a comprehensive criticality evaluation that *may* encompass any or all of the following areas of review:

1. criticality design criteria and features
2. fuel specification
3. model specification
 - a. configuration
 - b. material properties
4. criticality analysis
 - a. computer programs
 - b. multiplication factor
 - c. benchmark comparisons
5. supplemental information

III. Regulatory Requirements

Spent fuel storage systems must be designed to remain subcritical unless at least two unlikely independent events occur. Moreover, the spent fuel cask must be designed to remain subcritical under all credible conditions. Regulations specific to nuclear criticality safety of the cask system are specified in 10 CFR 72.124 and 72.236(c). Other pertinent regulations include 10 CFR 72.24(c)(3), 72.24(d), and 72.236(g). Normal and accident conditions to be considered are also identified in 10 CFR Part 72.

IV. Acceptance Criteria

In general, the DCSS criticality evaluation seeks to ensure that the given design fulfills the following acceptance criteria:

1. The multiplication factor (k_{eff}), including all biases and uncertainties at a 95-percent confidence level, should not exceed 0.95 under all credible normal, off-normal, and accident conditions.
2. At least two unlikely, independent, and concurrent or sequential changes to the conditions essential to criticality safety, under normal, off-normal, and accident conditions, should occur before an accidental criticality is deemed to be possible.
3. When practicable, criticality safety of the design should be established on the basis of favorable geometry, permanent fixed neutron-absorbing materials (poisons), or both. Where solid neutron-absorbing materials are used, the design should provide for a positive means to verify their continued efficacy during the storage period.
4. Criticality safety of the cask system should not rely on use of the following credits:
 - a. burnup of the fuel
 - b. fuel-related burnable neutron absorbers

Criticality Evaluation

- c. more than 75 percent for fixed neutron absorbers^a when subject to standard acceptance tests.

V. Review Procedures

Review the criticality design features and criteria in SAR Chapters 1 and 2. Also review SAR Chapter 6 for any additional details concerning criticality design features and criteria. Assess the bounding specifications for the spent fuel. Examine the models used by the applicant in the criticality analyses. Verify that the applicant has addressed criticality safety considerations under normal, off-normal, and accident conditions. Verify that the cask system design complies with 10 CFR Part 72. In addition, verify that the criticality calculations determine the highest k_{eff} that might occur under all loading states under normal, off-normal, and accident conditions involving handling, packaging, transfer, or storage. To the extent practicable, use independent methods to perform any k_{eff} calculations to evaluate the applicant's design.

1. Criticality Design Criteria and Features

Review the principal criticality design criteria presented in SAR Chapter 2, as well as any related detail provided in SAR Chapter 6. Also review the general cask description presented in SAR Chapter 1 and any related information provided in Chapter 6. Verify that the information in Chapter 6 is consistent with the information in Chapters 1 and 2. Also, verify that all drawings, figures, and tables are sufficiently detailed to support in-depth staff evaluation.

In addition to the general dimensions of the cask components and spacing of fuel assemblies in the basket, the criticality design often relies on neutron poisons. These may be in the form of fixed poisons in the basket structure and/or soluble poisons in the water of the spent fuel pool. The NRC staff accepts the use of borated water as a means of criticality control if the applicant specifies a minimum boron content, and strict controls are established to ensure that the minimum required boron concentration is maintained, which in turn becomes an operating control and limit in SAR Chapter 12. These operating controls should also be discussed in the SER. If borated water is used for criticality control, administrative controls and/or design features should be implemented to ensure that accidental flooding with unborated water cannot occur, or the criticality evaluation should consider accidental flooding with unborated water. If the cask is also intended for transport, borated water cannot be relied upon for criticality control.

2. Fuel Specification

Review the specifications for the ranges or types of spent fuel that will be stored in the cask as presented in SAR Sections 1 and 2, as well as any related information provided in SAR Sections 6. Verify that the spent fuel specifications given in Section 6 are consistent with, or bounded by, the specifications given in Section 1 and 2.

Of primary interest is the type of fuel assemblies and maximum fuel enrichment, which should be specified and used in the criticality calculations. Some boiling water reactors (BWR) use multiple fuel pin enrichments, in which case, the criticality calculations should use the maximum fuel pin enrichment present. Depending upon the fuel design, an applicant may propose use of assembly averaged, or lattice averaged enrichments. This may be acceptable if the applicant can demonstrate that any averaging techniques are technically defensible and, for the criticality calculation, produce conservative results. Because of the natural uranium blankets present in many BWR designs, use of an assembly-averaged enrichment is not normally considered appropriate or conservative for BWR fuel.

Although the burnup of the fuel affects its reactivity, the NRC staff does not currently allow credit for burnup, either in depleting the quantity of fissile nuclides or in producing fission product poisons for spent fuel storage or transport casks. Specifications for the fuel that will be stored in the cask should be included in Section 12 of both the SAR and SER and should also be explicitly listed in the Certificate of Compliance.

The fresh fuel assumption should be used in the criticality analyses; therefore, inadvertent loading of the cask with unirradiated fuel is not a major concern. Nonetheless, detailed loading procedures may need to

^a For greater credit allowance, special, comprehensive fabrication tests capable of verifying the presence and uniformity of the neutron absorber are needed.

Standard Review Plan for Spent Fuel Dry Storage Facilities

Final Report

**Manuscript Completed: February 2000
Date Published: March 2000**

**Spent Fuel Project Office
Office of Nuclear Material Safety and Safeguards
U.S. Nuclear Regulatory Commission
Washington, D.C. 20555-0001**

even grow by a chain reaction, which can produce as many or more neutrons than are absorbed. In criticality terminology, the term, k-effective or k_{eff} is the net ratio of neutrons produced per neutron absorbed in a mass of fissionable material. A k_{eff} of 1.0 indicates a critical mass whereas a k_{eff} of less than 1.0 is an indication of a subcritical condition.

8.4.1 Criticality Design Criteria and Features

8.4.1.1 Criteria

The regulatory requirements given in 10 CFR 72.40 and 10 CFR 72.124 identify acceptable design criteria. The NRC generally considers the design criteria identified below to be acceptable to meet the criticality requirements of 10 CFR 72 for storage confinement casks:

- The multiplication factor, k_{eff} , including all biases and uncertainties at a 95 percent confidence level, must not exceed 0.95 under all credible normal, off-normal, and accident conditions and events.
- Conditions for criticality safety (satisfaction of the limit on multiplication factor, k_{eff}) of subject radioactive material while at the Independent Spent Fuel Storage Installations (ISFSI) or Monitored Retrievable Storage (MRS) must include:
 - no burnup credit. (The conservative assumption of fresh unburned fuel provides a worst case criticality analysis; however, 10 CFR 72.3 requires that spent fuel have been irradiated and cooled at least one year as a condition for storage.) Alternately, burnup credit may be taken using the guidelines described in section 8.4.5 of this SRP.
 - no credit taken for flammable neutron absorbers or for any solid poisons that may melt or lose any significant mass from the original solid form by melting or vaporization at any of the temperature and pressure conditions that may be experienced while in use
 - no credit taken for liquid neutron shielding material (except that k_{eff} for the situation of a loaded confinement cask with liquid that serves as both shielding and absorber and is used in the confinement cask during loading operations or in the pool shall be based on presence of the water and bounding level(s) of poison)
 - no more than 75 percent credit for fixed neutron absorbers, unless comprehensive fabrication acceptance tests capable of verifying the presence and uniformity of the neutron absorber are implemented
 - determination and use of optimum (i.e., most reactive) moderator density

Standard Review Plan for Transportation Packages for Radioactive Material

Manuscript Completed: March 31, 1999

Spent Fuel Project Office
Office of Nuclear Material Safety and Safeguards
U.S. Nuclear Regulatory Commission
Washington, DC 20555-0001

6.5.3.2 Material Properties

Verify that the appropriate mass densities and atom densities are provided for materials used in the models of the packaging and contents. Material properties should be consistent with the condition of the package under the tests of §71.71 and §71.73, and any differences between normal conditions of transport and hypothetical accident conditions should be addressed.

Ensure that materials relevant to the criticality design (e.g., poisons, foams, plastics, and other hydrocarbons) are properly specified. No more than 75% of the specified minimum neutron poison concentration should generally be considered in the criticality evaluation. Verify that materials will not degrade during the service life of the packaging.

6.5.3.3 Computer Codes and Cross-Section Libraries

Verify that the application uses an appropriate computer code (or other acceptable method) for the criticality evaluation. Standard codes should be clearly referenced. Other codes or methods should be described in the application, and appropriate supplemental information should be provided.

Ensure that the criticality evaluations use an appropriate cross-section library. If multigroup cross sections are used, confirm that the neutron spectrum of the package has been appropriately considered and that the cross sections are properly processed to account for resonance absorption and self-shielding. Additional information regarding cross-sections is provided in NMSS Information Notice No. 91-26 and NUREG/CR-6328.

Verify that the code has been properly used in the criticality evaluation. Key input data for the criticality calculations should be identified. These include number of neutrons per generation, number of generations, convergence criteria, mesh selection, etc., depending on the code used. The application should include at least one representative input file for a single package, undamaged array, and damaged array evaluation. Verify, as appropriate, that the information from the criticality model, material properties, and cross sections is properly input into the code.

At least one representative output file (or key sections) should be included in the application. Ensure that the calculation has properly converged and that the calculated multiplication factors from the output files agree with those reported in the evaluation.

6.5.3.4 Demonstration of Maximum Reactivity

Verify that the analyses demonstrate the most reactive configuration of each case listed in Section 6.5.1.2 (single package, array of undamaged packages, and array of damaged packages). Assumptions and approximations should be clearly identified and justified.

Ensure that the analysis determines the optimum combination of internal moderation (within the package) and interspersed moderation (between packages), as applicable. Confirm that preferential flooding of different regions within the package is considered as appropriate. As noted in Section 6.5.2, the maximum allowable fissile material is not necessarily the most reactive contents.

**Standard Review Plan
for Transportation Packages for Spent Nuclear Fuel**

Final Report

Manuscript Completed: January 2000
Date Published: March 2000

Spent Fuel Project Office
Office of Nuclear Material Safety and Safeguards
U.S. Nuclear Regulatory Commission
Washington, D.C. 20555-0001

6.3.5 Evaluation of Package Arrays under Normal Conditions of Transport

The SAR must evaluate arrays of packages under normal conditions of transport to determine the maximum number of packages that may be transported in a single shipment. [10 CFR 71.35 and 10 CFR 71.59]

6.3.6 Evaluation of Package Arrays under Hypothetical Accident Conditions

The SAR must evaluate arrays of packages under hypothetical accident conditions to determine the maximum number of packages that may be transported in a single shipment. [10 CFR 71.35 and 10 CFR 71.59]

6.3.7 Benchmark Evaluations

The package must be evaluated to demonstrate that it satisfies the criticality safety requirements of 10 CFR Part 71. [10 CFR 71.31(a)(2) and 10 CFR 71.35]

6.3.8 Burnup Credit

There are no regulatory requirements that are specific to burnup credit. The general criticality requirements apply. However, based on experience, the staff has developed guidelines to facilitate the review of burnup credit, when it is included in the analysis. Burnup credit evaluations are performed in accordance with Sections 6.4.8.1 through 6.4.8.6.

6.4 ACCEPTANCE CRITERIA

6.4.1 Description of Criticality Design

The regulatory requirements in Section 6.3.1 identify the acceptance criteria.

6.4.2 Spent Nuclear Fuel Contents

The regulatory requirements in Section 6.3.2 identify the acceptance criteria.

6.4.3 General Considerations for Criticality Evaluations

In addition to the regulatory requirements identified in Section 6.3.3, the packaging model for the criticality evaluation should generally consider no more than 75% of the specified minimum neutron poison concentrations. The model for the SNF should include no burnable poisons. Methods for including fuel burnup in the criticality calculations need to have prior approval by NRC.

The sum of the effective multiplication factor (k_{eff}), two standard deviations (95% confidence), and the bias adjustment should not exceed 0.95 to demonstrate subcriticality by calculation. A bias that reduces the calculated value of k_{eff} should not be applied.

Examine the Structural Evaluation and Thermal Evaluation sections of the SAR to determine the effects of the normal conditions of transport and hypothetical accident conditions on the packaging and its contents. Verify that the models used in the criticality calculation are consistent with these effects.

Examine the sketches or figures of the model used for the criticality calculations. Verify that the dimensions and materials are consistent with those in the drawings of the actual package. Differences should be identified and justified. Within the specified tolerance range, dimensions should be selected to result in the highest reactivity.

Verify that the SAR considers deviations from nominal design configurations. For example, the fuel assemblies might not always be centered in each basket compartment, and the basket might not be exactly centered in the package. In addition to a fully flooded package, the SAR should address preferential flooding as appropriate. This includes flooding of the fuel-cladding gap and other regions (e.g., flux traps) for which water density might not be uniform in a flooded package.

Determine whether the SAR includes a heterogeneous model of each fuel rod or homogenizes the entire assembly. With current computational capability, homogenization should generally be avoided. If such homogenization is used, the SAR must demonstrate that it is applied correctly or conservatively. As a minimum, this demonstration should include calculation of the multiplication factor of one assembly and several benchmark experiments (see Section 6.5.7) using both homogeneous and heterogeneous models.

6.5.3.2 Material Properties

Verify that the appropriate mass densities and atom densities are provided for all materials used in the models of the packaging and contents. Material properties should be consistent with the condition of the package under the tests of 10 CFR 71.71 and 10 CFR 71.73, and any differences between normal conditions of transport and hypothetical accident conditions should be addressed. The sources of the data on material properties should be referenced.

No more than 75% of the specified minimum neutron poison concentration of the packaging should generally be considered in the criticality evaluation. In addition, because of differences in net reactivity due to depletion of fissile material and burnable poisons, no credit should be taken for burnable poisons in the fuel. Ensure that neutron absorbers and moderators (e.g., poisons and neutron shielding) are properly controlled during fabrication to meet their specified properties. Such information should be discussed in more detail in the Acceptance Tests and Maintenance Program section of the SAR. Additional guidance on neutron poisons is provided in NUREG-1647.

Review materials to identify any criticality properties that could degrade during the service life of the packaging. If appropriate, ensure that specific controls are in place to assure the effectiveness of the packaging during its service life. Such information should also be discussed in more detail in the Acceptance Tests and Maintenance Program or Operating Procedures sections of the SAR.

6.5.3.3 Computer Codes and Cross Section Libraries



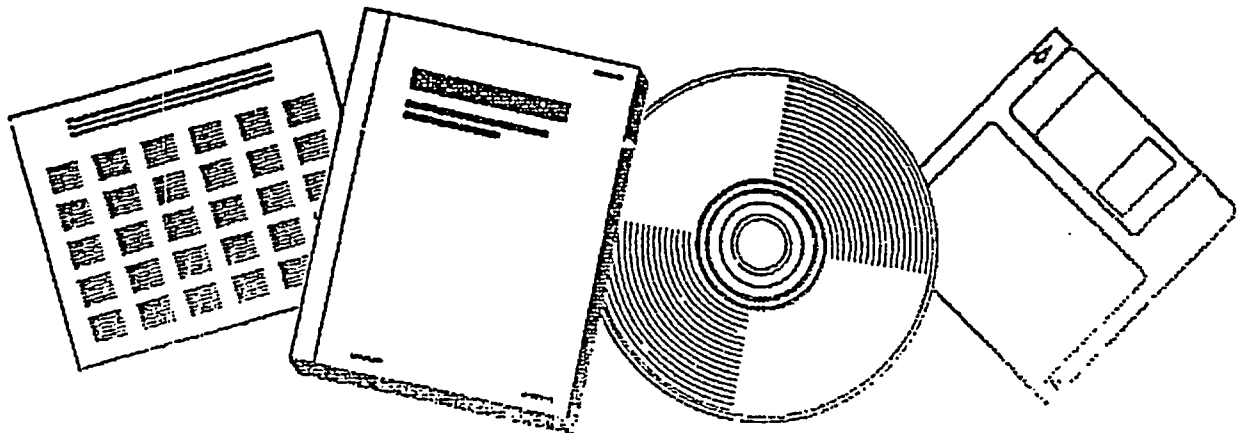
NUREG/CR-5661

NTIS
Information is our business.

RECOMMENDATIONS FOR PREPARING THE CRITICALITY SAFETY EVALUATION OF TRANSPORTATION PACKAGES

OAK RIDGE NATIONAL LAB., TN

APR 97



U.S. DEPARTMENT OF COMMERCE
National Technical Information Service



Recommendations for Preparing the Criticality Safety Evaluation of Transportation Packages

Prepared by
H. R. Dyer, C. V. Parks

Oak Ridge National Laboratory

Prepared for
U.S. Nuclear Regulatory Commission

REPRODUCED BY
U.S. DEPARTMENT OF COMMERCE
NATIONAL TECHNICAL
INFORMATION SERVICE

AVAILABILITY NOTICE

Availability of Reference Materials Cited in NRC Publications

Most documents cited in NRC publications will be available from one of the following sources:

1. The NRC Public Document Room, 2120 L Street, NW., Lower Level, Washington, DC 20555-0001
2. The Superintendent of Documents, U.S. Government Printing Office, P. O. Box 37082, Washington, DC 20402-9328
3. The National Technical Information Service, Springfield, VA 22161-0002.

Although the listing that follows represents the majority of documents cited in NRC publications, it is not intended to be exhaustive.

Referenced documents available for inspection and copying for a fee from the NRC Public Document Room include NRC correspondence and internal NRC memoranda; NRC bulletins, circulars, information notices, inspection and investigation notices; licensee event reports; vendor reports and correspondence; Commission papers; and applicant and licensee documents and correspondence.

The following documents in the NUREG series are available for purchase from the Government Printing Office: formal NRC staff and contractor reports, NRC-sponsored conference proceedings, international agreement reports, grantee reports, and NRC booklets and brochures. Also available are regulatory guides, NRC regulations in the *Code of Federal Regulations*, and *Nuclear Regulatory Commission Issuances*.

Documents available from the National Technical Information Service include NUREG-series reports and technical reports prepared by other Federal agencies and reports prepared by the Atomic Energy Commission, forerunner agency to the Nuclear Regulatory Commission.

Documents available from public and special technical libraries include all open literature items, such as books, journal articles, and transactions. *Federal Register* notices, Federal and State legislation, and congressional reports can usually be obtained from these libraries.

Documents such as theses, dissertations, foreign reports and translations, and non-NRC conference proceedings are available for purchase from the organization sponsoring the publication cited.

Single copies of NRC draft reports are available free, to the extent of supply, upon written request to the Office of Administration, Distribution and Mail Services Section, U.S. Nuclear Regulatory Commission, Washington, DC 20555-0001.

Copies of industry codes and standards used in a substantive manner in the NRC regulatory process are maintained at the NRC Library, Two White Flint North, 11545 Rockville Pike, Rockville, MD 20852-2738, for use by the public. Codes and standards are usually copyrighted and may be purchased from the originating organization or, if they are American National Standards, from the American National Standards Institute, 1430 Broadway, New York, NY 10018-3308.

DISCLAIMER NOTICE

This report was prepared as an account of work sponsored by an agency of the United States Government. Neither the United States Government nor any agency thereof, nor any of their employees, makes any warranty, expressed or implied, or assumes any legal liability or responsibility for any third party's use, or the results of such use, of any information, apparatus, product, or process disclosed in this report, or represents that its use by such third party would not infringe privately owned rights.



BIBLIOGRAPHIC DATA SHEET

(See instructions on the reverse)

NUREG/CR-5661
ORNL/TM-11935

2. TITLE AND SUBTITLE

Recommendations for Preparing the Criticality Safety Evaluation of Transportation Packages

3. DATE REPORT PUBLISHED

MONTH | YEAR
April | 1997

4. FN OR GRANT NUMBER
B0009

5. AUTHOR(S)

H.R. Dyer, C.V. Parks

6. TYPE OF REPORT

7. PERIOD COVERED (Inclusive Dates)

8. PERFORMING ORGANIZATION - NAME AND ADDRESS (If NRC, provide Division, Office or Region, U.S. Nuclear Regulatory Commission, and mailing address; if contractor, provide name and mailing address.)

Oak Ridge National Laboratory
Oak Ridge, TN 37831-8370

9. SPONSORING ORGANIZATION - NAME AND ADDRESS (If NRC, type "Same as above"; if contractor, provide NRC Division, Office or Region, U.S. Nuclear Regulatory Commission, and mailing address.)

Spent Fuel Project Office
Office of Nuclear Material Safety and Safeguards
U.S. Nuclear Regulatory Commission
Washington, DC 20555-0001

10. SUPPLEMENTARY NOTES

11. ABSTRACT (200 words or less)

This report provides recommendations on preparing the criticality safety section of an application for approval of a transportation package containing fissile material. The analytical approach to the evaluation is emphasized rather than the performance standards that the package must meet. Where performance standards are addressed, this report incorporates the requirements of 10 CFR Part 71.

12. KEY WORDS/DESCRIPTORS (List words or phrases that will assist researchers in locating the report.)

transportation, criticality safety, safety analysis, fissile material

13. AVAILABILITY STATEMENT

unlimited

14. SECURITY CLASSIFICATION

(If a Page)

unclassified
classified
not classified

15. NUMBER OF PAGES

10

ABSTRACT

This report provides recommendations on preparing the criticality safety section of an application for approval of a transportation package containing fissile material. The analytical approach to the evaluation is emphasized rather than the performance standards that the package must meet. Where performance standards are addressed, this report incorporates the requirements of 10 CFR Part 71.

7 SUMMARY	29
8 REFERENCES	31
APPENDIX A. EXAMPLE OF CALCULATIONAL MODELS AND RESULTS	33
A.1 GENERAL DESCRIPTION (Example)	33
A.2 PACKAGE DESCRIPTION	33
A.2.1 CONTENTS	34
A.2.2 PACKAGING	34
A.2.2.1 Inner Container Assembly	34
A.2.2.2 Inner Container	34
A.2.2.3 Drum	36
A.3 CRITICALITY SAFETY ANALYSIS MODELS	36
A.3.1 GENERAL MODEL	36
A.3.1.1 Dimensions	36
A.3.1.2 Materials	36
A.3.1.3 Models—Actual Package Differences	39
A.3.2 CONTENTS MODEL	39
A.3.3 SINGLE PACKAGES	39
A.3.4 PACKAGE ARRAYS	40
A.4 METHOD OF ANALYSIS	41
A.4.1 COMPUTER CODE SYSTEM	41
A.4.2 CROSS SECTIONS AND CROSS-SECTION PROCESSING	42
A.4.3 CODE INPUT	42
A.4.4 CONVERGENCE OF CALCULATIONS	42
A.5 VALIDATION OF CALCULATION METHOD	44
A.6 CRITICALITY CALCULATIONS AND RESULTS	44
A.6.1 SINGLE PACKAGE	44
A.6.2 PACKAGE ARRAYS	45
A.6.3 TRANSPORTATION INDEX	47

LIST OF FIGURES

<u>Figure</u>	<u>Page</u>
1 Typical plots of array k_{eff} vs interspersed water moderator density	25
A.1 Axial cross section of the single-package model	37
A.2 Radial cross section of single-package model	38
A.3a Sample input file f-2_4	43
A.3b Sample input file f-2_4a	43
A.4 k_{eff} vs pitch for 4.01 wt % ^{235}U UO_2 pellets	45

LIST OF TABLES

Table	Page
1 Example format of table for single-package calculations	22
2 Example format of table for array calculations	22
3 Requirements of 10 CFR § 71.59	27
A.1 Uranium isotopic distribution	34
A.2 Material specifications	35
A.3 Material specifications for Figs. A.1 and A.2	39
A.4 Single-package calculations	45
A.5 Results for triangular-pitch array calculations	46

ACKNOWLEDGMENTS

The authors gratefully acknowledge the overall direction and specific contributions provided during the preparation of this report by staff of the U.S. Nuclear Regulatory Commission's Spent Fuel Project Office. In particular, the efforts of the Technical Monitor, M. G. Bailey, in consolidating and communicating the NRC comments was an invaluable asset to the completion of this report. R. H. Odegaarden, private consultant, contributed valuable ideas and initial text for this document, and J. J. Lichtenwaller used the final draft to prepare Appendix A. Lichtenwaller's contributions were partially supported by his role as a participant in the post-graduate research program administered by the Oak Ridge Institute for Science and Education. The technical review comments provided by Lichtenwaller and C. M. Hopper were helpful in preparing the document for publication. The timely and carefully prepared manuscript and many drafts by Lindy Norris are also greatly appreciated.

1 INTRODUCTION

1.1 BACKGROUND

This report provides recommendations on preparing the criticality safety section of an application for approval of a transportation package containing fissile material. This report was prepared in consultation with the staff of the Spent Fuel Project Office of the U.S. Nuclear Regulatory Commission (NRC).

Packages used to transport fissile and Type B quantities of radioactive material are designed and constructed to meet the performance criteria specified in Title 10 of the Code of Federal Regulations, *Part 71—Packaging and Transportation of Radioactive Material* (10 CFR Part 71).¹ To assist an applicant in preparing an application for approval of such packaging, the NRC issued Regulatory Guide 7.9, *Standard Format and Content of Part 71 Applications for Approval of Packaging for Radioactive Material* (Standard Format Guide).² The Standard Format Guide indicates the information to be provided in the application and establishes a uniform format for presenting that information. This report (NUREG/CR-5661) supplements Chapter 6, *Criticality*, of the Standard Format Guide. This report should not be considered a substitute for referring to the Standard Format Guide or to 10 CFR Part 71.

1.2 PURPOSE AND SCOPE

The purpose of this report is to clarify the design information and analysis information that should be included in the criticality safety section of an application for approval of a package. This report also recommends an acceptable analytical approach for performing the criticality safety evaluation. The criticality calculations performed herein use the SCALE code system³ to illustrate the analysis approach. However, the report does not endorse any particular computational tool and stresses that any computational tools (SCALE system or any other code) used in the evaluation must be demonstrated as valid for the criticality safety analysis of the specific package design.

In this report, the performance requirements of 10 CFR Part 71 or the Standard Format Guide have not been emphasized; it is assumed that the reader is familiar with these documents. The completed criticality evaluation should address and demonstrate compliance with all applicable performance requirements, and the application should follow the Standard Format Guide. Sections 2 through 6 of this report have been compiled assuming that the recommendations in this report will be implemented in an application that has been prepared to demonstrate compliance with the requirements of 10 CFR Part 71 and in accordance with the Standard Format Guide.

1.3 SUMMARY RECOMMENDATIONS

This report recommends information and assumptions to be considered in the criticality section of an application for approval of a transportation package. A summary of these recommendations is listed below. The list provides the information and assumptions that should be considered; additional information and/or assumptions may need to be considered depending on the package design and the approach used in the safety evaluation.

1. Provide a complete description of the contents and the packaging (including maximum and minimum mass of all materials, maximum ²³⁵U enrichment, physical parameters, type, form, and composition). See Sect. 2 for more details.

2. Provide a description (including sketches with dimensions and materials) of the calculational models, point out the differences between the models and actual package design, and discuss how these differences affect the calculations. See Sect. 3 for more details.
3. For packages equipped with fixed neutron absorbers, assume no more than 75% of the minimum neutron absorber content, unless comprehensive acceptance tests are implemented that are capable of verifying the presence and uniformity of the neutron absorber. See Sect. 3.1.3.
4. Demonstrate and consider the most reactive content loading and the most reactive configuration of the contents, the packaging, and the package array in the criticality evaluation. For spent fuel packages, assume unburned (fresh) fuel isotopic concentrations; however, do not take credit for any fixed burnable absorbers in the fuel. See Sects. 3.2-3.4 for more details.
5. Provide a description of the code(s) and cross-section data used in the safety analysis, together with references that provide complete information. Discuss software capabilities and limitations of importance to the criticality safety evaluations. See Sect. 4 for details.
6. Use appropriate validation procedures to justify the bias and uncertainties associated with the calculational method. In addition to the bias and uncertainties, the NRC position is that transportation packages should have a minimum administrative subcritical margin of $0.05 \Delta k$. See Sect. 5 for more details.
7. For the following cases, demonstrate that the effective neutron multiplication factor (k_{eff}) calculated in the safety analysis is limited to 0.95 after consideration of appropriate bias and uncertainties (see Sect. 5.4).
 - a. a single package with optimum moderation within the containment system, close water reflection, and the most reactive packaging and content configuration (consistent with the effects of normal conditions of transport or hypothetical accident conditions, whichever is more reactive);
 - b. an array of 5N undamaged packages (packages subject to normal conditions of transport) with nothing between the packages and close water reflection of the array; and
 - c. an array of 2N damaged packages (packages subject to hypothetical accident conditions) if each package were subjected to the tests specified in §71.73, with optimum interspersed moderation and close water reflection of the array.

See Sects. 3.4 and 6.1-6.2 for more details.

8. Calculate and report the transport index (TI) for criticality control based on the value of N determined in the array analyses. See Sect. 6.3 for more details.
9. Provide sufficient information in the application to support independent analyses without reference to external documents.

2 PACKAGE DESCRIPTION

The criticality section of the application for approval of a transportation package should include a description of the packaging and its contents. Descriptions of the packaging and contents should be consistent with the engineering drawings and with other figures and text provided in other sections of the application. Other sections of the application may be referenced to ensure consistency and to limit duplication. However, a description of the package sufficient for understanding the criticality evaluation should be provided without reference to other sections. This description should focus on the package dimensions and material components that can influence k_{eff} (e.g., fissile material inventory and placement, neutron absorber material and placement, reflector materials), rather than structural information such as bolt placement and trunnions. This section of the report clarifies the information that is expected in the criticality safety section of the application.

2.1 CONTENTS

The criticality safety section of the application should have a complete and detailed description of the contents of the packaging. This should include content quantities, dimensions, and configurations that are most limiting in terms of criticality safety. The application should clearly state the full range of contents for which approval is requested. Thus parameter values (e.g., maximum ^{235}U enrichment, multiple fuel assembly types, fuel pellet diameter, fuel masses) needed to bound the packaging contents within prescribed limits should be provided. For packages with multiple loading configurations, each configuration should also be specifically described, including all possible partial-load configurations. The description of the contents should include

1. the type of materials (e.g., fissile and nonfissile isotopes, reactor fuel assemblies, packing materials, and neutron absorbers),
2. the form and composition of materials (e.g., gases, liquids, and solids as metals, alloys, or compounds),
3. the quantity of materials (e.g., masses, densities, ^{235}U enrichment, isotopic distribution, H/X, and C/X), including tolerances for any nominal values given, and
4. other physical parameters (e.g., geometric shapes, configurations, dimensions, orientation, spacing, and gaps), including tolerances for any nominal values given.

The criticality safety section of the application should also describe the configuration of the contents after the package has been subjected to the hypothetical accident conditions. Appropriate references to the structural and thermal sections of the application should be made. Any changes from the normal conditions content configurations should be described.

2.2 PACKAGING

The criticality section of the application should include a description of the packaging with emphasis on the design features pertinent to the criticality safety evaluation. The features that should be emphasized are

1. the materials of construction and their relevance to criticality safety.
2. pertinent dimensions and volumes, including tolerances and allowable deviations.

3. the limits on design features relied on for criticality safety (e.g., minimum dimensions for fixed neutron absorbers, minimum loading of neutron absorber material, minimum separation distances), and
4. other design features that contribute to criticality safety.

The application should also describe the configuration of the packaging after the package has been subjected to the hypothetical accident conditions. Appropriate references to the structural and thermal sections of the application should be made. Any changes from the normal condition packaging configuration which may affect the criticality evaluation should be described.

2.3 SPECIFICATION OF TRANSPORT INDEX

The application should specify the TI for criticality control. The TI is the dimensionless number (rounded up to the next tenth) that designates the degree of control (e.g., limits package accumulation) to be provided by the carrier. The TI is defined by 10 CFR Part 71 to address concerns for radiation protection (TI value is maximum dose in millirem per hour at 1 m from the package surface) and criticality control. The TI for criticality control is calculated by dividing 50 by the number "N." The number "N" used to determine the TI for criticality control is derived from separate consideration (see Sects. 6.2 and 6.3) of the number of damaged and undamaged packages that can be adequately subcritical in an array subject to the conditions of 10 CFR § 71.59(a).

3 CRITICALITY SAFETY ANALYSIS MODELS

The application for approval of transportation packages should provide specific information on all calculational models used to perform the criticality safety evaluation. This section provides recommendations on the information that should be provided for each calculational model.

3.1 GENERAL

The applicant should perform criticality safety analysis for single packages and arrays of packages. In each case, the package conditions under normal conditions of transport (i.e., an undamaged package) and the package conditions under hypothetical accident conditions (i.e., damaged package) should be considered. For each evaluation, a calculational model should be developed. An exact model of the package may not be necessary. However, the calculational models should explicitly include the physical features important to criticality safety. Also, any modeling approximations should be shown to be conservative or essentially neutral relative to a more exact model.

The applicant should provide three types of calculational models: contents models, the single-package models, and package array models. The contents models should include all geometric and material regions out to the containment boundary (or to a convenient boundary, such as the strongback of a fresh fuel assembly package). Each contents model should dimensionally fit inside the undamaged and damaged package models used in the single-package and package array evaluations. Additional calculational models may be needed to describe the range of contents or the various array configurations or damage configurations that should be analyzed.

The criticality section of the application should contain a detailed description of the calculational models. Sections 3.1.1 through 3.1.4 discuss the items that should be included with the description of the calculational models.

3.1.1 Sketches

The criticality section of the application should include simplified, dimensioned sketches of the calculational models. Sketches drawn specifically for the various portions of the model are preferable to engineering drawings. However, the sketches should be consistent with the engineering drawings. Any differences with the engineering drawings, or with other figures in the application, should be noted and explained.

The sketches should be simplified by limiting the dimensional features on each sketch and by providing multiple sketches, with each sketch building on the previous one. Multiple sketches for each calculational model may be necessary to show sufficient detail. Also, multiple sketches may be necessary to show different undamaged and damaged package configurations.

3.1.2 Dimensions

The sketches discussed in Sect. 3.1.1 should show the dimensions that are used in the calculations (see examples in Appendix A). Any difference between dimensions used in the sketches and those in the engineering drawings, or other figures of the application, should be noted and explained. The dimensions on the sketches should be specified in both SI and English units.

The criticality section should address dimensional tolerances of the packaging, including components containing neutron absorbers. When developing the calculational models, adjustments should be made for tolerances that tend to add conservatism (i.e., produce higher k_{eff} values). For example, subtraction of the

negative tolerance from the nominal wall thickness of steel should be conservative for array calculations and may have no significant effect on the single-package calculation.

3.1.3 Materials

The range of material specifications (including tolerances and uncertainties) for the packaging and contents should be addressed in the criticality section of the application. Specifications and tolerances for all fissile materials, neutron-absorbing materials, materials of construction, and moderating materials should be confirmed with the engineering drawings of the packaging or the specified design criteria. The range of material specifications should be used to select parameters that produce the highest k_{eff} value consistent with normal and hypothetical accident conditions. For example, the ^{235}U enrichment of the fuel should be maximized, while the ^{10}B enrichment of a neutron poison component should be minimized. In practice, the effect of small variations in dimensions or material specifications may also be considered by determination of a reactivity allowance that covers the k_{eff} change due to the parameter changes under consideration. This additional reactivity allowance should be positive and included as an additional element of the calculational uncertainty (see Sect. 5.4).

For each calculational model, the atom density of any neutron absorber (e.g., boron, cadmium, or gadolinium) added to the packaging for criticality control should be limited to 75% of the minimum neutron absorber content specified in the application. This minimum neutron absorber content should be verified by chemical analysis, neutron transmission measurements, or other acceptable methods. A percentage of neutron absorber material greater than 75% may be considered in the analysis only if comprehensive acceptance tests, capable of verifying the presence and uniformity of the neutron absorber, are implemented. The adequacy of these tests will be considered on a case-by-case basis. Use of independent tests that verify the presence of the absorber material and adequate demonstration that the tests have appropriate sensitivity to the quantities of concern (presence and uniformity of absorber constituents) are issues that should be considered.

Limiting added absorber material credit to 75% without comprehensive tests is based on concerns for potential "streaming" of neutrons due to nonuniformities. It has been shown that boron carbide granules embedded in aluminum permit channeling of a beam of neutrons between the grains and reduce the effectiveness for neutron absorption. The experimental work of Refs. 4 and 5 shows that for a monoenergetic neutron beam, the granulated boron carbide areal density of 0.040 g/cm^2 of ^{10}B is equivalent to a homogeneous areal density of 0.033 g/cm^2 of ^{10}B . The efficiency of boron as a neutron absorber allows credit for only 75% of the poison to be a manageable value for most transportation package designs. The 75% value demonstrated by this work is conservative for several reasons: (1) many neutron poisons tend to be distributed homogeneously through a component of the packaging and are not distributed in a granular fashion, and (2) the experimental work is based on the use of a monodirectional beam of neutrons, while in most package designs an isotropic source of neutrons will be impinging on the wall (thus reducing the potential for intragranular transmission). Nevertheless, the 75% value is a prudent value consistent with demonstrated percentages found in experimental work.

A table should be provided in the application that identifies all of the different material regions in the criticality safety calculational models. This table should list the following for each region: the material in each region, the density of the material, the constituents of the material, the weight percent and atom density of each constituent, the region mass represented by the model, and the actual mass of the region (consistent with the contents and packaging description discussed in Sect. 2). The materials, densities, and masses provided in the sketches should be consistent with the corresponding items in the engineering drawings and should have the

same numerical values used in the input of the calculational method. For each sketch representing a portion of the calculation model, there should be a corresponding subsection discussing the material compositions and densities of each region shown in the sketch. All density values that are used, whether input by the analyst or retrieved by the code from a software database, should be reported in the application.

The source of all material density values should be reported. If a density value other than that found in standard references (e.g., materials or engineering handbook) is used in the calculation, the applicant should explain why the density is different, how the value was determined, and how the value affects the k_{eff} . Compositional differences should also be discussed.

3.1.4 Differences Between the Models and the Actual Package Configuration

The calculational models described in the criticality safety section of the application should be consistent with the undamaged and damaged package configurations as described in other sections (general, structural, thermal) of the application. Any differences (e.g., in dimensions, material, geometry) between the calculational models and the package configurations should be identified. The applicant should show how these different values (in dimensions, densities, etc.) were determined and justify the values used in the calculational models. Also, the applicant should discuss and explain how the differences impact the calculated k_{eff} values.

3.2 CONTENTS MODELS

The contents model should provide a detailed description of the packaging contents as they are assumed to be configured in the single-package and package array calculations. Models that show the contents under normal conditions of transport and under hypothetical accident conditions should be included in the application. A contents model representing each of the different loading configurations (full- and partial-load configurations) should also be provided. A single-contents model that will encompass different loading configurations should be considered only if the justification is clear and straightforward.

Each contents model should provide a description of the fissile contents of a package in its most reactive configuration, consistent with its physical and chemical form within the containment vessel under the normal or hypothetical accident conditions considered by the model. If the contents can vary over some parameter range (e.g., mass, enrichment, spacing), the criticality safety analysis should demonstrate that the model describes and uses the parameter specification that provides the maximum k_{eff} value under normal and hypothetical accident conditions. In designing the calculational models, tolerances that tend to add conservatism (i.e., produce higher k_{eff} values) should be included. Any assumed fissile material distribution that limits the maximum k_{eff} of the package contents should be justified.

The contents models for packages that transport loose pellets should ensure that variations in pellet size and spacing are considered in determining the configuration that produces the maximum k_{eff} value. The maximum pellet enrichment should be considered in the criticality safety evaluation. Fuel elements should consider the actual fuel pin spacing provided by the element.

At this time, the NRC does not accept burnup credit for spent fuel transportation packages. Therefore, unburned (fresh) fuel isotopics should be considered in the evaluation of packages containing spent fuel; however, no credit should be taken for any fixed burnable absorbers in the fuel when the fuel has been irradiated.

Other fissile materials should assume a particle spacing that results in maximum reactivity. Packages that transport isotopic waste containing fissile material should ensure that the limiting concentration and/or mix of fissile material is used in the safety analysis. Contents that are unknown or uncertain must be assumed to have a value that maximizes k_{eff} .

3.3 SINGLE-PACKAGE MODELS

The single-package models, together with the contents model(s), should depict the configuration of the packaging and contents under normal conditions of transport and under hypothetical accident conditions. These models should be those used to demonstrate that a single package remains adequately subcritical (see Sect. 5.4) per the requirements of 10 CFR § 71.55. The calculational model (single-package and contents model) for the single-package evaluation should consider the following items:

1. The undamaged single-package model should represent the physical condition of a package subjected to the test specified in 10 CFR § 71.71 (normal conditions of transport).
2. The damaged single-package model should represent the physical condition of a package subjected to the tests specified in 10 CFR § 71.73 (hypothetical accident conditions).
3. The packaging and contents should be in the most reactive configuration consistent with the chemical and physical form of the material. Determination of the most reactive configuration should account for the effects of both the normal and hypothetical accident conditions. In development of the damaged package models, the applicant should consider (a) the change in internal and external dimensions due to impact; (b) loss of material, such as neutron shield or wooden overpack, due to the fire test; (c) rearrangement of fissile material or neutron absorber material within the containment system due to impact, fire, or immersion; and (d) the effects of temperature changes on the package material and/or the neutron interaction properties.
4. Water moderation should be considered to occur to the most reactive extent possible. Partial flooding or preferential flooding (i.e., uneven flooding among the regions of a package to the most reactive extent), if possible, should be considered. If the contents are cladded fuel rods, flooding of the pellet-to-clad-gap regions should be considered. If fuel rods or pellets are annular, flooding of the annulus should also be considered, even if the rods or pellets are cladded. Moderation by other packaging materials should also be considered.
5. The containment system should be reflected closely on all sides by at least 30 cm of water. Package materials that are present and are better reflectors than water should be considered. For example, a lead shield around the containment system may provide more effective reflection than water.

In many cases, one model can be used to envelop both the undamaged and the damaged single-package models. If only one model is used in the single-package analysis, the applicant should justify that this model bounds the most reactive undamaged and damaged configuration of the package.

3.4 PACKAGE ARRAY MODELS

The package array models should depict the arrangements of packages that are used in the calculation necessary to fulfill the requirements of 10 CFR § 71.59. At least two array models are needed: an array of

5N undamaged packages (normal conditions of transport) and an array of 2N damaged packages (hypothetical accident conditions). The configuration of the individual packages (undamaged and damaged) used in the respective array models should be the worst case for the array of packages, which may not be the same as the worst case for a single package. The dimensions of the array that provides the limiting subcritical k_{eff} value should be determined as described in Sect. 6.2. The calculational models for the array analysis should consider the following items:

1. The applicant should demonstrate that the most reactive array configuration has been considered in the criticality safety evaluation. The exact lattice arrangement may be represented by a simplified arrangement if justification is provided.
2. The applicant should consider all types of array arrangements. Often an array model that provides the lowest surface-to-volume ratio (typically one with equal dimensions on each side of the array) is a good initial arrangement because this model should minimize neutron leakage from the array (see Sect. 6.2).
3. The array of packages should be reflected on all sides by a close-fitting water reflector at least 30 cm thick.
4. The following criteria for moderation in the containment system should be assessed and separately applied for normal conditions of transport and hypothetical accident conditions. Optimum moderation is the condition that produces the highest k_{eff} value over the range of moderation conditions. Sources of moderation in the containment system are water leaking into the containment system, and the packaging materials and contents inside the containment system.

Typically, the analysis for the array of undamaged packages can assume that the packages are dry internally, provided that there is no water leakage into the package, including the containment system, when the package is subjected to the tests specified in 10 CFR § 71.71.

The analysis for the array of damaged packages should assume water leakage into the containment system to the most reactive degree. For those cases where water inleakage is not assumed, the application must adequately demonstrate that water inleakage would not occur under hypothetical accident conditions. The adequacy of such demonstrations will be assessed on a case-by-case basis. The acceptance criteria for these demonstrations are beyond the scope of this report.

Regardless of whether water inleakage is assumed, internal moderation provided by the materials and contents (e.g., plastics, foam, impurities, or residual moisture in the fuel) in the package should be considered when determining optimum moderation. If the moderation provided by the packaging materials or contents overmoderates the package contents, and by its physical and chemical form cannot leak from the containment vessel, then its overmoderating properties can be considered in the model. For example, a solid moderator which is shown to overmoderate the fissile material can be considered in the calculational model if its continued presence is demonstrated under normal conditions of transport and hypothetical accident conditions.

5. If there can be leakage of water into the package, then partial and preferential flooding should be considered in determining optimum moderation. For fuel with pellet-to-clad gaps, flooding of the gap region should be considered.

6. Optimum interspersed hydrogenous moderation should be determined in the evaluation of arrays of damaged packages. Optimum interspersed moderation is the degree of hydrogenous moderation between packages that results in the highest k_{eff} value. In addition to interspersed moderation, moderation in regions of the package outside the containment system should also be considered if these regions consist of voids, hydrogenous or other moderating materials, or water-absorbing materials (e.g., foam, wood). The overmoderating or "isolating" effect of a packaging material may be considered, provided that the material remains in place and maintains its overmoderating or "isolating" properties under hypothetical accident conditions. Note that moderation between packages, moderation in regions of the package outside the containment system, and moderation within the containment system need to be considered concurrently to the most reactive extent.

4 METHOD OF ANALYSIS

This section of the report discusses the information that should be supplied on the computer code, nuclear cross-section data, and technique used to complete the criticality safety evaluation.

4.1 COMPUTER CODE SYSTEM

The computer codes used in the safety evaluation should be identified and described in the application or adequate references should be included. Verification that the software is performing as expected is important. The applicant should identify all hardware and software (titles, versions, etc.) used in the calculations as well as pertinent configuration control information. Correct installation and operation of the computer code should be demonstrated by performing and reporting (in the application or by reference) the results of the sample problems or general validation problems provided with the software package. Capabilities and limitations of the software that are pertinent to the calculational models should be discussed with particular attention to limitations that may affect the calculated k_{eff} value.

Computational methods that fully consider the anisotropic angular terms of the Boltzmann radiation transport equation are preferred for use in criticality safety analysis. The deterministic discrete-ordinates technique and the Monte Carlo statistical technique are the most rigorous and flexible techniques available to consider the anisotropic scattering terms. These techniques solve, respectively, the differential and integral eigenvalue (e.g., the k_{eff} value) form of the Boltzmann equation. Monte Carlo analyses are prevalent because these codes can better model the geometry detail needed for most criticality safety analyses. Well-documented and well-validated computational methods, such as those provided in the SCALE code system,³ may require less description than a limited-use and/or unique computational method. The use of computational methods that limit or eliminate the angular terms in the Boltzmann equation (e.g., diffusion theory) or use simpler methods to estimate k_{eff} should be thoroughly justified.

When using a Monte Carlo code, the applicant should consider the imprecise nature of the k_{eff} value provided by the statistical technique. Every k_{eff} value should be reported with a standard deviation, σ . Typical Monte Carlo codes provide an estimate of the standard deviation of the calculated k_{eff} . The applicant may wish to obtain a better estimate for the standard deviation (Monte Carlo code estimates typically underpredict σ) by repeating the calculation with different valid random numbers and using this set of k_{eff} values to estimate σ . If fewer than 20 to 25 k_{eff} values are provided in the set, the estimation of σ should be calculated using the student-t distribution formula. Also, because of the statistical nature of Monte Carlo methods, this method should not be used to determine changes in k_{eff} due to small problem parameter variations. The change in k_{eff} due to a parameter change should be statistically significant (greater than at least 3σ) to indicate a trend in k_{eff} .

The geometry model limitations of deterministic discrete-ordinates methods typically restrict their applicability to calculation of bounding, simplified models and investigation of the sensitivity of k_{eff} to changes in system parameters. These sensitivity analyses can use a model of a specific region of the full problem (e.g., a fuel pin or homogenized fissile material unit surrounded by a detailed basket model) to demonstrate changes in reactivity with small changes in model dimensions or material specification. Applicants should consider such analyses when necessary to ensure or demonstrate that the full package model has utilized conservative assumptions relative to calculation of the system k_{eff} value. For example, a one-dimensional fuel pin model may be used to demonstrate the reactivity effect of tolerances in the clad thickness.

4.2 CROSS SECTIONS AND CROSS-SECTION PROCESSING

The calculational method consists of both the computer code and the neutron cross-section data used by the code. The criticality safety evaluation should be performed using cross-section data that are derived from measured data involving the various neutron interactions (e.g., capture, fission, and scatter). Although not infallible, unmodified data processed from compendiums of evaluated nuclear data (e.g., the various versions of the Evaluated Nuclear Data Files in the United States or the Joint European Files) should be considered as the major sources of such data.

The neutron cross-section data and any codes used to process the data for the criticality safety analyses should be identified, described, and referenced in the application. The codes used to process the data are subject to the same recommendations provided in the initial paragraph of Sect. 4.1. The application should identify the source of the neutron cross-section data (e.g., specific version of an evaluated nuclear data file) and supply pertinent references that document the content of the cross-section library, the procedure used to generate the cross-section library, and its range of applicability. Verification that the data library consists of the cross-section data described and referenced in the application is important. The applicant should demonstrate correct installation and operation of the data library by performing and reporting the results of any sample problems or general validation problems provided with the software package. Capabilities and limitations of the data library that are pertinent to the calculational models should be discussed with particular attention to discussing limitations that may affect the calculations. For example, the 123-group library once provided in the SCALE code package did not have resonance data for ^{235}U . Although not an issue for low-enriched, well-moderated systems that the library was generated to analyze, this lack of data made the library inappropriate for high-enriched, low-moderation systems.⁶

Continuous energy and multienergy-group (multigroup) cross-section libraries are acceptable. The number of energy groups and the energy boundaries of each group should be specified for a multigroup library. Known limitations (e.g., omission or limited range of resonance data, limited order of scattering) that may affect the analysis should be provided. The temperature range over which the cross-section data are applicable needs to be considered in the analyses and specified in the application. For multigroup cross sections, the order of scatter available on the library and applied in the calculation should be indicated. For continuous energy data, the number of points in the nuclide set should be specified. Computer programs and methods used to perform functions such as cross-section mixing for problem materials, problem-dependent resonance self-shielding, or cell-weighting of mixtures to represent heterogeneous configurations should be identified and discussed consistent with the recommendations of Sect. 4.1.

Any special techniques used in the analysis to improve the adequacy or use of the cross-section data should be discussed. For example, the SCALE system sequences automatically perform a problem-dependent resonance calculation for only one type of unit cell within a lattice. If deemed important, resonance-corrected data for materials outside the lattice, or for other types of unit cells within the lattice, can be calculated separately and provided via an optional input field.

4.3 CODE INPUT

All major code input parameters or options used in the criticality safety analysis should be identified and discussed in the application. This identification and discussion of code input should be provided in addition to the actual case inputs (or at least a sampling of the inputs for the various types of calculational models). For a Monte Carlo analysis, the applicant should indicate, among other things, the neutron starting distribution, the

number of histories tracked (number of generations and particles per generation), boundary conditions selected, order of scatter selected (for multigroup codes), any special reflector treatment, and any special biasing option. For a discrete-ordinates analysis, the applicant should specify the spatial mesh used in each region, the angular quadrature used, the order of scatter selected, the boundary conditions selected, and the flux convergence criteria. Any of these input parameters can influence the accuracy of the results; therefore, the selection of the input values should be carefully considered and, to the extent possible, be consistent with the data used in the validation analyses.

4.4 ADEQUACY OF CALCULATION

The criticality safety section of the application should review and discuss calculational issues that are important in ensuring an accurate k_{eff} value is obtained. Adequate problem-dependent treatment of multigroup cross sections, use of sufficient cross-section energy groups (multigroup) or data points (continuous energy), and proper convergence of the numerical results are examples of issues the applicant may need to review and discuss in the criticality section of the application. To the degree allowed by the code, the applicant should demonstrate or discuss any checks made to confirm that the calculational model prepared for the criticality safety analysis is consistent with the code input. For example, code-generated plots of the geometry models and outputs of material masses by region may be beneficial in this confirmation process. The statistical nature of Monte Carlo calculations is such that there are no fixed rules, criteria, or tests for judging when calculational convergence has occurred. Thus the applicant should discuss the code output or other measures used to confirm the adequacy of convergence. For example, many Monte Carlo codes provide output edits that should be reviewed to determine adequate convergence, including:

1. the k_{eff} by generation run,
2. plot of average k_{eff} by generation run,
3. final k_{eff} edit table by generation skipped,
4. plot of k_{eff} by generation skipped, and
5. frequency distribution bar graph.

Other conditions in the output that may indicate a convergence problem should be reviewed, for example,⁷

1. upward or downward trends in k_{eff} by generation run over the last half of the total generations,
2. upward or downward trends in k_{eff} by generation for the first half of generations skipped,
3. sudden changes of greater than one standard deviation in either k_{eff} plot,
4. abnormally high or low generation k_{eff} ($\pm 20\%$ of calculated mean), and
5. a calculated result that is not consistent with expected results based on previous experience (may be indicative of other problems).

It is also advisable to check for adequate sampling of isolated fissile regions by examining the printed regionwise fission event data and associated statistics.

If necessary, the applicant should review the code documentation as well as literature (such as Refs. 7 and 8) to obtain practical discussions on the uncertainties associated with Monte Carlo codes used to calculate k_{eff} and advice on output features and trends that should be observed. If convergence problems were encountered by the applicant, a discussion of the problem and the steps taken to obtain an adequate k_{eff} value should be provided. For example, calculational convergence may be achieved by selecting a different neutron starting distribution or running additional neutron histories. Modern personal computers and workstations allow a significant number of particle histories to be tracked; a minimum of 200,000 histories is now typical

As a minimum, portions of output (such as the plots of k_{eff} by generation run and k_{eff} by generation skipped) from selected cases should be included in the application. In selecting the output to provide, the applicant should consider that the goal is to demonstrate that the calculations have been performed as described and run to successful completion.

5 VALIDATION OF CALCULATIONAL METHOD

The application should demonstrate that the calculational method (codes and cross-section data) used to establish criticality safety has been validated against measured data that can be shown to be applicable to the package design characteristics. The validation process should provide a basis for the reliability of the calculational method and should justify that the calculated k_{eff} , plus bias and uncertainties, for the necessary package conditions will ensure an actual package $k_{eff} \leq 0.95$.

The applicant should comply with the following guidelines⁹ in performing and documenting the validation process:

1. bias and uncertainties should be established through comparison with critical experiments that are applicable to the package design;
2. the range of applicability for the bias and uncertainty should be based on the range of parameter variation in the experiments;
3. any extension of the range of applicability beyond the experimental parameter field should be based on trends in the bias and uncertainty as a function of the parameters and use of independent calculational methods; and
4. a margin of subcriticality should be included. The NRC currently regards $0.05 \Delta k$ as the minimum administrative margin of subcriticality that should be considered for transportation packages.

Although significant reference material is available to demonstrate the performance of many different criticality safety codes and cross-section data combinations, the application needs to demonstrate that the specific calculational method used by the applicant (e.g., code version, cross-section library, and computer platform) is validated in accordance with the above process. The remainder of this section of the report provides recommendations on the assumptions that should be made and the information that should be provided in performing and documenting the validation process.

5.1 SELECTION OF CRITICAL EXPERIMENTS

The first phase in the validation process should be to establish an appropriate bias and uncertainty for the calculational method by using well-defined critical experiments that have parameters (e.g., materials, geometry, etc.) that are characteristic of the package design. The single-package configuration, the array of packages, and the normal and hypothetical accident conditions should be considered in selecting the critical experiments for the validation process. Ideally, the set of experiments should match the package characteristics that most influence the neutron energy spectrum and reactivity. These characteristics include:

1. the fissile isotope (^{233}U , ^{235}U , ^{238}Pu , ^{239}Pu , and ^{241}Pu according to the definition of 10 CFR 71), form (e.g., homogeneous, heterogeneous, metal, oxide, fluoride), and isotopic composition of the fissile material;
2. hydrogenous moderation, consistent with the normal conditions of transport and hypothetical accident conditions, in and between packages that results in maximum k_{eff} (if substantial amounts of other moderators such as carbon or beryllium are in the package, these should also be considered);
3. the type (e.g., boron, cadmium), placement (between, within, or outside the contents), and distribution of absorber material and materials of construction;

4. the single-package contents configuration (e.g., homogeneous or heterogeneous) and packaging reflector material (e.g., lead, steel); and
5. the array configuration including spacing, interstitial material, and number of packages.

Unfortunately, it is unlikely that the complete combination of package characteristics will be found from available critical experiments, and critical experiments for large arrays of packages do not currently exist. Thus the applicant should model a sufficient variety of critical experiments to demonstrate the capability of the calculational method in predicting k_{eff} for each individual experiment that has characteristics that are also judged to be important to the k_{eff} of the package (or array of packages) under normal conditions of transport and hypothetical accident conditions.

Reference 10 provides general guidance on selecting critical experiments and provides descriptions of a significant number of critical experiments appropriate for low-enriched lattice systems. The critical experiments that are selected by the applicant should be briefly described in the application with references provided for detailed descriptions. The applicant should indicate any deviation from the reference experiment description including the basis for the deviation (e.g., discussions with experimenter, experiment log books). Since validation and supporting documentation may result in a voluminous report, it is acceptable to summarize the results in the application and reference the validation report for specific information.

5.2 ESTABLISHMENT OF BIAS AND UNCERTAINTY

For validation using critical experiments, the bias in the calculational method is the difference between the calculated k_{eff} value of the critical experiment and unity (1.0). Typically, a calculational method is termed to have a positive bias if it overpredicts the critical condition (i.e., calculated $k_{eff} > 1.0$) and a negative bias if it underpredicts the critical condition (i.e., calculated $k_{eff} < 1.0$). A calculational methodology should have a bias that either has no dependence on a characteristic parameter or is a smooth, well-behaved function of characteristic parameters. The applicant should analyze a sufficient number of critical experiments to determine if trends may exist with parameters important in the validation process [e.g., hydrogen-to-fissile ratio (H/X), ^{235}U enrichment, neutron absorber material]. As indicated in Sect. 4.1, the k_{eff} values should change by at least 3σ to indicate any type of parametric trend. The bias for a set of criticals should be taken as the difference between the best fit of the calculated k_{eff} data and 1.0. Where trends exist, the bias will not be constant over the parameter range. If no trends exist, the bias will be constant over the range of applicability. For trends to be recognized, they must be statistically significant.

The applicant should consider three general sources of uncertainty: the experimental data or technique, the calculational method, and the particular analyst and calculational models. Examples of uncertainties in experimental data are uncertainties reported in material or fabrication data or uncertainties due to an inadequate description of the experimental layout. Examples of uncertainties in the calculational method are uncertainties in the approximations used to solve the mathematical equations, uncertainties due to solution convergence, and uncertainties due to cross-section data or data processing. Interpretation of the calculated results, individual modeling techniques, and selection of code input options are possible sources of uncertainty due to the analyst or calculational model.

In general, all of these sources of uncertainty should be cumulatively observed in the variability of the calculated k_{eff} results obtained for the critical experiments. The variability should include the Monte Carlo standard deviation in each calculated critical experiment k_{eff} value as well as any change in the calculated value

caused by the consideration of experimental uncertainties. Thus these uncertainties will be included in the bias and uncertainty in the bias. This variation or uncertainty in the bias should be established by a valid statistical treatment of the calculated k_{eff} values for the critical experiments. Methods exist (see Ref. 10) that allow the bias and uncertainty in the bias to be evaluated as a function of changes in a selected characteristic parameter.

Calculational models used to analyze the critical experiments should be provided or adequate references to such discussions should be provided. Input data sets used for the analysis should be provided along with an indication of whether these data sets were developed by the applicant or obtained from other identified sources (e.g., published references, data bases). Known uncertainties in the experimental data should be identified, along with a discussion of how (or if) they were included in the establishment of the overall bias and uncertainty for the calculational method. The statistical treatment used to establish the bias and uncertainty should be thoroughly discussed in the application with suitable references where appropriate. Relative to experimental uncertainties, the applicant should provide a discussion on the approach used to model the experiments (i.e., with nominal dimensions and material compositions or with conservative tolerances, with simplifications in the geometry and material specifications, etc.).

5.3 ESTABLISHMENT OF RANGE OF APPLICABILITY

As an integral part of the code validation effort, the applicant should define the range of applicability for the established bias and uncertainty. The applicant should demonstrate that, considering both normal and hypothetical accident conditions, the package is within this range of applicability and/or the applicant should define the extension of the range necessary to include the package. The range of applicability should be defined by identifying the range of important parameters (see Ref. 10 for guidance on identifying important parameters) and/or characteristics for which the code was (or was not) validated. The procedure or method used to define the range of applicability should be discussed and justified in the application for approval. For example, the method of Ref. 10 indicates the range of applicability to be the limits (upper and lower) of the characteristic parameter used to correlate the bias and uncertainties. The characteristic parameter may be defined in terms of, for example, the hydrogen-to-fissile ratio (e.g., $H/X = 10$ to 500), the average energy causing fission, the ratio of total fissions to thermal fissions (e.g., $F/F_{th} = 1.0$ to 5.0), or the ^{235}U enrichment.

Use of the bias and uncertainty for the evaluation of a package with characteristics beyond the defined range of applicability is endorsed by consensus guidance.⁹ This guidance indicates the extension should be based on trends in the bias as a function of system parameters and, if the extension is large, confirmed by independent calculational methods. However, the applicant should consider that extrapolation can lead to a poor prediction of actual behavior. Even interpolation over large ranges with no experimental data can be misleading (see Ref. 6 for an example). The applicant should also consider the fact that comparisons with other calculational methods can illuminate a deficiency or provide concurrence; however, given discrepant results from independent methods, it is not always a simple matter to determine which result is "correct" in the absence of experimental data (see Ref. 11 for an illustration).

The applicant should recognize that there is no available guidance on what constitutes a "large" extension, nor any guidance on how to extend trends in the bias. In fact, it is not just the trend in the bias that the applicant should consider, but the trend in the uncertainties and bias. The paucity of experimental data near one end of a parameter range may cause the uncertainty to be larger in that region. (Note: Any extension of the uncertainty using the method of Ref. 10 should consider the behavior of the uncertainty as a function of the parameter, not just the maximum value of the uncertainty.) Proper extension of the bias and uncertainty means the applicant should determine and understand the trends in the bias and uncertainty. The applicant should exercise extreme

care in extending the range of applicability and provide in the application a detailed justification for the need for an extension, along with a thorough description of the method and procedure used to estimate the bias and uncertainty in this extended range.

5.4 ESTABLISHMENT OF ACCEPTANCE CRITERIA

The criticality safety section of the application should demonstrate how the bias and uncertainty determined from the comparison of the calculational method with critical experiments are used to establish a minimum k_{eff} value [i.e., upper subcritical limit (USL)] so that similar systems with a higher calculated k_{eff} are considered to be critical. The USL should be established with an additional margin of subcriticality (often termed a safety margin) included.⁹ The following general relationship (see Ref. 10) for establishing the acceptance criteria should be used in the application for approval:

$$k_c - \Delta k_u \geq k_{eff} + 2\sigma + \Delta k_m,$$

where

- k_c = mean value of k_{eff} resulting from the calculation of benchmark critical experiments using a specific calculational method and data;
- Δk_u = an allowance for the calculational uncertainty;
- Δk_m = a required margin of subcriticality (minimum of 0.05 for applications of approval for packaging);
- k_{eff} = the calculated value obtained for the package or array of packages;
- σ = is the standard deviation of the k_{eff} value obtained with Monte Carlo analysis.

If the calculational bias β is defined as $\beta = k_c - 1$, then the bias is negative if $k_c < 1$ and positive if $k_c > 1$. Thus the acceptance criteria may be rewritten as

$$1.00 + \beta - \Delta k_u \geq k_{eff} + 2\sigma + 0.05,$$

or

$$k_{eff} + 2\sigma \leq 0.95 - \Delta k_u + \beta.$$

The maximum USL that should be used for a package evaluation is

$$USL = 0.95 - \Delta k_u + \beta.$$

The uncertainty, Δk_u , will always be greater than or equal to zero, whereas the bias, β , can be positive or negative. However, a positive bias is not recommended; therefore, the equation should be revised to

$$USL = 0.95 - \Delta k_u + \bar{\beta}$$

$$\text{where } \bar{\beta} = \begin{cases} \beta & \text{if } \beta \leq 0 \\ 0, & \text{if } \beta > 0. \end{cases}$$

The applicant should consider that the value for Δk_m (=0.05) may need to be increased by an arbitrary amount if there is a lack of sufficient critical data to adequately determine the calculational bias and uncertainty. The statistical method of Ref. 10 provides a technique to estimate Δk_u and Δk_m based on available data. The estimate for Δk_m can be used to demonstrate that the value of 0.05 for the margin of subcriticality is adequate.

for the given set of critical experiments used in the validation. A paucity of critical experiment data or the need to extend beyond the range of applicability may indicate the applicant should consider the adequacy of the 0.05 value. Also, for high-reactivity worth systems where the value of k_{eff} is particularly sensitive to parameter changes in the package, a margin of subcriticality greater than 0.05 Δk should be considered by the applicant.

6 CRITICALITY CALCULATIONS AND RESULTS

This section of the report describes the criticality calculations that should be performed and documented in the criticality safety section of the application for approval of a package. The criticality safety evaluation should demonstrate the subcriticality of a single package and an array of packages during normal conditions of transport and hypothetical accident conditions, and determine the TI for criticality control of a shipment. For the purposes of this evaluation, the applicant should consider the term "subcriticality" to mean that the calculated k_{eff} value (including any Monte Carlo standard deviation) is less than the USL defined by Sect. 5.4.

The calculations that the applicant should include in the criticality safety section will depend on the various parameter changes and conditions that should be considered, the packaging design and features, the contents, and the damaged condition of the package. The calculated results should be presented in a tabular form with a case identifier, a brief description of the conditions for each case, and the case results. Values of k_{eff} obtained from Monte Carlo codes should always indicate the estimated standard deviation. Additional information should be included in the table if it supports and simplifies the description in the text. The case description should be clearly presented in the tables to permit easy cross-reference between the table and the text. Tables 1 and 2 show an example of the format desired to summarize the results of single-package and package array calculations.

The following subsections present a logical, generic approach to the calculational effort that should be described in the application for approval. Two series of calculational cases should be performed: (1) a series of single-package cases and (2) a series of array cases. Both series should consider normal and hypothetical accident conditions. Subsets of the array series for different size arrays or different package arrangements may also be necessary. Each array series should include calculations to determine the number of undamaged packages that will ensure subcriticality of an array under normal conditions of transport, as well as calculations to determine the number of damaged packages that ensure subcriticality of an array under hypothetical accident conditions. A TI for criticality control should be derived (see Sect. 6.3) from these array sizes based on the prescription of 10 CFR § 71.59.

6.1 SINGLE PACKAGE

The applicant should perform a series of calculations to demonstrate that the single package remains subcritical under normal conditions of transport and hypothetical accident conditions (per the requirements of 10 CFR § 71.55).

The single-package calculations also provide useful points of reference for subsequent calculations involving variations of certain parameters.

The single-package series of calculations must consider a model of the single containment vessel fully reflected by water (a 30-cm-thick region of full-density water is recommended). The containment vessel should be optimally moderated with the fissile content in its most reactive credible configuration. This water-reflected, optimally moderated containment vessel analysis should be compared with one where the water reflector is replaced by the package material (including water flooding in voids) that surrounds the containment system. Package materials such as lead may provide better reflection of the containment system than water. Demonstration that these two single, undamaged cases are adequately subcritical satisfies the requirements of 10 CFR § 71.55(b).

Table 1 Example format of table for single-package calculations

Case	Water reflected ^a	Internal moderation ^b	$k_{eff} \pm \sigma^c$
SU1	No	0.0	
SU2	Yes	0.0	
SU3	Yes	0.001	
SU4	Yes	0.003	
.	.	.	
SUx	Yes	1.0	
SUy	No	1.0	

^aWhen fully reflected, water should be at least 30-cm thick on all faces.

^bInternal moderation is the specific gravity water equivalent of hydrogenous content within all void spaces inside the package, including the containment vessel.

^c σ is one standard deviation of the calculated Monte Carlo result.

Table 2 Example format of table for array calculations

Case ^a	Array size	Internal moderation ^b	Interspersed moderation ^c	$k_{eff} \pm \sigma^d$
IA1	Infinite	0.0	0.0	
IA2	Infinite	0.0	0.001	
IA3	Infinite	0.0	0.003	
.	.	.	.	
IAx	Infinite	0.0	1.0	
FA1	7 × 7 × 7			
FA2	7 × 7 × 7			
FA3	7 × 7 × 7			
.	.	.	.	
FA10	5 × 5 × 5			
FA11	5 × 5 × 5			
.	.	.	.	

^aCase identifier IA represents infinite arrays and FA represents finite arrays; all finite arrays should be reflected by at least 30 cm of water on all faces.

^bInternal moderation is the specific gravity water equivalent of hydrogenous content within all void spaces inside the package, including the containment vessel.

^cInterspersed moderation is the specific gravity water equivalent of hydrogenous content between packages.

^d σ is one standard deviation of the calculated Monte Carlo result.

The remaining single-package cases provided in the application should systematically investigate progressive states of water flooding and package reflection representative of the normal and hypothetical accident conditions. If the hypothetical accident conditions cause damage to the contents or packaging, the damaged configuration of the package should be considered. If a package has multiple void regions, including regions within the containment system, flooding each region independently and consecutively should be considered. Variations in the flooding sequence should be considered by the applicant [e.g., partial flooding, variations caused by the package lying in horizontal or vertical orientations, flooding (moderation) at less than full-density water, progressively flooding regions from the inside out]. Water flooding of cladded fuel rod gap regions should be considered. The final case of this single-package series should represent a package completely water-flooded and water-reflected. The primary objectives of the single-package cases should be

1. to demonstrate that a single package is subcritical when subjected to the normal conditions of transport and hypothetical accident conditions as specified by 10 CFR § 71.55, and
2. to identify the specific conditions that produce the highest k_{eff} value.

For packages with different fissile material loading configurations (including partial-load configurations), the applicant should use a similar approach for each different loading, unless a limiting-contents model is developed and demonstrated in the application to provide a bounding reactivity for the different loadings. The results of the single-package calculations can influence the approach and the number of calculations required for the array series calculations, particularly if there are different content loading configurations.

6.2 EVALUATION OF PACKAGE ARRAYS

The applicant should perform the package array calculations to obtain the information needed to determine the TI for criticality control as prescribed by 10 CFR § 71.59. The applicant may consider beginning the array calculations with an infinite array model because, if the infinite array is adequately subcritical under normal and hypothetical accident conditions, no additional array calculations should be necessary. If the infinite array under normal and hypothetical accident conditions is shown to be above the USL, a large (number of packages) finite array should be selected and all cases recalculated. Successively smaller finite arrays may be required until the array sizes for normal and hypothetical accident conditions are found to be below the USL. As an alternative, an applicant may initiate the analyses using any array size—for example, one that is based upon the number of packages planned to be shipped on a vehicle.

Care should be taken so that the most reactive array configuration of packages has been considered in the criticality safety assessment. In investigating different array arrangements, the competing effects of leakage from the array system and of interaction between packages in the array should be considered. Array arrangements that minimize the surface-to-volume ratio decrease leakage and should, in simplistic terms, maximize k_{eff} . Preferential geometric arrangement of the packages in the array should be considered. For example, consider packages where the fissile material is loaded off-center. In this case, the need to optimize the interaction may mean that an array is more reactive when packages are grouped in a single or double layer. The effect of the external water reflector also needs to be considered. For some array cases there may be little moderator present within the array, so increasing the surface area may lead to more moderation and possibly higher reactivity. The exact package arrangement may be represented by a simplified arrangement if adequate justification is provided. For example, Appendix A demonstrates a case where a triangular-pitch arrangement of packages can, in simple cases, be represented by using an appropriately modified package model within a square-pitch lattice arrangement. In more complex cases, the effect of having a triangular pitch may be

important, since interaction between three triangularly pitched packages could be a dominating factor. Because there are so many competing effects, any simplifications made in the assessment need to be justified; something that is obvious from the point of view of array leakage may not be as obvious from the point of view of package interaction. All finite arrays of packages should be reflected on all sides by a close-fitting, full-density water reflector at least 30 cm thick.

Each array model for undamaged packages is not required to include interspersed moderation; however, moderation built into the packaging (e.g., due to hydrogenous packaging materials) or added to the packaging due to normal conditions of transport (e.g., the spray test) should be included to the most reactive extent possible under normal conditions. For damaged packages, varying amounts of hydrogenous moderation should be added in all regions that can be flooded within (see discussion of Sect. 6.1 for single package) and between the packages (i.e., interspersed moderation) by varying the density of water in these regions. If water in-leakage is considered (see Sect. 3.4), then the water density should be varied from zero to full density in increments such that the optimum moderator density is determined. The applicant should provide a plot of the k_{eff} value as a function of the moderator density to demonstrate the trend and the location of the highest k_{eff} value.

As an interspersed moderator is added to the region between packages, the spacing of the packages may become important because of the amount of moderator that may be present. For this reason, it is sometimes convenient to model an infinite array of packages using an array unit cell consisting of the individual package and a tight-fitting repeating boundary. If the k_{eff} response to increasing interspersed moderator density for this array with the units in contact has an upward trend (positive slope) at full-density moderation, the applicant should consider increasing the size of the unit cell and recalculating k_{eff} as a function of moderation density. Increasing the size of the unit cell provides an increased edge-to-edge spacing between packages and makes more volume available for the interspersed moderator. The applicant should stop this procedure only after confirming that the packages are isolated and that added interstitial space is only providing additional water reflection.

To illustrate this recommended procedure, consider a cylindrical shipping package with a diameter of one unit and a height (or length) of two units. With a tight-fitting cuboid around the cylinder, 21.5% of the cuboid's volume is outside the package and is available for an interspersed moderator. By increasing the cuboid's dimensions so that the edge-to-edge spacing between the packages in all directions is 10% of the package diameter, then 38.2% of the cuboid's volume is outside the package and is available for an interspersed moderator. This small increase in edge-to-edge spacing corresponds to a 126% increase in volume available for the interspersed moderator. Therefore, if the k_{eff} value is increasing at full water density with the packages in contact, then increasing the packaging spacing to permit additional interspersed moderation may be necessary.

The applicant should consider combinations of density and spacing variation (consistent with normal and hypothetical accident conditions) that may cause a higher k_{eff} value to be calculated and should provide a discussion in the application that demonstrates the maximum k_{eff} value has been determined. Figure 1 depicts some typical plots of k_{eff} versus interspersed water moderator density illustrating the moderation, absorption, and reflection characteristics that may be encountered in packaging safety evaluations. These curves represent changes in array moderation for a fixed package spacing. Curves A, B, and C represent arrays for which an array of packages at the selected spacing is overmoderated and increasing water moderation only lowers (curves B and C) or has no effect (curve A) on the k_{eff} value. Curves D, E, and F represent arrays for which the array is undermoderated at zero water density, and increasing the moderator density causes the k_{eff} value to

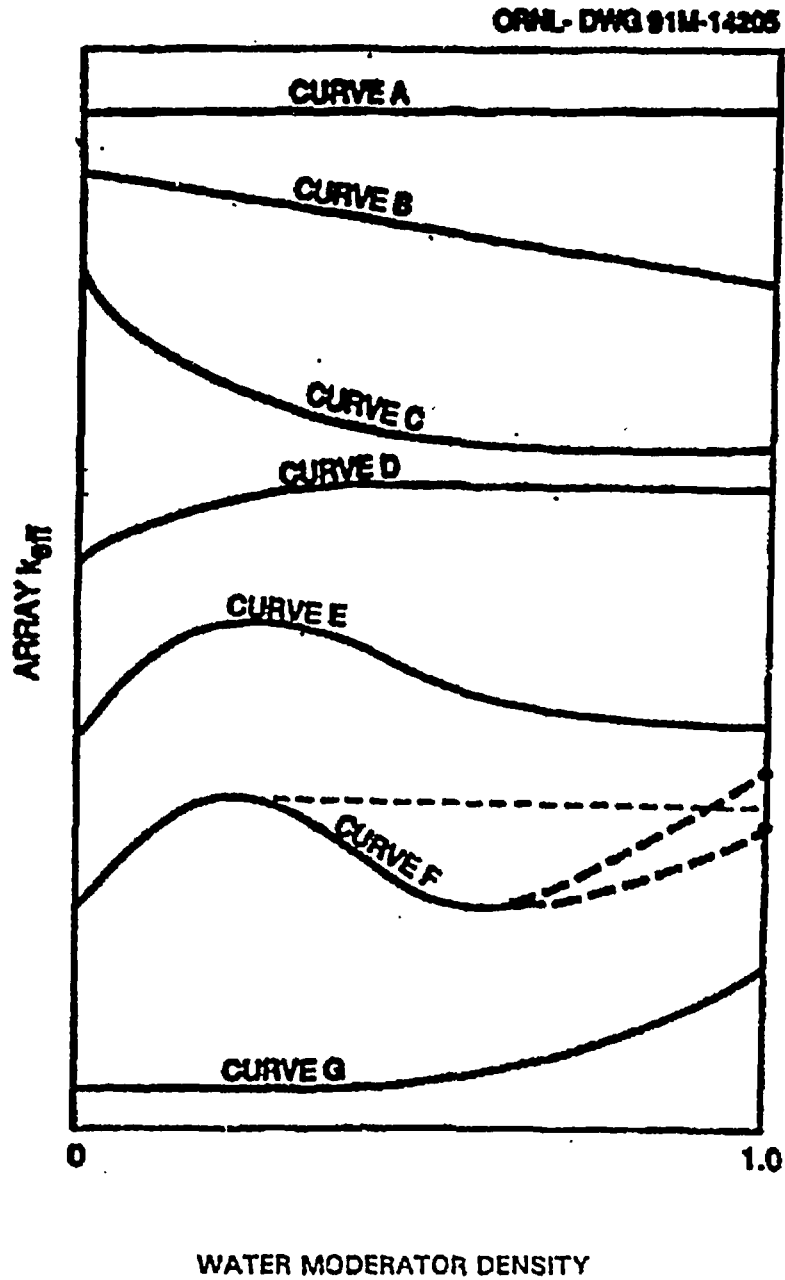


Figure 1 Typical plots of array k_{eff} vs interspersed water moderator density

increase. Then as the water density increases further, neutron absorption comes into effect, neutron interaction between packages decreases, and the k_{eff} value levels out (curve D) or decreases (curves E and F). The applicant should consider that peaking effects such as seen in curves E and F frequently occur at very low moderator density (e.g., 0.001 to 0.1 fraction of full density). Therefore, the applicant should exercise care when selecting the values of interspersed moderator density to calculate in the search for the maximum k_{eff} value.

As indicated above, optimum moderation conditions for the array of packages represented by curves D, E, and F have been obtained; and the only mechanism that could make the k_{eff} value of curve D, E, or F rise above the value at full-density water is increased reactivity due to increased reflection provided by more interspersed water (i.e., additional spacing between packages). If the array k_{eff} at full-density moderation is less than the k_{eff} of the flooded and reflected single unit, the edge-to-edge spacing of the packages is not sufficient to permit full reflection.

However, for responses such as those illustrated in curves D, E, and F, there is no need to increase spacing and recalculate the array k_{eff} because the maximum k_{eff} of the array will be that of the reflected single unit, or the k_{eff} of the optimally moderated array (i.e., the first local maxima of curves D, E, and F), whichever is larger. For curves A through F, the packages in the array are essentially isolated at full-density moderation and the corresponding k_{eff} will typically be the same (within statistical limits) as the flooded and reflected single-unit case.

Curve G represents an array where the optimum array moderator density has not been achieved even with full-density water, and the maximum k_{eff} has not been determined. For this situation, the applicant should increase the center-to-center spacing of the packages in the array and all cases should be recalculated. The center-to-center spacing must be sufficiently large for the curve to reach a plateau (like curve D) or to peak and then decrease (like curves E and F).

The treatment of array moderation can be easy or complex, depending on the placement of the materials of construction and their susceptibility to damage from hypothetical accident conditions. For all of these conditions and combinations of conditions, the applicant should carefully investigate the optimum degree of internal and interspersed moderation consistent with the chemical and physical form of the material and the packaging, and should demonstrate that subcriticality is maintained. The applicant should consider the numerous conditions for which the effects of moderation must be investigated, such as

1. moderation from packing materials that are inside the primary containment system,
2. moderation due to preferential flooding of different regions in the packages,
3. moderation from hydrogenous materials of construction (e.g., thermal insulation and neutron shielding),
and
4. interspersed moderation in the region between the packages in an array.

In determining the TI of an array of packages under normal conditions of transport, the applicant should consider only the possible ranges of hydrogenous (or other) moderators present in the package [items (1) and (3) above and, if applicable, item (2) above]; interspersed moderation between packages [item (4) above] from conditions such as mist, rain, snow, or flooding need not be considered (per the specifications of 10 CFR § 71.59). In determining the TI of an array of damaged packages, the applicant should carefully consider all four of the above conditions, including how each form of moderation can change under hypothetical accident conditions. As an example, consider a package with thermally degradable insulation. The applicant should evaluate the array with the insulation for the normal conditions of transport. For the hypothetical accident

conditions, the applicant should investigate moderation effects caused by changes in the insulation due to the thermal tests. The applicant should carefully evaluate the varying degrees of internal moderation in the containment.

6.3 RELATING ANALYSES TO TRANSPORT INDEX

The TI for criticality control should be determined by the applicant using the information from the array analyses on the number of packages that will remain subcritical (below the USL) under normal and hypothetical accident conditions. The USL should be determined using the criteria discussed in Sect. 5.4. Table 3 illustrates the tabular form that the applicant should use to summarize the results on the limiting number of packages shown to be subcritical in the analysis of the package arrays. The value N in the table can be defined so that

- N = maximum number of packages per shipment for a nonexclusive use shipment, where $5 \leq N \leq \infty$.
 $2N$ = maximum number of packages per shipment for an exclusive use shipment, where $0.5 \leq N \leq \infty$.

Table 3 Requirements of 10 CFR § 71.59

Case	No. of fissile packages that must be subcritical
Undamaged	$5N$ with nothing between packages
Damaged	$2N$ with optimum interspersed moderation

With the information provided in Table 3, the applicant can determine the TI for criticality control using the expression

$$TI = 50 \div N.$$

7 SUMMARY

This report provides recommendations on the information that should be included in the criticality safety section of an application for approval of a transportation package. The emphasis has been on the design information, analysis models, and computational results and discussion that should be in the application. However, the applicant should recognize that the recommendations may not be exhaustive and that additional information or analyses may be needed for selected applications.

Section 2 of the report discusses the design information that the applicant should include in the criticality safety section of the application. Specification of the contents (e.g., form, type, mass, composition) considered in the application should be provided, including any anticipated variations and uncertainties.

Section 3 of the report reviews the description and figures that should be included in the application to adequately explain the calculational models. In preparing these models, the applicant should limit the use of fixed neutron absorbers to 75% of the composition, unless adequate (see Sect. 3.1.3) consideration is made for testing the presence and uniformity of the absorber. Fixed, burnable poisons should not be considered in spent fuel packages. And, until the NRC provides direction on use of spent fuel isotopics, it is recommended that unburned (fresh) fuel isotopics be assumed in applications for spent fuel packages. Water moderation and reflection specifications based on the normal and accident conditions of 10 CFR Part 71 must be considered in the development of the analysis models.

Sections 4-5 of the report recommend the information that should be considered by the applicant in selecting and using an appropriate analysis method (code and nuclear data) for determination of the neutron multiplication factor. Codes that adequately model the kinematics of neutron transport, including angular scattering, are needed to provide the best estimate of k_{eff} . The codes and data used in the application should be validated against critical experiments appropriate for the package conditions and contents. This validation provides a basis for development of a USL that considers bias and uncertainties (determined from the validation), the statistical nature of the analysis method, and a margin of subcriticality. The minimum margin of subcriticality accepted by the NRC for transportation packages is $0.05 \Delta k$.

Section 6 of the report discusses the analyses that should be considered to demonstrate that the requirements of 10 CFR § 71.55 and 71.59 are met. This section provides practical information on how to proceed with the analyses, the single-package and array conditions that should be considered, and a process for determination of the TI for criticality control. Development and analysis of the array models should carefully consider the various conditions that could lead to an increased k_{eff} value. Optimum moderation of the packages according to the normal and accident conditions, package arrangement and spacing for optimum interaction between packages, and proper water reflection of the array should be considered.

8 REFERENCES

1. "Compatibility with the International Atomic Energy Agency (IAEA); Final Rule," Part II, 10 CFR Part 71 of *Federal Register* 60(188), 50248-50289 (September 28, 1995).
2. *Standard Format and Content of Part 71, Applications for Approval of Packaging for Radioactive Material*, Regulatory Guide 7.9 (Proposed Revision 2), U.S. Nuclear Regulatory Commission, Washington, DC (May 1986).
3. *SCALE: A Modular Code System for Performing Standardized Computer Analyses for Licensing Evaluation*, Vols. I-III, NUREG/CR-0200, Rev. 4 (ORNL/NUREG/CSD-2/R4) (April 1995).
4. A. H. Wells, D. R. Marnon, and R. A. Karam, "Criticality Effect of Neutron Channeling Between Boron Carbide Granules in Boral for a Spent Fuel Shipping Cask," *Trans. Am. Nucl. Soc.* 54, 205-206 (1987).
5. W. R. Burrus, "How Channeling Between Chunks Raises Neutron Transmission Through Boral," *Nucleonics* 16, 1, 91 (January 1958).
6. C. V. Parks, R. Q. Wright, and W. C. Jordan, "Validation of the 123-Group Cross-Section Library for Criticality Analyses of Water-Moderated Uranium Systems," NUREG/CR-6328 (ORNL/TM-12970), U.S. Nuclear Regulatory Commission, August 1995.
7. N. F. Landers and L. M. Petrie, "Uncertainties Associated with the Use of the KENO Monte Carlo Criticality Codes," p. 289 in *Proc. International Topical Meeting on Safety Margins in Criticality Safety*, San Francisco, California, November 26-30, 1989.
8. R. A. Forster, T. E. Booth, T. J. Urbatsch, K. A. Van Riper, and L. S. Waters, "Analyses and Visualization of MCNP Criticality Results," *Trans. Am. Nucl. Soc.* 1, Albuquerque, New Mexico, September 17-21, 1995.
9. *American National Standard for Nuclear Criticality Safety in Operations with Fissionable Materials Outside Reactors*, ANSI/ANS-8.1-1983 (Revision of ANSI N16.1-1975), American Nuclear Society, 1983.
10. J. J. Lichtenwalter and S. M. Bowman, *Criticality Benchmark Guide for Light-Water-Reactor Fuel in Transportation and Storage Packages*, NUREG/CR-6361 (ORNL/TM-13211), U.S. Nuclear Regulatory Commission, 1997.
11. C. V. Parks, W. C. Jordan, L. M. Petrie, and R. Q. Wright, "Use of Metal/Uranium Mixtures to Explore Data Uncertainties," *Trans. Am. Nucl. Soc.* 73, 217 (1995).
12. M. D. DeHart and S. M. Bowman, *Validation of the SCALE Broad Structure 44-Group ENDF/B-V Cross-Section Library for Use in Criticality Safety Analyses*, ORNL/TM-12460. Oak Ridge Natl. Lab., September 1994.

APPENDIX A

EXAMPLE OF CALCULATIONAL MODELS AND RESULTS

This appendix uses a simple example of a fictitious transport package to illustrate many of the recommendations provided in this report regarding the content of the criticality safety section of the application for a transport package. This example package and analysis have not been approved by the NRC, and there has been no assessment as to whether the package would meet all of the requirements for approval. The descriptions provided herein do not include all the information that would be necessary for an actual package evaluation; rather they provide an illustrative sampling of the type of information discussed in this report.

The following sections provide information as if it were imbedded as the criticality section of the application. However, since this is intended to be an illustrative example, only that information pertinent to developing the calculational models is included. The dimensional and material specifications provided are the minimum to support the calculations in this appendix and do not represent certified container loadings or configurations. Also, the descriptions, calculations, and justifications presented here may not be complete or acceptable to the NRC.

A.1 GENERAL DESCRIPTION (Example)

The transport package uses a 55-gal steel drum overpack [22.5-in. (57.15-cm) inside diam by 40.5-in. (102.87-cm) inside height]. The drum body and bottom are fabricated from a 16-gauge [0.064-in. (0.16-cm)] low carbon steel sheet. The drum lid (head) is fabricated from a 14-gauge [0.080-in. (0.20-cm)] low-carbon steel sheet. Two approximately equally spaced, rolling hoops are swaged into the drum body. The removable head is closed by means of a bolt-locking ring.

The inner container (containment vessel) is the containment boundary. The inner container is fabricated from a 0.25-in. (0.64-cm)-thick carbon steel plate. The inner container [12.0-in. (30.48-cm) inside diam by 28.0-in. (71.12-cm) inside height] has a welded bottom plate and welded cover plate.

The 55-gal drum is filled between the drum wall and inner container with insulating fiber board that provides thermal insulation and vibration and shock isolation, and centers the inner container within the drum. The insulating fiber board provides a thickness between the inner container and drum of 5.0 in. (12.7 cm) radially and 5.0 in. (12.7 cm) axially (top and bottom).

The package shall be used to transport unirradiated uranium dioxide (UO_2) pellets of 0.325-in. (0.83-cm) nominal outside diameter. The contents are not to exceed 116.16 kg of UO_2 pellets at an enrichment in the ^{235}U isotope of 4.01%.

A.2 PACKAGE DESCRIPTION

Sections A.2.1 and A.2.2 describe the package contents and packaging, specifically the dimensions and material components that influence k_{eff} .

Preceding page blank

A.2.1 CONTENTS

The package shall be used to transport right cylindrical UO_2 pellets of 10.40 g/cm^3 oxide density. The pellets have a 0.325-in. (0.83-cm) nominal outside diameter and height and a maximum enrichment of 4.01 wt % ^{235}U . The uranium isotopic distribution is given in Table A.1.

Table A.1 Uranium isotopic distribution

Isotope	wt %
^{234}U	0.02
^{235}U	4.01
^{236}U	0.02
^{238}U	95.95

A.2.2 PACKAGING

The packaging consists of the inner container assembly (DWG-X12G64) comprising 316 stainless steel tubes that accommodate the fuel pellets, the inner container or containment vessel (DWG-D184K), plywood board, insulating fiber board, and the 55-gal drum (DWG-4201V).

A.2.2.1 Inner Container Assembly

Pellets and end plugs are contained in 27.75-in. (70.49-cm)-long stainless steel tubes of 0.350-in. (0.89-cm) inside and 0.366-in. (0.93-cm) outside diam. Each of the 316 tubes is filled with 80 pellets. The composition and atom densities of the 304-stainless steel tubes and other package materials are given in Table A.2. The tube ends are sealed with 0.350-in. (0.89-cm)-diam, 1.0-in. (2.54-cm)-long top and 0.75-in. (1.91-cm)-long bottom stainless steel plugs that are welded in place. The tube bottoms are welded into 0.75-in. (1.91-cm)-deep recesses on a 0.528-in. (1.34-cm)-square pitch of a 1.0-in. (2.54-cm)-thick, 12.0-in. (30.48-cm)-diam stainless steel bottom plate. The tube tops extend through 0.375-in. (0.95-cm)-diam holes to the top of a 1.0-in. (2.54-cm)-thick, 12.0-in. (30.48-cm)-diam stainless steel top plate. Rubber o-rings between the tubes and plate holes provide a tight tube-to-top-plate fit. The top plate is connected by four 26.0-in. (66.04-cm)-long, 0.667-in. (1.69-cm)-diam stainless steel support rods to the bottom plate. The structural evaluation has shown that the inner container assembly remains intact, and the pellets remain inside the tubes, under normal conditions of transport and hypothetical accident conditions.

A.2.2.2 Inner Container

The inner container is fabricated from 0.25-in. (0.635-cm)-thick carbon steel plate. The inner container [12.0-in. (30.48-cm)-inside diameter by 28.0-in. (71.12-cm) inside height] has a welded 0.25-in. (0.635-cm)-thick bottom plate with a welded 0.25-in. (0.635-cm)-thick cover plate.

Table A.2 Material specifications

Material	Density (g/cm ³)	Constituent	Atomic density (atoms/b-cm)
304 stainless steel	7.92	Fe	5.935e-2
		Cr	1.7428e-2
		Ni	7.7188e-3
		Mn	1.7363e-3
Insulating fiber board	0.24	H	8.914e-3
		C	5.348e-3
		O	4.457e-3
Plywood	0.45	H	1.671e-2
		C	1.003e-2
		O	8.357e-3
Water	0.9982	H	6.675e-2
		O	3.338e-2
Carbon steel	7.821	C	3.9250e-3
		Fe	8.3498e-2
Rubber	1.321	C	3.8414e-2
		H	5.1298e-2
		Ca	2.2627e-3
		S	4.2182e-4
		O	1.0988e-2
		Si	8.4972e-5

A.2.2.3 Drum

The transport package uses a 55-gal steel drum overpack [22.5-in. (57.15-cm) inside diameter by 40.5-in. (102.87-cm) inside height]. The drum body and bottom are fabricated from a 16-gauge [0.064-in. (0.163-cm)] low-carbon steel sheet. The drum lid (head) is fabricated from a 14-gauge [0.080-in. (0.20-cm)] low-carbon steel sheet. Two approximately equally spaced, rolling hoops are swaged into the drum body. The removable head is closed by means of a bolt-locking ring.

The 55-gal drum is filled between the drum wall and inner container with insulating fiber board that provides thermal insulation and vibration and shock isolation, and centers the inner container within the drum. The drum is loaded top-to-bottom with (1) a 5.0-in. (12.7-cm)-thick, 22.5-in. (57.15-cm)-diam insulating fiber board block, (2) a 1.0-in. (2.54-cm)-thick, 22.5-in. (57.15-cm)-diam plywood load bearing plate, (3) the inner container assembly, centered, and surrounded by a 22.5-in. (57.15-cm)-outer-diam, 12.5-in. (31.75-cm)-inner-diam, 13.75-in. (34.93-cm)-thick insulating fiber board ring, followed by a 1.0-in. (2.54-cm)-thick, 22.5-in. (57.15-cm)-outer-diam, 12.5-in. (31.75-cm)-inner-diam plywood support ring, followed by a 22.5-in. (57.15-cm)-outer-diam, 12.5-in. (31.75-cm)-inner-diam, 13.75-in. (34.93-cm)-thick insulating fiber board ring, (4) a 1.0-in. (2.54-cm)-thick, 22.5-in. (57.15-cm)-diam plywood load-bearing plate, and (5) a 5.0-in. (12.7-cm)-thick, 22.5-in. (57.15-cm)-diam insulating fiber board block.

A.3 CRITICALITY SAFETY ANALYSIS MODELS

Section A.3.1.1 provides dimensioned sketches of a modeled package. The material specifications for regions of the sketches in Sect. A.3.1.1 are given in Sect. A.3.1.2. Section A.3.1 identifies differences between the models and actual package configurations. Section A.3.2 describes the contents models representing each of the different loading configurations. Models depicting the configuration of packaging and contents of a single package under normal and accident conditions are discussed in Sect. A.3.3. Section A.3.4 contains a discussion on the package array models.

A.3.1 GENERAL MODEL

A.3.1.1 Dimensions

Figure A.1 represents the vertical elevations of the package seen along the vertical centerline of the package. A cross section of the package along A-A of Fig. A.1 is displayed in Fig. A.2. The figures' dimensions were used in the calculations.

Note: Although not included in this example, a real application should not *a priori* use nominal dimensions, but instead should address dimensional tolerances of the package that tend to add conservatism to the models.

A.3.1.2 Materials

Figures A.1 and A.2 show cross sections of the single-package calculational model. Table A.3 identifies the regions, materials, material densities, and masses as used in the calculations, and the actual masses.

Note: Although not included in this example, a real application should not *a priori* use nominal material specifications, but instead should address maximum and minimum fissile, neutron-absorbing moderating, and structural materials parameter values that produce conservative k_{eff} results within the allowable tolerances.

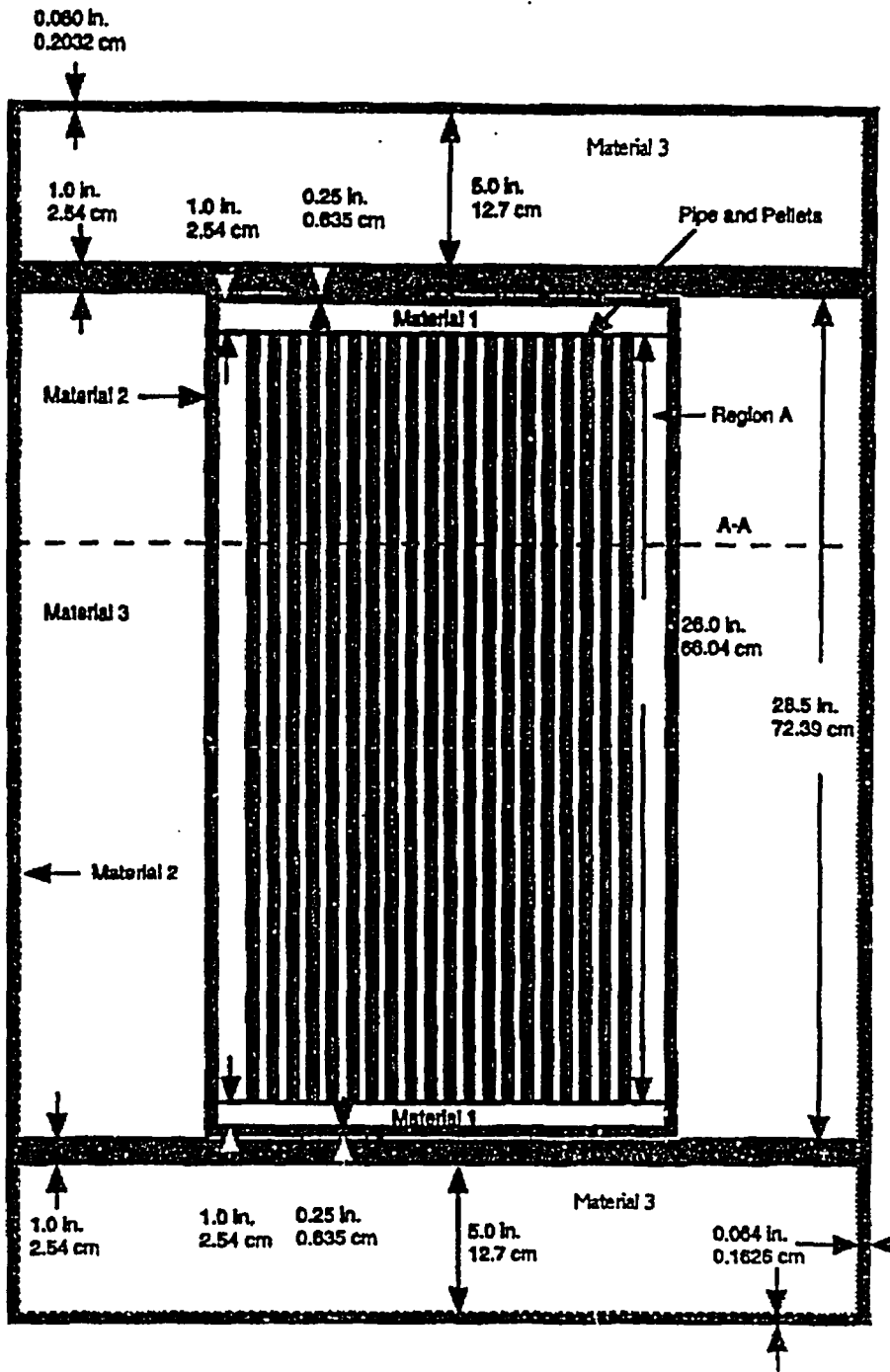


Figure A.1 Axial cross section of the single-package model

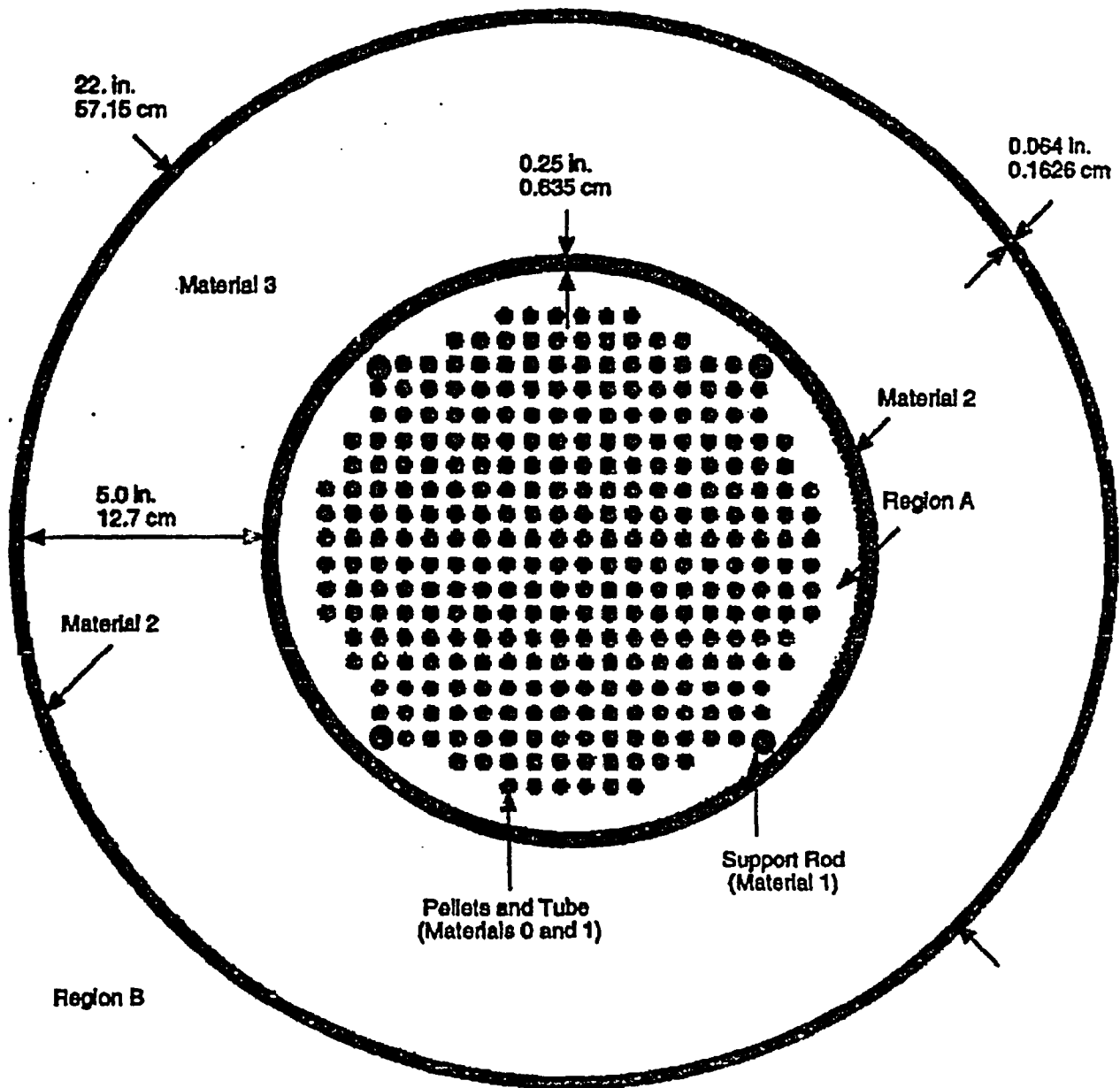


Figure A.2 Radial cross section of single-package model

Table A.3 Material specifications for Figs. A.1 and A.2

Material No.	Material	Density (g/cm ³)	Model mass (kg)	Actual mass (kg)
0	UO ₂	10.40	116.19	116.16
1	SS-304	7.92 ^a	41.87	42.12
2	Carbon steel	7.8212 ^a	73.37	77.23
3	Insulating fiber board	0.24	46.42	44.29
4	Plywood	0.45	5.860	8.796

^aSCALE Standard Composition Library values.

A.3.1.3 Models—Actual Package Differences

The single-package calculational model of the 55-gal drum differs from the actual drum in the treatment of the drum wall. In the model, the drum wall is a straight wall cylinder without the rolling hoops. The drum model does not have the top and bottom inset into the drum wall, bolts, locking rings, etc.

The rubber o-ring fittings around the tubes in the top plate of the inner container assembly were treated as stainless steel, the surrounding material. The change constitutes such a small change in stainless steel mass in the positive axial direction relative to the fuel region that the impact on k_{eff} would be negligible. To simplify the modeling, the center plywood support ring was modeled as insulating fiber board, the surrounding material. The exchange of materials would have a negligible effect on k_{eff} because the constituents of the two materials are identical and the thickness of the region is small relative to the radial surface of the containment vessel (i.e., -4% of the surface available for radial neutron leakage).

A.3.2 CONTENTS MODEL

Figure A.2 shows the package contents (pellets in tubes) configured for both the single-package and package-array calculations. Each tube is physically restricted to a maximum loading of 80 pellets. Partial-loading (variable-mass) configurations are allowed, as are variations in pellet enrichment (up to 4.01 wt % ²³⁵U). However, partial loadings must be from the inner tubes outward with only the last loaded tube containing less than 80 pellets (see Chapter 1). Because of this restriction and the fixed tube spacing, partial loadings do not require further analysis because they are bounded by the more reactive configuration of full loading. Chapter 2 of the application for approval has shown that the tube spacing remains at 1.34 cm (0.528 in.), and that the pellets remain inside the tubes, under normal conditions of transport and hypothetical accident conditions.

A.3.3 SINGLE PACKAGES

To meet the general requirements for fissile material packages, 10 CFR § 71.55, a package must be designed and its contents so limited that it would be subcritical under the most reactive configuration of the material, optimum moderation, and close reflection of the containment system by water on all sides or surrounding materials of the packaging. Models of both reflective conditions have been considered. The package was subjected to the tests specified in 10 CFR § 71.71. Normal Conditions of Transport, and, as reported in

Appendix A

Chapters 2 and 3, the geometric form of the package was not substantially altered, no water leakage into the containment occurred, and no substantial reduction in the effectiveness of the packaging was observed. In short, the damage incurred will not affect the technical evaluation, and the package contents under normal conditions of transport will be less reactive than the contents under the aforementioned general requirements, requiring no further analysis.

To address the requirement of 10 CFR § 71.55(e), a single package was analyzed with optimum internal moderation and a 30-cm water reflector on all sides. The damaged package experienced a 4.7% reduction in diameter due to impact testing (see Chapter 2, Structural Evaluation). The packaging diameter reduction is to be analyzed as a reduction in insulating fiber board and plywood thicknesses while conserving the carbon steel drum, insulating fiber board, and plywood masses. Limited material loss occurred as a result of fire testing (see Chapter 3, Thermal Evaluation). The outer 0.8 in. (2.03 cm) of insulating fiber board (axially and radially) and plywood (radially) exhibited charring and off-gassing during the fire test. The regions were modeled as residual carbon and water (immersion test). The water from the immersion test optimally moderates the inner containment. The minimal damage resulting from crush and puncture tests (see Chapter 2, Structural Evaluation) will not influence the reactivity of the packages.

A.3.4 PACKAGE ARRAYS

Cylindrical transport packages such as this example package may be shipped in a tightly packed triangular-pitch configuration (or may be shifted to that configuration because of hypothetical accident conditions). This arrangement may provide a more reactive configuration than a square-pitch arrangement because the triangular pitch provides absolute minimum center-to-center spacing of the fissile contents, the maximum density of fissile units, and thus the greatest potential for increased neutron interaction between fissile contents. To avoid the complex modeling required to analyze triangular-pitch arrays with the computational method used in this application, a square-pitch array model with a modified single-package model was developed to emulate the effects of a triangular-pitch package array. The single-package modification involved a reduction of the drum diameter by 7% to produce an array density in a square-pitch lattice equal to the array density of a triangular-pitch lattice of packages with the full-diameter package. If the mass of steel of the drum and the mass of the insulating fiber board are conserved, the neutron reaction rates within the array are essentially identical. To conserve the mass of steel in this example, the drum wall density was increased; and to conserve the mass of the insulating fiber board in this example, the insulating fiber board density was increased. The diameter reduction was applied only to regions of the "array package model," not the "contents model."

The justification for the 7% diameter reduction is seen in the following derivation. Consider three full-diameter packages in contact on triangular pitch and four reduced-diameter packages in contact on square pitch. The equivalent array density of each configuration is

$$\rho_t = \frac{3(m/6)}{\left(\frac{1}{2}\right)(d_t)\left(\frac{\sqrt{3}}{2}\right) \times (d_t)(h)} = \frac{m}{(d_t^2)(\sqrt{3}/2)(h)}$$

and

$$\rho_s = \frac{4(m/4)}{(d_s^2)(h)} = \frac{m}{(d_s^2)(h)}$$

where

the subscripts r and s indicate triangular and square pitch, respectively,
 d is the package diameter,
 h is the package height (same for both packages), and
 m is the fissile material mass (same for both packages).

If ρ_r is set equal to ρ_s and d_r is calculated in terms of d_s , the diameter of a square pitch is 0.9306 that of the triangular pitch, to produce the equivalent array density. If a constant mass of materials is maintained outside the fissile unit (i.e., the thermal insulation and steel outer drum), the neutron reaction rates between fissile units remain constant. Because the drum is smaller in diameter, the mass of thermal insulation is conserved by increasing the density, and the mass of steel in the outer drum is conserved by increasing the steel density.

Two array model types are included in the evaluation. The first model type consists of an infinite array of close-packed, triangular-pitch, undamaged packages consistent with the normal conditions of transport. From 10 CFR § 71.59, standards for arrays of fissile material packages, undamaged package arrays are evaluated with void between the packages. The second model type consists of various size finite arrays of close-packed triangular-pitch, damaged packages. As required by 10 CFR § 71.59, the damaged packages are evaluated as if each package was subjected to the tests specified in 10 CFR § 71.73, Hypothetical Accident Conditions, with optimum interspersed hydrogenous moderation. Further, the finite array of packages must be reflected by 30 cm of water on all sides.

Various finite array sizes had to be investigated in order to ascertain the number of subcritical packages under hypothetical accident conditions. The condition of each damaged package in the array is that described in Sect. A.3.3 for the single package.

A.4 METHOD OF ANALYSIS

Sections A.4.1 and A.4.2 describe the sequences and modules of the SCALE-4.3 system used in the analysis of these computational models. Section A.4.3 identifies all major code input parameters. Section A.4.4 discusses the adequacy of the calculations.

All calculations were performed on CA02 and CA29, IBM RS/6000 workstations in the Computational Physics and Engineering Division at ORNL with SCALE version 4.3 (1/6/97 production date) and the 44-group ENDF/B-V cross-section library.

A.4.1 COMPUTER CODE SYSTEM

SCALE is a computational system consisting of a set of well-established codes and data libraries suitable for analyses of nuclear fuel facility and package designs in the areas of criticality safety, radiation shielding, source-term characterization, and heat transfer. The codes are compiled in a modular fashion and are called by control modules that provide automated sequences for standard system analyses in each area. The CSAS control module contains automated sequences that perform problem-dependent cross-section processing and three-dimensional (3-D) Monte Carlo calculations of neutron multiplication.

KENO V.a, a 3-D multigroup Monte Carlo criticality code, determines the effective multiplication factor (k_{eff}) from the problem-dependent cross-section data and the user-specified geometry data. Other calculated

Appendix A

KENO V.a quantities include average neutron lifetime and generation time, energy-dependent leakages, energy- and region-dependent absorptions, fissions, fluxes, and fission densities.

A.4.2 CROSS SECTIONS AND CROSS-SECTION PROCESSING

All neutronic control sequences use the SCALE Material Information Processor to calculate material number densities, prepare geometry data for resonance self-shielding and optional flux-weighting cell calculations, and create data input files for the cross-section processing codes. The BONAMI and NITAWL-II codes are then used to perform problem-specific (resonance- and temperature-corrected) cross-section processing. BONAMI applies the Bondarenko method of resonance self-shielding for nuclides that have Bondarenko data included in the cross-section library. NITAWL-II uses the Nordheim integral treatment to perform resonance self-shielding corrections for nuclides that have resonance parameters included with their cross-section data.

The analyses discussed in this evaluation were performed using the broad-structure, 44-group neutron cross-section library. The 44-group library was chosen because the evaluated package contents have many similarities (e.g., form, enrichment) to light-water-reactor (LWR) fuel, and the 44-group library has demonstrated markedly improved performance in LWR-type fuel analyses over the ENDF/B-IV 27-group library. The reason: the 44-group neutron cross-section library was collapsed from the 238-group AMPX master-format neutron cross-section library contains data for all the nuclides available in ENDF/B-V, and the 44-group library was collapsed using a fuel cell spectrum based on a 17×17 Westinghouse pressurized-water-reactor (PWR) fuel assembly.

Additionally, the broad-group structure was designed to accommodate two windows in the oxygen cross-section spectrum, a window in the iron cross-section spectrum, the Maxwellian peak in the thermal range, and the 0.3-eV resonance in ^{239}Pu (which, because of low energy and lack of resonance data, cannot be modeled by the Nordheim integral treatment in NITAWL-II).

A.4.3 CODE INPUT

All problems were started with a flat initial neutron distribution over the system, in fissile material only. All problems were run for 305 generations of 400 neutrons per generation, skipping the first five generations, for a total of 120,000 histories. Mirror image reflection was applied to the orthogonal-plane boundaries of the single-package model to simulate infinite array-package models. A 12-in. (30.48-cm) water differential albedo with four incident angles was applied to the outer boundary of the single-package models and finite-array models to simulate tight, full-density water reflection. Biasing options were not applied.

Figures A.3(a) and A.3(b) are sample input files. The files correspond to cases f-2_4 and f-2_4a, a $4 \times 4 \times 1$ array of optimally moderated, damaged packages in square, with diameter correction factor of Sect. A.3.4, and triangular-pitch arrays.

A.4.4 CONVERGENCE OF CALCULATIONS

UO_2 mass data for each problem were checked against KENO V.a output. The input geometries were checked by examining the 2-D plots generated by KENO V.a. Problem convergence was determined by examining plots of k_{eff} by generation run and skipped, as well as the final k_{eff} edit tables. No trends were observed either in k_{eff} by generation run over the last half of total generations or, correspondingly, in k_{eff} by generation skipped over the first half of total generations. No sudden changes of greater than one standard deviation in k_{eff} by


```

=csas25
KENO-V.a, 4x4x1 array, optimally moderated damaged
'packages, square pitch, 4.7% and 7% diameter reduction
4% latt
uo2 1 0.9489 293 92235 4.01 92234 0.02 92236 0.02 92238
95.95 end
h2o 2 1.0 end
ss304 3 1.0 end
c 4 0 3.9250e-3 end
fe 4 0 8.3498e-2 end
h 5 0 1.293e-2 end
c 5 0 7.127e-3 end
o 5 0 6.464e-3 end
h 6 0 2.128e-2 end
c 6 0 1.277e-2 end
o 6 0 1.064e-2 end
c 7 0 4.550e-3 end
fe 7 0 9.879e-2 end
h 8 0 1.135e-2 end
c 8 0 6.809e-3 end
o 8 0 5.674e-3 end
c 9 0 7.757e-3 end
h2o 9 0.001 end
c 10 0 6.809e-3 end
h2o 10 0.001 end
h2o 12 1.0 end
end comp
squarepitch 1.34 0.8255 1 2 0.9296 3 0.889 12 end
read parm run=yes plt=no gen=305 npg=400 nsk=5 end parm
read geom
unit 1
cylinder 1 1 0.4128 2p33.02
cylinder 2 1 0.4445 2p33.02
cylinder 3 1 0.4648 2p33.02
cuboid 2 1 4p0.670 2p33.02
unit 2
cylinder 3 1 0.4648 2p33.02
cuboid 2 1 4p0.670 2p33.02
unit 3
array 2 -4.02 0 0 0 0
unit 4
array 3 -6.7 0 -33.02
unit 5
array 4 0 -4.02 -33.02
unit 6
array 5 0 -6.7 -33.02
unit 7
array 1 -10.72 -10.72 -33.02
cylinder 2 1 15.24 2p33.02
hole 6 10.72 0 0
hole 6 -12.06 0 0
hole 5 12.06 0 0
hole 5 -13.41 0 0
hole 4 0 10.72 0
hole 4 0 -12.06 0
hole 3 0 12.06 0
hole 3 0 -13.41 0
reflector 3 1 0 2r2.54 1
reflector 4 1 3r0.635 1
reflector 5 1 7.4165 2r0 1
reflector 6 1 2.032 2r0 1
reflector 9 1 0 2r2.54 1
reflector 8 1 0 2r10.668 1
reflector 10 1 0 2r2.032 1
reflector 7 1 0.1626 0.2032 0.1626 1
cuboid 0 1 4p25.4862 51.6383 -51.5977
global unit 8
array 6 3*0.0
end geom
read array
ara=1 nux=16 nuy=16 nuz=1 fill 2 14r1 2 224r1 2 14r1 2
end fill
ara=2 nux=6 nuy=1 nuz=1 fill 6r1 end fill
ara=3 nux=10 nuy=1 nuz=1 fill 10r1 end fill
ara=4 nux=1 nuy=6 nuz=1 fill 6r1 end fill
ara=5 nux=1 nuy=10 nuz=1 fill 10r1 end fill
ara=6 nux=4 nuy=4 nuz=1 fill 16r7 end fill
end array
rc.d bnds all=h2o end bnds
end data
end

```

Figure A.3a Sample input file f-2_4

```

=csas26
KENO-VI, 4x4x1 array, optimally moderated damaged
'packages, triangular pitch, 4.7% diam. reduction
4% latt
uo2 1 0.9489 293 92235 4.01 92234 0.02 92236 0.02 92238
95.95 end
h2o 2 1.0 end
ss304 3 1.0 end
c 4 0 3.9250e-3 end
fe 4 0 8.3498e-2 end
h 5 0 1.029e-2 end
c 5 0 6.173e-3 end
o 5 0 5.144e-3 end
h 6 0 1.841e-2 end
c 6 0 1.105e-2 end
o 6 0 9.207e-3 end
c 7 0 4.167e-3 end
fe 7 0 8.864e-2 end
h 8 0 9.821e-3 end
c 8 0 5.892e-3 end
o 8 0 4.910e-3 end
c 9 0 6.173e-3 end
h2o 9 0.001 end
c 10 0 5.892e-3 end
h2o 10 0.001 end
h2o 11 1.0 end
end comp
squarepitch 1.34 0.8255 1 2 0.9296 3 0.889 11 end
read parm run=yes plt=no gen=305 npg=400 nsk=5 end parm
read geom
unit 1
cylinder 10 0.4128 2p33.02
cylinder 20 0.4445 2p33.02
cylinder 30 0.4648 2p33.02
cuboid 40 4p0.670 2p33.02
media 1 1 10
media 2 1 20 -10
media 3 1 30 -20 -10
media 2 1 40 -30 -20 -10
boundary 40
unit 2
cylinder 10 0.667 2p33.02
cuboid 20 4p0.670 2p33.02
media 3 1 10
media 2 1 20 -10
boundary 20
unit 3
cuboid 10 4p0.670 2p33.02
media 2 1 10
boundary 10
unit 4
cylinder 10 15.24 2p33.02
array 1 10 place 12 12 1 -0.67 -0.67 0
cylinder 20 15.24 2p35.56
cylinder 30 15.875 2p36.195
cylinder 40 25.1922 2p36.195
cylinder 50 25.1922 2p36.195
cylinder 60 27.2242 2p38.435
cylinder 70 27.2242 2p39.403
cylinder 80 27.2242 2p41.435
cylinder 90 27.3868 51.6383 -51.5976
hexprism 100 27.3869 51.6383 -51.5977
media 3 1 20 -10
media 4 1 30 -20
media 5 1 40 -30
media 9 1 50 -40
media 6 1 60 -50
media 8 1 70 -60
media 10 1 80 -70
media 7 1 90 -80
media 0 1 100 -90
boundary 100
unit 5
hexprism 10 27.3869 51.6383 -51.5977
media 2 1 10
boundary 10
global unit 6
cylinder 10 189.74 51.6383 -51.5977
array 2 10 place 5 5 1 -27.3869 -27.3869 0
cylinder 20 225 2p82.
media 2 1 20 -10
boundary 20
end geom
read array
ara=1 nux=24 nuy=24 nuz=1 fill 14r3 9r3 6r1 2r3 7r3 10r3
7r3 4r3 2 14r1 2 4r3 4r3 15r1 4r3 1q24 1r3 18r1 5r3 1q24
2r3 20r1 2r3 5q24 3r3 18r1 3r3 1q24 1r3 16r1 4r3 1q24 4r3
2 14r1 2 4r3 7r3 10r1 7r3 9r3 6r1 9r3 4r3 end fill
ara=2 typ=t-1 nux=10 nuy=10 nuz=1 fill 10r5 4r5 1r5
3r5 4r5 5r5 4r5 3r5 2r5 4r5 4r5 30r5 end fill
end array
end data
end

```

Figure A.3b Sample input file f-2_4a

Appendix A

generation run or skipped, resulting from an abnormal k_{eff} generation, were found. Frequency distribution bar graphs appear to approximate normal distribution with single peaks and no significant outlying values.

A.5 VALIDATION OF CALCULATION METHOD

For the purpose of this example, a negative value of 0.01 will be assumed for the bias and uncertainty ($\Delta k_u - \beta$) associated with using SCALE-4.3 and the 44-group cross-section library. This is consistent with published information on validation of this computational method using low-enriched lattice criticals.^{10,12} Note: The applicant should demonstrate the justification for the bias and uncertainty in the application for approval.

Using the general equation for the USL from Sect. 5.4 and the requirements of 10 CFR 71, it can be found that for the calculations to be considered subcritical, the following condition should be satisfied:

$$k_{eff} + 2\sigma \leq 0.95 - \Delta k_u + \bar{\beta} ,$$
$$k_{eff} + 2\sigma \leq 0.94 .$$

A.6 CRITICALITY CALCULATIONS AND RESULTS

This evaluation demonstrates the subcriticality of a single package (Sect. A.6.1) and an array of packages (Sect. A.6.2) during normal conditions of transport and hypothetical accident conditions. The determined TI for criticality control of a damaged and undamaged shipment is given in Sect. A.6.3.

A.6.1 SINGLE PACKAGE

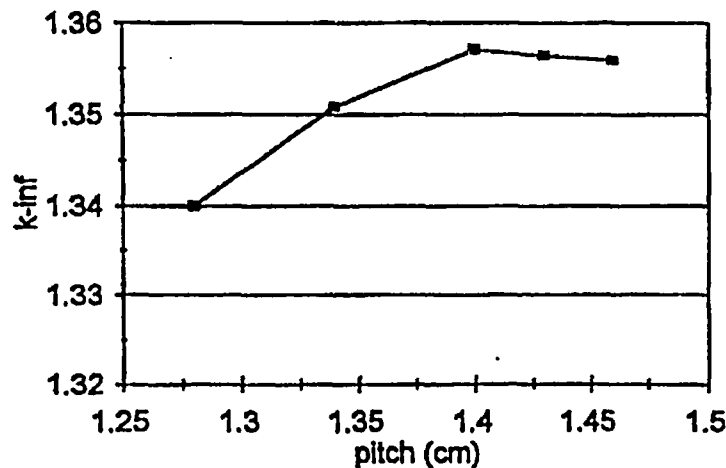
Calculations show that a single package remains subcritical under general requirements for fissile material packages under normal conditions of transport and under hypothetical accident conditions. To meet the general requirements for fissile material packages, 10 CFR § 71.55, a package must be designed and its contents so limited that it would be subcritical under the most reactive configuration of the material, optimum moderation, and close reflection of the containment system by water on all sides or surrounding materials of the packaging. Case s-0 of Table A.4 represents the optimally moderated inner containment reflected on all sides by 30 cm of water. For case s-1, the container reflection is provided by the surrounding materials of the packaging and 30 cm of water. In both cases, the gap region between the tubes and pellets are completely flooded with full-density water, as is the void region in the inner container (Region A of Fig. A.2). Full-density water is optimum in both regions because the fissile content of the package is slightly undermoderated at a tube pitch of 1.34 cm (see Fig. A.4). The highest single-package k_{eff} of 0.8942 ± 0.0019 is considered subcritical (i.e., $0.8942 + 2 \cdot 0.0019 = 0.8980 < 0.94$).

Case s-2 in Table A.4 is the result for a single damaged package with internal water flooding and 30 cm of water reflection on all sides. As with the undamaged cases, the reported k_{eff} is less than the established USL of 0.94. The results for a reflected, damaged containment system would have been identical to the undamaged case (case s-0) because the configurations of the containment system or contents did not change under hypothetical accident conditions.

All calculations (damaged and undamaged) were performed at the maximum allowable ²³⁵U enrichment (4.6 wt %) to ensure maximum reactivity and eliminate the need for calculations at lower possible enrichments.

Table A.4 Single-package calculations

Case	Description	$k_{eff} \pm \sigma$
s-0	Optimally moderated, reflected undamaged containment	0.8942 ± 0.0019
s-1	Optimally moderated, reflected undamaged package	0.8798 ± 0.0019
s-2	Optimally moderated, reflected damaged package	0.8820 ± 0.0018

Figure A.4 k_{inf} vs pitch for 4.01 wt % ^{235}U UO_2 pellets

A.6.2 PACKAGE ARRAYS

The calculational results of Table A.5 show that an infinite array of packages is adequately subcritical under normal conditions of transport. Case i-1, an infinite, triangular-pitch array of dry packages under normal conditions, calculates at a k_{eff} of 0.5343 ± 0.0012 . An infinite array of packages under hypothetical accident conditions, however, is not subcritical. Case i-2_7 represents an infinite array of close-packed, triangular-pitch (diameter reduction factor), flooded packages with optimum moderated contents, a 4.7% reduction in diameter, effects due to charring and off-gassing, and optimum interspersed moderation. The k_{eff} for case i-2_7 is 0.9755 ± 0.0021 , which exceeds the subcritical limit (i.e., $0.9755 + 2 \cdot 0.0021 = 0.9797 > 0.94$). Since the infinite array under hypothetical accident conditions calculates above the USL, finite array calculations are necessary.

Cases i-3_1 through i-3_3 are variants of i-2_7 that investigate flooding of the insulating fiber board charred region. The optimally moderated package array i-3_2 has full-density water inside the package containment, has $0.001 \text{ g H}_2\text{O/cm}^3$ in the charred region of the packaging, and has void between packages.

Table A.5 Results for triangular-pitch array calculations

Case	Interspersed H ₂ O density (g/cm ³)	Description	$k_{eff} \pm \sigma$
i-1	0	Infinite array, normal conditions of transport	0.5343 ± 0.0012
f-1	-	1×1×1 array, hypothetical accident conditions	0.8820 ± 0.0018
i-2_1	0.9982	Infinite, hypothetical accident conditions	0.9238 ± 0.0021
i-2_2	0.95	Infinite, hypothetical accident conditions	0.9237 ± 0.0021
i-2_3	0.5	Infinite, hypothetical accident conditions	0.9297 ± 0.0023
i-2_4	0.1	Infinite, hypothetical accident conditions	0.9618 ± 0.0025
i-2_5	0.01	Infinite, hypothetical accident conditions	0.9716 ± 0.0024
i-2_6	0.001	Infinite, hypothetical accident conditions	0.9718 ± 0.0024
i-2_7	0 ^a	Infinite, hypothetical accident conditions	0.9755 ± 0.0021
i-3_1	0	Infinite, hypothetical accident conditions, 0 g H ₂ O/cm ³ charred region	0.9755 ± 0.0021
i-3_2	0	Infinite, hypothetical accident conditions, 0.01 ^b H ₂ O/cm ³ charred region	0.9772 ± 0.0027
i-3_3	0	Infinite, hypothetical accident conditions, 0.01 g H ₂ O/cm ³ charred region	0.9759 ± 0.0022
f-2_1	0	2×2×1 array, hypothetical accident conditions	0.9103 ± 0.0018
f-2_2	0	2×2×2 array, hypothetical accident conditions	0.9158 ± 0.0018
f-2_3	0	3×3×1 array, hypothetical accident conditions	0.9270 ± 0.0017
f-2_4	0	4×4×1 array, hypothetical accident conditions	0.9369 ± 0.0019
f-2_4a	0	4×4×1 array, hypothetical accident conditions	0.9335 ± 0.0028 ^c
f-2_5	0	3×3×2 array, hypothetical accident conditions	0.9306 ± 0.0017
f-2_6	0	5×5×1 array, hypothetical accident conditions	0.9284 ± 0.0019
f-2_7	0	3×3×3 array, hypothetical accident conditions	0.9405 ± 0.0023
f-2_8	0	4×4×2 array, hypothetical accident conditions	0.9359 ± 0.0017

^aDetermined to be near optimum interstitial moderation via CSAS4 search.

^bDetermined to be new optimum moderation via CSAS4 search

^cKENO-VI calculation.

Cases f-2_1 through f-2_8 are variants of case i-3_2 and represent finite arrays of close-packed, triangular-pitch packages (diameter reduction factor) that have optimally moderated contents, a reduced diameter by 4.7%, charred insulating fiber board, varying interstitial moderation, and 30 cm of full-density water reflection tightly fit on the array boundary. The finite array of $4 \times 4 \times 2$ (case f-2_8) packages is considered just subcritical because $0.9359 + 2 \cdot 0.0017 = 0.9393$ falls below the USL of 0.94.

Case f-2_4a is equivalent to case f-2_4a except that f-2_4a was modeled with KENO-VI, which allows explicit modeling of triangular-pitch arrays and does not require the use of the drum diameter reduction factor of Sect. A.3.4. The calculational results of f-2_4 and f-2_4a are statistically the same, attesting to the correctness of the diameter reduction factor.

A.6.3 TRANSPORTATION INDEX

The TI for criticality control is determined by the number of packages that remain below the USL. For normal conditions of transport, an infinite array of packages is subcritical. However, under hypothetical accident conditions, only up to 32 damaged packages would remain subcritical. Thus a maximum of 16 packages may be shipped for a nonexclusive shipment, and the $TI = 3$.

Note: The example presented in this appendix is for illustrative purposes only. The fictitious transport package used in this example has not been approved by the NRC, and no assessment has been made as to whether the package would meet the requirements for NRC approval. Also, the descriptions, calculations, and justifications presented in this example have not been fully reviewed by the NRC, and may not be complete or acceptable to the NRC.

THE MAGAZINE OF

TITANIUM ••• BORAL

Magnesium

Published Quarterly By BROOKS & PERKINS, INC.

August 1956



MAGNESIUM HAS
BEEN CHOSEN!

B & P becomes the first industry producer of BORAL

Brooks & Perkins has just become the first commercial supplier of Boral. This is a new material. It is used as a neutron shield in atomic energy installations and atomic power plants.

Boral is said to offer as much neutron shielding protection as 26 inches of concrete where the neutrons are of thermal energies. It does not shield against the passing of gamma rays.

The Atomic Energy Commission developed Boral at their Oak Ridge Plant, where it has been produced by the Government in limited amounts only. The product consists of a core of boron carbide uniformly dispersed in aluminum, clad on both sides with commercially pure aluminum. Boral can be produced with the core material having various concentrations of boron carbide.

Now that atomic power plants are operating in submarines and in an experimental airplane, and several industrial power plants are in the development stage, it has

become advisable to have a commercial supplier of Boral. B&P is highly qualified, primarily because of its successful pioneering of methods for working some of the newer metals, including zirconium; also the fact that it operates a rolling mill at nearby Livonia. Here B&P has just installed a new 3000 cycle ultra high frequency induction furnace, now used for the production of the Boral core material.

The grade of Boral offered by B&P has a 35% concentration of boron carbide. The Boral plate is rolled $\frac{1}{8}$ " and $\frac{1}{4}$ " thick. Standard sizes offered are 30" x 96", 30" x 48", 15" x 96", and 15" x 48". The approximate weight per square foot of $\frac{1}{4}$ " thick 35% Boral plate is 3.4 pounds.

Boral and zirconium are, in a sense, companion products. Both are used in atomic applications. B&P has been deep-drawing zirconium for the past two years. Unlike Boral, zirconium is transparent to the passage of neutrons while acting as the container of the atomic fuel.



Microphoto of cross section of $\frac{1}{4}$ " thick Boral plate, 10 X magnification. Shows crystalline structure of boron carbide in center, with aluminum cladding on top and bottom.

Rolling mill superintendent J. G. Merritt is looking at a formed Boral cylinder. The three-inch-thick rolling slab, ready for break-down, is a cast Boral core surrounded by pure aluminum cladding.



J.M.C.

U.S. DEPARTMENT OF COMMERCE
Office of Technical Services

distributes this and thousands of similar reports in the interest of science, industry and the public—for which research and new products mean better health, better living, and a stronger economy.



A GOVERNMENT RESEARCH REPORT

HOW TO GET OTHER REPORTS

The Office of Technical Services is the Nation's clearinghouse for reports of research supported by the Army, Navy, Air Force, Atomic Energy Commission, and other Government agencies.

Abstracts of new reports available are published semi-monthly in U.S. GOVERNMENT RESEARCH REPORTS (\$15 a year domestic).

Selected Reports of particular interest to small business are described monthly in TECHNICAL REPORTS NEWSLETTER (\$1 a year domestic).

Translations of foreign technical material are also available from the Office of Technical Services and other sources. These are listed or abstracted semi-monthly in TECHNICAL TRANSLATIONS (\$12 a year domestic).

The above periodicals may be ordered from Superintendent of Documents, U.S. Government Printing Office, Washington 25, D. C. or through a U.S. Department of Commerce Field Office.

Inquiries about the availability of reports and translations on any particular subject may be directed to Office of Technical Services, U.S. Department of Commerce, Washington 25, D. C. or to any Commerce field office.

Microfilm.—Any reports available from the Office of Technical Services will be provided in microfilm (35 mm) on request. The following prices are charged for microfilm: 1 through 20 pages, 80 cents minimum; and three cents per page for every page in excess of 20 pages.

Reports and translations are published by the Office of Technical Services for use by the public. Thus, you may use the know-how or reprint the information therein except that where patent questions appear to be involved the usual preliminary search is advised, and where copyrighted material is used permission should be obtained for its further publication.

microfilm
Photocopy \$ 3.60

UNITED STATES-ATOMIC ENERGY COMMISSION

AECD-3625

BORAL: A NEW THERMAL NEUTRON SHIELD

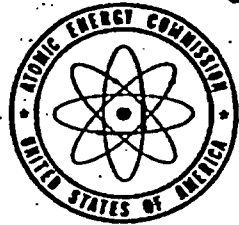
By
V. L. McKinney
Theodore Rockwell, III

SUPPLEMENT I

By
A. S. Kitzes
W. Q. Hullings

May 1954
[TIS Issuance Date]

Technical Division and Reactor Experimental
Engineering Division
Oak Ridge National Laboratory
Oak Ridge, Tennessee



Technical Information Service, Oak Ridge, Tennessee

Subject Category, PHYSICS
Operated by Carbide and Carbon Chemicals Company
for the U. S. Atomic Energy Commission under Contract
No. W-7405-eng-26.

This report has been reproduced with minimum alteration directly from manuscript provided the Technical Information Service in an effort to expedite availability of the information contained herein.


Reproduction of this information is encouraged by the United States Atomic Energy Commission. Arrangements for your republication of this document in whole or in part should be made with the author and the organization he represents.

Issuance of this document does not constitute authority for declassification of classified material of the same or similar content and title by the same authors.

BORAL: A NEW THERMAL NEUTRON SHIELD, was issued as ORNL-242 in 1949, and was declassified June 16, 1953.

SUPPLEMENT I, was issued as ORNL-981 on July 3, 1951, and was declassified December 4, 1952. (AECD-3476).

This combined report replaces both of the above reports and is complete without omission.

Printed in USA.  Available from the Office of Technical Services, Department of Commerce, Washington 25, D. C.

BORAL: A NEW THERMAL NEUTRON SHIELD

By

V. L. McKinney and Theodore Rockwell, III

May 1954
[TIS Issuance Date]

AECD-3625

3

1.0 Abstract

A technique has been developed for making large sheets or castings of B_4C and aluminum complex for absorption of thermal neutrons without production of hard gamma radiation. The $\frac{1}{4}$ " sheet has the following properties:

Boron Content: 50% B_4C (or 40% B) by volume.
0.91 g B/cm³ or 0.58 g B/cm² of $\frac{1}{4}$ " sheet.

Thermal Neutron Attenuation of 10^{10} in $\frac{1}{4}$ " (based on $\sum_{th}^B = 100 \text{ cm}^{-1}$).

Density: 2.53 g/cm³ or $\frac{1}{4}$ #/ft²

Cost: 15-20 \$/ft²

Tensile Strength: 5500 psi (10 times concrete, 1/10 mild steel, about equal best plastics).

Thermal Conductivity: Somewhat better than steel (more precise measurements in progress).

Can be sheared, sawed, welded, punched, drilled, tapped, rolled, and hot-pressed. Sheets 7' by 33' by $\frac{1}{4}$ " are in preparation for shearing to 5' x 6' test sheets.

It is felt that this material will have many uses where a large thermal neutron flux must be absorbed without production of hard gammas, e.g. inner section of reactor shields, shutters for thermal columns, instrumentation.

2.0 Introduction

The absorption of thermal neutrons without production of hard gamma radiation can be a very important function. For example, if the radiation impinging upon a shield is such that the thermal neutrons outnumber the quanta of hard gammas by a factor of 100, and these thermal neutrons are absorbed in the shield to produce hard gammas (the usual result), then the incident gamma flux which must be shielded has been effectively increased by this factor, i.e., an additional 26" of concrete (or equivalent) must be added to the shield. If instead, these incident thermal neutrons were absorbed without hard gamma production (e.g. in a thin film of boron), the 26" of hypothetical concrete could be removed. E. Creutz of Carnegie Institute of Technology estimates that a comparable thickness of concrete added to the CIT cyclotron shield would have cost over \$20,000 in materials and floor space. In a stationary reactor shield it might cost ten times this amount. It might tip the balance of feasibility in a mobile reactor shield.

The $B^{10}(n,\alpha)Li^7$ reaction is uniquely suited for such a function. Natural boron, containing 18.8% B^{10} , has a cross-section of 703 barns for this reaction at thermal energy, falling off as $1/v$ to about 0.1 barn at 1 MeV where the function becomes irregular. The residual activity is negligible and the 0.42 MeV gamma, which is emitted after 93% of the captures, is soft enough to be easily absorbed. Cadmium, by contrast, emits a 6 MeV gamma and leaves four unstable isotopes after irradiation.

Boron can be bought in many forms: Nearly pure crystalline boron at \$200 - 300 per pound, amorphous boron at \$15 per pound, and $B_{12}C$ in various grades and prices starting near \$7 per pound. The crystalline B is quite pure, the amorphous B 60-80%, the $B_{12}C$ 75-80% B. $B_{12}C$ is not only the cheapest form of highly concentrated boron, it is also exceedingly refractory, chemically inert, mechanically hard, and atomically dense; in each of these properties it exceeds almost all other known materials. For \$8 to 10 per pound, it can be obtained quite pure.

Being difficult to work, it seems desirable to bind the $B_{12}C$ with a more docile material for handling. Aluminum appears to be the most promising cementing agent: it has a low cross-section for the production of hard capture gammas, it is ductile and easily fabricated, has high thermal conductivity, is inexpensive, light weight, and corrosion resistant.

The question of radiation damage naturally arise. Since aluminum is the continuous phase, it should not suffer from destruction of the embedded $B_{12}C$ particles. Radiation damage studies on aluminum show that, with the possible exception of warpage, no deleterious effects should be expected. The diffusion of helium (from the n,α reaction) through the aluminum is expected to take place without damage. Irradiation tests will be made.

3.0 Early Experiments

The objective was to achieve as high a fraction as possible of $B_{12}C$. In addition it was felt that no $B_{12}C$ should be exposed at the surface and no loose $B_{12}C$ should exist within the sheet. In this way

it was hoped to minimize the possibility of escape of B_4C from the sheet due to blistering during operation or machining during fabrication. Arbitrarily a 1:1 ratio by volume of B_4C to aluminum was chosen. For a $\frac{1}{8}$ " sheet, this is sufficient to give a 10^{10} attenuation of thermal neutrons, assuming a macroscopic cross-section for boron of 100 cm^{-1} , or for boral, 40 cm^{-1} . Actually a 1:1 weight ratio was used for the unclad material, giving a volume ratio of 2.7 B_4C : 2.45 Al, but this is compensated for by the cladding on both sides which occupies a total of 16% of the thickness. It was found that a significantly larger fraction of B_4C could not be obtained without seriously impairing the mechanical and thermal properties of the material. In the rare cases where greater quantities of boron are needed, a thicker sheet can more easily be used.

Experimental work was started in December 1948 under Frank Kerze of the Engineering Materials Section and was shortly thereafter moved to the new Y-12 facilities of the Shielding Group.

3.1 Foil and Powder Method (See Figure 1)

B_4C powder was sprinkled in thin layers between ten .005" aluminum foils, around which was a wrapper of .064" 2S aluminum sheet. This was hot-rolled at $1130^\circ F$, reducing the laminated assembly .050" each pass through the rolls until the laminate had been reduced to $\frac{1}{8}$ ". The results of this experiment were unsatisfactory because only a small amount of the B_4C embedded itself in the aluminum foil, leaving most of the powder loose between the laminations. The loose B_4C prevented the bonding of the layers of foil and a considerable amount of powder blew out during rolling, preventing bonding of the outside wrapper. Figure 1 shows a sheared section of the finished sheet. Note that the laminations are not bonded to each other.

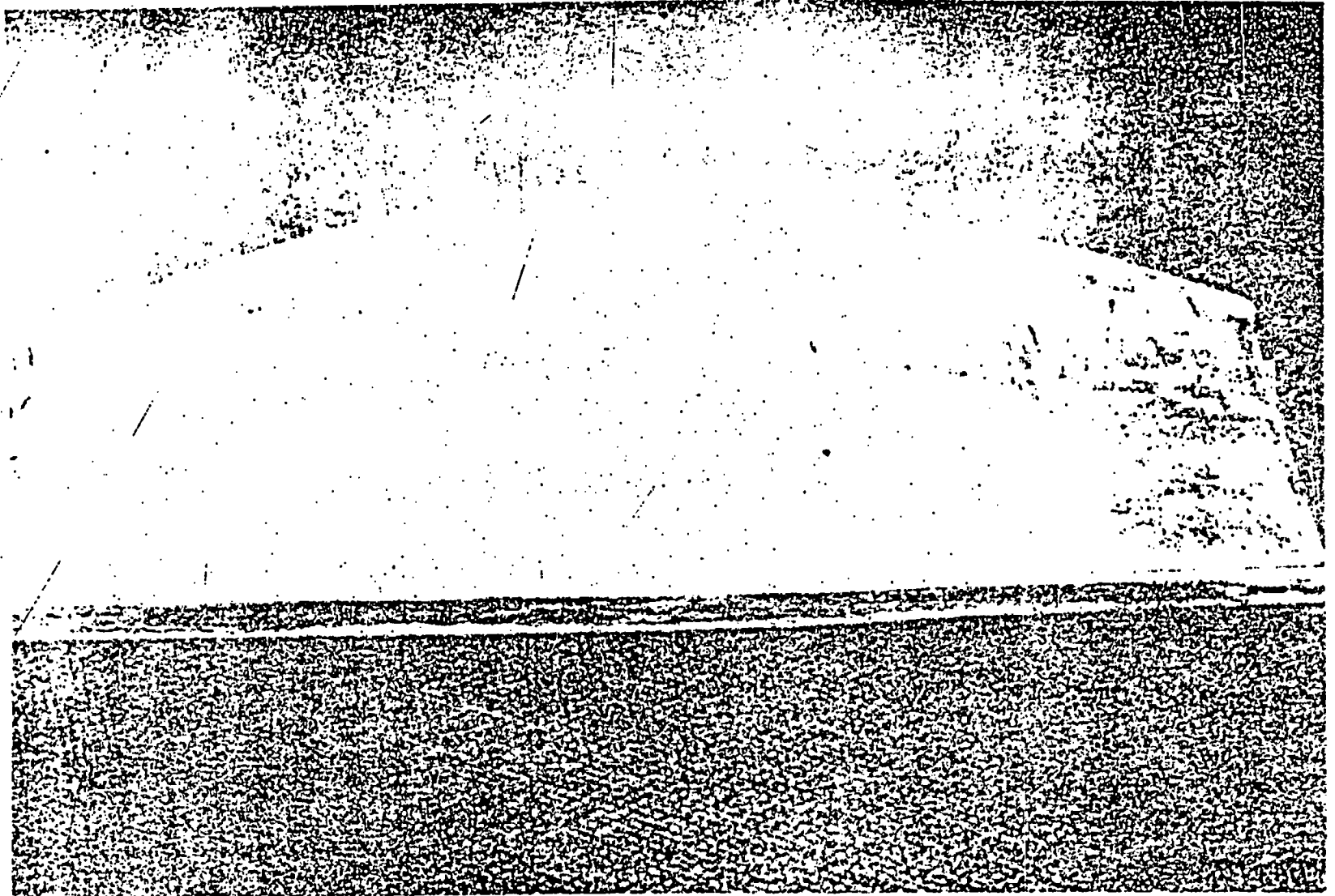


Fig. 1—Al foil and B₄C powder, hot rolled.

3.2 Two-Powder Method. (See Figures 2 and 3)

A mixture of B₄C and Al powder was placed in an envelope of Al foil (to prevent dusting during rolling) and this mixture was fitted carefully into an aluminum "picture frame". The frame was covered top and bottom with a single 1/8" wrapper sheet, and the assembly was then soaked at 1130°F for one hour. It was rolled at this temperature, being heated 10 minutes between passes, and reduced to 1/4".

The first attempts (see Figure 2) were fairly satisfactory, but several serious difficulties arose. The picture frame generally bonded to the wrapper on the first pass, trapping air in the powder mix inside. To minimize this, the envelope containing the powder was pressed within the picture frame on a 100 psi Studebaker pneumatic press, before heating and rolling. In spite of this, a large blister was formed and a vent hole had to be drilled through the wrapper. When the finished sheet was examined, it was found that the wrapper was not bonded to the inner material and there was considerable loose B₄C apparent. In an attempt to improve upon this, several sheets were made, varying the aluminum particle size from approximately 20 mesh to 1/4" chips, and the B₄C from 100 mesh to 18 mesh. These gave no significant improvement.

A larger sheet was tried by this method, starting with a 9 1/2" x 9 1/2" x 1" (inside dimensions) picture frame (see Figure 3). In addition to the above difficulties, the wrapper became quite soft at the soaking temperature, and handling the large assembly proved quite difficult. It was decided at that time that large satisfactory

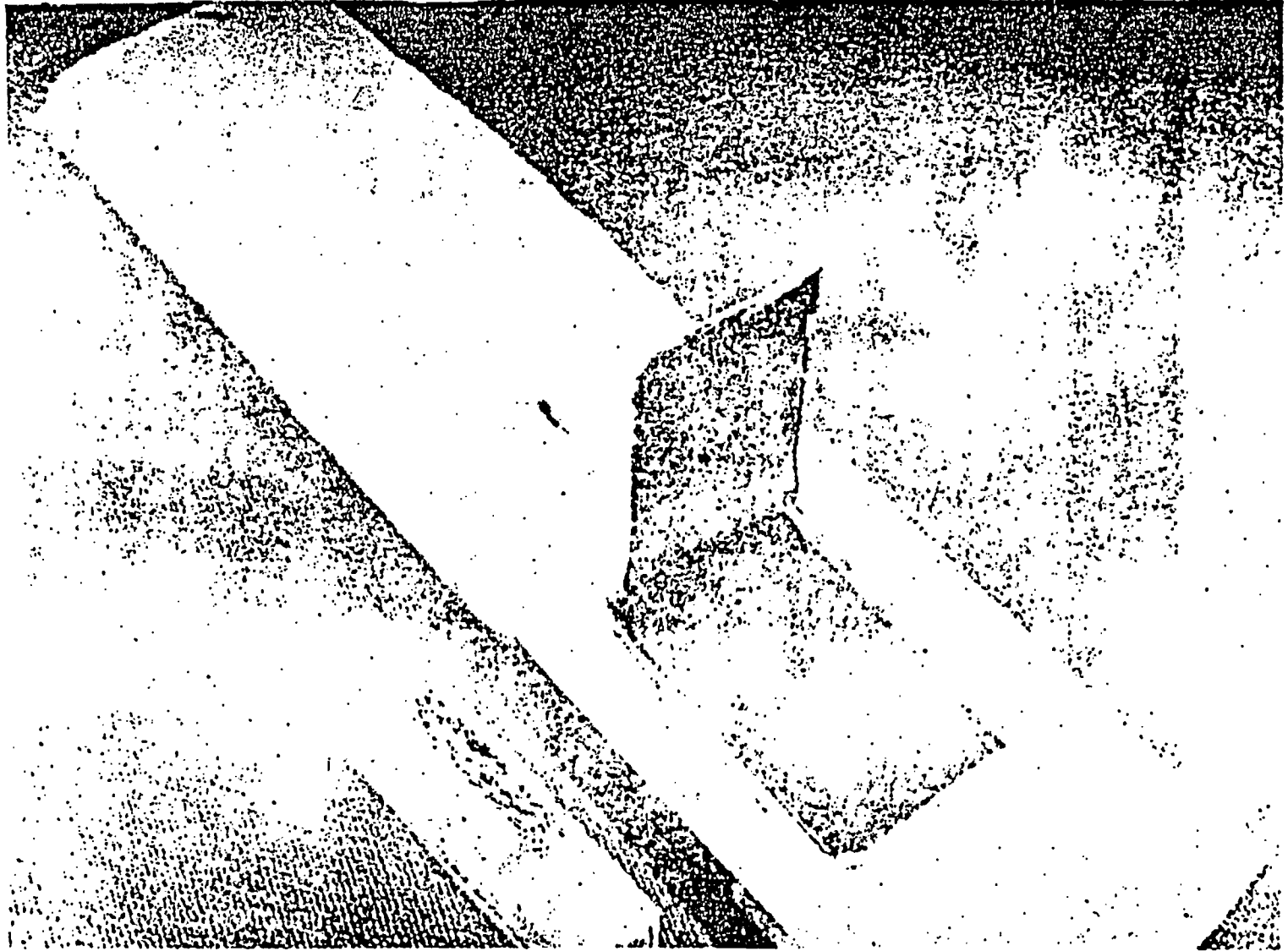


Fig. 2—Al and B₄C powders in picture frame.



AMMO-3629

Fig. 3—Large two-powder attempt.

sheets could not be rolled unless the B_4C and aluminum were in the form of a rigid structure during rolling.

3.3 Cast Ingot Method (Figure 4)

Several small-scale attempts were made to mix B_4C powder with molten aluminum. The aluminum did not wet the B_4C and the resultant mix when cooled was crumbly and incohesive. Preheating the B_4C , precipitating B_2O_3 or Al_2O_3 on the B_4C surface, and varying the temperature range, had little effect. Attempts to make an ingot from B_4C and aluminum powder were equally unsuccessful. A non-oxidizing atmosphere seemed to make little difference.

Finally a successful ingot was made as follows: (Figure 4) Half of the aluminum, as powder, and all of the B_4C , were mixed cold and added slowly with stirring to the remaining aluminum which was molten. The temperature, which seemed critical, was kept at $1230^{\circ}F \pm 20$. The resultant ingot was somewhat porous (density 2.25 g/cc), but very strong and homogeneous. The porosity was nearly eliminated during rolling, resulting in a sheet with a density of 2.53 g/cc. This method was refined and was the basis of the present fabrication technique.

4.0 Present Fabrication Technique (Figures 5 and 6)

The capacity of the rolling mill at ORNL limits the sheet width to 27" and the billet thickness (including wrapper) to $1\frac{1}{2}$ ". Therefore it has been decided to roll a billet $1\frac{1}{4}$ " x 7" x 12", with an $1/8$ " wrapper on each side, which produces a trimmed sheet 20" x 20" x $\frac{1}{4}$ ". Since the B_4C powder alone stacks to nearly 50% voids, the boral ingot holds B_4C particles which are nearly touching, resulting in a very rigid mass which cannot be poured, even at high temperature. Therefore



Fig. 4—Sections of first ingot and sheet.

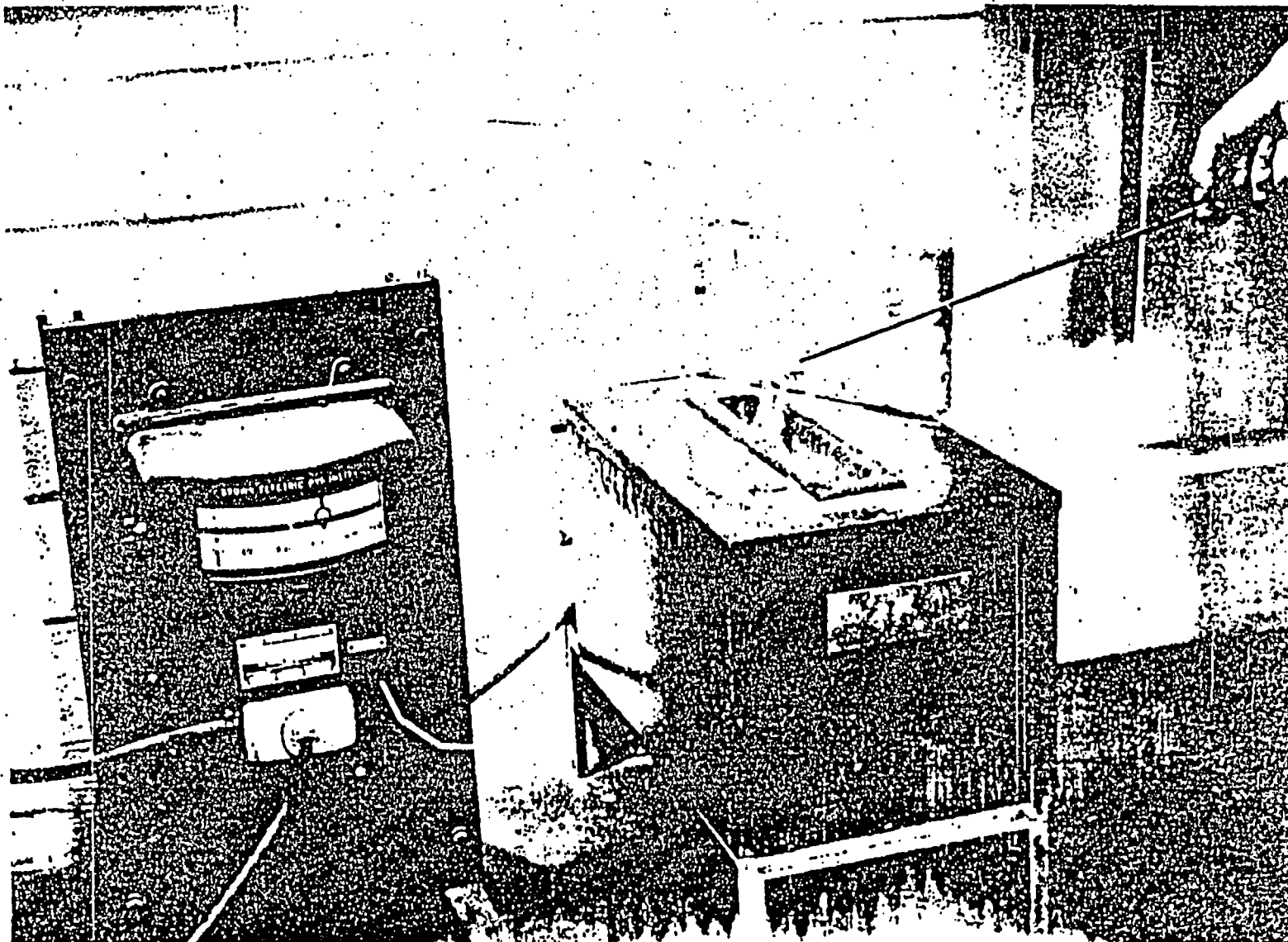


Fig. 5—Casting boron Ingot.

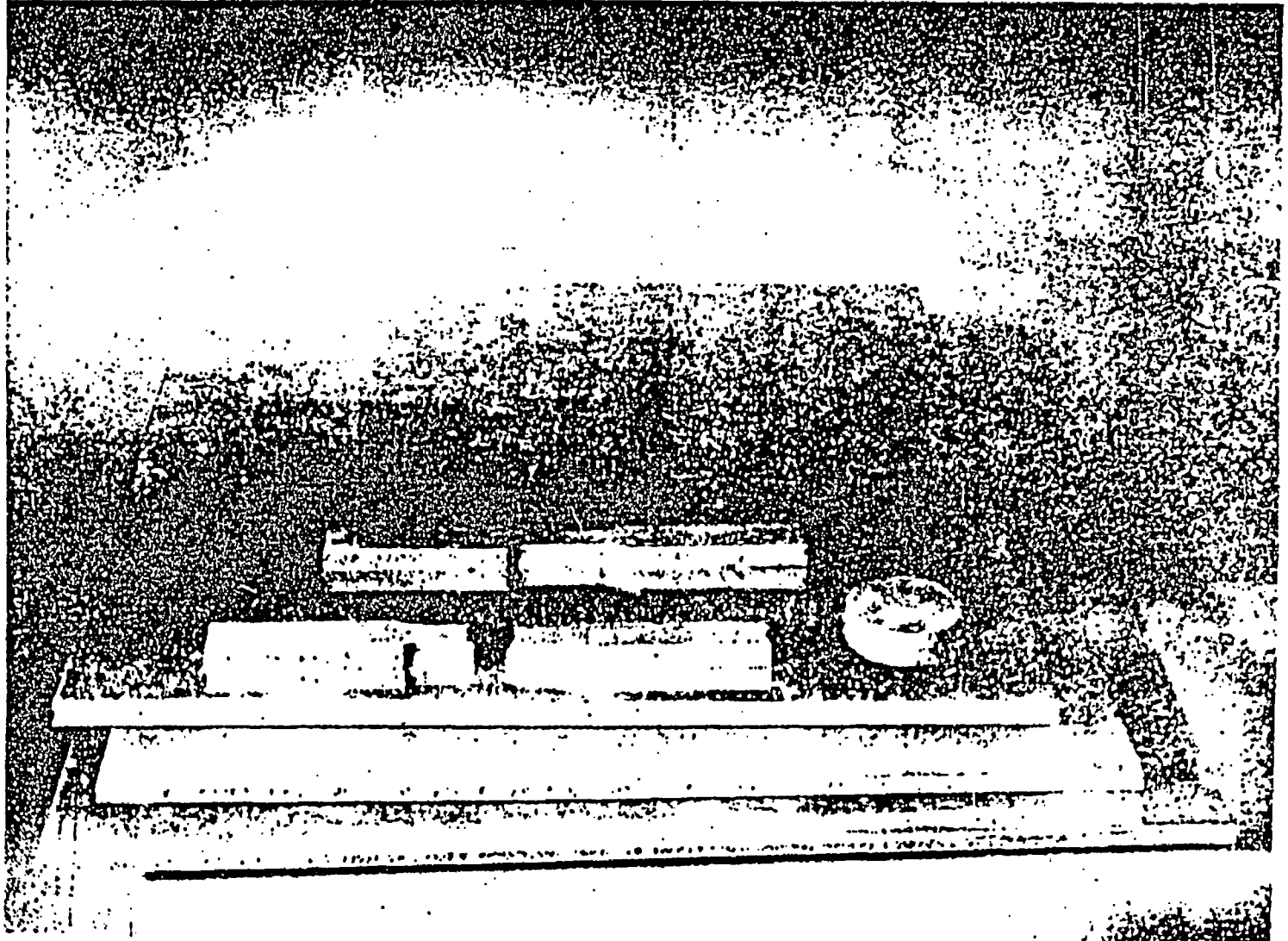


Fig. 6—Finished boral sheets and pieces

it is desirable that the rolling billet be the original casting, and not recast from a larger pig. For this purpose, a special furnace has been built from two standard 6" x 12" muffle furnace elements, which heats a graphite crucible with inside dimensions 7" x 12" x $\frac{1}{4}$ " with $\frac{1}{16}$ " taper. The temperature is controlled by a Brown electric pyrometer from a thermocouple set in the graphite, and the mixed powders are stirred into the molten aluminum with a $\frac{3}{8}$ " steel rod, as shown in Figure 5. A typical ingot is shown on the furnace. To produce an ingot this size requires 825 grams of 2S aluminum pig. To this a cold mixture of 1650 grams B_4C (through 20 on 100 mesh) and 825 grams of aluminum powder (approximately 20 mesh), is added gradually while stirring in order to wet and suspend the B_4C particles in the molten aluminum.

After removing the ingot from the crucible mold, it is then metal-sprayed with a thin coat of aluminum to cover completely any exposed particles of B_4C . A wrapper of $\frac{1}{8}$ " 2S aluminum sheet, which has been wire-brushed to remove excess oxide and dirt to facilitate bonding, is placed around the ingot to form a cladding of approximately .020" on the $\frac{1}{4}$ " finished sheet. The assembly is then placed in a Lindberg forced-circulation electric furnace and heated to 1130°F for approximately one hour and rolled. The billet is reduced approximately 10% each pass through the rolls. The material retains considerable ductility at low temperatures and work-heats appreciably during rolling, so that reheating between passes is not necessary if the rolling is carried out at a reasonable pace.

The first heats were run with only the ingot and a wrapper sheet. Since there was nothing to confine the edges of the ingot during rolling, excessive crumbling, edge-cracking, and unevenness resulted. Present runs employ a welded aluminum picture frame to confine the ingot, and this technique yields straight edges, free from cracks. The edges of the wrapper sheet are bent over and tack-welded to the outside of the picture frame, which has several vent holes drilled through it.

5.0 The 250 ft² Sheets (Figures 7 and 8)

As indicated above, the maximum width which could be rolled at ORNL was 27". There is a need for several 40" x 43" shutters for the ORNL attenuation facility and several 56" x 66" sheets for experimental work. Arrangements have been made with the Lukens Steel Company of Coatesville, Pennsylvania, to roll two sheets 84" x 396" x $\frac{1}{4}$ ", from which ten 56" x 66" sheets and four 40" x 33" shutters can be cut. Two ingots, 6" x 36" x 32", weighing 450 pounds each, will be cast and wrapped at Y-12, then shipped to Lukens for rolling. The expenses for this job are being partly borne by NEPA, and the sheets will be used for the joint ORNL-NEPA shield tests in the ORNL attenuation facility.

The method of wrapping is essentially that described in paragraph 4.0 and is shown in detail in Figure 7. The special furnace for casting the ingots (Figure 8) is scaled up from that shown in Figure 5, except that a non-tapered steel crucible is being used. A separate report, ORNL-243, covering this project, will be written as soon as the sheets are rolled.

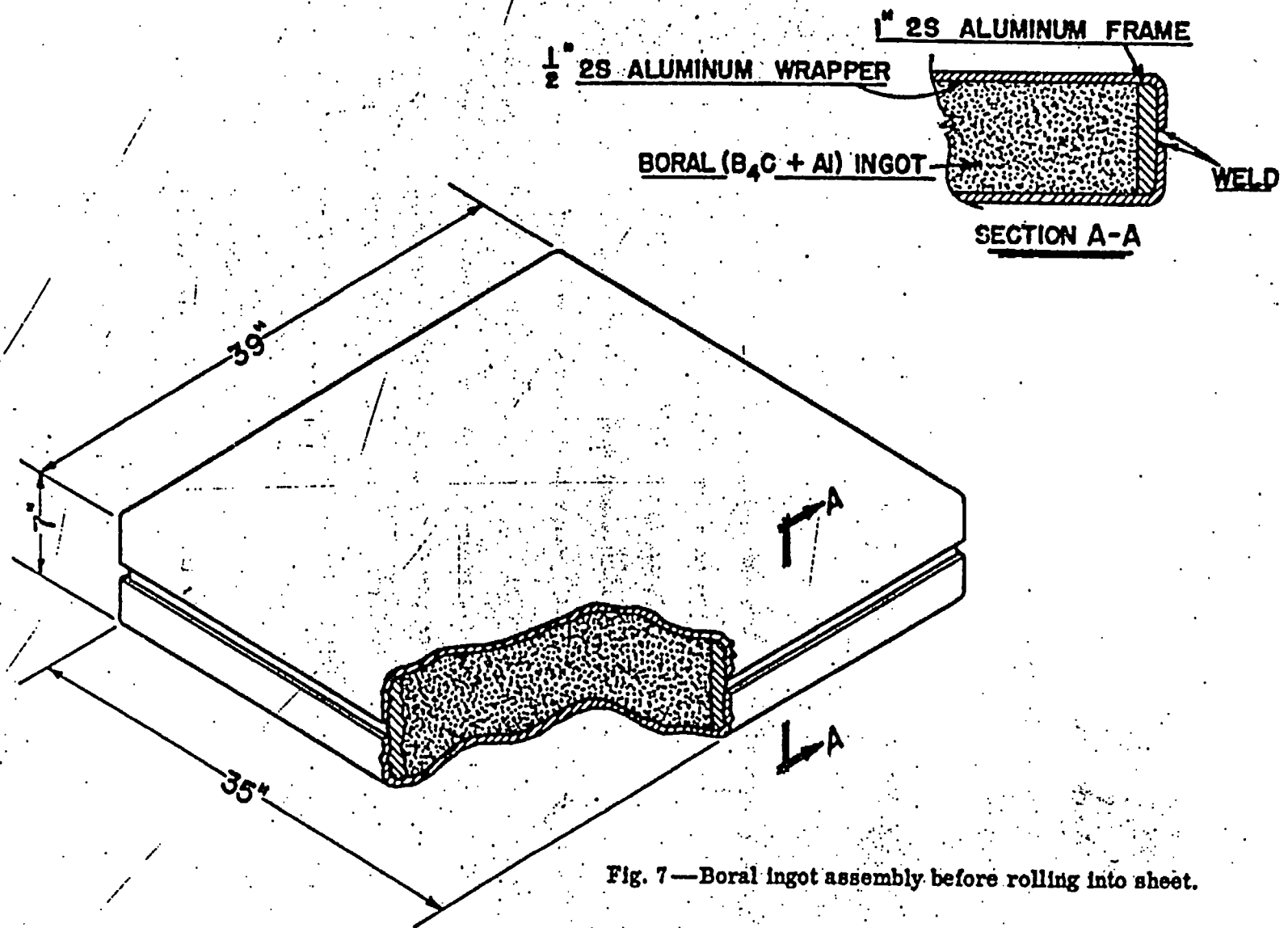


Fig. 7 — Boral ingot assembly before rolling into sheet.

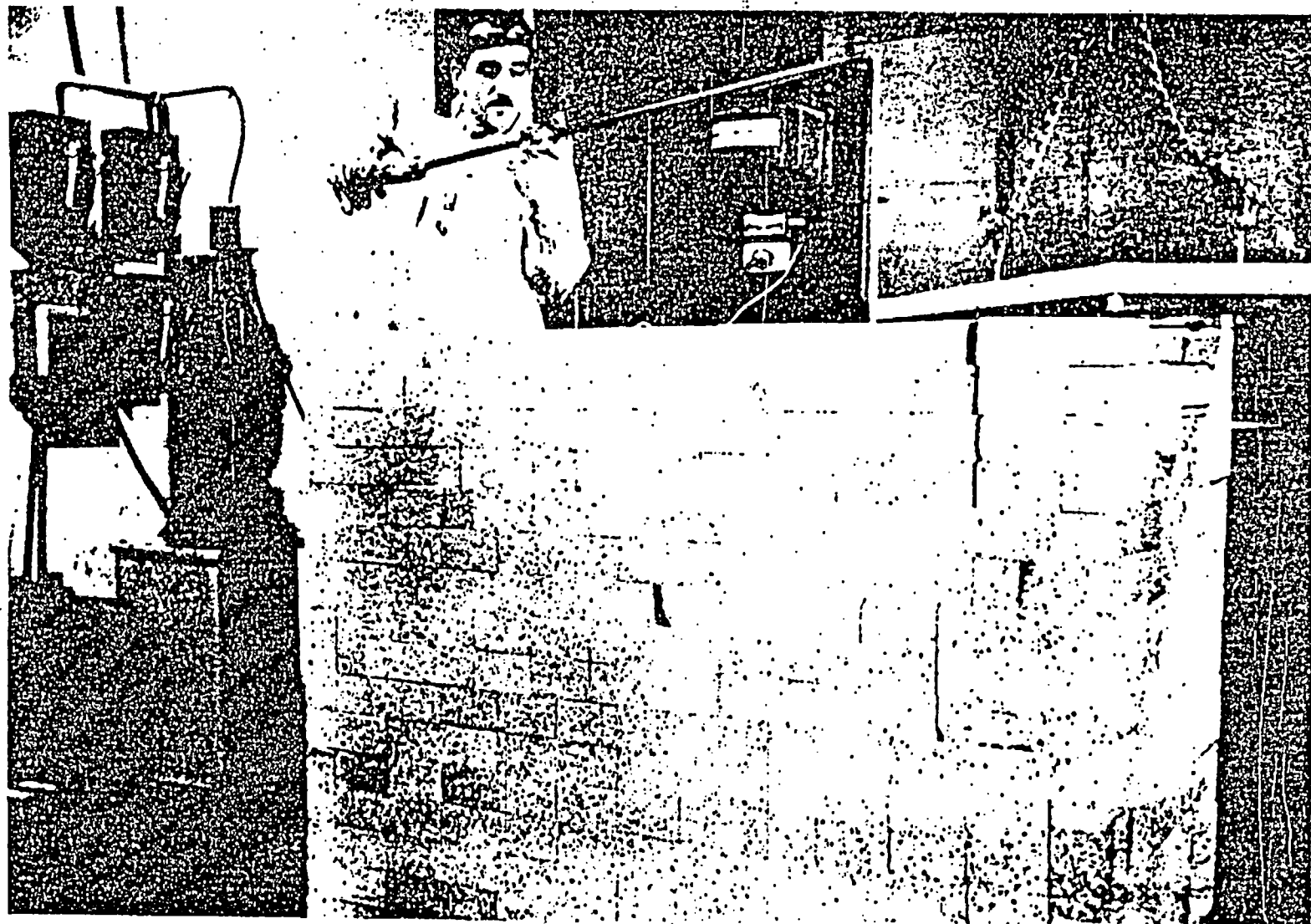


Fig. 8—Casting 36" x 32" x 6" boral ingot.

6.0 Physical Properties6.1 Data

1. Composition (for $\frac{1}{8}$ " sheet, including .020" Al cladding on each side).
50% (vol.) B_4C , 50% Al.

	<u>% (wt)</u>	<u>mg-mol/cm³</u>	<u>g/cm³</u>	<u>g/cm²</u>
B	36.0	84.2	0.911	0.578*
Al	55.1	51.7	1.394	0.886
C	8.9	18.7	.225	0.143

* This is sufficient to give 10^{10} attenuation of thermal neutrons

2. Density: 2.53 g/cc.
0.09 lb/in³
 $3\frac{1}{8}$ lb/ft² for $\frac{1}{8}$ " sheet

3. Strength

- a) Tensile 5,500 psi
b) Elongation 0.4 %
c) Shear 8,237 psi
d) Welded tensile specimens did not fail at weld

4. Thermal Properties

- a) Conductivity: somewhat better than steel (more precise measurements in progress).
b) Specific Heat: 0.175 Btu/lb x °F or g-cal/g x °C
c) Melting Point: Maintains mechanical strength up to 1500°F (800°C), above which oxidation is excessive.
d) Heat Generation from n, α Reaction: 7.4×10^{-10} watts/ft² x unit thermal neutron flux.
5. Cost: 15-20 \$/ft² for $\frac{1}{8}$ " sheet.
6. Workability: Can be sheared, sawed, welded, punched, drilled, tapped, rolled, hot-formed, and experimentally die-cast.

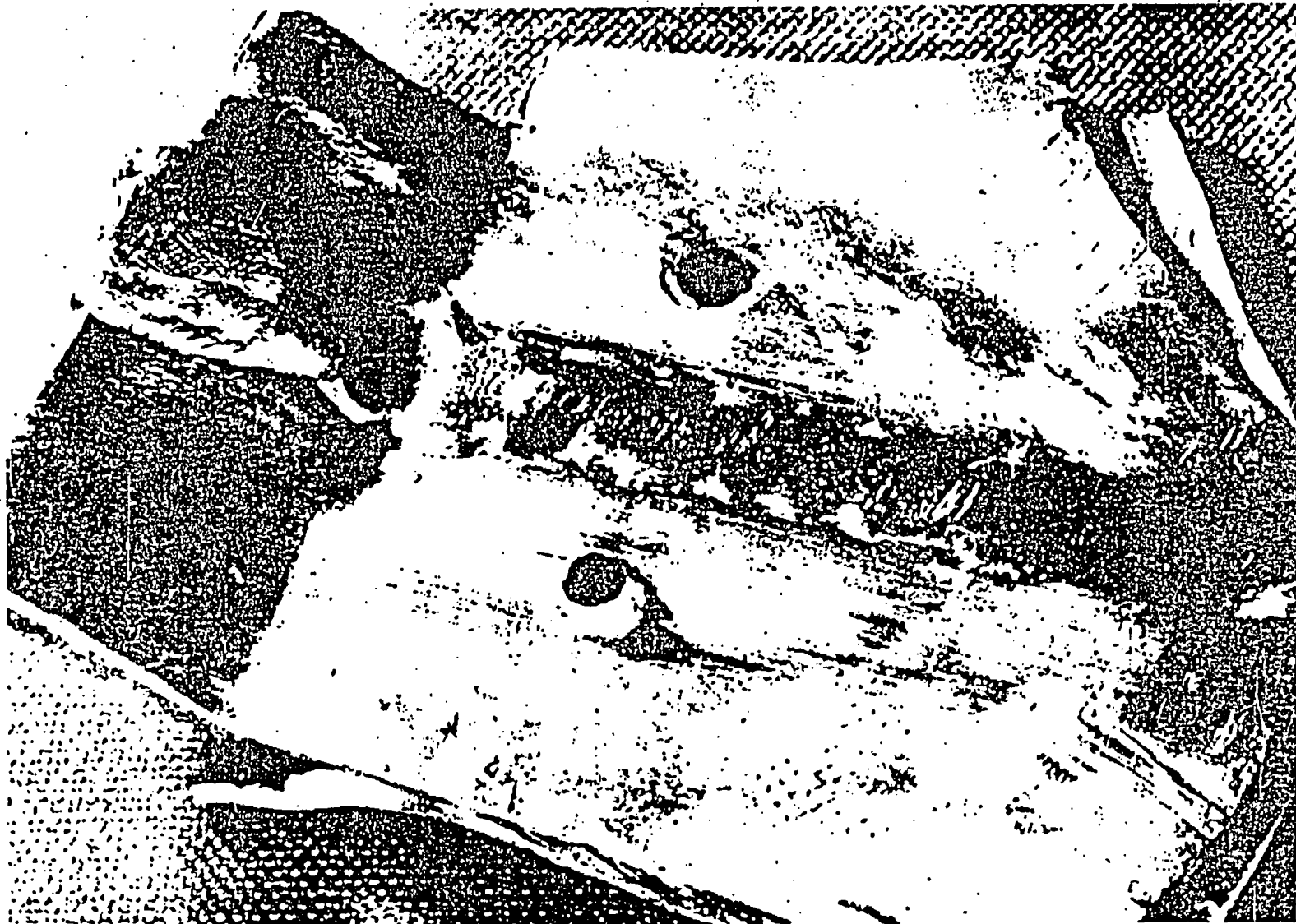


Fig. 9—Boral sawed, welded, punched, and drilled.

6.2 Testing and Calculation Methods

1. Composition

Calculations are based on 1:1 (vol) B₁C : Al composition.

Densities assumed are 2.45 and 2.70 g/cc respectively.

2. Density is based on gross volume measurement and also water displacement, with no significant difference.

3. Tensile strength on 8 normal and 3 welded specimens, as per ASTM (e.g. B209-46T, 1946 ed, Part IB, p 572, fig. 1).

Shear strength on three $\frac{1}{4}$ " x 2" x 8" strips, in modified

Johnson Shear Tool (ASTM C102-36, 1946 ed, Part II, p 228, fig. 1)

4. Thermal Conductivity was made by comparing temperature drops through Al rod, Al discs, and boral discs, through which a constant heat flux flows axially (see Figure 9). Comparison of the Al rod and discs gives an approximation of the temperature drop through the brazed interfaces of discs, and this correction, applied to the boral discs, gives the drop through boral compared to drop through Al for same heat flux. Precision was poor and precise tests are being made on new equipment.

$$\text{Heat Generation} = 5 \text{ Mev} \alpha/n \text{ capture} \times 929 \text{ nv} \frac{\text{captures}}{\text{ft}^2 \times \text{sec}} \times 1.6 \times 10^{-13} \frac{\text{watts}}{\text{MeV}}$$

5. Cost: \$12/ft² for B₁C, \$0.40 for Al, \$1 for rolling.

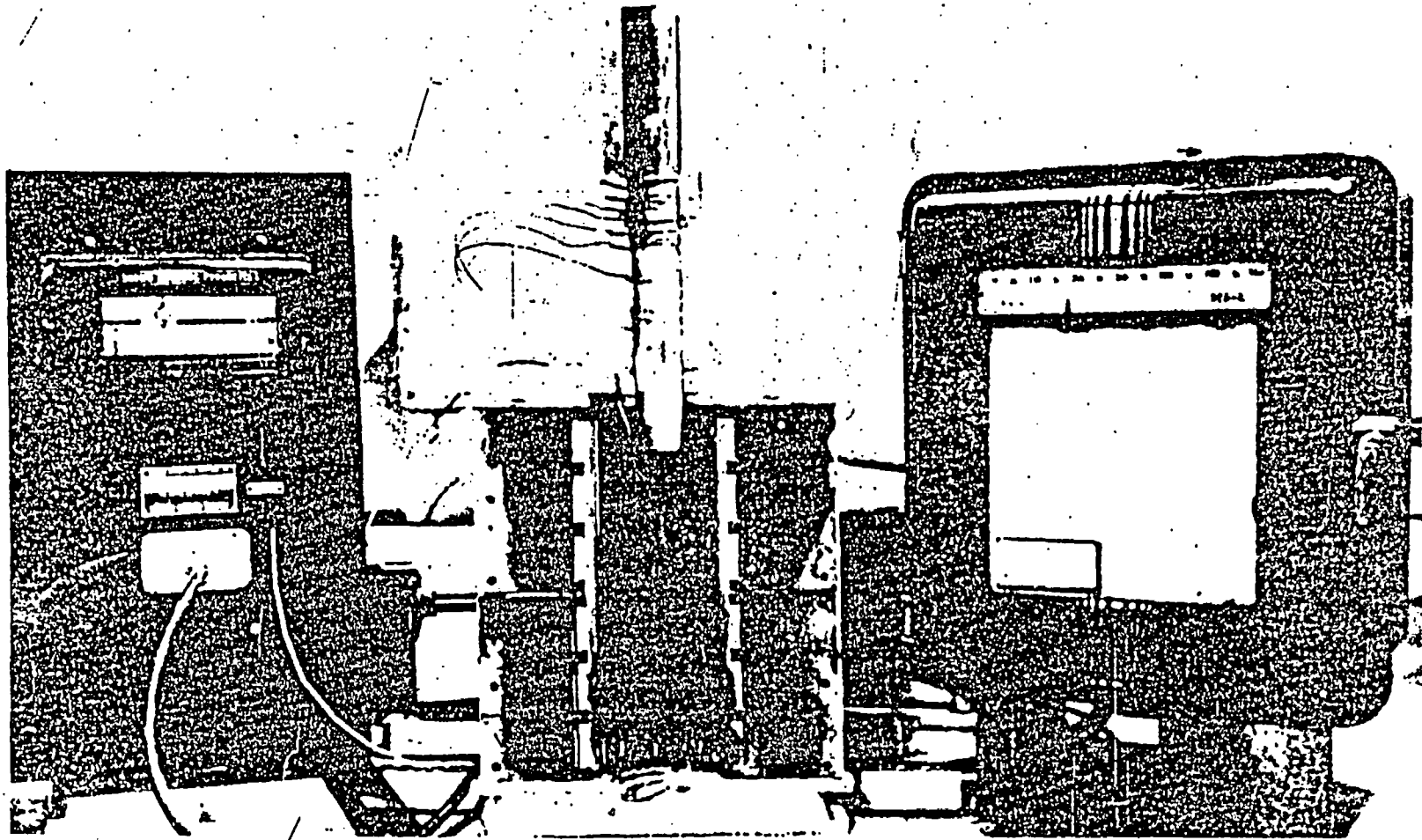


Fig. 10—Sectional view of thermal conductivity apparatus.

7.0 Analyses of Raw Materials for Boral

	<u>Al Powder</u>	<u>Large Al Pig</u>	<u>Small Al Pig</u>	<u>Boral</u>
Ag	<.04%	T	--	T
Al	>.10	VS	VS	VS
B	<.015	--	--	VS
Be	<.004	--	--	--
Ca	<.08	--	--	--
Cd	<.15	--	--	--
Co	<.08	--	--	--
Cr	<.15	--	--	--
Cu	<.08	W	W	T
Fe	<.15	W	W	S*
In	<.08	--	--	M*
Mg	<.04	M	W	S*
Mn	<.04	T	T	W
Mo	<.15	T	--	--
Ni	<.08	--	--	T
Pb	<.08	--	--	--
Pt	<.08	--	--	--
Si	<.20	W	T	W
Sn	<.08	--	--	--
Ti	<.04	--	--	--
V	<.08	--	--	--
Zn	<.31	--	--	--
Zr	<.15	--	--	--

*Chemical analyses being made

Symbols for spectrographic analyses: VS very strong
 S strong
 M medium
 W weak
 T trace
 -- not detected

Analyses were made for all elements listed

Wrapper sheet and spray-metal being analyzed

SUPPLEMENT I

By

A. S. Kitzes and W. Q. Hurlings

ABSTRACT

The technique for making large sheets of boral described in ORNL-242, which consists of mixing B_4C with aluminum has been modified and simplified. Recommendations are given for casting and rolling ingots into sheets.

Additional physical property data are included. Tensile strength measurements of boral indicate no serious damage upon irradiation with a total of 2.6×10^{19} nvt in the ORNL reactor. Thermal conductivity for the 50-50 mixture was found to be 25.0 Btu/hr-ft²-°F/ft at 200 °F and 19.0 Btu/hr-ft²-°F/ft at 500 °F.

A method for measuring thermal conductivities is described.

In order to make boral available to other sites, ORNL has agreed to accept urgent requests for small amounts of boral as sheets not larger than 24" x 96" x 1/4" or 1/8", other program commitments permitting. Requests or purchase orders for sheet stock or simple fabrication parts may be submitted directly to ORNL, giving detailed requirements.

INTRODUCTION

Boral, as described in ORNL-242, is an engineering material for the absorption of thermal neutrons.

Boral is a mixture of boron carbide (B_4C) and aluminum in which the boron carbide is suspended in molten aluminum and the resultant product allowed to solidify into a form suitable for rolling. It is useful because of its light weight, its high boron content for the absorption of thermal neutrons without production of hard gammas, its good heat conductivity and its thermal stability up to the melting point of aluminum.

In ORNL-242, "Boral: A New Thermal Neutron Shield", McKinney and Rockwell adequately discuss the history, development, and fabrication of boral and establish a procedure for producing large quantities of this material. However, they were unable to conclude their program for the production of large sheets of boral. This report summarizes the work done in concluding the program initiated by McKinney and Rockwell. Additional physical property data and information relative to the availability and fabrication of large quantities of boral are included.

In ORNL-242, McKinney and Rockwell reported that small scale attempts to mix B_4C powder with molten aluminum were unsuccessful. The aluminum did not

wet the $B_{14}C$ and the resultant mix when cooled was crumbly and incohesive. Preheating the $B_{14}C$, coating the $B_{14}C$ with B_2O_3 or Al_2O_3 and varying the temperature had little effect. A successful ingot was finally made by stirring a mixture of aluminum powder and $B_{14}C$ into molten aluminum, keeping the temperature at $1230^{\circ}F \pm 20^{\circ}$. This method was therefore established as the standard procedure for casting ingots.

EXPERIMENTAL DEVELOPMENT PROGRAM

Additions to make Aluminum wet $B_{14}C$

In the McKinney-Rockwell procedure, it is difficult to understand and interpret the action of the aluminum powder in causing the molten aluminum to wet the $B_{14}C$. In an effort to understand the mechanisms involved, a series of experiments was performed in which varying percentages of Al_2O_3 were substituted for part of the aluminum powder and added to the molten aluminum with the $B_{14}C$. The results were negative; the $B_{14}C$ floated on top of the molten metal.

In a second series of tests, varying percentages of B_2O_3 were mixed with the $B_{14}C$ and added to the molten aluminum, omitting the use of aluminum powder. Good workable mixes were obtained resulting in strong homogeneous ingots. The B_2O_3 content varied from 5-50% of the weight of the $B_{14}C$. During the addition of the B_2O_3 - $B_{14}C$ mixture to the molten metal, a black smoke was given off and green flames popped on the surface of the melt. This same reaction was observed in the McKinney-Rockwell process.

Since the addition of B_2O_3 caused the aluminum to wet the B_4C , a B_2O_3 coating was placed on the carbide by oxidizing it for one hour in a muffle furnace. The oxidized carbide was then added to the molten aluminum. Good workable mixes and perfect ingots were obtained. No black smoke or green flames were evident. This method is now the basis of the present fabrication technique.

The mechanism of how the B_2O_3 influences the wetting of B_4C by the aluminum is still not known. The B_2O_3 probably acts as a fluxing agent and as such helps to minimize the absorption of gases and the oxidation of the aluminum. Since inert atmospheres above the melts made no difference, their use was discontinued. Although either the oxidized carbide or B_2O_3 and carbide can be added freely to the molten aluminum, the oxidized carbide is preferred.

Effect of Temperature During Mixing of B_4C into Aluminum

The temperature at which the oxidized B_4C was added to the molten aluminum was not critical as long as it was below that at which the oxidation of aluminum became severe. No apparent difficulty was observed when oxidized B_4C was added to molten aluminum at $1400^\circ-1450^\circ F$; however, the temperature was usually kept at $1300^\circ-1350^\circ F$ and the B_4C was added at a rate which did not reduce the temperature of the molten aluminum by more than $25^\circ-35^\circ F$. Adding big slugs of carbide to the melt caused the mix to cool as much as $400^\circ F$ and resulted in a loss of time required to reheat the mixture. When the required temperature was again reached, more B_4C was added, and only occasionally when the mix was cooled too much through the addition of larger doses of carbide it was impossible to remelt the mixture without excessive oxidation of the aluminum.

TECHNIQUE FOR CASTING INGOTS

The capacity of the ORNL rolling mill limited the sheet width to 24" and the billet thickness to 1 1/2" including covers. For this reason it was decided to roll ingots, 1" x 20" x 24" with 1/4" cover plates on each side, which produced a trimmed sheet, 24" x 108" x 1/4". A 150 KW Ohio Crankshaft Company "Tocco" tilting type induction furnace was used to heat a graphite crucible 9" in diameter with 1" wall thickness. The temperature was controlled by a Micromax electric pyrometer from a thermocouple set in the graphite. The pre-oxidized B_4C (oxidized at 1000 °F for one hour) was stirred into the molten aluminum by hand with stainless steel paddles, and the mix was then allowed to stand for 10-15 minutes in order to attain a uniform temperature.

While the carbide was stirred into the molten aluminum, a graphite mold, 20" x 24" x 1" was heated electrically to between 800°-900°F. One continuous pour was then made into the heated mold; the residual mix in the crucible was incorporated into the next pour.

During cooling, the ingot shrank sufficiently for easy removal from the mold. It was then prepared for rolling according to the procedure outlined in ORNL-242 except that the operation of metal spraying with aluminum was eliminated.

To produce an ingot, 20" x 24" x 1" containing 35% B_4C by weight, 13.5 lbs B_4C and 24.5 lbs 2S aluminum pig were required. The B_4C content was decreased from 50%, the percentage used by McKinney and Rockwell, to 35% to facilitate rolling and fabrication of the sheet stock. This phase of the work is more fully discussed in the section entitled, "Rolling at Lukens Steel Company."

Proposed Changes for Casting Ingots

Minor changes which will lower costs and simplify the operation are being incorporated in the aforementioned ingot-casting procedure. Instead of pouring the boron carbide into the mixture by hand, it will flow, at a controlled rate, by gravity from an electrically heated hopper. After oxidation in a muffle furnace, the carbide will be transferred to the hopper and kept at a temperature, probably between $800^{\circ} - 1000^{\circ} F$, permitting it to flow freely. This will minimize the temperature drop of the melt during the addition of the carbide and reduce the temperature gradient between the top and bottom of the crucible.

It is also planned that mechanical stirring will replace the manual operation, and the casting mold will be cooled from the bottom by forced air circulation, allowing the entrapped gases to escape from the top.

Advantages of the New Casting Technique over McKinney-Rockwell Method

- 1) Ten to twelve ingots can be mixed before replacing the crucible and mold. In the McKinney-Rockwell procedure, one crucible per ingot was expended.

- 2) Elimination of the aluminum powder minimizes the oxidation of the molten aluminum.
- 3) Elimination of the metal spraying operation prior to cladding the ingots and the use of nitrogen during mixing lowers the cost of the finished sheet.

ROLLING BORAL INGOTS INTO LARGE SHEETS

Rolling at Lukens Steel Company

Unsuccessful attempts at large-scale experimental rolling were made by Lukens Steel Company, Coatesville, Pennsylvania. Two ingots, 27" x 36" x 6", containing 50% B_4C by weight and prepared according to the procedure outlined in ORNL-242, were scheduled for rolling into sheets, 56 1/2" x 66 1/2" x 3/16". Failure of the rolling attempt was attributed to rough handling of the ingots during rolling. Greater care could not be used because the mill designed primarily for steel ingots could not be slowed down to the desired speed and the rolls could not be lubricated with kerosene.

Upon examination of the damaged sheets there was evidence of insufficient aluminum to coat all the B_4C in the 50-50 mixture. It is possible that this defect, which apparently was not too important when rolling small ingots, became more prominent in rolling the larger ones and contributed to the unsuccessful rolling attempt. It was therefore decided to lower the B_4C content in an effort to improve the rolling characteristics.

Even at the lower $B_{4}C$ concentration, sufficient attenuation of thermal neutrons can be obtained for more applications without using excessively thick sheets.

Rolling at Republic Steel Company

A successful rolling was accomplished at the South Division Plant of the Republic Steel Company in Canton, Ohio. Republic was chosen for this experiment because it had hand-fed or jobber rolling mills which were more suited for the rolling of boral. Two ingots, 23" x 14" x 2", containing 35% $B_{4}C$ by weight, were prepared, placed in 2" aluminum frames and covered with 1/2"-sheet 2S aluminum. These ingots were then heated to 1100 °F, reduced 50%, reheated to 1000 °F, and rolled into sheets 52" wide, 92" long, and 3/16" thick, the minimum attainable thickness on the rolls. Cold rolls, frequently lubricated with kerosene were used. After a few more large scale experimental rollings, boral could be supplied commercially in sheets, 5' x 10' x 3/16" if this is warranted.

Rolling at ORNL

Because of the small quantities required to meet present commitments, boral was rolled in the ORNL rolling mill. Since the capacity of this mill limited the maximum width of the finished sheet to 24", sheets 24" x 84"-96" x 1/4" or 1/8" were rolled, and wider sheets were fabricated by joining several smaller ones. Ingots were prepared according to the procedure outlined in the section entitled, "Technique for Casting Ingots", placed in 1" frames and clad with 1/4" aluminum. The rolling procedure was essentially the same as the one used at Republic.

PHYSICAL PROPERTIES

Data

- 1) Composition (for 1/4" sheet including Al cladding on each side)

	<u>Sandwich Material</u> <u>35% B₄C by Weight</u>		<u>Sandwich Material</u> <u>50% B₄C by Weight</u>	
	<u>%(wt)</u>	<u>mg/cm²</u>	<u>%(wt)</u>	<u>mg/cm²</u>
B	15.7	254	22.4	342
C	4.3	71.6	6.2	100.1
Al	80.0	1303.0	71.4	1103.5

Borals with B₄C contents varying from 10 - 50% in the core can be supplied.

- 2) Strength

- a) Tensile

Tensile specimens containing 50% B₄C by weight were exposed to radiations in the X-10 pile for 14 months with no serious damage.

<u>Weeks of Exposure</u>	<u>Total nvt</u>	<u>Average Tensile Strength (psi)</u>
0	0	5000
6	3.1×10^{18}	6335
8	4.8×10^{18}	7500
30	1.2×10^{19}	5650
60	2.6×10^{19}	5500

Additional samples are now being exposed in the Hanford piles - no results are available at this time.

- b) Elongation - 0.4% (ORNL-242)
 c) Sbear - 8,237 psi (ORNL-242)

3) Thermal Properties - 50% B₄C by weight

a) Thermal Conductivity (Btu/hr-ft-°F)

Temp. (°F)	200	450	500
k	25	19.2	19.0

The above values are being rechecked and additional values for pure B₄C and for boral with varying B₄C content are being obtained.

b) Heat Content: .175 Btu/lb-°F (ORNL-242)

4) Density: 2.5 g/cc

5) Cost: \$15-\$17/ft² for material containing 35% B₄C in the core

6) Workability:

Recommended methods for working boral are shearing and punching. Boral with 35% B₄C can be sawed at low speeds with Do-All saws. All welding must be done with heliarc. Boral tubes can be hot turned or pressed.

7) Availability:

In order to make boral available to other sites, ORNL has agreed to accept urgent requests for small amounts of boral as sheets not larger than 24" x 96" x 1/4" or 1/8", other program commitments permitting. Requests or purchase orders for sheet stock or simple fabricated parts may be submitted directly to ORNL, giving detailed requirements.

8) Other Applications:

Boral can be sprayed onto mild steels. However, the bond between the sprayed material and the base needs improvement.

ACKNOWLEDGEMENTS

The authors wish to acknowledge the assistance of V. L. McKinney and the Y-12 Shops in setting up the casting procedure for producing ingots and of C. D. Smith and his group at ORNL in rolling the boral.

APPENDIX

Principle of Proposed Method for Determining Thermal Conductivities

Longitudinal heat flow through a specimen was measured by the temperature rise of a metered amount of water passing through a heat exchanger located at the base of the sample. The temperature drop across the specimen was measured with thermocouples embedded in the sample a known distance apart. Radiation, conduction and convection losses were minimized by employing an electrically heated guard ring system in which the cavity between the sample and the walls of the guard ring was filled with a powdered thermal insulation, Sil-O-Cel. Under these conditions, the thermal conductivity was computed by means of the relationship

$$k = \frac{Wc_p (\Delta T)_w L}{A (\Delta T)_s}$$

k = thermal conductivity, Btu/hr-ft- $^{\circ}$ F

c_p = specific heat of water, Btu/hr-lb

$(\Delta T)_w$ = temperature rise in water, $^{\circ}$ F

L = distance between thermocouples embedded in sample, ft

A = cross-sectional area of sample, ft 2

$(\Delta T)_s$ = temperature drop in sample, $^{\circ}$ F

Application of Proposed Method for Determining Thermal Conductivity

In an effort to simulate experimentally the method set forth in the section entitled, "Principle of Proposed Method for Determining Thermal Conductivity," the apparatus diagrammatically shown in Figure 1 was set-up. The Specimen (D), 2 cm in diameter and 5 cm in length was sandwiched between a heat source (A) and a heat exchanger (C) and the complete assembly was held tightly together by a spring loaded clamp (3)(4) to assure thermal contact between the various metal faces. The temperature of the heat source, a solid cylinder of copper wound with high resistance nichrome wire was controlled by a variac. The heat exchanger was also made of copper with water flowing in a baffled path as the heat exchange medium. Knowing the water flow rates, the quantity of heat being conducted was computed from the temperature rise in the water. A thermopile made of fluorethene, containing six iron-constantin thermocouples was used to measure the temperature rise of the water.

The temperature drops of the specimen and simulator (B) were measured with chromel-alumel thermocouples sealed into small holes with saureisen. The simulator or guard assembly (F), a brass tube wound with high resistance nichrome wire was cooled by water (5) as shown in order to effect the same temperature drop in the simulator and specimen. The cavity between the sample and simulator walls was filled with powdered Sil-O-Cel to minimize heat losses. Data were taken when the system reached steady state.

Other Testing and Calculation Methods

- 1) Density - gross volume measurements
- 2) Tensile Strength - ASTM B209-46T, 1946 Ed., Part 1B, p 572
- 3) Shear - ASTM C102-36, 1946 Ed., Part II, p 228

UNCLASSIFIED

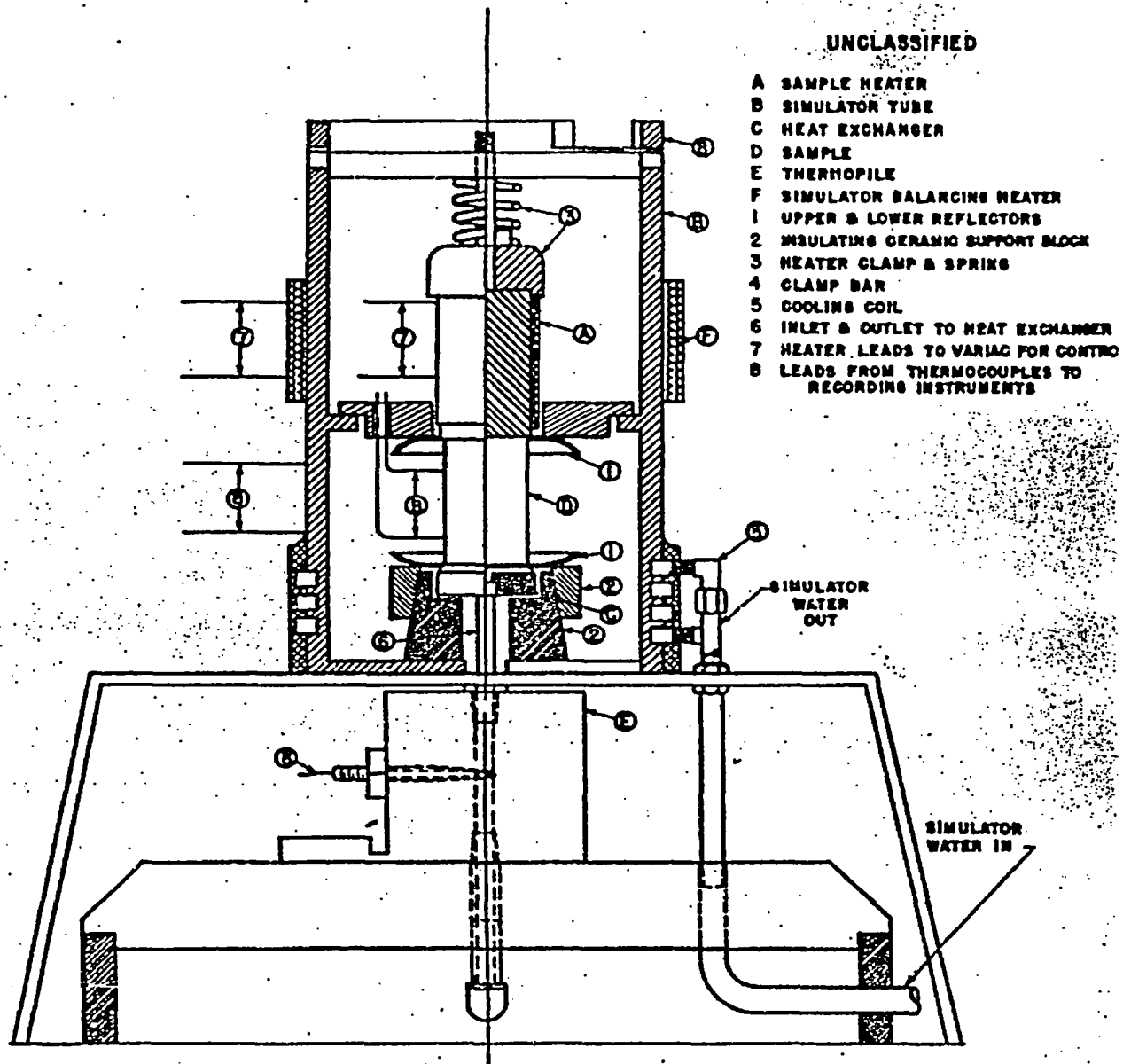


Fig. 1—Thermal conductivity apparatus.

Howard Perkins

9/9/55

**RESULTS OF A SURVEY ON THE
USE OF BORAL IN SHIELDING**

**A Paper Presented at
The Atomic Energy Commission Conference
on**

**Radiation Shielding
May 13 and 14, 1954
Knolls Atomic Power Laboratory
Schenectady, New York**

by

**Neil F. Ritchey
Atomic Energy Advisor
Reynolds Metals Company
Louisville, Kentucky**

RESULTS OF A SURVEY ON THE USE OF BORAL IN SHIELDING

Before discussing the results of the Boral survey, I want to make sure that everyone knows what Boral is. For the benefit of new members and guests here today who may not be familiar with Boral, I want to describe very briefly what it is.

Boral is an engineering shielding material that is used to absorb thermal neutrons. Essentially it is a mixture of boron carbide (B_4C) and aluminum, rolled into sheet. The mixture is not used bare in this form, however. It is clad with commercially pure aluminum.

Figure No. 1 shows schematically how ORNL produces Boral. There are no technical details in this sketch, because I only want to show the principle of Boral construction. To make this sketch correct, I would have to show the picture frame cladding around the edges.

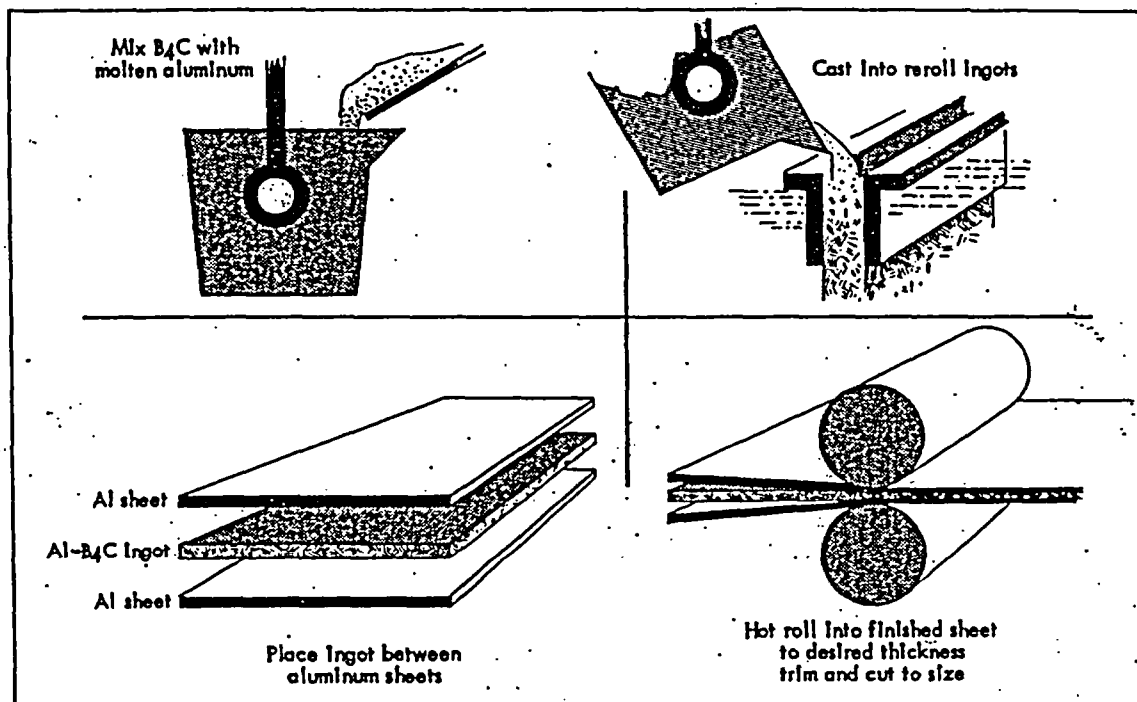


Figure 1

FLOW CHART FOR MAKING BORAL AT ORNL
(SEE ORNL 981 AND ORNL 242)

MAY 1954

You may not be interested in the detailed engineering properties of Boral. I do think you would like to know how Boral compares with other familiar metals. Figure No. 2 shows relative properties of Boral, Aluminum, Copper, Iron and Stainless Steel.

PROPERTY	BORAL	ALUMINUM (ANNEALED)	COPPER (ANNEALED)	IRON (ANNEALED)	STAINLESS STEEL (ANNEALED)
TENSILE STRENGTH (PSI)	5,000	13,000	32,500	38,500	80,000
ELONGATION (PERCENT)	0.4	45	37	45	55
THERMAL CONDUCTIVITY (BTU/IN/FT ² /LB/°F) (AT 200°F)	25	1,509 <i>25 = 1518</i>	2,700 <i>0.757 = 2832</i>	743 <i>0.144 = 519</i>	200
SPECIFIC HEAT BTU/LB/°F	.175	<i>145 = 226</i> .226	.09	.126	.150
DENSITY (GMS/CM ³)	2.5	2.7	8.9	7.8	8.0

Figure 2

PROPERTIES OF BORAL COMPARED TO
SEVERAL COMMON METALS
MAY 1954

You can see that Boral has low strength; it is brittle; the thermal conductivity is very low - in fact you might say it has high insulating value (k for concrete is about 12; wood is in the range 0.5 to 1.5).

Specific heat or heat capacity of Boral is in between the values for Iron and Aluminum. Its low density has advantages that may have more significance in aircraft shielding than land based reactors.

Figure No. 3 summarizes the results of our survey. The questions we asked are across the top of the chart. The replies received are listed under each column heading.

Most people visualize the use of Boral for stationary reactors component to the concrete shield. Mounting Boral against a flat concrete wall greatly minimizes the manufacturing problems. I have some design ideas to show you in the illustration to follow.

Several aircraft companies indicate that if Boral could be formed into contour shapes, considerable quantities might be used over the long range future. Specific suggested uses include the use of Boral in the form of fabricated boxes to enclose electronic equipment and other radiation sensitive devices. Aside from the reactor shield, some people believe ultimate use of Boral will be made to shield easily activated components of aircraft, particularly the engine.

COMPANIES AND ORGANIZATIONS QUERIED	APPLICATION AGAINST WALL	FABRICATED INTO VESSELS	MINIMUM BORON CONCENTRATION GMS/CM ²	MINIMUM TENSILE STRENGTH PSI.	PREFERRED WIDTH AND LENGTH	PREFERRED THICKNESS	COMMENTS ON QUANTITY, PRICE, ETC.
1	X		.18	5,000	4' X 8'	1/4"	SMALL QUANTITIES
2	X		.04	SELF SUPPORTING	2-4' X 8'	1/8" - 1/4"	3-4,000 SQ. FT. PER REACTOR
3	X		.10	---	---	1/4"	SHOULD BE COMPETITIVE TO LEAD EQUIVALENT
4	X		---	SELF SUPPORTING	4' X 6'	1/2"	~\$5 PER SQ. FT. - SMALL DEMAND
5	X	X	.10	STRONGER THE BETTER	NOT IMPORTANT	THIN AS POSSIBLE	---
6	X		.25	~ 3,000	4' X 8'	1/8"	\$2-\$5 PER SQ. FT. - SMALL DEMAND
7	X		.25	NOT IMPORTANT	4' X 8'	1/4"	SMALL DEMAND
8	X		.25	NOT IMPORTANT	SMALL WIDTHS O.K. SMALL SEAMS PERMISSIBLE	1/4"	500 SQ. FT. PER REACTOR NOT LARGE MARKET
9	X		.11 MINIMUM .05 NOT EFFICIENT	---	4' X 8'	THIN AS POSSIBLE	SMALL DEMAND
10	X	X	.11	TO PERMIT NORMAL HANDLING	3' X 8'	1/8" = 100 ATTN. 1/4" = 10,000 ATTN.	IN AVIATION SHIELD FOR ACCESSORIES AND ENGINE

Figure 3

RESULT OF MAY 1954 BORAL SURVEY

The minimum concentration of Boron believed necessary was quite well agreed upon. Most values were in the range 0.10 to 0.25 grams/cc. As a means of comparison, Boral containing 35% of B₄C by weight of 1/4" total thickness will contain approximately 0.254 gms/cc.

The survey showed that as long as Boral will support itself against a wall, and not fall apart during normal handling, potential users are satisfied.

The dimensions of the sheet are more important to the manufacturer than to you. I will only say that most survey replies stated that panels should be about 4' x 8' and 1/4" thick.

The conclusion I draw from the survey is that the physical and mechanical properties of Boral are satisfactory for stationary land base reactor shielding. For aircraft reactors your indications were that it would be desirable to improve the mechanical properties so that Boral could be formed into simple and semi-complex shapes. For use in shipboard reactors, Boral would not only have to be formed into complex shapes, but it would have to possess high shock resistance.

The most overwhelming agreement from replies to the survey was on the prediction of Boral's future. All except one company could not see a very bright future for Boral. The basis for prediction was the number of reactors that might be built in the future. I will agree that reactors are not going to be mass produced in the next 5 or 10 yrs. But after that it is anyone's guess. It is my opinion that Boral has not been fully considered in the light of new fabrication techniques common to aluminum technology today.

I want to show you several illustrations of recent developments in the aluminum industry. I don't have shield designs incorporating these new aluminum developments with Boral. My only reason for bringing them up at this meeting is to stir up ideas that someday you may recall.

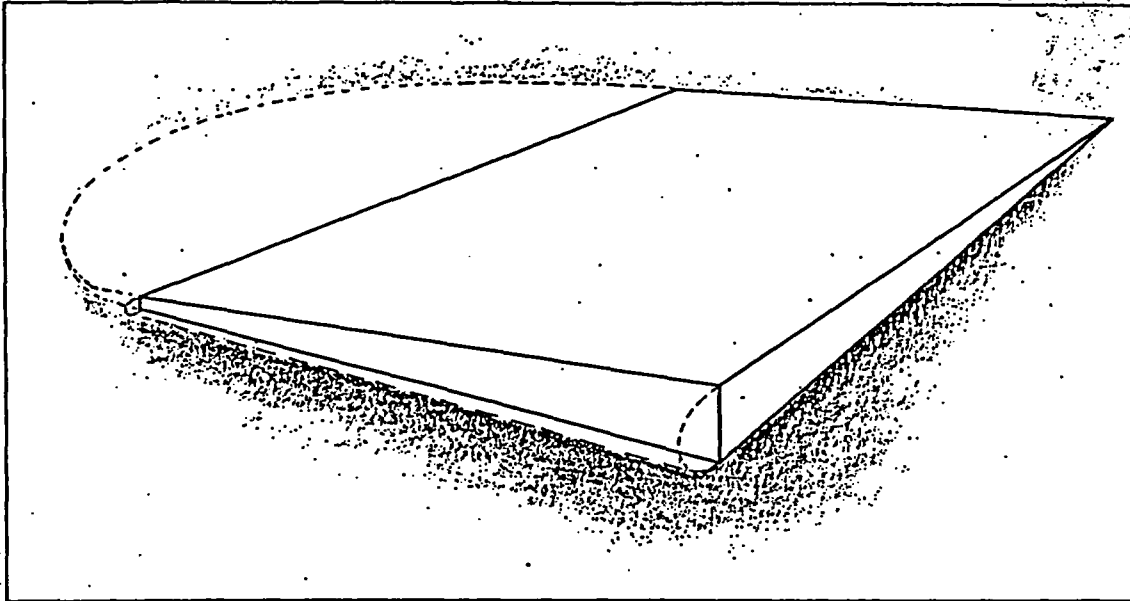


Figure 4
TAPERED ALUMINUM SHEET
MAY 1954

Figure No. 4 shows tapered sheet that the aluminum industry has been called to produce for high speed jets. Notice we outlined in the wing of a plane to give you an idea of how the sheet tapers in two directions. This product will be manufactured on a high production basis using a taper rolling technique.

Why do I bring it up here? Because here is a possibility for obtaining variable Boron concentration to meet cosine flux distribution. If Boral can be hot rolled, we ought to be able to convert it into tapered sheet. The cladding problem might be tough but not insurmountable. Perhaps you may have a problem someday that will make tapered Boral sheet look promising.

Figure No. 5 was made from a sketch presented by Helmer Enlund of the Detroit Edison Company. Mr. Enlund cautions against the use of Boral in flat contact with the bulk shield if heat removal is a problem.

I hope Mr. Enlund will correct me if I have incorrectly interpreted his reason for not wanting direct contact. Due to the irregularity of the concrete and possible inefficient bonding of the Boral to the concrete, cooling of the shield would be difficult.

At any rate, these two designs are good ideas for getting around the cooling problem.

I don't know myself how the heat developed in the bulk shield, due to primary gammas, compares to the heat resulting from secondary neutron capture gammas. I would think the answer to that question is important, because it tells us whether Boral is effective in suppressing a portion of shield heat.

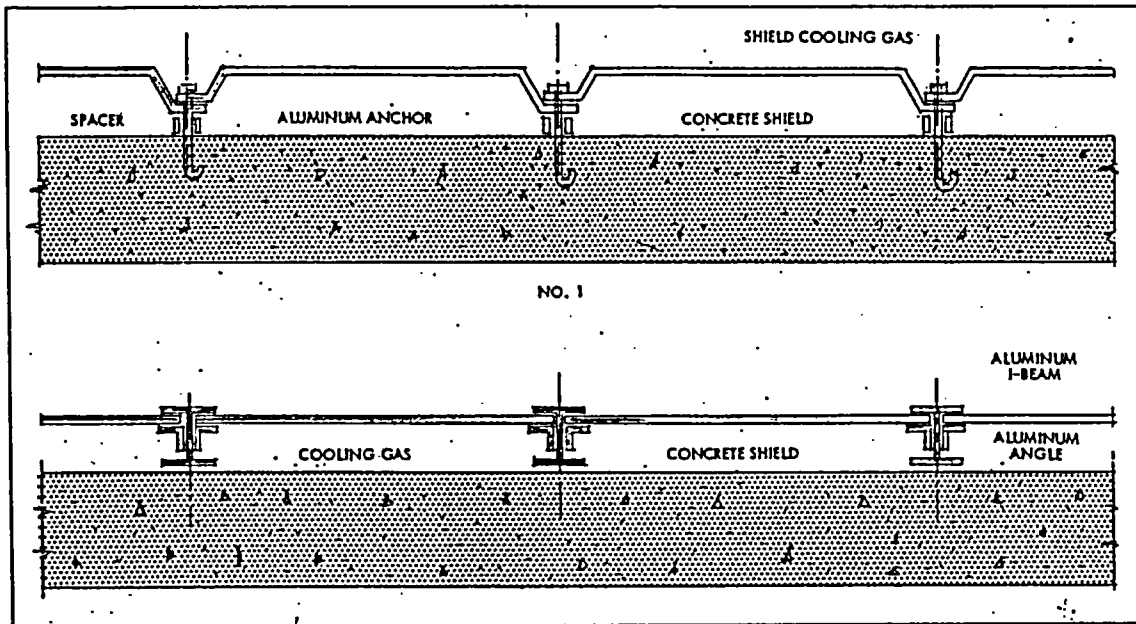


Figure 5

SUGGESTED BORAL SHIELD DESIGNS
FOR DEPRESSION OF HEAT INDUCED BY η - γ HEATING
SUBMITTED BY H. L. F. ENLUND, DETROIT EDISON CO.
MAY 1954

Figure 6 is a schematic chart depicting the principle of a new product called heat transfer sheet. The principle ought to lend itself very nicely to Boral.

What we do here is print a circuit on one sheet of aluminum using an anti-weld or non-bonding agent. Our newest facility now under construction will use the silk screen printing process for higher production.

Next, we lay another sheet over the first. Tack it around the edges - spot welding is satisfactory. Then we hot roll the two sheets to the finished size.

Where the circuit is printed the two sheets do not bond. The last step is to insert an air nozzle in one end of the circuit and expand.

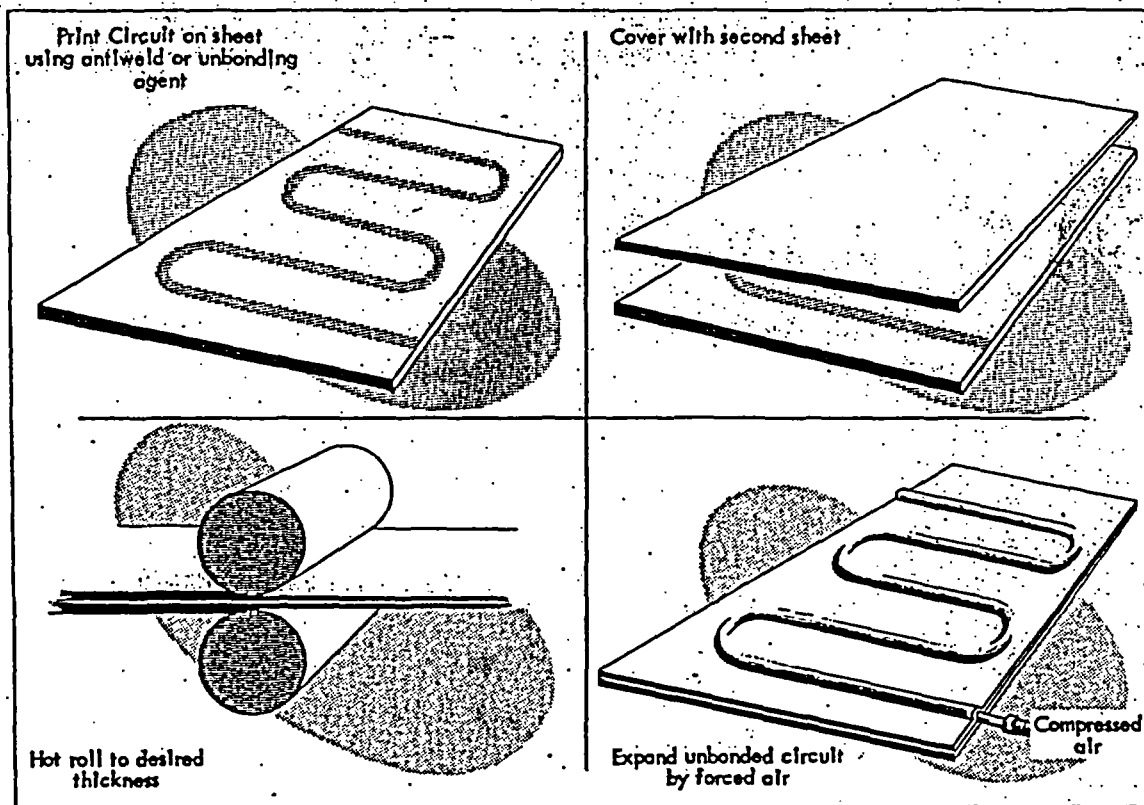


Figure 6

METHOD OF MANUFACTURING HEAT TRANSFER PLATES

(ROLL BONDED AND EXPANDED)

MAY 1954

The net result is sheet with built-in cooling coils ready for use.

Figures 7 and 8 show what can be done for stiffened sheet. Figure No. 7 is called integrally stiffened sheet. As you can see, it is first extruded into a tube. The tube is then slit longitudinally and straightened. The flattened section is about 30" wide. We have to extrude in the tube form first, because the largest extrusion presses today will only take shape within a 12" circumscribed circle.

Figure No. 8 illustrates the various roll passes necessary to produce rolled ribbed sheet. Both applications are stiffened aircraft skin.

To sum up, I think our survey shows that there is a definite place for Boral as an engineering material for shielding. It serves as a protector against high energy capture gamma ray generation. It will at the same time provide protection against induced activation.

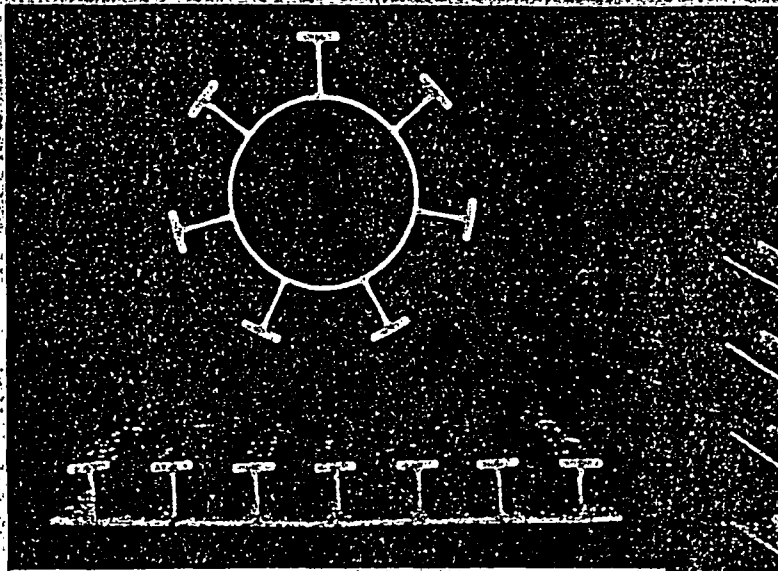


Figure 7

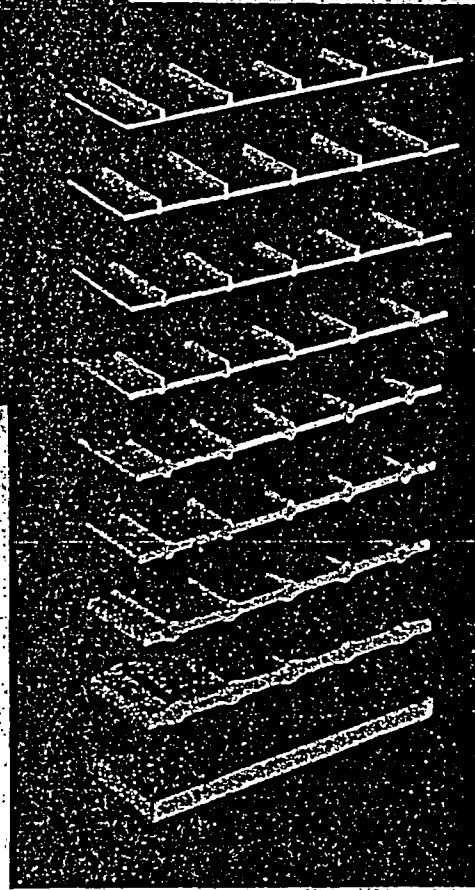


Figure 8

I believe more might be done with Boral if its fabricating and forming properties are evaluated more fully. More familiarity with new techniques in aluminum technology might lend impetus to design usefulness of Boral.

The relatively high cost of Boral can be brought down in proportion to the extent that its need grows. The future of reactor production and, therefore, the demand for neutron shields is bright. Just how bright and how far away that future is, we don't know.

I want to thank everyone who kindly took the time to answer our survey. To those interested people who I didn't contact, I sincerely hope you will report any comments or experience you have had with Boral, either in the discussion today or by letter at a later date.

How Channeling between Chunks Raises Neutron Transmission through Boral

By WALTER R. BURRUS*
Lockheed Aircraft Corp.
Marietta, Georgia

Boral is a mixture of boron carbide and aluminum encased between two thin layers of aluminum. Since boron carbide has a large $B^{10}(n,\alpha)Li^7$ cross section at thermal-neutron energies and the accompanying gamma ray is only 0.42 Mev, boral is valuable for use in nuclear shields where a large thermal flux must be absorbed without the production of hard gammas.

However, conventional calculations of the absorption of boral do not consider the channeling of neutrons through the spaces between the boron-carbide chunks. The results of a calculation for the transmission of $\frac{3}{8}$ -in. and $\frac{1}{4}$ -in. boral that considers the channeling effect are in much better agreement with experimental data than earlier calculations neglecting channeling.

Calculation

The transmission of a slab consisting of randomly distributed chunks of average chord l (normally incident monoenergetic radiation) is given by

$$T = (1 - VF)^{1/l}$$

where T is fractional transmission, V is the volume fraction of the slab occupied by chunks, F is the average absorption of a single chunk, t is the thickness of the slab, and l is the average chord of a chunk.

The average transmission of one layer of the slab of thickness l is $1 - VF$. Since the chunks are assumed to be randomly placed, adjacent layers are statistically independent, and the overall transmission is the product of the transmission of t/l sublayers.

If the chunks are nearly spherical (l)

$$F = \frac{2}{(2r\Sigma)^2} \left[\frac{1}{2}(2r\Sigma)^2 - 1 + (1 + 2r\Sigma)e^{-2r\Sigma} \right]$$

* PRESENT ADDRESS: Physics Department, Ohio State University, Columbus, Ohio.

TABLE 1—Size Distribution for B_4C Chunks

Mesh	Average particle diameter (in.)	$l (= \frac{4}{3}r)$ (in.)	Volume fraction
20-30	0.038	0.0253	17%
36-46	0.024	0.0160	11%
60-70	0.016	0.0107	6%
80-120	0.009	0.0060	6%

where Σ is the linear attenuation coefficient of chunk material and r is the radius of a sphere (or equivalent radius on the basis of volume).

For a chunk of any shape without cavities a theorem due to Gauss states that the average chord l is given by $l = 4v/s$, where v is the volume of the chunk and s is its total surface area. For a sphere this gives $l = \frac{4}{3}r$.

If $VF \ll 1$, the transmission is approximately $T \approx e^{-VF/l} \approx e^{-VF\Sigma_{eff}}$. From the equations for F and l we can verify that for the limits of opaque and almost transparent chunks $\Sigma_{eff} = F/l \approx 1/l$ if $\Sigma \gg 1$ and $\Sigma_{eff} = F/l \approx \Sigma$ if $\Sigma \ll 1$. It should be noted that the effective linear attenuation coefficient for opaque chunks is $1/l$ and does not depend on Σ since all the trans-

TABLE 2—Theoretical and Experimental Neutron Transmission through Boral*

Sample	Neutron source	Detector	Experimental transmission	Channeling calculation	Conventional calculation	Ref.
$\frac{3}{8}$ -in. Alcoa (two samples)	Collimated beam from ORNL graphite reactor	Current detector (LiI xtal Cd difference)	$7.0 \times 10^{-3} \pm 40\%$ (preliminary value)	9.6×10^{-3}	1.3×10^{-3}	5
$\frac{1}{4}$ -in. Alcoa	"	"	5.0×10^{-3} (preliminary value)	7.7×10^{-3}	4.8×10^{-4}	9
$\frac{3}{8}$ -in. Brooks and Perkins	Water thermal column of ORNL graphite reactor	Thin indium foil	7.0×10^{-3} 10^{-2}	2.7×10^{-3} **	2.0×10^{-3}	4
$\frac{3}{8}$ -in. ORNL	"	"	9.4×10^{-3} 10^{-2}	2.7×10^{-3}	2.0×10^{-3}	4
$\frac{1}{4}$ -in. Brooks and Perkins	"	"	5.6×10^{-3}	1.7×10^{-3}	4.5×10^{-4}	4
$\frac{1}{4}$ -in. ORNL	"	"	7.6×10^{-3}	1.7×10^{-3}	4.5×10^{-4}	4

* Since the first two samples were measured with a different neutron source and detector, there is no direct comparison with the others.

** There may be some more errors in this Table, but the figures 1, 2, and 3 appear to be correct.

For an isotropic angular distribution of neutrons upon Boral, the transmission for neutron current is different from the transmission for neutron flux; thus the transmission is calculated for both current and flux detectors, (e.g. think foils and thin foils).

mitted radiation channels around the chunks.

If the chunks consist of several groups with average chords l_1, l_2, \dots (and corresponding $V_1, V_2, \dots, \Sigma_1, \Sigma_2, \dots$), the transmission can be generalized to give $T \approx \exp -t (V_1 \Sigma_{a1} + V_2 \Sigma_{a2} + \dots)$, where $V_i^* = V_i / (1 - \text{volume fraction of all larger chunks})$. It is necessary to multiply V_i by $1 / (1 - \text{volume fraction of all larger chunks})$ to account for the crowding together of the smaller chunks by the larger ones.

This equation treats the distribution of chunks as if the chunks of various sizes were in separate layers. The result is always too small since it ignores voids that would be present in a layer if the larger chunks were separated out. Nevertheless, the result is correct for limiting cases of opaque and transparent chunks and is qualitatively correct in any case.

To calculate the transmission of $3/8$ -in. boral, it was assumed that the chunks of boron carbide were spherical. The size distribution shown in Table 1 is typical (Σ) of 20-100-mesh boron carbide usually used in boral. Other parameters used for the calculation are $\Sigma = 190.5 \text{ in.}^{-1}$ at 2,200 m/sec (S) (neglecting attenuation in aluminum), $t = 0.085 \text{ in.}$ (not including aluminum cladding), $V = 40\%$ (not including aluminum cladding) $\approx 25\%$ over all.

The resulting transmission from the last equation is plotted against energy in Fig. 1. (It is assumed that Σ is proportional to $1/\text{velocity}$.) The conventional calculation, assuming no channeling, is shown for comparison. Note that the transmission approaches the opaque-chunk limit at the low-energy end of the scale.

Since the chunks were assumed to be randomly distributed, there is no preferred direction for transmission. The transmission for neutrons incident at an angle θ with the normal can be found by replacing t by $t/\cos \theta$, the slant penetration. Figure 2 shows the transmission averaged over incident angles for an isotropic incident flux. Since transmitted neutron current in the forward direction is relatively greater than the isotropic flux, the range is carried out for both types of detectors. Figure 3 shows the results for $1/4$ -in. boral.

A more extensive description of the method is given in an ORNL report now being published (6).

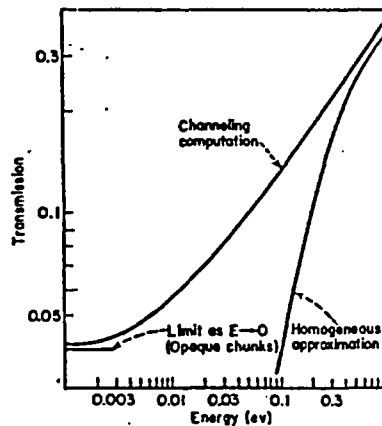


FIG. 1. Channeling computation departs from homogeneous approximation at low energies. Computations are for $3/8$ -in. boral with typical 20-100-mesh B,C distribution

Experimental Verification

Experiments performed to test boral have been gross-transmission measurements using various neutron detectors. It is possible to compare the results with calculations only if the angle and energy distribution of incident neutrons and the angle and energy sensitivity of the detector are known. The table on page 91 attempts to compare the calculations with several experiments performed at ORNL.

For the calculations it was assumed that the thermal-neutron spectrum was Maxwellian and that the angular distribution from the thermal column was of the Fermi type (7). Effective temperature of the neutrons was taken as room temperature, 293.6° K. The channeling calculations are an average of the results of Figs. 2 and 3 over the Maxwellian spectrum for the appropriate detector. The conventional calculations are based on the thermal-neutron absorption coefficients discussed by Zahn and Laporte (8). These coefficients take into account both spectrum hardening and angular distribution.

In the table the channeling calculation is too great in most cases by a factor of 2 or 3. The result of the conventional calculation is too small by more than a factor of 10 for $1/4$ -in. samples.

A considerable difficulty in accurately comparing experiment and calculation is the lack of standardization of boral. After initial development, fabrication was standardized, but the ingot size, cladding thickness, fraction of boron carbide, and particle-size dis-

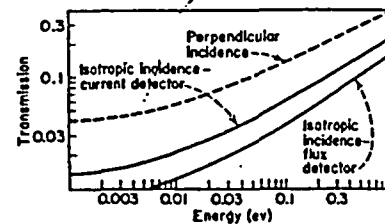


FIG. 2. Transmission of $3/8$ -in. boral with perpendicular incidence compared with current and flux from isotropic incidence

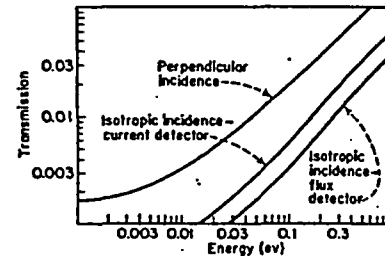


FIG. 3. Computations of Fig. 2 produce these results for $1/4$ -in. boral

tribution have not been rigorously fixed. In comparing experiments and calculations one must determine or guess the fractional weight of boron carbide, cladding thickness, and the size distribution.

* * *

This work was initiated at the Lid Tank Shielding Facility of the Oak Ridge National Laboratory while the author was on loan from the Wright Air Development Center Materials Laboratory. The author would like to acknowledge the assistance of R. W. Pelle and J. R. Smolen at ORNL and the cooperation of Alan Liebschutz at Lockheed and Stanley Szaulewicz at Wright Air Development Center. The basic method employed makes use of suggestions proposed by R. R. Coveyou and N. M. Smith at ORNL in 1947.

BIBLIOGRAPHY

1. K. M. Case, F. de Hoffmann, G. Placzek, "Introduction to the Theory of Neutron Diffusion," vol. 1, section 10 (U. S. Government Printing Office, 1954)
2. Norton Co., Worcester, Mass., "A Handbook on Boron Carbide, Elemental Boron and Other Stable, Boron-Rich Materials" (1955)
3. D. J. Hughes, J. A. Harvey, Neutron cross sections, BNL-325 (1955)
4. R. O. Maak, B. E. Prince, F. C. Rekemeyer, Boral attenuation characteristics, MIT Engineering Practice School Memo EPS-X-282 (1957)
5. J. Krisan, Thermal cross section and homogeneity test of boral and other shielding materials, ORNL BSF Monthly Report (Aug. 23, 1956)
6. W. R. Burrus, Transmission through boral, ORNL (to be published)
7. E. Fermi, *Rivista di Fisica*, 7, 3 (1936); H. A. Bethe, *Rev. Mod. Phys.* 9, 133 (1937)
8. C. T. Zahn, O. Laporte, *Phys. Rev.* 52, 67 (1935)
9. G. de Saussure, A nuclear test for thermal neutron absorbing material (Information Meeting on Thermal Neutron Shielding Materials, Oak Ridge National Laboratory, Sept. 20, 1956)

MASSACHUSETTS INSTITUTE OF TECHNOLOGY
ENGINEERING PRACTICE SCHOOL
UNION CARBIDE NUCLEAR COMPANY
A DIVISION OF UNION CARBIDE AND CARBON CORPORATION

MEMORANDUM

EPS-X-282

KT-251

November 27, 1956

TO: E.P. Blizard
FROM: R.O. Maak, B.E. Prince, and P.C. Rekemeyer
SUBJECT: Boral Radiation Attenuation Characteristics

DISTRIBUTION:

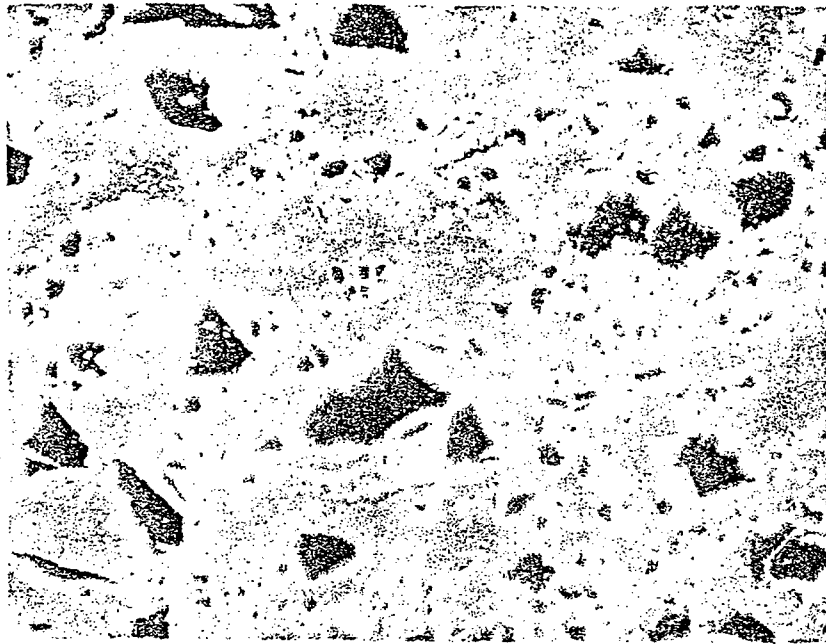
E.P. Blizard (10)	J.E. Vivian
T.V. Blosser	T.F. Wagner
J.A. Cox	C.D. Zerby
F.O. Lewis	ORGDP Plant Records (2)
F.C. Maienschein	ORNL Laboratory Records (4)
R.C. Reid	M.I.T. Practice School Files (10)

INTRODUCTION

Boral, a mixture of boron carbide and aluminum encased between two thin layers of aluminum, has many uses as a thermal neutron shielding material. Since the $B^{10}(n,\alpha) Li^7$ reaction has such a large cross section of 735 barns at thermal energies and the accompanying gamma ray is only 0.42 Mev, boral is uniquely suitable for shields where a large thermal neutron flux must be absorbed without production of hard gammas, e.g., inner section of reactor shields, shutters for thermal columns, and instrumentation.

Figures 1 and 2 are dark field illuminated magnified photographs of a cross section of sample boral manufactured by the Oak Ridge National Laboratory. Figures 3 and 4 are photographs of a sample manufactured by Brooks and Perkins in an attempt to improve on the quality of this material. Since the boron carbide is heterogeneously dispersed throughout the aluminum, the gamma ray linear attenuation coefficient and the thermal neutron absorption cross section are a function of the amount of boron carbide content, its particle size, and the degree of dispersion. This investigation is concerned with the experimental determination of the attenuation characteristics of these two samples, and an attempt to theoretically predict, using a Monte Carlo type calculation, the effective macroscopic thermal neutron cross section.

*Duke
Studen*

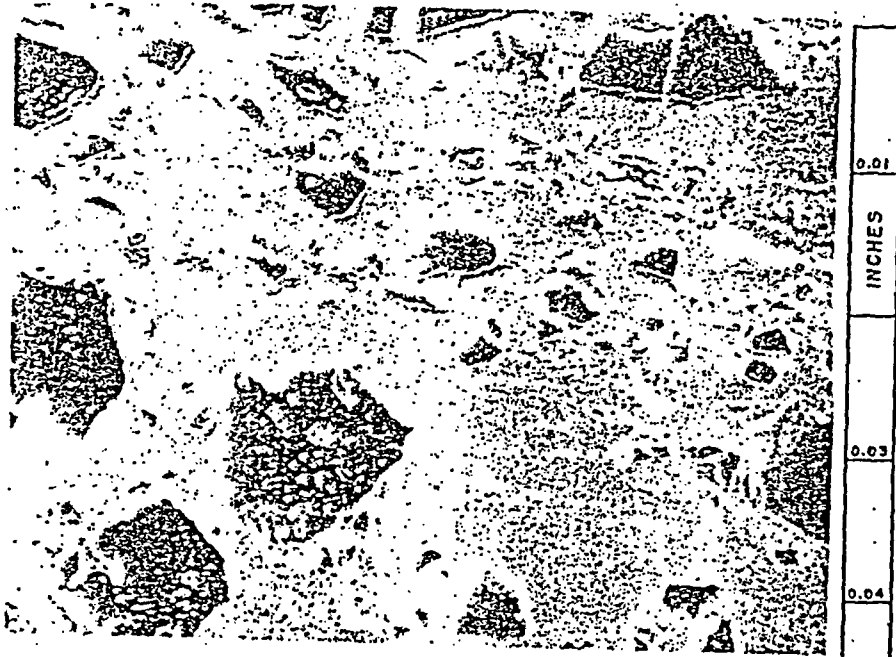


0.01
INCHES
0.03
0.04

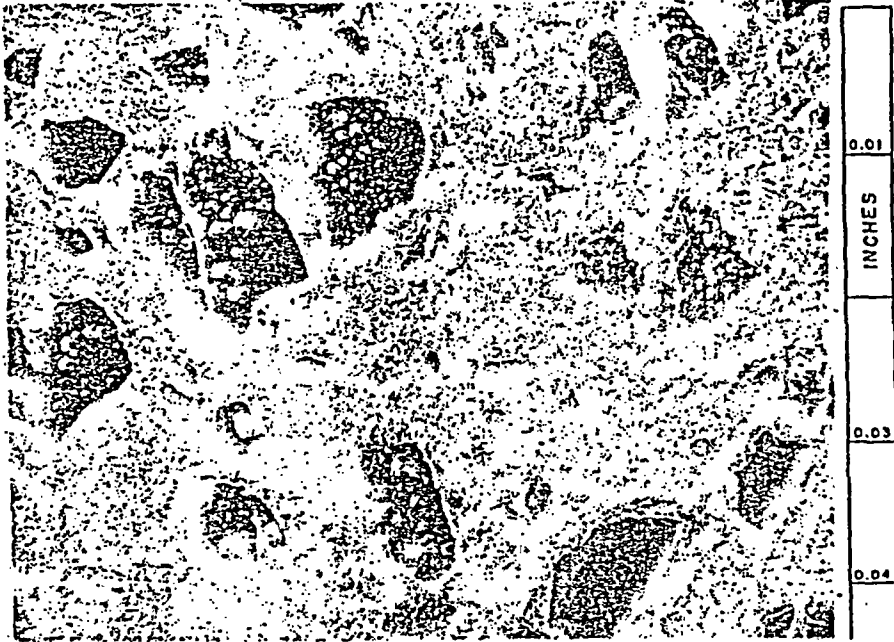


0.01
INCHES
0.03
0.04

MASSACHUSETTS INSTITUTE OF TECHNOLOGY ENGINEERING PRACTICE SCHOOL UNION CARBIDE NUCLEAR COMPANY <small>A Division of Union Carbide and Carbon Corporation</small>			
Dark Field Illuminated Microphotographs of unetched 1/8 inch ORNL samples			
DATE	DRAWN BY	FILE NO.	FIG.
11/27/56		EPS-X-282	1



MASSACHUSETTS INSTITUTE OF TECHNOLOGY ENGINEERING PRACTICE SCHOOL UNION CARBIDE NUCLEAR COMPANY <small>A Division of Union Carbide and Carbon Corporation</small>			
Dark Field Illuminated Microphotographs of Unetched 1/4 inch ORNL samples			
DATE 11/27/56	DRAWN BY	FILE NO. EPS-X-282	FIG. 2



MASSACHUSETTS INSTITUTE OF TECHNOLOGY ENGINEERING PRACTICE SCHOOL UNION CARBIDE NUCLEAR COMPANY <small>A Division of Union Carbide and Carbon Corporation</small>			
Dark Field Illuminated Microphotographs of Unetched 1/8 inch Brooks and Perkins samples			
DATE 11/27/56	DRAWN BY	FILE NO. EPS-X-282	FIG. 3



MASSACHUSETTS INSTITUTE OF TECHNOLOGY ENGINEERING PRACTICE SCHOOL UNION CARBIDE NUCLEAR COMPANY <small>A Division of Union Carbide and Carbon Corporation</small>			
Dark Field Illuminated Microphotographs of Unetched 1/4 inch Brooks and Perkins samples			
DATE 11/27/56	DRAWN BY	FILE NO. EPS-X-282	FIG. 4

PROCEDUREGamma Ray Attenuation

The gamma ray linear attenuation coefficient, μ , was determined by measuring the attenuation of the 0.661 Mev gamma rays from a ten curie cesium-137 source for various thicknesses of the two samples. Readings were taken on an ion chamber at distances of 10, 15, and 20 cm from the top of the source container, and μ determined as the slope of a plot of the log of the counter reading versus plate thickness.

An indication of the effect of non-homogeneity of the boral on γ ray attenuation was obtained by taking x-rays of the two samples.

Neutron Attenuation

Experimental:

The attenuation of thermal neutrons was experimentally determined by activating indium foils secured to both sides of a boral sample placed in the water thermal column of the ORNL graphite reactor. A removal cross section, Σ , was defined by the equation $I = I_0 e^{-\Sigma x}$, where I and I_0 are the upward neutron currents measured by the indium foils. Only upward moving neutrons were detected since the foils were backed with a cadmium cover to remove any thermal neutrons diffusing downward.

Theoretical:

The activation of an indium foil placed in back of an irradiated sample may be determined by solving the integral,

$$Z = \frac{\int_{\Omega/A} F(\underline{\Omega}) e^{-\Sigma_b x_p^b(\underline{\Omega}, A) - \Sigma_a \left(\frac{t_p}{\cos \theta} - x_p^b(\underline{\Omega}, A) \right) \left(1 - e^{-\frac{\Sigma_f t_f}{\cos \theta}} \right) d\Omega}{\int dA}$$

where Z = neutrons/sec-cm² absorbed by foil.

$F(\underline{\Omega})$ = thermal neutrons/unit solid angle, sec.

x_p^b = thickness of B_4C seen by a neutron.

Σ_b = macroscopic total thermal cross section for boron carbide.

Σ_a = macroscopic total thermal cross section for aluminum.

Σ_f = macroscopic total thermal cross section for indium.

$\underline{\Omega}$ = unit vector in direction of neutron velocity.

t_p = thickness of boral plate.

t_f = thickness of indium foil.

θ = angle the neutron path makes with the normal to the plate.

A = area of the plate.

This integral was solved by random sampling of the variables θ and A , and actually measuring $x_p^b(\theta, A)$ using a magnified picture of an 1/8" ORNL sample cross section.

The activation of the foil without the plate was analytically calculated from the expression.

$$Z = \int_{\underline{\Omega}} F(\underline{\Omega}) (1 - e^{-\Sigma_f t_f / \cos \theta}) d\underline{\Omega}$$

The ratio of $Z/Z_0 = R$ should be the ratio of the foil readings and an effective cross section may be determined by $R = e^{-\Sigma x}$.

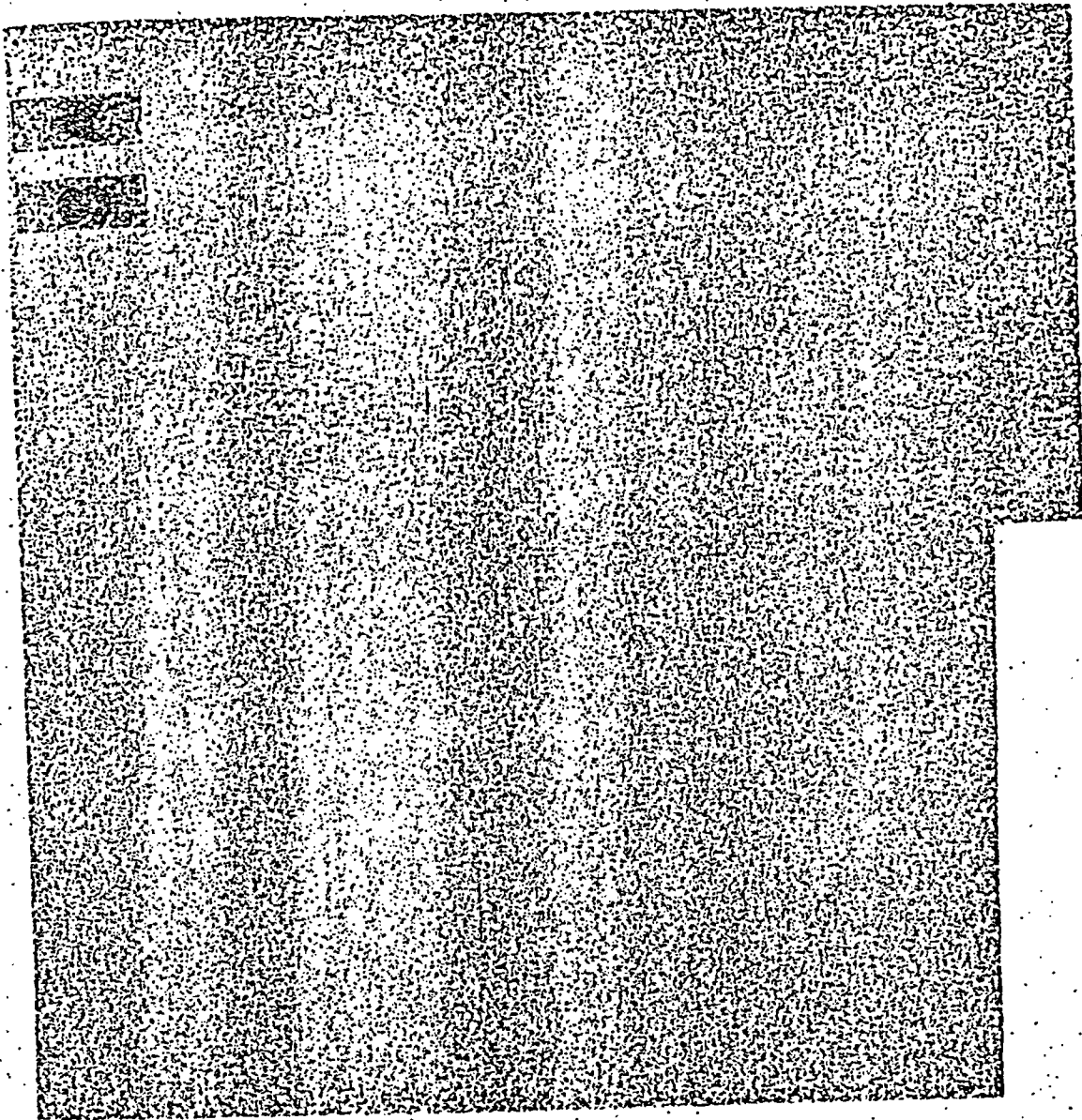
A complete description of the method followed in using this procedure along with the derivation of an expression for $F(\underline{\Omega})$ is given in the Appendix.

RESULTS

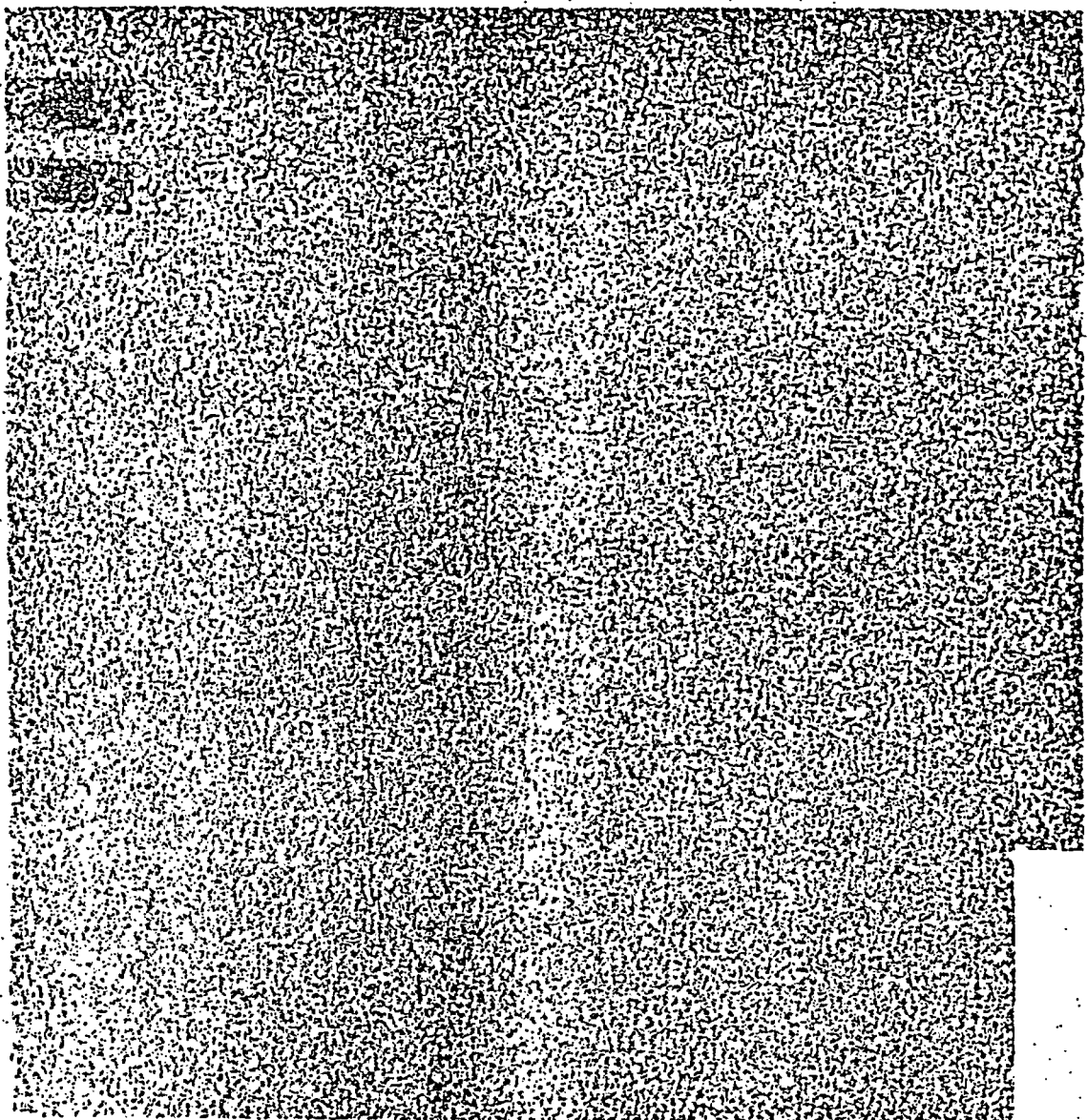
The results of the experimental determination of the gamma ray linear attenuation coefficient gave a μ of 0.183 cm^{-1} for the Brooks and Perkins sample and a μ of 0.193 cm^{-1} for the ORNL sample. For pure 2S aluminum, a coefficient of 0.202 cm^{-1} was obtained.

X-ray pictures of the two samples are shown in Figures 5 through 8; where $B_{14}C$ particles are shown white.

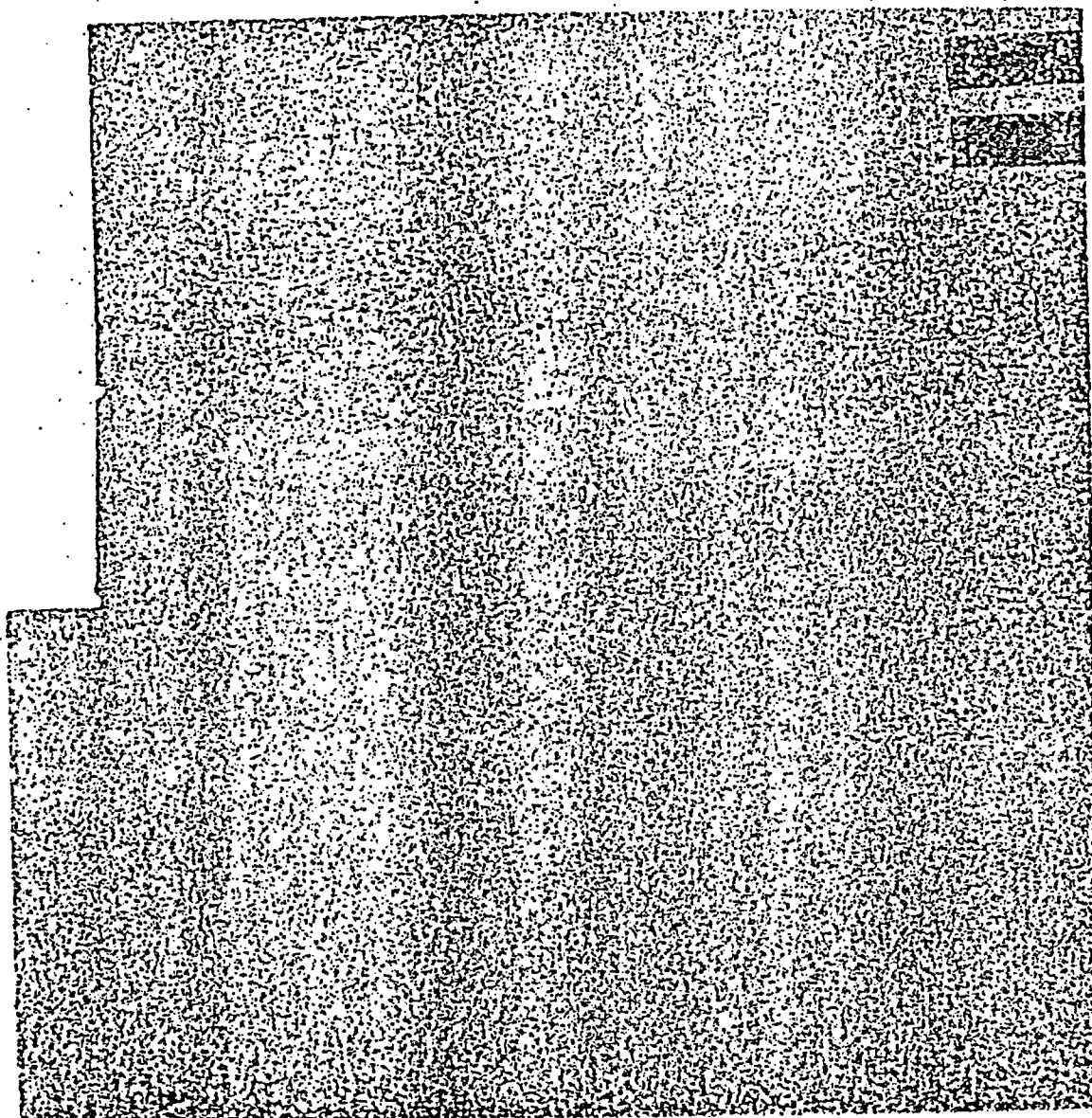
The results of the experimental determination of an effective neutron removal cross section are shown in Table I.



MASSACHUSETTS INSTITUTE OF TECHNOLOGY ENGINEERING PRACTICE SCHOOL UNION CARBIDE NUCLEAR COMPANY <small>A Division of Union Carbide and Carbon Corporation</small>			
X-Ray Photograph of 1/8 inch ORNL Sample			
DATE 11/27/56	DRAWN BY	FILE NO. EPS-X-282	FIG. 5



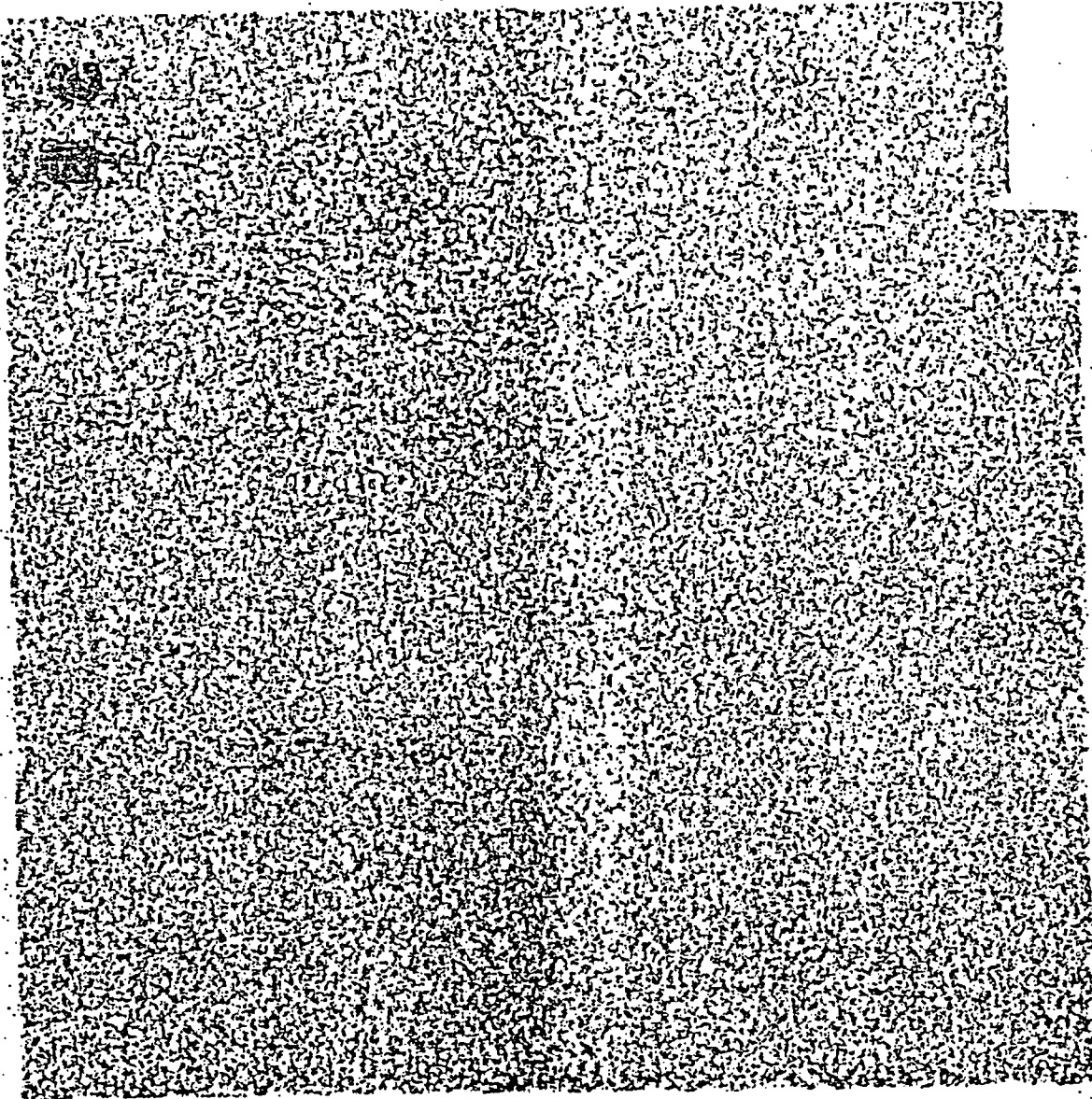
MASSACHUSETTS INSTITUTE OF TECHNOLOGY ENGINEERING PRACTICE SCHOOL UNION CARBIDE NUCLEAR COMPANY <small>A Division of Union Carbide and Carbon Corporation</small>			
X-Ray Photograph of 1/4 inch ORNL Sample			
<small>DATE</small> 11/27/56	<small>DRAWN BY</small>	<small>FILE NO.</small> EPS-X-282	<small>FIG.</small> 6



MASSACHUSETTS INSTITUTE OF TECHNOLOGY
ENGINEERING PRACTICE SCHOOL
UNION CARBIDE NUCLEAR COMPANY
A Division of Union Carbide and Carbon Corporation

X-Ray Photograph of 1/8 inch
Brooks and Perkins Sample

DATE	DRAWN BY	FILE NO.	FIG.
11/27/56		EPS-X-282	7



MASSACHUSETTS INSTITUTE OF TECHNOLOGY ENGINEERING PRACTICE SCHOOL UNION CARBIDE NUCLEAR COMPANY <small>A Division of Union Carbide and Carbon Corporation</small>			
X-Ray Photograph of 1/4 inch Brooks and Perkins Sample			
DATE 11/27/56	DRAWN BY	FILE NO. EPS-X-282	FIG. 8

TABLE I

Sample	$\Sigma_{\text{removal}} \text{ cm}^{-1}$
1/8" Brooks and Perkins	15.6
1/8" ORNL	14.7
1/4" Brooks and Perkins	11.8
1/4" ORNL	11.3

The calculated removal cross section for the 1/8" ORNL sample using the Monte Carlo technique gave Σ_{removal} of 13.4 cm^{-1} .

Σ_{removal} for a homogeneous mixture of boron carbide and aluminum containing 25% B_4C by volume is 18.9 cm^{-1} .

DISCUSSION OF RESULTS AND CONCLUSIONS

Since the neutron attenuation experiments were not conducted in "good geometry", the current does not fall off at an exponential rate given by $I_0 e^{-\Sigma x}$. This is due to the neutrons entering the boral at all different angles; thus the average neutron will pass through an amount of boral greater than just the thickness, x . This is indicated in the results by a Σ_{removal} for the 1/8" sample larger than that for a 1/4" sample. The first 1/8" of a boral sheet is clearly more effective in removing neutrons than the next 1/8". This effective removal cross section, although it does not have a precise physical significance may be used, however, to obtain an indication of neutron attenuation. A good estimate of the true thermal neutron cross may be obtained by linear extrapolation of the results of the 1/8" and 1/4" thick samples to zero thickness. This gives a value of $\Sigma_a = 18.1 \text{ cm}^{-1}$ for the ORNL boral and $\Sigma_a = 19.4 \text{ cm}^{-1}$ for the Brooks and Perkins sample, both in good agreement with the Σ_a obtained by homogenization.

The good agreement between the experimental Σ_{removal} of 14.7 and Monte Carlo calculated value of 13.4 cm^{-1} for the 1/8" ORNL sample demonstrates that these removal cross sections may be predicted fairly accurately by this procedure. The Monte Carlo type calculation has its disadvantages, however, in that it is tedious and time consuming, and electronic computers are of little help. The measurement of x_p^b , the distance a neutrons "sees", must be determined visually.

Robert O. Maak
Robert O. Maak

Blynn E. Prince
Blynn E. Prince

Peter C. Rekemeyer
Peter C. Rekemeyer

APPENDIX

A. Angular Distribution of Neutrons from Thermal Column (6)

An expression is derived below for $F(\underline{\Omega})$, the angular distribution of neutrons from the top of the graphite thermal column. The derived distribution should closely approximate the physical case, and can be readily applied in a hand Monte Carlo calculation (Appendix B).

The graphite thermal column is shown schematically in Figure 9. The boron sample is placed in close proximity to the top of the column and will be assumed to be at $w = 0$. The thermal neutron flux in the column is well represented by an exponential decrease in the vertical direction and a cosine variation in the horizontal x, y plane (2). Since the center of the column is several diffusion lengths from the x, y boundaries, leakage in these directions will be neglected, i.e., the column is assumed infinite in the x, y plane. Then,

$$\phi = \phi_0 e^{-k w} \quad (1)$$

where k is determined experimentally and ϕ_0 is the flux at the top of the fuel region.

The scattering collision density in the graphite is,

$$H(w) = \Sigma_s \phi_0 e^{-k w} \text{ collisions/cm}^3\text{-sec} \quad (2)$$

Then the number of scattering collisions per sec in the volume element, dV , is $H(w) dV$. If the scattering is assumed isotropic, the scattered neutrons will leave dV equally in all directions. The number crossing unit area of a sphere of radius r about dV is:

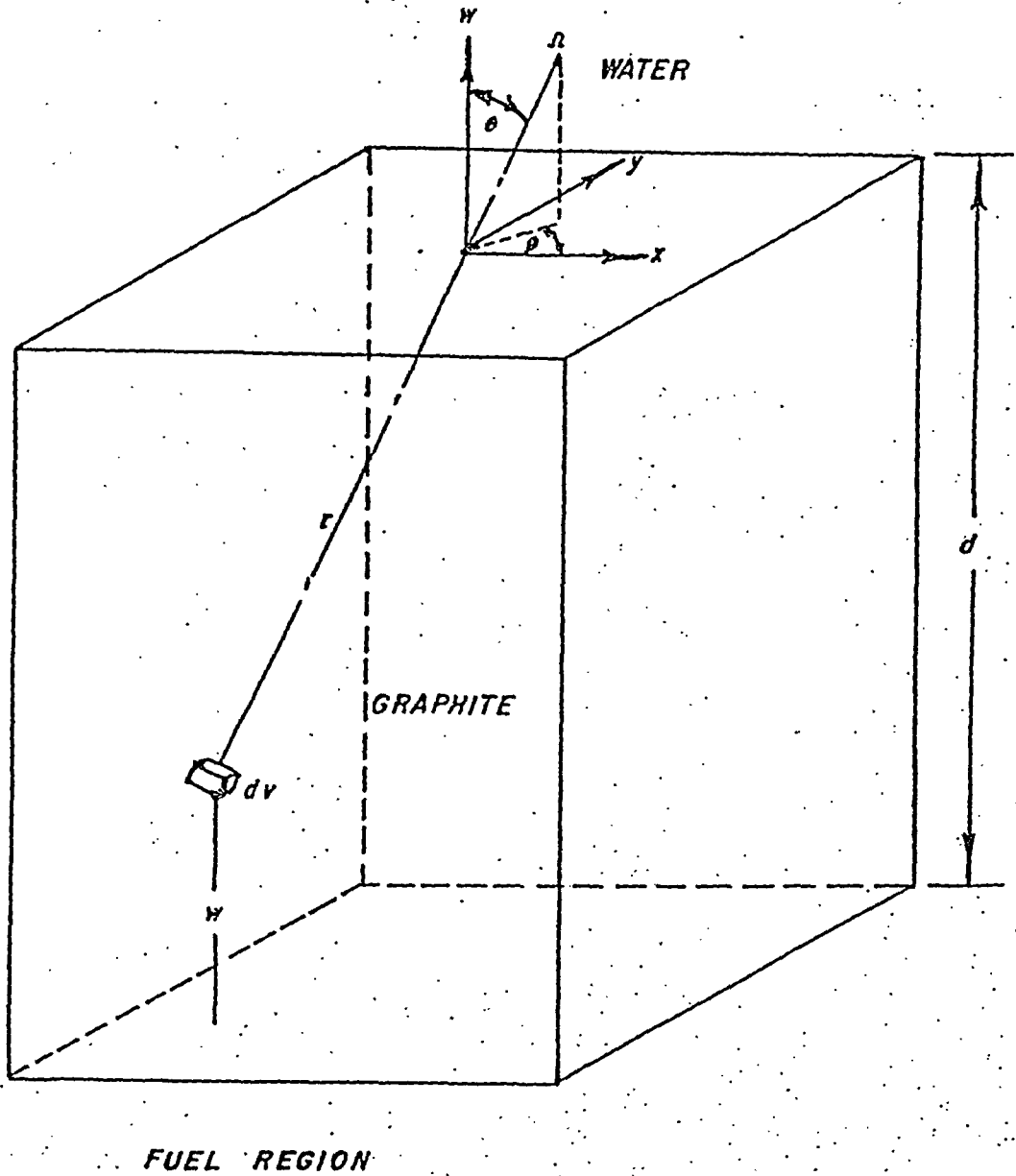
$$\frac{H(w) dV e^{-\Sigma r}}{4\pi r^2} \text{ neutrons/cm}^2\text{-sec} \quad (3)$$

The corresponding number crossing unit area in the x, y plane about the origin and moving in the direction $\underline{\Omega}$ is given by multiplying (3) by $\cos \theta$. Integration over the volume of the graphite results in the total outward neutron current S_0 .

$$S_0 = \int_V \frac{dV H(w) e^{-\Sigma r} \cos \theta}{4\pi r^2} \text{ neutrons/cm}^2\text{-sec} \quad (4)$$

If the neutron current were isotropic, the angular distribution would be given by:

$$F_{\text{isotropic}}(\underline{\Omega}') = \frac{S_0}{2} = \text{(neutrons per cm}^2\text{-sec, moving in the direction } \underline{\Omega}' \text{ per unit solid angle)} \quad (5)$$



MASSACHUSETTS INSTITUTE OF TECHNOLOGY
 ENGINEERING PRACTICE SCHOOL
 UNION CARBIDE NUCLEAR COMPANY
A Division of Union Carbide and Carbon Corporation

*SCHEMATIC DIAGRAM OF
 THERMAL COLUMN*

DATE 11-27-56	DRAWN BY R.O.M.	FILE NO. EPS-X-282	FIG. 9
------------------	--------------------	-----------------------	-----------

The actual distribution from the column follows by writing the contribution to $F(\underline{\Omega}')$ from dV :

$$\begin{aligned} dF(\underline{\Omega}') &= \frac{H(w) e^{-\Sigma r} \cos \theta}{4\pi r^2} \frac{f(\underline{\Omega} - \underline{\Omega}') dV}{2\pi} \quad (6) \\ &= (\text{neutrons per cm}^2\text{-sec from } dV \text{ going in the} \\ &\quad \text{direction } \underline{\Omega}' \text{ per unit solid angle)} \end{aligned}$$

In spherical coordinates $dV = r^2 \sin \theta d\theta d\phi dr = r^2 dr d\underline{\Omega}$. Thus,

$$F(\underline{\Omega}') = \int_r dr \int_{\underline{\Omega}} d\underline{\Omega} H(w) e^{-\Sigma r} \cos \theta f(\underline{\Omega} - \underline{\Omega}') \quad (7)$$

The Dirac delta function has the property (1),

$$f(\underline{\Omega} - \underline{\Omega}') = 0, \quad \underline{\Omega} \neq \underline{\Omega}' \quad (8)$$

and

$$\int_{4\pi} f(\underline{\Omega} - \underline{\Omega}') d\underline{\Omega} = 1 \quad (9)$$

where the integration variable $\underline{\Omega}$ ranges over $\underline{\Omega}'$.

In spherical coordinates (9) becomes,

$$\int_{\phi=0}^{2\pi} \int_{\theta=0}^{\pi/2} f(\cos \theta - \cos \theta') f(\phi - \phi') \sin \theta d\theta d\phi = 1 \quad (10)$$

Rewriting (7) explicitly, noting $w = d - r \cos \theta$,

$$\begin{aligned} F(\underline{\Omega}') &= \int_0^{2\pi} d\phi' \int_0^{\pi/2} d\theta' \int_0^{d/\cos \theta'} dr \frac{\Sigma_s \phi}{8\pi^2} e^{-k(d - r \cos \theta) - \Sigma r} \\ &\quad \cos \theta \sin \theta f(\cos \theta - \cos \theta') f(\phi - \phi') \quad (11) \\ &\quad 0 \leq \theta' \leq \pi/2 \quad 0 \leq \phi' \leq 2\pi \end{aligned}$$

or,

$$F(\underline{\Omega}') = \int_0^{2\pi} d\phi' \int_0^1 d\mu' \int_0^{d/\mu'} dr \frac{\Sigma_s \phi}{8\pi^2} e^{-k(d - r\mu) - \Sigma r} \mu f(\mu - \mu') f(\phi - \phi') \quad (12)$$

where $\mu = \cos \theta$

performing the integration over r ,

$$F(\underline{\Omega}') = \int_{\phi=0}^{2\pi} d\phi \int_{\mu=0}^1 d\mu \frac{\Sigma_s \phi_0}{8\pi^2} \left(\frac{e^{-\Sigma d/\mu} - e^{-kd}}{k\mu - \Sigma} \right) \mu f(\mu - \mu') f(\phi - \phi') \quad (13)$$

The integral over μ and ϕ follows from the definition of the delta function (1),

$$F(\underline{\Omega}') = \frac{\Sigma_s \phi_0}{8\pi^2} \left(\frac{e^{-\Sigma d/\mu'} - e^{-kd}}{k\mu' - \Sigma} \right) \mu' \quad (14)$$

Equation (14) can be further simplified by noting the relative magnitudes of the parameters Σ , k , and d (Appendix D).

$$\Sigma = 0.533 \text{ cm}^{-1} \quad k = 0.0312 \text{ cm}^{-1} \quad d = 308 \text{ cm}$$

Thus, $F(\underline{\Omega})^*$ will be closely approximated by neglecting the first term in comparison to the second.

$$F(\underline{\Omega}) = F(\theta) \cong \frac{\Sigma_s \phi_0}{8\pi^2} \left(\frac{e^{-kd} \cos \theta}{\Sigma - k \cos \theta} \right) \quad (15)$$

Note that $F(\underline{\Omega})$ is independent of azimuth, as expected from symmetry considerations.

Consider next the neutron distribution in polar angle $f(\theta)$. In the subsequent application of the Monte Carlo method (Appendix B), interpretation of the following will be simplified if use is made of probability density functions (5). Define $f(x)dx$ as the probability that x lies in the interval dx at x . Then $f(x)$ is the probability density function for x . Let the interval of x be $(-\infty, +\infty)$. Since the point x must lie within the interval,

$$\int_{-\infty}^{\infty} f(x) dx = 1$$

The probability that x is between $-\infty$ and x_0 is,

$$P(x_0) = \int_{-\infty}^{x_0} f(x) dx$$

*The primed symbol on the angular coordinates is dropped in the remainder of this section.

It is next shown that the neutron angular distributions can be interpreted as probability density functions.

$$\int_{2\pi} F(\underline{\Omega}) d\underline{\Omega} = S_0 \quad (16)$$

Define the normalized distribution $F'(\underline{\Omega})$ by:

$$\int_{2\pi} F'(\underline{\Omega}) d\underline{\Omega} = 1 \quad (17)$$

thus,

$$F'(\underline{\Omega}) = \frac{1}{S_0} F(\underline{\Omega}) = \frac{F(\underline{\Omega})}{\int_{2\pi} F(\underline{\Omega}) d\underline{\Omega}} \quad (18)$$

The denominator of Equation (18) is evaluated as follows. From the aximuthal symmetry, $d\underline{\Omega} = 2\pi \sin \theta d\theta$. Thus,

$$\begin{aligned} \int_{2\pi} F(\underline{\Omega}) d\underline{\Omega} &= \int_0^{\pi/2} \frac{\Sigma_s \phi_0}{8\pi^2} e^{-k\lambda \frac{\cos \theta}{\Sigma - k \cos \theta}} 2\pi \sin \theta d\theta \\ &= \frac{\Sigma_s \phi_0}{4\pi} \int_0^1 \frac{\mu d\mu}{\Sigma - k\mu} \\ &= \frac{\Sigma_s \phi_0}{4\pi} e^{-k\lambda} \left(\frac{\Sigma}{k^2} \ln \left(\frac{\Sigma}{\Sigma - k} \right) - \frac{1}{k} \right) \end{aligned} \quad (19)$$

Equation (18) becomes,

$$F'(\underline{\Omega}) = F'(\theta) = \left(\frac{1}{2\pi \left(\frac{\Sigma}{k^2} \ln \left(\frac{\Sigma}{\Sigma - k} \right) - \frac{1}{k} \right)} \right) \frac{\cos \theta}{\Sigma - k \cos \theta} \quad (20)$$

From the form of (17), $F'(\underline{\Omega})$ can be interpreted as the probability density function (p.d.f.) for $\underline{\Omega}$. The corresponding p.d.f. in polar angle θ follows from (17) by noting,

$$\int_0^{\pi/2} f(\theta) d\theta = 1 \quad (21)$$

Rewriting Equation (17),

$$\int_{2\pi} F'(\underline{\Omega}) d\underline{\Omega} = \int_0^{\pi/2} F'(\theta) 2\pi \sin \theta d\theta$$

Thus,

$$f(\theta) = 2\pi F'(\theta) \sin \theta \tag{22}$$

or,

$$f(\theta) = \frac{1}{N} \frac{\cos \theta \sin \theta}{\Sigma - k \cos \theta} \tag{23}$$

$$\text{where } N = \left(\frac{\Sigma}{k^2} \ln \left(\frac{\Sigma}{\Sigma - k} \right) - \frac{1}{k} \right) \tag{24}$$

In the application of the Monte Carlo method, the integrated probability curve, $P(\theta)$, is necessary.

$$\begin{aligned} P(\theta) &= \int_0^\theta f(\theta') d\theta' = \frac{1}{N} \int_0^\theta \frac{\cos \theta' \sin \theta' d\theta'}{\Sigma - k \cos \theta'} \\ &= \frac{1}{N} \left[\frac{\Sigma}{k^2} \ln \left(\frac{\Sigma - k \cos \theta}{\Sigma - k} \right) + \frac{(\cos \theta - 1)}{k} \right] \end{aligned} \tag{25}$$

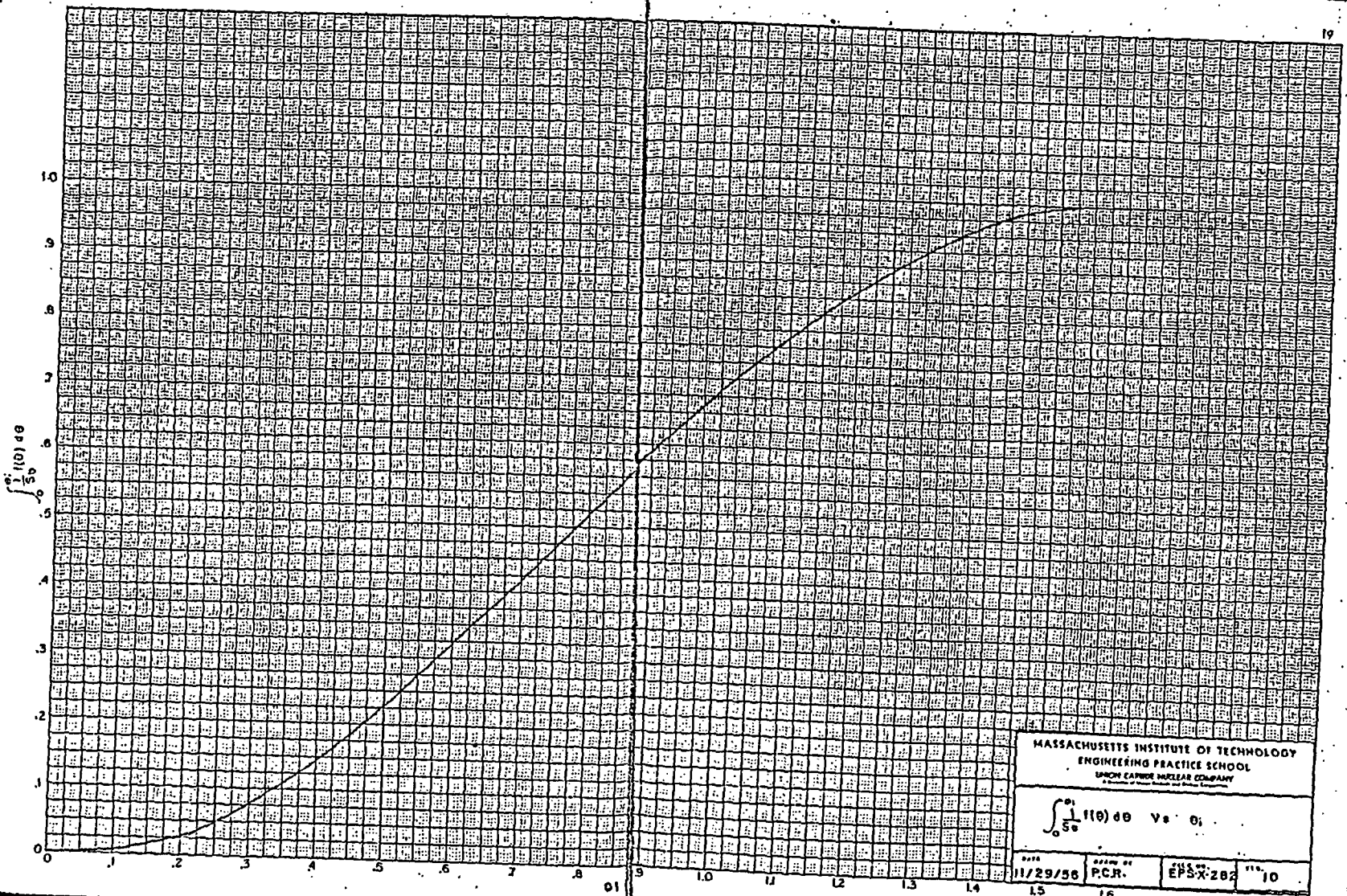
where the normalization factor, N , is given by Equation (24)

This curve is plotted in Figure 10 for the parameters of the graphite column listed in Appendix D.

B. Monte Carlo Procedure for Theoretical Determination of Neutron Attenuation by Boral (6)

A mathematical model is given below expressing the attenuation of thermal neutrons by a boral plate. It is then shown how the Monte Carlo procedure can be applied to this model to obtain numerically the attenuation and effective absorption cross section of Boral.

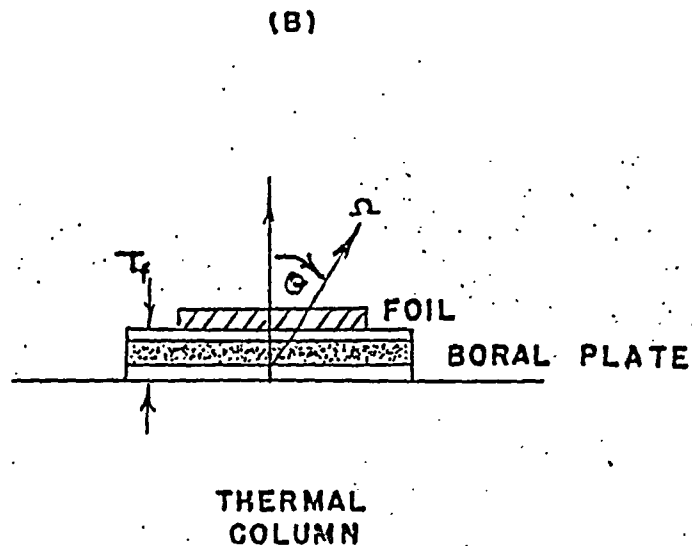
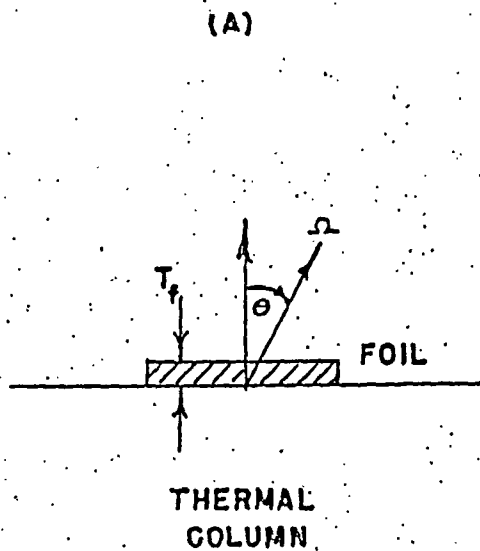
In Figure 11a a thin absorbing foil is shown representing the indium exposed to the thermal neutrons from the column. The saturated activity of the foil per unit area, Z_0 , is derived from first principles. The differential activity, dZ_0 , from absorption of $F(\underline{\Omega}) dA d\underline{\Omega}$ neutrons, which cross dA at A , in the direction range $d\underline{\Omega}$ about $\underline{\Omega}$ is,



MASSACHUSETTS INSTITUTE OF TECHNOLOGY
 ENGINEERING PRACTICE SCHOOL
 SPENCER CARPENTER NUCLEAR COMPANY

$$\int_0^{\theta} f(t) dt \quad \text{vs. } \theta$$

DATE 11/29/58	DRAWN BY P.C.R.	EPS# 282	FIG. 10
------------------	--------------------	-------------	------------



MASSACHUSETTS INSTITUTE OF TECHNOLOGY
 ENGINEERING PRACTICE SCHOOL
 UNION CARBIDE NUCLEAR COMPANY
 A Division of Union Carbide and Carbon Corporation

SCHEMATIC DIAGRAM OF INDIUM FOIL
 (A). BARE
 (B). BACKED BY BORAL PLATE

DATE
 11-27-56

DRAWN BY
 ROM

FILE NO.
 EPSX-282

FIG.
 11

$$\begin{aligned}
 dZ_o &= F(\underline{\Omega}) (1 - e^{-\Sigma_f t_f / \cos \theta}) d\underline{\Omega} dA \\
 Z_o &= \frac{\int_{\underline{\Omega}} \int_A F(\underline{\Omega}) (1 - e^{-\Sigma_f t_f / \cos \theta}) d\underline{\Omega} dA}{\int_A dA} \quad (26)
 \end{aligned}$$

Since the foil is homogeneous, the integral over A will not affect the result. This will not be true, however, for the case of a foil backed by the heterogeneous boron plate (Figure 11b). The differential foil activity, dZ, is now given by,

$$dZ = \left(\begin{array}{l} \text{neutrons crossing } dA \text{ at} \\ A \text{ in the direction range} \\ d\underline{\Omega} \text{ about } \underline{\Omega} \end{array} \right) \left(\begin{array}{l} \text{probability of} \\ \text{penetrating} \\ \text{plate} \end{array} \right) \left(\begin{array}{l} \text{probability} \\ \text{of absorption} \\ \text{by foil} \end{array} \right)$$

Since the boron carbide has a large absorption cross section ($\Sigma_a = 72.2 \text{ cm}^{-1}$) (Appendix D), the assumption is made that any neutrons scattering in the plate are changed in direction and effectively absorbed by the boron. Let $x_p^b(\underline{\Omega}, A)$ and $x_p^a(\underline{\Omega}, A)$ be the respective thicknesses "seen" by a neutron crossing dA at A in the direction range d\underline{\Omega} at \underline{\Omega}. The probability or fraction of neutrons penetrating the plate is,

$$e^{-(\Sigma_b x_p^b + \Sigma_a x_p^a)}$$

$x_p^a(\underline{\Omega}, A)$ is related to $x_p^b(\underline{\Omega}, A)$ by:

$$x_p^a(\underline{\Omega}, A) = t_p / \cos \theta - x_p^b(\underline{\Omega}, A) \quad (27)$$

then,

$$dZ = F(\underline{\Omega}) e^{-\Sigma_b x_p^b(\underline{\Omega}, A) - \Sigma_a (t_p / \cos \theta - x_p^b(\underline{\Omega}, A))} (1 - e^{-\Sigma_f t_f / \cos \theta}) d\underline{\Omega} dA$$

and the average activity per unit area induced in the foil is,

$$Z = \frac{\int_{\underline{\Omega}} d\underline{\Omega} \int_A dA F(\underline{\Omega}) e^{-\Sigma_b x_p^b(\underline{\Omega}, A) - \Sigma_a (t_p / \cos \theta - x_p^b(\underline{\Omega}, A))} (1 - e^{-\Sigma_f t_f / \cos \theta})}{\int dA} \quad (28)$$

Since the boron carbide particles are distributed in random sizes and positions within the aluminum matrix, analytical solution of this integral is not possible. Instead, it is proposed to apply the Monte Carlo procedure to obtain an approximate solution. Interpretation of the remainder of this section will be simplified if Equation (28) is rewritten in terms of probability density functions (Appendix A). Define:

$$g(A) = \frac{1}{\int dA} = \frac{1}{A_0} \quad (29)$$

where A_0 is the total area of the plate exposed to the neutron beam. Then,

$$\int_{A_0} g(A) dA = 1 \quad (30)$$

Thus $g(A)$ is the probability density function in position A . Physically Equation (29) states that the neutrons are randomly incident over the plate area, A_0 , i.e., for one incident neutron the probability $g(A)dA$ of striking dA is the fraction of the total area A_0 , represented by dA .

From Appendix A, $F(\underline{r})$ is related to the probability distribution, $f(\theta)$ by,

$$f(\theta)d\theta = \frac{F(\underline{r})d\underline{r}}{S_0} = \frac{2\pi F(\theta) \sin \theta}{S_0} \quad (31)$$

$$\text{where } F(\underline{r}) = F(\theta)$$

Assuming that, on the average, $x_p^b(\underline{r}, A)$ is independent of azimuth, the integral (28) can now be rewritten:

$$\bar{Z} = \int_{\theta} d\theta \int_A dA Z(\theta, A) f(\theta)g(A) dA \quad (32)$$

where;

$$Z(\theta, A) = S_0 e^{-\Sigma_b x_p^b(\theta, A) - \Sigma_a (t_p / \cos \theta - x_p^b(\theta, A))} (1 - e^{-\Sigma_f t_f / \cos \theta}) \quad (33)$$

In Equation (33), $Z(\theta, A)$ can be interpreted as the foil activity per unit area induced by S_0 neutrons per cm^2 incident on the boron plate at A in the direction θ . The weighted average with respect to the probability distributions in θ and A , of the neutrons from the column gives the average foil activity per unit area.

The Monte Carlo method consists in solving Equation (32) by sampling of the

variables θ and A , and studying the individual histories of the neutrons traversing the plate. Let N be the total number of histories studied, and i be the index for the i^{th} sample neutron. If \hat{Z} is the estimate of \bar{Z} obtained from this procedure:

$$\hat{Z} = \frac{1}{N} \sum_{i=1}^N Z(\theta_i, A_i) \quad (34)$$

In the method of random selection of the variables θ_i and A_i , decisions are made by means of random numbers. In this problem, random selection of A_i and an alternative method of systematic sampling of θ_i was used. It is shown in Appendix C that use of the latter method reduces the statistical variance of \hat{Z} . A description of the sampling procedure is given below.

A random number, y , lying in the interval $(0, L)$ is a number equally probable to lie at any point in that interval. It is convenient to restrict y to the particular interval $(0, 1)$. Thus y is defined by the rectangular distribution function:

$$g(y) = \begin{cases} 0 & y > 1 \\ 1 & 0 \leq y \leq 1 \\ 0 & y < 0 \end{cases} \quad (35)$$

$$\int_{-\infty}^{\infty} g(y) dy = 1 \quad (36)$$

In the method of random sampling, the decision for the random number y results from comparing the probability that θ lies between θ and $\theta + d\theta$ to the probability that y lies between y and $y + dy$;

$$f(\theta)d\theta = g(y) dy \quad (37)$$

$$g(A)dA = g(y)dy \quad (38)$$

Then,

$$\int_0^{\theta_2} f(\theta) d\theta = \int_{-\infty}^{y_1} g(y) dy = \int_0^{y_1} 1 dy = y_1 \quad (39)$$

$$\int_0^{A_i} g(A) dA = \int_{-\infty}^{y_1} g(y) dy = y_1 \quad (40)$$

If the plate area, A_0 , is normalized to unity, from Equation (29),

$$g(A) = g(y) \tag{41}$$

$$A_i = y_i \tag{42}$$

Alternatively, if the total area is A_0 ,

$$A_i = y_i A_0 \tag{43}$$

If random selection is also used for θ_i ,

$$\int_0^{\theta_i} f(\theta) d\theta = P_i(\theta_i) = y_i \tag{44}$$

The alternative procedure of systematic selection of θ_i is described next. The physical interpretation is that the θ_i 's are chosen at the midpoints of small finite intervals which represent equal probability ranges for θ from zero to $\pi/2$. The neutron history studied at θ_i is assumed to be the average history over the corresponding angular interval.

Mathematically, θ_i is selected according to the formula;

$$P(\theta_i) = \int_0^{\theta_i} f(\theta) d\theta = \frac{i - 1/2}{N} \quad i = 1, 2, \dots, N \tag{45}$$

In Figure 10, where the integrated probability curve $P(\theta)$ is shown, Equation 45 is interpreted graphically by dividing the total probability interval,

$$P(\pi/2) = 1 = \int_0^{\pi/2} f(\theta) d\theta \tag{46}$$

into N equal parts. θ_i is read from the curve, corresponding to the midpoint of the i^{th} interval on the $f(\theta)$ axis. Letting θ_i^L and θ_i^U represent the lower and upper limits of the i^{th} angular interval;

$$P(\theta_i^L \leq \theta \leq \theta_i^U) = \int_{\theta_i^L}^{\theta_i^U} f(\theta) d\theta = \frac{1}{N} \tag{47}$$

= probability that θ is between θ_i^L and θ_i^U .

θ_i , determined from Equation (45) has the property $\theta_i^L < \theta_i < \theta_i^U$. Thus,

$$\int_{\theta_i^L}^{\theta_i^U} f(\theta) d\theta = \frac{1}{N} \approx f(\theta_i) \Delta\theta_i \approx f(\theta) d\theta \quad (48)$$

where it is assumed that N is large.

The procedure for the Monte Carlo calculation of \hat{Z} is now complete. Rewriting Equation (26) in terms of $f(\theta)$,

$$Z_0 = \int_{\theta=0}^{\pi/2} S_0 (1 - e^{-\Sigma_f t_f / \cos \theta}) f(\theta) d\theta \quad (49)$$

The thermal neutron attenuation by the boron plate is the ratio of the foil activities,

$$R = \frac{\hat{Z}}{Z_0} \quad (50)$$

where it is noted that the magnitude of the total neutron current S_0 will cancel from the result. The effect thermal absorption cross section Σ_B is given by,

$$R = e^{-\Sigma_B t_p} \quad (51)$$

C) Analysis of Variance (6)

In this section a discussion is given of the accuracy of the Monte Carlo calculation of \hat{Z} . The reason for the use of systematic sampling of θ is shown by proving that the procedure will reduce the variance of \hat{Z} .

The variance of a single estimate of \hat{Z} , obtained from N neutron histories, is given by;

$$\begin{aligned} V &= \frac{(\hat{Z} - \bar{Z})^2}{N} = \frac{Z^2 - 2Z\bar{Z} + \bar{Z}^2}{N} \\ &= \frac{\bar{Z}^2 - \bar{Z}^2}{N} \quad (52) \end{aligned}$$

Since the true value of Z cannot be known accurately, the best estimate of the variance is given by,

$$\begin{aligned}
 v &\hat{=} \frac{\hat{Z}^2 - \hat{Z}^2 *}{N - 1} \\
 &\hat{=} \frac{\sum_{i=1}^N \frac{Z_i^2}{N} - \left(\sum_{i=1}^N \frac{Z_i}{N} \right)^2}{N - 1} \hat{=} \sigma^2
 \end{aligned} \tag{53}$$

where σ is the standard deviation of the calculated value \hat{Z} .

Suppose the variables θ and A are selected randomly. Let \hat{Z}_1 be the estimate of Z obtained from this procedure.

$$\hat{Z}_1 = \frac{1}{N} \sum_{i=1}^N Z_i(\theta_i, A_i) \tag{54}$$

and,
$$v_1 = \frac{1}{N} (Z_1 - \bar{Z})^2 \tag{55}$$

$$= \frac{1}{N} \iint [Z(\theta, A) - \bar{Z}]^2 f(\theta) g(A) d\theta dA \tag{56}$$

Define the conditional average,

$$\bar{Z}(j\theta) = \int Z(\theta, A) g(A) dA \tag{57}$$

Verbally, $\bar{Z}(j\theta)$ is the average value of Z given θ . Add and subtract this quantity to the bracketed term under the integral of Equation (56).

$$v_1 = \frac{1}{N} \iint [(Z - \bar{Z}(j\theta) + \bar{Z}(j\theta) - \bar{Z})]^2 f(\theta) g(A) d\theta dA \tag{58}$$

Algebraically expanding the bracketed term,

$$[Z(\theta, A) - \bar{Z}]^2 = [(Z - \bar{Z}(j\theta))^2 + 2(Z - \bar{Z}(j\theta))(\bar{Z}(j\theta) - \bar{Z}) + (\bar{Z}(j\theta) - \bar{Z})^2] \tag{59}$$

$$(Z - \bar{Z}(j\theta))(\bar{Z}(j\theta) - \bar{Z}) = Z \bar{Z}(j\theta) - Z\bar{Z} - \bar{Z}(j\theta)^2 + \bar{Z}(j\theta)\bar{Z} \tag{60}$$

Upon integration over A , noting the definition of $\bar{Z}(j\theta)$, Equation (59) becomes,

$$\bar{Z}(j\theta)^2 - \bar{Z}(j\theta)\bar{Z} - \bar{Z}(j\theta)^2 + \bar{Z}(j\theta)\bar{Z} = 0 \tag{61}$$

*The factor $N - 1$ eliminates small sample bias.

Hence,

$$V_1 = \frac{1}{N} \iint \left\{ \left[Z - \bar{Z}(j\theta) \right]^2 + \left[\bar{Z}(j\theta) - \bar{Z} \right]^2 \right\} f(\theta) g(A) d\theta dA \quad (62)$$

$$\begin{aligned} &= \frac{1}{N} \left[\overline{Z_1 - \bar{Z}(j\theta)}^2 + \overline{\bar{Z}(j\theta) - \bar{Z}}^2 \right] \\ &= \frac{V(j\theta)}{N} + \frac{\left[\bar{Z}(j\theta) - \bar{Z} \right]^2}{N} \end{aligned} \quad (63)$$

Consider next the case where θ_1 is sampled systematically and A_1 is randomly selected. Let the estimate of \bar{Z} obtained by this procedure be \hat{Z}_2 ;

$$\hat{Z}_2 = \frac{1}{N} \sum_{i=1}^N Z_2(\theta_1, A_i)$$

The average value of Z_2 is given as;

$$\begin{aligned} \bar{Z}_2 &= \frac{1}{N} \sum_{i=1}^N \int Z(\theta_1, A) g(A) dA \\ &= \frac{1}{N} \sum_{i=1}^N \bar{Z}(j\theta_1) \end{aligned} \quad (64)$$

where the averaging is only done over the variable A , since the θ_1 values are fixed. The variance is given by:

$$V_2 \approx \overline{(\hat{Z}_2 - \bar{Z}_2)^2} \quad (65)$$

$$\begin{aligned} &\approx \overline{\left\{ \frac{1}{N} \sum_{i=1}^N \left[Z_2(\theta_1, A_i) - \bar{Z}(j\theta_1) \right] \right\}^2} \\ &= \frac{1}{N^2} \overline{\left\{ \sum_{i=1}^N \left[Z_2(\theta_1, A_i) - \bar{Z}(j\theta_1) \right] \right\}^2} \\ &= \frac{1}{N^2} \overline{\sum_{i=1}^N \left[Z_2(\theta_1, A_i) - \bar{Z}(j\theta_1) \right]^2} \end{aligned}$$

The summation sign can be taken outside the average, since all the cross terms will cancel when averaged. Thus:

$$V_2 = \frac{1}{N} \sum_{i=1}^N V(j\theta_1) \quad (66)$$

From Appendix B;

$$\frac{1}{N} \approx \int f(\theta) d\theta \quad (67)$$

Hence,

$$v_2 \approx \frac{1}{N} \int v(j\theta) f(\theta) d\theta = \overline{\frac{1}{N} v(j\theta)} \quad (68)$$

By comparing Equation (68) to (63), it is seen that the variance will be reduced if θ_1 is selected systematically.

D) Nuclear Constants

TABLE I

CROSS SECTIONS

Element	Absorption Cross Section at 2200 m/sec (3) (cm ² x 10 ⁺²⁴)	Average Thermal Scattering Cross Section (cm ² x 10 ⁺²⁴)	Density (7) (gms/cm ³)	Macroscopic Total Thermal Cross Section ^a (cm ⁻¹)
Aluminum	0.230	1.4	2.70	0.096
Boron	775	4	-	-
Carbon	0.0032	4.8	2.22	0.533
Boron Carbide	-	-	2.45 (4)	72.2
Indium	145 ^b	-	7.31	4.93 ^b

Thermal column characteristics:

$$k = 0.0312 \text{ cm}^{-1}$$

$$d = 308.6 \text{ cm}$$

Coil thickness:

$$t_f = 0.0127 \text{ cm}$$

^aAll thermal absorption cross sections are Maxwell-Boltzmann averaged.

^bActivation cross section for 54.1 minute Indium-116.

E) Sample Calculations

(1) Procedure

Photomicrographs were taken of the polished cross section of a 1/8" ORNL boron plate. A single frame from the total field scanned is shown in Figure 1. The magnification used was 75X. To obtain a field of the total cross sectional area, including the aluminum cladding, single frames were taken of overlapping sections, trimmed, and joined together. This resulted in a large photograph, representing a total field of 1/8" x 1/4". A 0.01 mm scale was then photographed at the same magnification and superimposed across the top of the picture, i.e., the top surface of the aluminum cladding. In this way, length measurements could be made directly in terms of the actual dimensions of the plate and the boron carbide particles. The total length of the top surface was 0.60 cm, scaled in units of 0.01 mm.

The neutron histories were studied individually by laying a straightedge across the picture, with origin at A_1 , measured from one end of the top scale, and inclined at the angle θ_1 from the normal to the top surface. In selecting A_1 , use was made of a table of random numbers, generated on Oracle. The sampling of A_1 and θ_1 is illustrated in the calculation of Z_1 below. The thickness $x_p^b(\theta_1, A_1)$ of boron carbide, "seen" by the neutron, was measured along the straightedge using the magnified scale.

For each angle θ_1 , paths clockwise and counterclockwise from the normal were taken and the corresponding distances in B_4C were averaged. Whenever edge effects were encountered, the point where the neutron path left the side of the film was extrapolated to the opposite side and the path was continued at the same angle.

(2) Calculations

Z_1 :

The first random number used was 0.508600678.

$$A_1 = 0.6 \times 0.508600678 = 0.3051604068 = 0.305 \text{ cm}$$

θ_1 is obtained from Figure 10.

$$P(\theta_1) = \frac{0.01}{2} = 0.005$$

$$\theta_1 = 0.105 \text{ radians} = 6.0^\circ$$

The values of x_p^b obtained from the photograph were:

$$x_p^b(+\theta_1, A_1) = 0.027 \text{ cm}$$

$$x_p^b(-\theta_1, A_1) = 0.034 \text{ cm}$$

$$x_p^b(\bar{\theta}_1, A_1) = 0.0305 \text{ cm}$$

The plate thickness measured from the microphotograph was,

$$t_p = 0.326 \text{ cm}$$

Substituting the cross sections and foil thickness given in Appendix D,

$$Z_1 = 0.006561$$

\hat{Z} :

Similar sampling of 100 neutron histories gave the following results:

$$\sum_{i=1}^{100} Z_i(\theta_i, A_i) = 0.1636$$

$$\sum_{i=1}^{100} Z_i^2(\theta_i, A_i) = 8.34 \times 10^{-4}$$

$$\hat{Z} = \frac{\sum_{i=1}^{100} Z_i}{100} = 0.001636$$

V :

$$V = \frac{\frac{\sum_{i=1}^{100} Z_i^2}{N} - \left(\frac{\sum_{i=1}^{100} Z_i}{N}\right)^2}{N-1}$$

$$= 5.73 \times 10^{-8}$$

$$\sigma = \sqrt{V} = 2.39 \times 10^{-4}$$

$$\hat{Z} = 0.00164 \pm 0.00024$$

Z_0 :

The activation of the foil without the boron plate was obtained by numerical integration of Equation (26), using the parameters listed in Appendix D.

$$Z_0 = 0.1085$$

R:

$$R = \frac{(0.164 \pm 0.024) \times 10^{-2}}{0.1085}$$

$$= (1.51 \pm 0.22) \times 10^{-2}$$

 Σ_B :

$$R = e^{-\Sigma_B t_B} = 1.51 \pm 0.22$$

$$\Sigma_B = 13.4 \text{ cm}^{-1}$$

F) Nomenclature

A_0 = Total area of plate exposed to neutron flux.

dA = Differential area element.

dV = Differential volume element.

d = Height of thermal column.

F = Neutron angular distribution function $jF(\underline{\Omega})$ is the number of neutrons from the thermal column, per unit surface area, moving in the direction $\underline{\Omega}$ per unit solid angle.

$F(\theta), F'(\underline{\Omega})$ = Probability density function in neutron direction.

$g(A), f(x)$ = Probability density function in neutron incident position.

H = Scattering collision density.

k = Experimentally determined neutron attenuation coefficient in thermal column.

N = Total number of histories studied.

$P(\theta)$ = Integrated probability distribution.

S_0 = Total outward neutron current from thermal column.

t_p = Thickness of boral plate.

t_f = Thickness of indium foil.

$x_p^b(\underline{\Omega}, A)$ = Thickness of boron carbide "seen" by a neutron going in the direction $\underline{\Omega}$ from the thermal column and incident at position A on the surface of the boral plate.

V = Variance.

Z_0 = Activity of indium foil per unit surface area with foil exposed to direct flux from column.

\bar{Z} = Average activity of indium foil per unit surface area with foil shielded by boral plate.

\hat{Z} = Monte Carlo estimate of \bar{Z} .

θ = Angle between neutron velocity and w-axis.

$\underline{\Omega}$ = Unit vector in direction of the neutron velocity.

Σ = Macroscopic total thermal cross section for graphite.

Σ_s = Macroscopic scattering cross section for graphite.

Σ_b = Macroscopic total thermal cross section for boron carbide.

Σ_a = Macroscopic total thermal cross section for aluminum.

Σ_f = Macroscopic total thermal cross section for indium.

σ = Standard deviation of calculated value of Z .

ϕ = Thermal neutron flux at any point x, y, w .

ϕ_0 = Thermal neutron flux at base of thermal column.

μ = $\cos \theta$.

μ = Linear gamma ray attenuation coefficient.

$\delta(\underline{\Omega} - \underline{\Omega}'), \delta(\theta - \theta')$ = Dirac delta function.

ORNL-2528

Copy _____

Contract No. W-7405-eng-26

Neutron Physics Division

RADIATION TRANSMISSION THROUGH BORAL AND SIMILAR HETEROGENEOUS
MATERIALS CONSISTING OF RANDOMLY DISTRIBUTED
ABSORBING CHUNKS

W. R. Burrus*

Date Issued

JAN 18 1960

OAK RIDGE NATIONAL LABORATORY
Oak Ridge, Tennessee
operated by
UNION CARBIDE CORPORATION
for the
U.S. ATOMIC ENERGY COMMISSION

*Now at Ohio State University, Department of Physics, Columbus, Ohio.

ABSTRACT

Shields that consist of randomly distributed absorbing chunks in a relatively transparent matrix must contain a greater mass of absorber than homogeneous shields which provide the same attenuation. This is the result of radiation "channeling" between the absorbing chunks. Channeling is particularly important for heterogeneous materials when the mean free path for absorption is comparable to the chunk size. A newly developed method for calculating the transmission of radiation through such heterogeneous shields is described. The numerical results of a calculation of the transmission of thermal neutrons by boral (a B_4C -Al mixture) are given, including the effects of energy and angular distributions on the predicted attenuation. The calculated results are in reasonable agreement with available experimental results.

ACKNOWLEDGEMENTS

This work was initiated in April, 1956 while the author was on assignment from the Wright Air Development Center to the ORNL Lid Tank Shielding Facility. At that time two other members of the LTSF staff, Dr. R. W. Peelle and Mr. J. R. Smolen, the latter on assignment from Pratt and Whitney Aircraft, were considering elementary aspects of the same approach, and many of their ideas are included in this report. Simultaneously, Mr. S. Auslender, also on assignment to ORNL from Pratt and Whitney Aircraft, was interested in the method, and he, too, assisted in the work reported here. The author later discovered that Mr. R. R. Coveyou and Dr. N. M. Smith, Jr. had proposed essentially the same approach at ORNL as early as 1947; in fact, the method of calculation proposed here is based on the Coveyou model.

This work was completed while the author was a consultant to the Nuclear Products Branch of the Lockheed Aircraft Corporation, and appreciation is expressed to that organization, especially to Mr. Alan Liebschutz, for granting this opportunity. The author is also grateful to Mr. Stanley Szawlewicz of WADC for his encouragement.

Mr. R. W. Peelle and Mrs. L. S. Abbott have kindly made extensive editorial contributions to the final manuscript.

TABLE OF CONTENTS

	<u>Page No.</u>
Abstract	iii
Acknowledgements	iv
Introduction	1
I. Method of Calculation	6
Formulas for Materials with Single-Sized Right Cylindrical Chunks	6
Formulas for Materials with Right Cylindrical Chunks of Multiple Sizes	12
Formulas for Materials with Arbitrary Chunk Shapes	18
Formulas Including Energy and Angular Distributions	20
II. Calculation of Neutron Transmission Through Boron	22
III. Comparison of Calculated and Experimental Results	24
IV. Conclusions	26

INTRODUCTION

One material commonly used as a thermal-neutron shield is boral,¹⁻³ a heterogeneous mixture of commercial-grade boron carbide and aluminum sandwiched between aluminum plates. The total sandwich is usually rolled to a thickness of 1/8 or 1/4 in. Since the mixture is not uniform, aluminum-filled regions exist between the chunks of B_4C in the B_4C -Al melt. This is apparent in the Dark Field Illuminated Photomicrograph⁴ of a sample of the melt in Fig. 1. The dark chunks are B_4C and the light background is aluminum. The B_4C is, of course, the attenuating material, and, in order to use boral to an optimum advantage, it is necessary to have a qualitative understanding of the effects of the B_4C size and distribution on the thermal-neutron transmission. The same is true of any other heterogeneous shield material which consists of "randomly distributed" chunks.

A first approximation of the transmission of a heterogeneous material may be obtained by assuming that the absorbing material is uniformly distributed instead of heterogeneously distributed and using the conventional theory for homogeneous materials, providing the density of the material used in the calculation is reduced to account for the voids. This "reduced density" is simply

$$(\text{reduced density}) = (\text{true absorbing material density}) \times V \quad (1)$$

where V is the volume fraction occupied by the absorbing material. This approximation will lead to a lower limit for the actual transmission since nonuniformity in the material will tend to augment the transmission. The importance of this effect has been demonstrated by experiments which have

1. V. L. McKinney and T. Rockwell, III, Boral: A New Thermal Neutron Shield, ORNL-242 (1949).
2. A. S. Kitzes and W. O. Hullings, Boral: A New Thermal Neutron Shield, Supplement 1, ORNL-981 (1951).
3. J. R. Smolen, ORNL-CP-56-6-163 (1956) (Classified).
4. R. O. Maak, B. E. Prince, and P. C. Rekemeyer, Boral Radiation Attenuation Characteristics, MIT Engineering Practice School, KT-251 (1956).

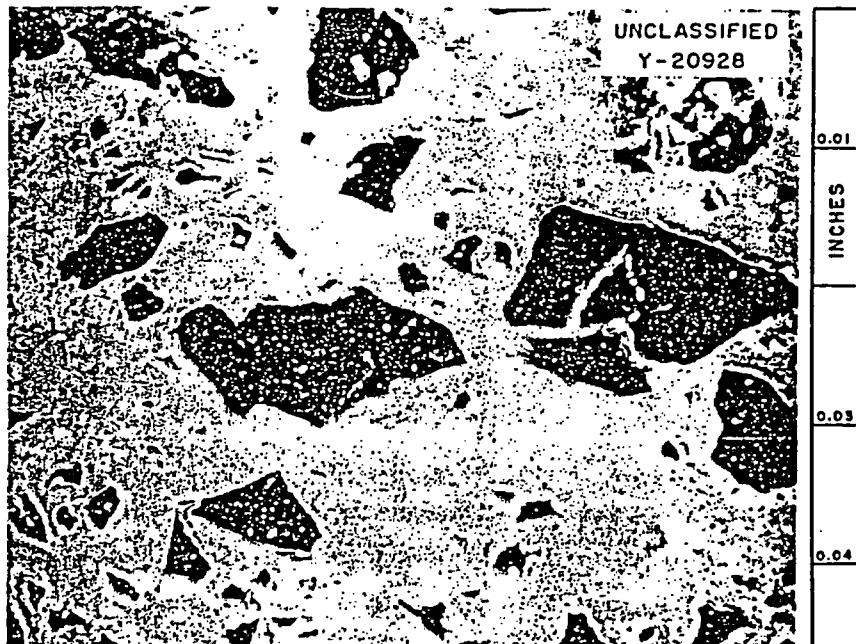


Fig.1. Typical Samples of ORNL-Fabricated $\frac{1}{8}$ -in.-thick "Boral". As-polished. 75X

shown that the transmission of thermal neutrons through 1/8-in.-thick boral is much greater (as much as a factor of 40) than the transmission indicated by a homogeneous calculation. Therefore, some other method must be used for computing the transmission through materials such as boral.*

In principle, the transmission of radiation through nonuniform heterogeneous materials may be calculated if the location of the absorbing parts of the material is known. If scattering is neglected, the transmission through a slab of material consisting of a distribution of chunk sizes is given by:

$$T = \int_0^t P(x,t)\tau(x)dx \quad (2)$$

where

$P(x,t)dx$ = fraction of rays which encounter a thickness of absorbing material between x and $x + dx$ in traversing a total thickness t of material,

$\tau(x)$ = fraction of radiation transmitted through a chunk of material of thickness x .

$P(x,t)$ has been calculated for simple geometric shapes with various orientations (including random) by F. H. Murray,⁵ J. A. McLennan,⁶ and P. A. M. Dirac.⁷ Dirac also developed a general theory for nonuniform media consisting of arbitrarily shaped chunks. $\tau(x)$ may be calculated from the existing theory for the transmission of radiation through homogeneous materials.

*The absorption of dilute mixtures of strongly absorbing chunks was treated by H. Hurwitz and P. F. Zweifel, Nuclear Sci. Eng. 1, 438 (1956), but their formulation would not apply for a mixture as concentrated as boral.

5. F. H. Murray, Fast Effects, Self-Absorption, Fluctuation of Ion Chamber Reading, and the Statistical Distribution of Chord Lengths in Finite Bodies, CP-G-2922 (1945).
6. J. A. McLennan, APEX-197 (1955) (classified).
7. P. A. M. Dirac, Approximate Rate of Neutron Multiplication for a Solid Arbitrary Shape and Uniform Density, British Report MS-D-5 (n.d.).

N. M. Smith⁸ considered the case of randomly distributed chunks from another viewpoint. He assumed a hypothetical chunk which is physically similar to actual chunks but mathematically simpler to deal with. The statistical distribution of the thickness of his hypothetical chunk material is shown in Fig. 2 for a 20-cm-thick slab having two-thirds of its volume occupied by chunks which have an average diameter of about 3 cm. $\tau(x)$ is also shown in Fig. 2 for exponential attenuation with an attenuation length of 2 cm. It is obvious that the over-all transmission is much greater than it would be in the homogeneous case, in which all the rays pass through $(2/3) \times 20$ cm of material. In other words, the rays which statistically penetrate less than the average material thickness control the over-all transmission when the transmission $\tau(x)$ of a chunk is much less than unity. This geometrical channeling of rays between chunks is known as the "channeling effect."

R. R. Coveyou⁹ has suggested a model to calculate the approximate transmission of radiation through materials in which the channeling effect is important. The material is considered to be divided into layers that have a thickness characteristic of the size of the chunks. Each layer is analogous to a sieve made from attenuating material. Part of the radiation may pass unattenuated through the holes between the chunk material in a given layer, and the rest must pass attenuated through the chunk material. The holes in the layers are assumed to be located statistically independent of holes in adjacent layers so that the over-all transmission is the product of the transmission of each layer. As the chunks are made more attenuating, the radiation passing through the holes between the chunks becomes more important.

In the discussion that follows a method of calculation based on the Coveyou model is presented. The model itself is first discussed and then

8. N. M. Smith, Transmission and Scattering of Radiation in Random Aggregates of Pebbles, CNL-21, Revised (n.d.).

9. R. R. Coveyou, Oak Ridge National Laboratory, private communication.

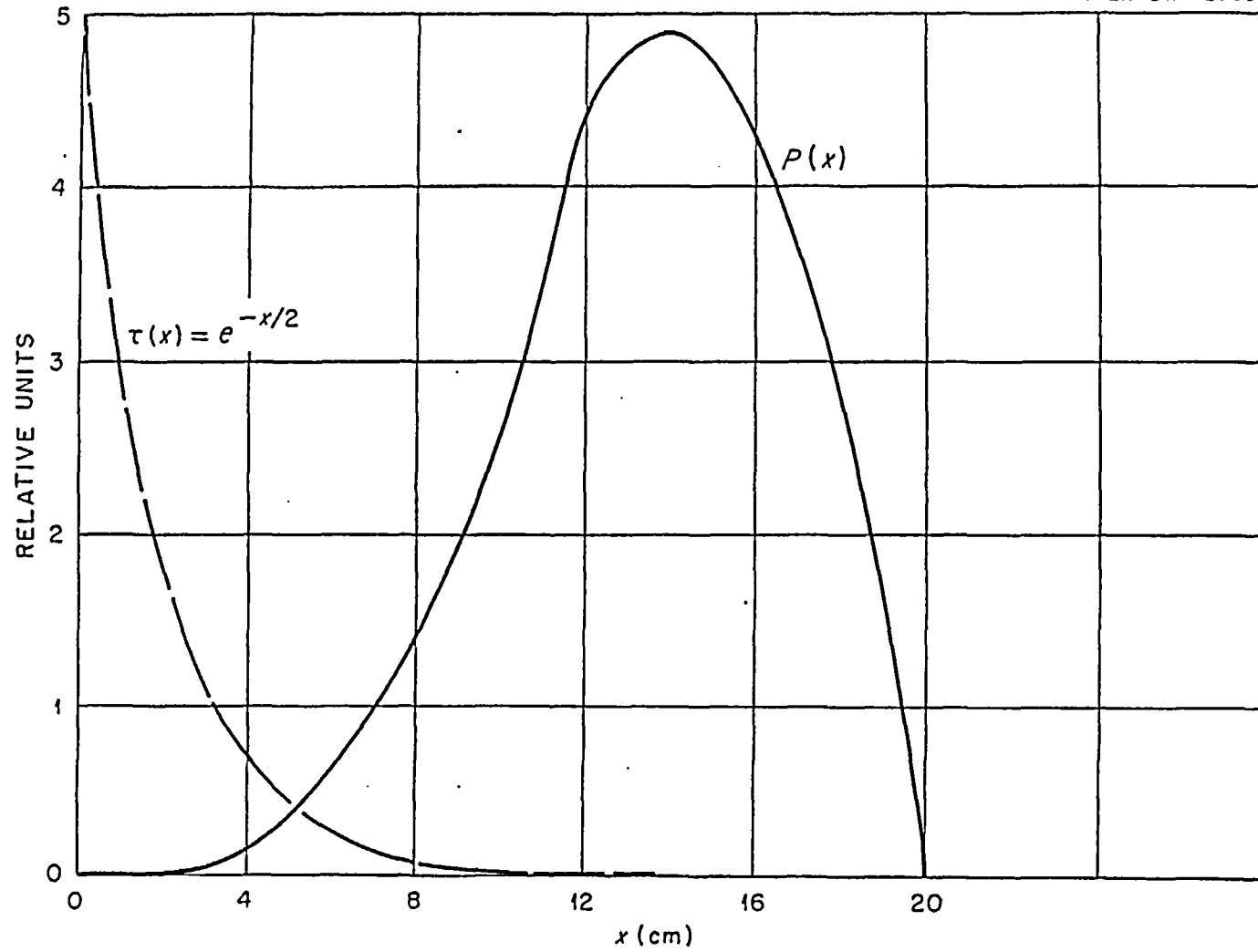


Fig. 2. The Probability $P(x)$ of Penetrating x cm of Chunk Material in Traversing a 20-cm Slab.

extended to include a distribution of various chunk sizes and materials. For simplicity, it is first assumed that the neutron radiation is monoenergetic and normally incident on the face of a plane slab. Exponential attenuation in the chunk material is assumed. The results are then extended to remove these restrictions. An attempt is made at all stages of the development to provide an insight into the relations between transmission and the physical parameters of the chunks involved, and approximations that clarify these relations are emphasized. Scattering is not considered in the calculation.

The applicability of the proposed method is demonstrated in the last two sections of the report in which the transmission of thermal neutrons through a 1/8-in. thickness of boral is calculated, and the results are compared with the transmission indicated by experiments.

I. METHOD OF CALCULATION

Formulas for Materials with Single-Sized Right Cylindrical Chunks

The transmission through a slab consisting of a "random distribution" of single-sized chunks is computed first because of its simplicity. It is assumed that the chunks are right cylinders (cubes, circular cylinders, etc.) with their generators normal to the surface of the slab. Right cylindrical chunks are chosen because it makes the division into layers easy and because a ray that passes through a normally oriented right cylinder always passes through a chunk thickness equal to the cylinder height.

The concept of "random distribution" may be clarified by describing an artificial procedure which yields such a distribution. Randomly selected coordinates (in the desired region) are picked for each chunk in the distribution. If this selection causes two or more chunks to overlap, the selection is rejected and another random assignment is made. Eventually, a selection will be found which is physically realizable. In the simple case of identical cubic chunks, any volume fraction up to unity may be obtained in this manner, although it will require a large number of trials to achieve a realizable distribution as the volume fraction approaches unity.

Chunks which are dumped into a container with no preference as to order or arrangement can be thought of as "randomly packed" chunks as opposed to "randomly distributed" chunks. Randomly packed chunks are usually in intimate contact with at least two neighboring chunks, whereas randomly distributed chunks are not likely to be in contact. If spheres are distributed within a container in the most compact manner, it is possible to obtain volume fractions of 0.74. If the spheres are dumped into the container so that they are "randomly packed," experimental volume fractions of about 0.5 to 0.6 are obtained, depending on the speed and uniformity of pouring, the conditions of the surface of the spheres, etc.

As the actual volume fraction of a distribution of chunks increases, the packing tends to make the material thickness distribution (Fig. 2) less skewed, i.e., with smaller variation in material thickness penetrations. Packing thus causes the over-all transmission to be smaller than that calculated by assuming a random distribution. However, the true transmission will always be bracketed between the random distribution value and the reduced density value. Materials which consist of discrete chunks which are separated by a vehicular medium so that the chunks are not in intimate contact with neighboring chunks are well represented by a "random distribution." Packing becomes a consideration when the volume fraction begins to approach the maximum experimental volume fraction which is about 0.5 for single-sized chunks that are not too different from spheres or cubes. Even when the chunks are closely packed, the randomly distributed transmission is expected to be closer to the true over-all average transmission than the reduced density transmission.

With a randomly distributed mixture of chunks, the transmission may vary statistically over the surface of a material, being unity over a small area (where there is an alignment of voids) and being much smaller than average (where there is an alignment of chunks). The variations are usually on a scale comparable with the attenuation of a single chunk, so that this effect is seldom noticed in practical experiments. If a slab were very thick, however, this effect would become more noticeable.

The slab is considered to be divided into an integral number (N) of layers of thickness (Δ) equal to the height of a cylinder of absorbing material. This division is made by translating the cylinders vertically (see Fig. 3) so that the center of a cylinder is moved to the center of the layer in which it falls. Allowing chunks to protrude beyond the surface is a fairly good approximation to chunks mixed in a binder if no effort is made to level off the surfaces after curing. If the chunks are mixed in a die under pressure, then no chunks will penetrate the surface. This distinction can be taken into account by noting that those chunks which protrude from the surface have their centers located within $\Delta/2$ of the surface. Thus, the apparent boundary of the slab is located a distance $\Delta/2$ inside the real boundary. The method is developed for chunks which may protrude but is applicable for chunks which do not protrude if the "reduced thickness" is used, thus accounting for the apparent boundary at such a surface being $\Delta/2$ inside the slab.

The transmission through a slab divided in this manner is the same as the transmission through the undivided slab since every normally incident ray sees the same thickness of chunk material in either case (as may be seen in Fig. 3). The probability that a given ray will encounter exactly n chunks is given by Bernoulli's binomial distribution:

$$P_n = V^n (1 - V)^{N-n} C_n^N ; \quad C_n^N = \frac{N!}{(N-n)! n!} \quad (3)$$

where

V = probability that a ray will encounter a chunk in passing through a layer (the volume fraction of chunks),

V^n = probability that n chunks will be encountered in n specified layers,

$(1 - V)^{N-n}$ = probability that the rest of the layers are not occupied by other chunks,

C_n^N = number of combinations of N things taken n at a time and is equal to the number of ways in which the n specified layers could be selected from N layers.

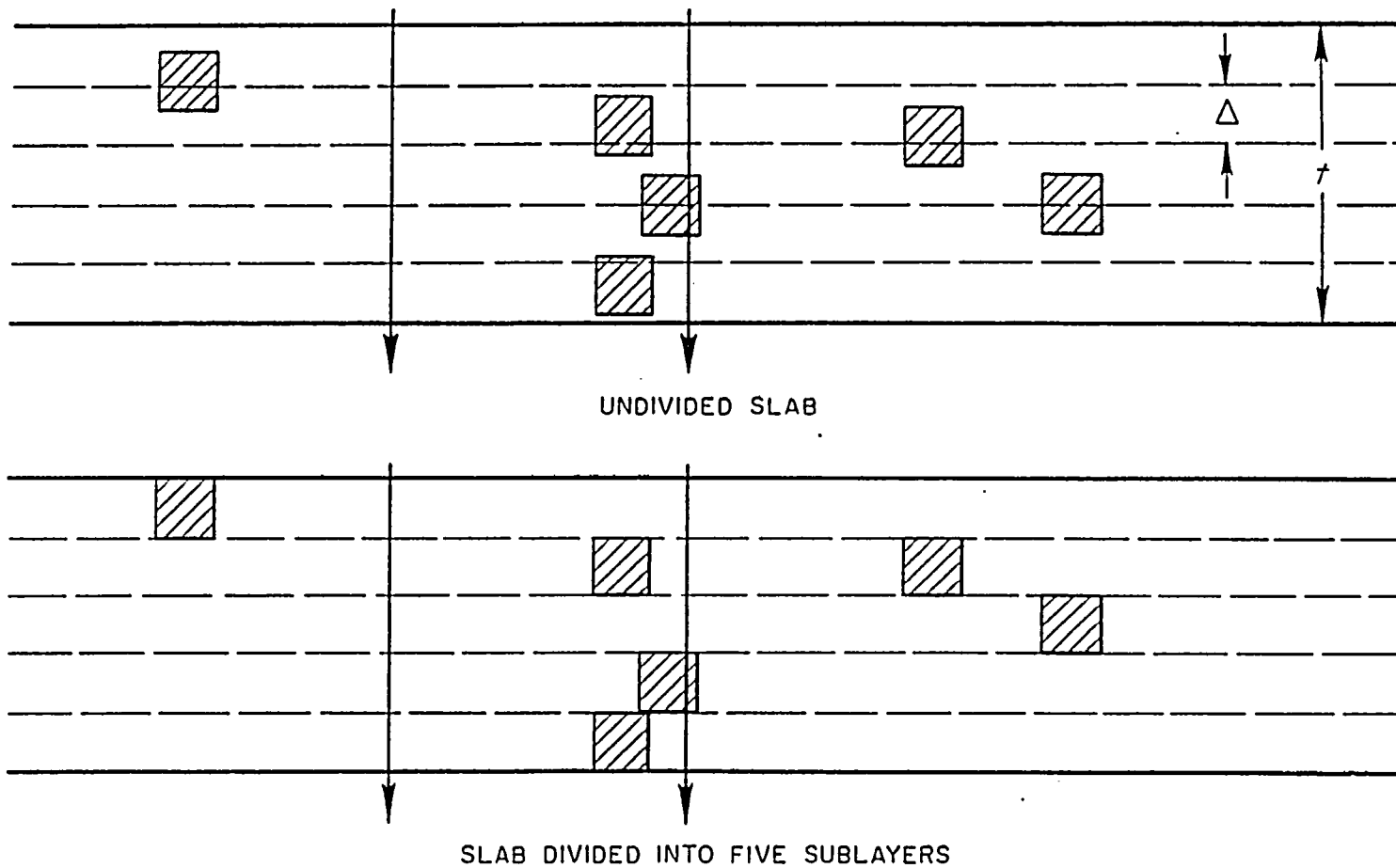


Fig. 3. Illustrating the Division of a Slab into Sublayers.

If exponential attenuation in the chunk material is assumed, then the probability that a given ray penetrates the slab is:

$$\tau(n) = e^{-\sum n \Delta} \quad (4)$$

where

\sum = linear attenuation coefficient for the chunk material,

n = number of chunks encountered,

Δ = height of a chunk,

$n\Delta$ = total chunk material thickness along this ray.

The over-all average transmission for the slab is:

$$\begin{aligned} T &= \sum_{n=0}^N P_n \tau(n) \quad (5) \\ &= \sum_{n=0}^N V^n (1-V)^{N-n} C_n^N e^{-\sum n \Delta} \end{aligned}$$

By the binomial theorem, this may be written as:

$$\begin{aligned} T &= \sum_{n=0}^N C_n^N (V e^{-\sum \Delta})^n (1-V)^{N-n} \quad (6) \\ &= \left[V e^{-\sum \Delta} + 1 - V \right]^{N=t/\Delta} \end{aligned}$$

Equation 6 has a simple physical interpretation which could have given Eq. 6 at once. Since V is the probability that a ray will encounter a chunk at a given layer, $(1 - V)$ is the probability that a ray will miss the chunks in a layer. $V e^{-\sum \Delta}$ is the probability that those rays that hit a chunk will penetrate the layer. Thus the quantity in brackets is just the average transmission through one layer. Since the chunks are randomly distributed,

each layer acts independently and the over-all average transmission T is the product of the transmission of all N sublayers. Equation 6 was derived with the assumption that there was an integral number of layers in the slab. When there is a fractional number of layers, Eq. 6 is still approximately correct since the transmission of such a slab will uniformly decrease as its thickness increases (if the volume fraction of chunks is kept constant), in agreement with the behavior of the equation.

Equation 6 may be written as:

$$T = e^{\frac{t}{\Delta} \ln [Ve^{-\sum \Delta} + 1 - v]} \quad (7)$$

This suggests the concept of an effective linear attenuation coefficient defined by:

$$T = e^{-v \sum_{\text{eff}} t} \quad (8)$$

Comparing Eq. 7 with Eq. 8 shows that:

$$\begin{aligned} \sum_{\text{eff}} &= \frac{-\ln [Ve^{-\sum \Delta} + 1 - v]}{v \Delta} \\ &= \frac{-\ln [1 - v(1 - e^{-\sum \Delta})]}{v \Delta} \end{aligned} \quad (9)$$

Equation 9 may be expanded in a series:

$$\sum_{\text{eff}} = \frac{v(1 - e^{-\sum \Delta})}{v \Delta} + \frac{1}{2} \frac{v^2(1 - e^{-\sum \Delta})^2}{v \Delta} + \dots \quad (10)$$

For small values of $v(1 - e^{-\sum \Delta})$, Eq. 10 reduces to

$$\begin{aligned} \Sigma_{\text{eff}} &= \frac{1 - e^{-\Sigma \Delta}}{\Delta} \approx \Sigma \quad \text{if } \Sigma \Delta \ll 1 \\ &\approx \frac{1}{\Delta} \quad \text{if } \Sigma \Delta \gg 1 \end{aligned} \quad (11)$$

Equation 11 provides a valuable insight into the variation of the efficiency of a chunk with its size. The transmission approaches the reduced density value as the chunks become small or less opaque. The transmission of opaque chunks depends only on Δ since the radiation that penetrates the slab channels around the chunks instead of penetrating them.

The case of opaque chunks is of special interest since it represents the extreme case where all the transmitted radiation channels through the slab. An opportunity to penetrate the slab exists only when the void spaces between chunks are lined up so that there is a direct path through the slab. In this case Eq. 6 becomes:

$$T = (1 - v)^{t/\Delta} \quad (12)$$

If V is small, this can be approximated by:

$$T \approx e^{-tV/\Delta} \quad (13)$$

It is interesting to note that the Poisson distribution function for the probability of straight paths through the slab encountering no chunks, which is only strictly valid when $V \ll 1$ and $N \gg n \gg 1$, gives the same answer for this approximation.

Formulas for Materials with Right Cylindrical Chunks of Multiple Sizes

The above treatment of a single chunk size is now extended to include more than one chunk size or material. For two different sized chunks, a division is made into layers and sublayers characteristic of the larger chunks and smaller chunks, respectively. The transmission of a layer is

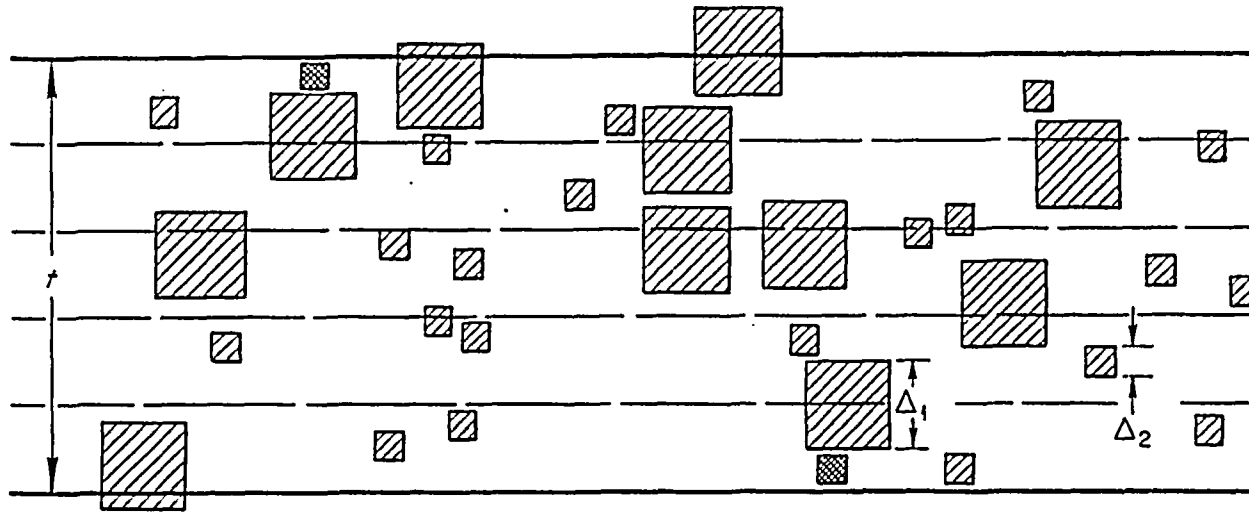
then found as before except that Eq. 6 is used to determine the transmission of the area between the large chunks. It is shown that the large chunks crowd the smaller ones together and hence the effectiveness of small chunks depends on the volume occupied by larger ones. The effective attenuation cannot be expressed simply as was the case for single-sized chunks, but it is possible to approximate the effective volume fraction in certain limiting cases.

It is assumed first that the chunk distribution is made up of two different sized cylinders (see Fig. 4) with heights Δ_1 and Δ_2 with $\Delta_1 \cong \Delta_2$. In deriving the approximate result it is assumed that Δ_1 is a multiple of Δ_2 . The volume fraction of the Δ_1 chunk is V_1 , and the volume fraction of the Δ_2 chunk is V_2 . The corresponding attenuation coefficients are Σ_1 and Σ_2 . The division of the chunks into sublayers is carried out by further dividing the layers into sublayers as shown in Fig. 4.

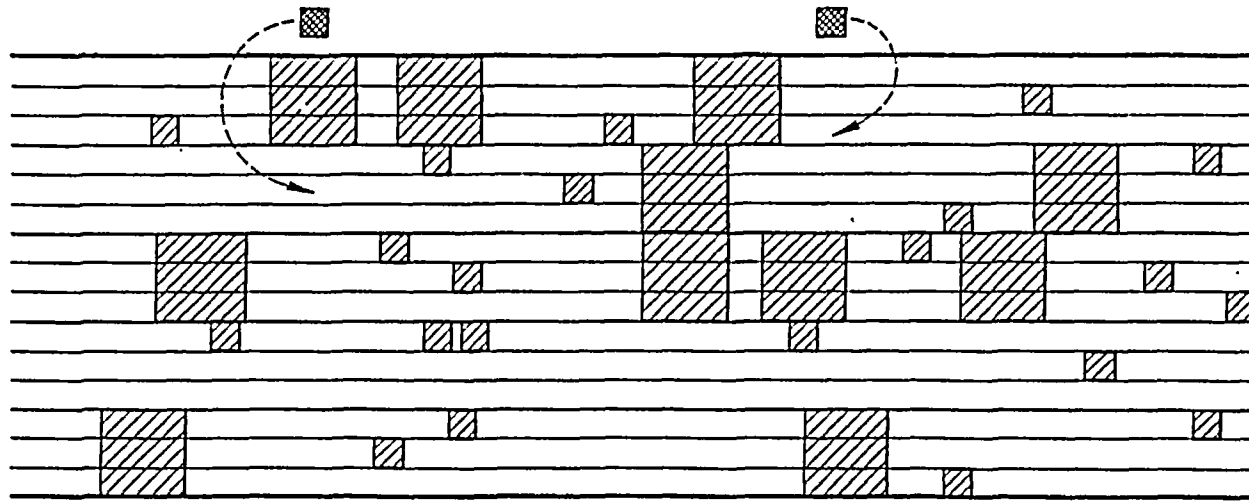
Each large (Δ_1) chunk is translated vertically so that it lies in the layer in which its center was formerly located, just as in the division of the single chunk size illustrated in Fig. 3. The small chunks are then translated so that each one lies in the sublayer in which its center was formerly located. Occasionally a small chunk should go into a sublayer which is occupied by a large chunk (see the cross-hatched small chunks in Fig. 4). In this case, the small chunk is translated vertically and inserted at random in some vacant spot. Thus, the original random distribution is divided into layers which are statistically independent of one another and the over-all slab transmission T can be found if the average transmission of one layer is known.

The transmission T_s of a single layer is given by an extension of Eq. 4.

$$T_s = V_1 e^{-\Sigma_1 \Delta_1} + (1 - V_1) \left[\frac{V_2 e^{-\Sigma_2 \Delta_2}}{1 - V_1} + 1 - \frac{V_2}{1 - V_1} \right]^{\Delta_1 / \Delta_2} \quad (14)$$



THE UNDIVIDED SLAB



THE DIVIDED SLAB

Fig. 4. The Division of a Slab Containing Two Chunk Sizes into Layers and Sublayers.

The first term is the transmission through the larger chunks. The second term is the transmission through the rest of the layer. This second term is identical in Eq. 6 except that the volume fraction of smaller chunks is adjusted to account for the space occupied by the larger chunks. For a given volume fraction of small chunks, the density is larger if there are large chunks present, since the total volume available for the small chunks is less. The volume available to the smaller chunks is $1 - V_1$ so that V_2 must be multiplied by $1/(1 - V_1)$ to account for the effect of the larger chunks. The over-all transmission of the slab is then:

$$T = \left\{ v_1 e^{-\sum_1 \Delta_1} + (1 - v_1) \left[\frac{v_2 e^{-\sum_2 \Delta_2}}{1 - v_1} + 1 - \frac{v_2}{1 - v_1} \right]^{\Delta_1/\Delta_2} \right\}^{t/\Delta_1} \quad (15)$$

This formula is applicable to chunks of different materials.

For more than two chunk sizes or materials, the above argument is extended to consider that sub-sublayers contain the next smaller Δ_3 chunks, etc. For three chunk sizes (with $\Delta_1 \geq \Delta_2 \geq \Delta_3$):

$$T = \left\{ v_1 e^{-\sum_1 \Delta_1} + (1 - v_1) \left(\frac{v_2 e^{-\sum_2 \Delta_2}}{1 - v_1} + \left[1 - \frac{v_2}{1 - v_1} \right] \left[\frac{v_3 e^{-\sum_3 \Delta_3}}{1 - v_1 - v_2} + 1 - \frac{v_3}{1 - v_1 - v_2} \right]^{\Delta_2/\Delta_3} \right)^{\Delta_1/\Delta_2} \right\}^{t/\Delta_1} \quad (16)$$

The extension to an arbitrary number of chunk sizes is evident. The general formula (with $\Delta_1 \geq \Delta_2 \dots \geq \Delta_n$) is:

$$T = \left\{ v_1' e^{-\sum_1 \Delta_1} + (1 - v_1') \left(v_2' e^{-\sum_2 \Delta_2} + [1 - v_2'] \left[\dots (1 - v_{n-1}') \right. \right. \right. \\ \left. \left. \left. \chi \left\{ v_n' e^{-\sum_n \Delta_n} + 1 - v_n' \right\}^{\Delta_{n-1}/\Delta_n} \dots \right]^{\Delta_2/\Delta_3} \right)^{\Delta_1/\Delta_2} \right\}^{t/\Delta_1} \quad (17)$$

V_i' is the volume fraction adjusted for the displacement of all larger chunks. The volume occupied by the chunks larger than the i th chunk is $(1 - V_1 - V_2 - \dots - V_{i-1})$ hence:

$$V_i' = \frac{V_i}{1 - V_1 - V_2 - \dots - V_{i-1}} \quad (18)$$

V_1 is the same as V_1' since there are no chunks with $\Delta_i > \Delta_1$. Equation 17 may be used to approximate a continuous distribution by choosing a sufficient number of discrete sizes in accord with the distribution. The smallest chunk size may be allowed to go to zero, so that in the limit, the equation is applicable to chunks distributed in a uniformly absorbing medium. In this case, the last bracket in Eq. 11 becomes:

$$\lim_{\Delta_n \rightarrow 0} \left\{ v_n' e^{-\sum_n \Delta_n} + 1 - v_n' \right\}^{\Delta_{n-1}/\Delta_n} = e^{-v_n' \sum_n \Delta_{n-1}} \quad (19)$$

It is desirable to find an effective value of the attenuation coefficient which indicates the effect of the chunk size distribution on the effectiveness of a particle of a given size. In general, the effectiveness of a chunk of a given size depends on the parameters of all the other chunk sizes, but for certain limiting cases, the effective attenuation can be simply obtained as follows:

I. For all chunks opaque $\therefore \left(\Delta_i \sum_i \gg 1 \text{ for all } i \right),$

$$T = e^{\left[\frac{1}{\Delta_1} \ln(1 - v_1') + \frac{1}{\Delta_2} \ln(1 - v_2') + \dots \right] t} \quad (20a)$$

17) II. For all chunks almost transparent $\left(\sum_i \Delta_i \ll 1 \text{ for all } i \right)$

$$T = e^{-(v_1 \sum_1 + v_2 \sum_2 + \dots) t} \quad (20b)$$

18) III. For first m chunks opaque and all others almost transparent,

$$T = e^{\left[\frac{1}{\Delta_1} \ln(1 - v_1^*) + \dots + \frac{1}{\Delta_m} \ln(1 - v_m^*) - v_{m+1}^* \sum_{m+1} - \dots \right] t} \quad (20c)$$

17) where

$$v_i^* = v_i / \left[1 - (\text{volume fraction of all opaque chunks with } \Delta > \Delta_i) \right]$$

IV. For total volume fraction of all chunk sizes $\ll 1$,

$$T = e^{- \left[v_1 \frac{1 - e^{-\sum_1 \Delta_1}}{\Delta_1} + v_2 \frac{1 - e^{-\sum_2 \Delta_2}}{\Delta_2} + \dots \right] t} \quad (20d)$$

All the above limiting cases can be collectively expressed by:

$$T = e^{- \left[v_1^* \sum_1^* + v_2^* \sum_2^* + \dots \right] t} \quad (21)$$

where

$$\sum_i^* = - \frac{\ln \left[v_i^* e^{-\sum_i \Delta_i} + 1 - v_i^* \right]}{\Delta_i v_i^*}$$

$$\text{and } v_i^* = v_i / \left[1 - (\text{volume fraction of all opaque chunks with } \Delta > \Delta_i) \right].$$

Note that \sum_i^* is the same as \sum_{eff} for the single chunk size distribution as given by Eq. 9. The physical significance of this result is that the transmission may be approximated in the limiting cases above by the product of the transmissions of separate layers containing a single chunk size if the volume fraction of the chunk in the layer is corrected for the volume occupied by larger opaque chunks in the slab. Each term of the exponent in Eq. 21 gives the transmission of one layer. When none of the approximations are valid, Eq. 21 gives a transmission which is too small since it ignores the voids which should be present in a layer when the larger chunks are separated out. In these cases, Eq. 17 must be used but the approximate Eq. 21 still is useful in qualitatively interpreting the effect of changing the chunk size distribution.

Formulas for Materials with Arbitrary Chunk Shapes

The discussion has thus far been restricted to aligned cylinders because of the simple formulas that resulted. The results can be extended in an approximate way to arbitrarily shaped chunks with random orientation by replacing $(1 - e^{-\Sigma\Delta})$ in the simple formula by F , which represents the absorption of a single chunk averaged over all orientations, and replacing the layer thickness Δ by $\bar{\Delta}$, the average chunk thickness. A theorem due to Gauss¹⁰ shows that for chunks with no concavities,

$$\bar{\Delta} = \frac{4v}{S} \quad (22)$$

where v is the volume of chunk and S is the total surface area of chunk. F is related to the collision probability P_c which is tabulated in Ref. 10 for many shapes of chunks, i.e.,

$$F = \bar{\Delta} \sum (1 - P_c) \quad (23)$$

10. K. M. Case, F. de Hoffmann, and G. Placzek, Introduction to the Theory of Neutron Diffusion, Vol. I, Section 10, Los Alamos Scientific Laboratory Report, Superintendent of Documents (1953).

For large chunks ($\Sigma \bar{\Delta} \gg 1$) with smooth edges (Ref. 10),

$$F = \left[1 - O \left(\frac{1}{\Sigma \bar{\Delta}} \right)^2 \right] \quad (24)$$

where $O \left(\frac{1}{\Sigma \bar{\Delta}} \right)^2$ means terms of the order of magnitude of $\left(\frac{1}{\Sigma \bar{\Delta}} \right)^2$.

For large chunks with irregular edges,

$$F = \left[1 - O \left(\frac{1}{\Sigma \bar{\Delta}} \right) \right] \quad (25)$$

For small chunks ($\Sigma \bar{\Delta} \ll 1$),

$$F = \Sigma \bar{\Delta} (1 - \nu^{1/3} \alpha \Sigma) \quad (26)$$

where α is a parameter ≈ 0.5 for spheres. For spheres (Ref. 10)

$$F = \frac{2}{(2r\Sigma)^2} \left[\frac{1}{2} (2r\Sigma)^2 - 1 + (1 + 2r\Sigma) e^{-2r\Sigma} \right] \quad (27)$$

In terms of F , Eq. 6 for single-sized aligned chunks becomes:

$$T = \left[1 - VF \right]^{t/\Delta} \quad (28)$$

The extension to several different types of chunks is straightforward and

(23)

ry
ratory

$$T = \left\{ v_1' (1 - F_1) + (1 - v_1') \left(v_2' (1 - F_2) + [1 - v_2'] \left[\dots \right. \right. \right. \right. \\ \left. \left. \left. \left. \dots (1 - v_{n-1}') \left\{ v_n' (1 - F_n) + 1 - v_n' \right\} \left. \begin{array}{l} \bar{\Delta}_{n-1}/\bar{\Delta}_n \\ \bar{\Delta}_2/\bar{\Delta}_3 \\ \bar{\Delta}_1/\bar{\Delta}_2 \end{array} \right] \right) \right] \right\} t/\bar{\Delta}_1 \quad (29)$$

in analogy with Eq. 17 for aligned cylinders. The generalized form of Eq. 21 remains:

$$T = e^{-\left[v_1^* \Sigma_1^* + v_2^* \Sigma_2^* + \dots \right] t} \quad (30)$$

where now $v_i^* = v_i / \left[1 - (\text{volume fraction of all opaque chunks with } \bar{\Delta} > \bar{\Delta}_i) \right]$,

$$\Sigma_i^* = - \frac{\ln [1 - v_i^* F_i]}{\bar{\Delta}_i v_i^*} \quad (31)$$

Formulas Including Energy and Angular Distributions

All the above discussion assumes a constant linear attenuation coefficient. This assumption is not valid in those cases for which the angular distribution is not collimated and spectrum hardening effects occur. If the chunks are randomly oriented, there will be no preferred direction of transmission in the slab. The transmission for incidence at the angle θ may therefore be calculated by replacing the thickness t by the slant penetration $t/\cos\theta$ in the previous formulas. Then the above formulas may be used to compute the transmission for a single entrance angle and energy and the result integrated in accordance with the prescribed neutron distributions. In general, the transmission including the effects of energy spectra and angular distribution is given by:

$$T(t) = \int_0^{\infty} \int_0^{\pi/2} T(t/\cos\theta, E) \phi(E) \psi(\theta) d\theta dE \quad (32)$$

where

$T(t/\cos\theta, E)$ = transmission for a given angle and energy,

$\phi(E)$ = effective neutron spectral function,

$\psi(\theta)$ = angular distribution function.

For normal incidence, Eq. 32 simplifies to:

$$T(t) = \int_0^{\infty} T(t, E) \phi(E) dE \quad (33)$$

For isotropic incidence, Eq. 32 becomes

$$T(t) = \int_0^{\infty} E_2 \left(-\ln T(t, E) \right) \phi(E) dE \quad (\text{flux detector}) \quad (34a)$$

$$= 2 \int_0^{\infty} E_3 \left(-\ln T(t, E) \right) \phi(E) dE \quad (\text{current detector}) \quad (34b)$$

where the neutron spectral function is (for a Maxwell-Boltzmann distribution):

$$\phi(E) = \sqrt{\frac{4}{\pi}} \frac{E^{1/2}}{(KT)^{3/2}} e^{-E/KT} \quad (\text{for } 1/v \text{ detector}) \quad (35a)$$

$$\phi(E) = \frac{E}{(KT)^2} e^{-E/KT} \quad (\text{for constant efficiency detector}) \quad (35b)$$

The functions E_2 and E_3 are the standard exponential integrals.¹¹

II. CALCULATION OF NEUTRON TRANSMISSION THROUGH BORAL

The foregoing method has been used to compute the transmission of neutrons through boral. For the calculation it was assumed that the boral sandwich was rolled to a thickness of 1/8 in. and that the thickness of the B_4C -Al mixture was 0.085 in. with 40 vol% boron carbide. This resulted in an over-all volume fraction of approximately 25% for the absorbing chunks, which were assumed to be spherical in shape. The chunks were first considered to be of 11 different sizes between 20 and 100 mesh (this size distribution was taken from Ref. 12); however, it was found that assuming only four sizes gave approximately the same results, and only four groups were used thereafter. The four groups were as follows:

Size Mesh	Avg. Particle Diameter (in.)	$\bar{\Delta} = (4/3)r$ (in.)	Vol%
20-30	0.038	0.0253	17.0
36-46	0.024	0.0160	11.0
60-70	0.016	0.0107	6.0
80-120	0.009	0.0060	<u>6.0</u>
			40.0

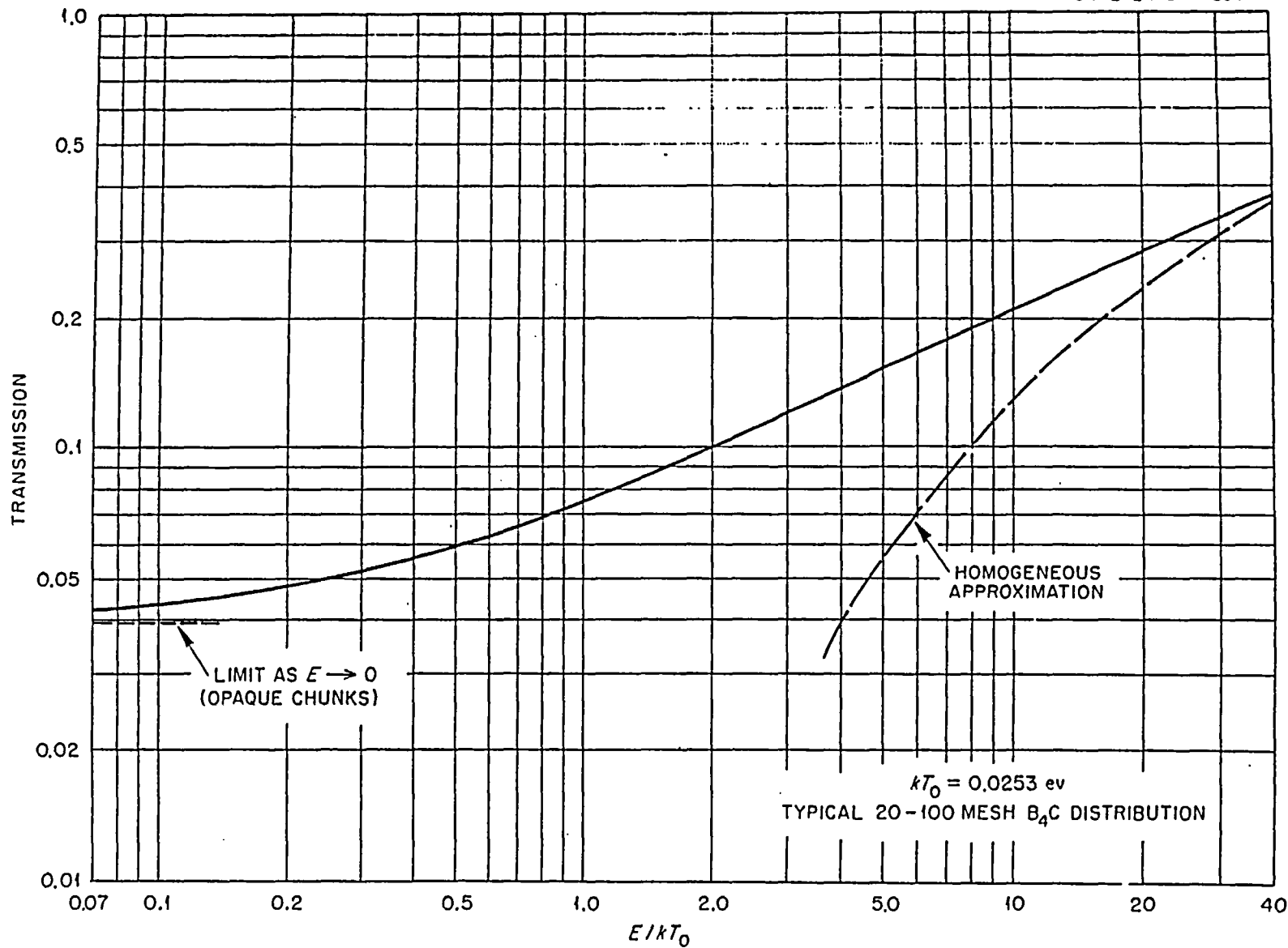
The transmission calculated by this method for normally incident 2200-m/sec (0.0253-ev) neutrons through 1/8-in.-thick boral was 0.076. This is to be compared with a transmission of 0.0015 calculated for normally incident 2200-m/sec neutrons by the homogeneous approximation.

The transmission of normally incident neutrons through a 1/8-in.-thick boral shield as a function of energy is shown in Fig. 5, along with the

11. Case, de Hoffman, and Placzek, op. cit., Appendix A.

12. A Handbook on Boron Carbide, Elemental Boron, and Other Stable, Boron-Rich Materials, Norton Company 1417-3PCMX-10-56 CP (1955).

UNCLASSIFIED
ORNL-LR-DWG 25040



limit as the chunks become opaque (low energies). The average transmission over the neutron distribution shown (Maxwell-Boltzmann distribution at room temperature) is 0.096 for a constant efficiency detector and 0.084 for a $1/v$ detector.

The transmission of isotropically incident neutrons through $1/8$ -in.-thick boral as a function of energy is shown in Fig. 6. For this case the average transmissions are 0.024 for a constant efficiency flux detector, 0.021 for a $1/v$ flux detector, 0.041 for a constant efficiency current detector, and 0.034 for a $1/v$ current detector.

III. COMPARISON OF CALCULATED AND EXPERIMENTAL RESULTS

The calculated results reported above can be compared with the results of two experiments which have been performed at ORNL to determine the transmission through $1/8$ -in. thicknesses of boral as measured by $1/v$ detectors. In the first experiment⁴ the radiation consisted of thermal neutrons escaping from a thermal column on top of the ORNL Graphite Reactor with an angular distribution of the $(1 + \sqrt{3} \cos\theta)$ type,¹³ which is more forwardly peaked than an isotropic flux. Consequently, the experimental values should be between the computed values for normal incidence and those for isotropic incidence. The transmission obtained for a Brooks and Perkins boral sample was 0.070, while the transmission for an ORNL sample was 0.094.

In the second experiment¹⁴ the radiation was a collimated beam of normally incident neutrons from a beam hole at the ORNL Graphite Reactor. The transmissions obtained for two different Alcoa samples were 0.065 and 0.070, respectively.

13. R. F. Christy et al., Lecture Series in Nuclear Physics, MDDC-1175 (1943; decl. 1945).

14. G. deSaussure, Oak Ridge National Laboratory, private communication.

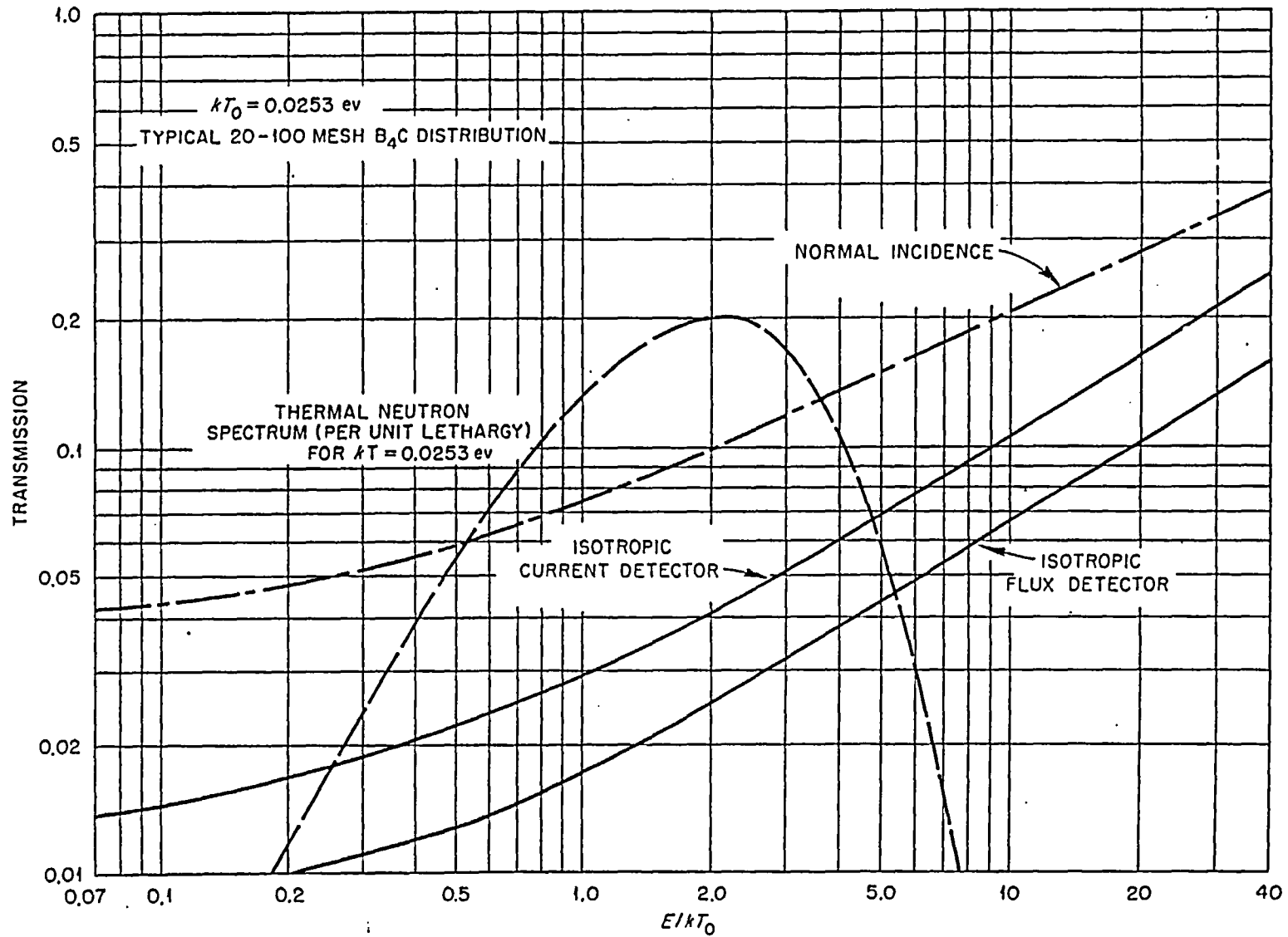


Fig. 6. Neutron Transmission Through $\frac{1}{8}$ -in.-thick Boron as a Function of Energy; Isotropically Incident Flux.

IV. CONCLUSION

The method proposed in this paper is less elegant than other methods proposed previously, for example, Smith's method,⁸ but it is more easily visualized. Furthermore, the degree of agreement between experimental and calculated results seems reasonably good since experimental details of particle size, energy, and angular distribution are incompletely known in each case. It may be concluded that the methods described in this paper can be used to provide useful estimates of the attenuation of radiation in heterogeneous media for which channeling between absorbing chunks is an important process.

MICHIGAN MEMORIAL PHOENIX PROJECT
THE UNIVERSITY OF MICHIGAN

FNR - PML REPORT 1-76

Experimental Observation of
BORAL Plates
Encased in Stainless Steel
Under the Influence of
Gamma and Neutron Fluxes

February, 1976

Prepared For
Brooks and Perkins, Incorporated
12633 Inkster Road
Livonia, Michigan 48150



Report No. 572

Prepared by

Brooks & Perkins, Inc.
Advanced Structures Division
12633 Inkster Road
Livonia, Michigan 48150

NOTE: All information contained in or disclosed by this document is considered confidential and proprietary by Brooks & Perkins, Inc., and must not be reproduced or copied, or used as the basis for the preparation of other designs, or for the manufacture or sale of apparatus or devices without specific permission of Brooks & Perkins, Inc., 12633 Inkster Road, Livonia, Michigan 48150.

EXPERIMENTAL OBSERVATION
OF BORAL PLATES ENCASED
IN STAINLESS STEEL UNDER
THE INFLUENCE OF GAMMA
AND NEUTRON FLUXES
(See FNR-PML Report 1-76)

FNR-PML REPORT 1-76

Experimental Observation of
BORAL Plates
Encased in Stainless Steel
Under the Influence of
Gamma and Neutron Fluxes

FORD NUCLEAR REACTOR
MICHIGAN MEMORIAL - PHOENIX PROJECT
THE UNIVERSITY OF MICHIGAN
Ann Arbor, Michigan

February, 1976

Prepared For
Brooks and Perkins, Incorporated
12633 Inkster Road
Livonia, Michigan 48150

ABSTRACT

Experimental observations were made of BORAL plates encased in stainless steel jackets. Samples were tested dry and with 25 ml distilled water, 70 ml 2000 PPM boron solution, and 20 ml 2000 PPM boron solution injected within the stainless jacket. Samples were subjected to gamma and neutron fluxes in the Ford Nuclear Reactor.

Under irradiation fluxes and water conditions expected in a power reactor spent fuel pool, the BORAL samples exhibited no detectable gas evolution, pressure buildup, or damage due to temperature or other effects.

In the presence of a neutron flux, hydrogen and oxygen gas were evolved from the BORAL samples injected with 2000 PPM boron solution.

TABLE OF CONTENTS

<u>Section</u>	<u>Page</u>
TITLE PAGE	1
ABSTRACT	2
TABLE OF CONTENTS	3
1. <u>INTRODUCTION</u>	
1.1 Purpose	4
1.2 Description	4
1.3 Experimental Conditions	4
2. RESULTS	6
3. CONCLUSION	12

APPENDIX 1: Deformation of the Ford Nuclear Reactor
Control Rods

1. INTRODUCTION

1.1 Purpose

The purpose of this report is to provide the results of experimental observations of BORAL plates encased in stainless steel jackets under gamma and neutron flux irradiations.

1.2 Description

Each BORAL sample was a 9 inch x 9 inch plate of 0.26 inch thickness. Each plate was encased in a thin, watertight jacket of stainless steel welded around the edges. A threaded connection was welded in the upper right corner of the face on one side of the stainless steel jacket. Irradiations were conducted in the Ford Nuclear Reactor pool at depths of 12 and 20 feet. An aluminum tube was run from the connection to the surface of the reactor pool for pressure measurements and gas collection.

Prior to testing, each sample plate was baked at 200°C for seven hours in a vacuum oven to remove moisture.

Each sample was tested to 10 P SIG internal pressure. Experimental pressures were limited to 5 P SIG as a reactor safety precaution.

Experimental measurements were made of pressure within each sample. Gas evolved during the tests was collected and analyzed. It was decided that temperature would not be measured. Each sample was observed after irradiation for damage due to pressure, temperature, or other effects.

Each sample was pressurized momentarily to 10 P SIG as it was inserted into the reactor pool to verify watertightness. Once each sample was placed in its experimental position, a 30 inch Hg vacuum was drawn to evacuate as much air as possible. The starting pressure for each test was the 30 inch Hg vacuum.

1.3 Experimental Conditions

The experimental sequence consisted of twelve steps derived from a combination of four different sample plates being subjected to three different irradiation conditions.

Sample 1 was a sealed, dry sample vented only through the gas collection line to the surface of the reactor pool. Sample 2 was identical to Sample 1 except that 25 ml of distilled water was injected within the stainless steel jacket. Sample 3 and Sample 4 were identical to Sample 1 except that 70 ml and 20 ml, respectively, of 2000 PPM boron solution were injected within the stainless steel jacket. The 2000 PPM boron solution was obtained by dissolving 1.23 grams of boric acid, H_3BO_3 , in 100 ml of distilled water.

Initially, in Condition 1, each sample was irradiated adjacent to spent reactor fuel in a gamma flux of 2×10^5 rad/hr. In Condition 2 each sample was placed in a holder adjacent to the reactor operating at a power level of 2 MW. The Condition 2 gamma flux was 4×10^7 rad/hr and thermal neutron flux was approximately 1×10^{12} N/cm²/sec, or 1×10^7 rad/hr. Finally, in Condition 3, each sample was left adjacent to the reactor core immediately after shutdown. Neutron flux was quite low, approximately five orders of magnitude below operating levels, while gamma flux was measured as 1.2×10^6 rad/hr.

The objective in these observations was to simulate conditions in a power reactor spent fuel pool:

<u>Description</u>	<u>Units</u>	<u>PWR</u>	<u>BWR</u>
Gamma Flux	rad/hr	1×10^6	1×10^6
Neutron Flux	rad/hr	Negligible	Negligible
Boron Concentration in Pool Water	PPM	1800	0

Combinations of Samples 2, 3, and 4 under Condition 3 closely simulate actual spent fuel pool conditions.

The 70 ml of boron solution placed in Sample 3 virtually filled the sample with liquid. It was decided to place a smaller liquid volume in Sample 4, 20 ml, and to thoroughly wet all surfaces with liquid prior to irradiation under the assumption that radiolysis, the breakdown of water into hydrogen and oxygen gas under the influence of radiation, would be enhanced by wetting all surfaces and providing a larger liquid to gas surface area within the sample.

2. RESULTS

Table 1 summarizes the observed effects of irradiation conditions on the BORAL samples. The total hours of irradiation per sample are noted in the array.

No pressure increase or gas evolution was observed under any condition for Sample 1, the dry sample, or Sample 2, the sample containing 25 ml of distilled water.

Sample 3 and Sample 4, the samples containing boron solutions, both generated gas when subjected to Condition 2, reactor at power and an irradiation flux of gamma rays and neutrons. Figure 1 is a plot of sample pressure increase as a function of time and dose. Gas was drawn from each sample and analyzed with a gas chromatograph. The results were:

<u>Sample</u>	<u>Sample Gas Constituents (%)</u>		
	<u>Hydrogen</u>	<u>Oxygen</u>	<u>Nitrogen</u>
3	6.5	20.4	73.1
4	41.1	21.6	37.3
4	41.0	21.8	37.2

The hydrogen percentage of Sample 3 was lower than might be expected, an approximate 2:1 hydrogen - oxygen ratio, because Sample 3 was not purged extensively prior to sampling. The chromatograph analysis results are included as Tables 2 - 4.

When Sample 3 and Sample 4 were subjected to gamma flux alone, gas was not evolved and no pressure increase was detected with irradiation time.

<u>SAMPLE 1</u>	<u>SAMPLE 2</u>	<u>SAMPLE 3</u>	<u>SAMPLE 4</u>
9" x 9" BORAL Plate Stainless Steel Jacket Dry	9" x 9" BORAL Plate Stainless Steel Jacket 25 ml Distilled Water	9" x 9" BORAL Plate Stainless Steel Jacket 70 ml - 2000 PPM Boron	9" x 9" BORAL Plate Stainless Steel Jacket 20 ml - 2000 PPM Boron

<u>CONDITION 1</u> Spent Fuel $\gamma - 2 \times 10^5$ Rad/hr N - Negligible	<u>42 Hours</u> No Detectable Effect	<u>25 Hours</u> No Detectable Effect	<u>19 Hours</u> No Detectable Effect	<u>4 Hours</u> No Detectable Effect
<u>CONDITION 2</u> Reactor at 2 MW $\gamma - 4 \times 10^7$ Rad/hr N - 1×10^7 Rad/hr	<u>24 Hours</u> No Detectable Effect	<u>6 Hours</u> No Detectable Effect	<u>48 Hours</u> Linear pressure increase with irradiation time. Gas Analysis: 6.5% Hydrogen 20.4% Oxygen	<u>152 Hours</u> Linear pressure increase with irradiation time. Gas Analysis: 41.1% Hydrogen 21.6% Oxygen
<u>CONDITION 3</u> Reactor Shutdown $\gamma - 1.2 \times 10^6$ Rad/hr N - Negligible	<u>4 Hours</u> No Detectable Effect	<u>4 Hours</u> No Detectable Effect	<u>12 Hours</u> No Detectable Effect	<u>96 Hours</u> No Detectable Effect

Table 1
Observed Effects of Irradiation Conditions on BORAL Samples

Figure 1
Sample Pressure Profile

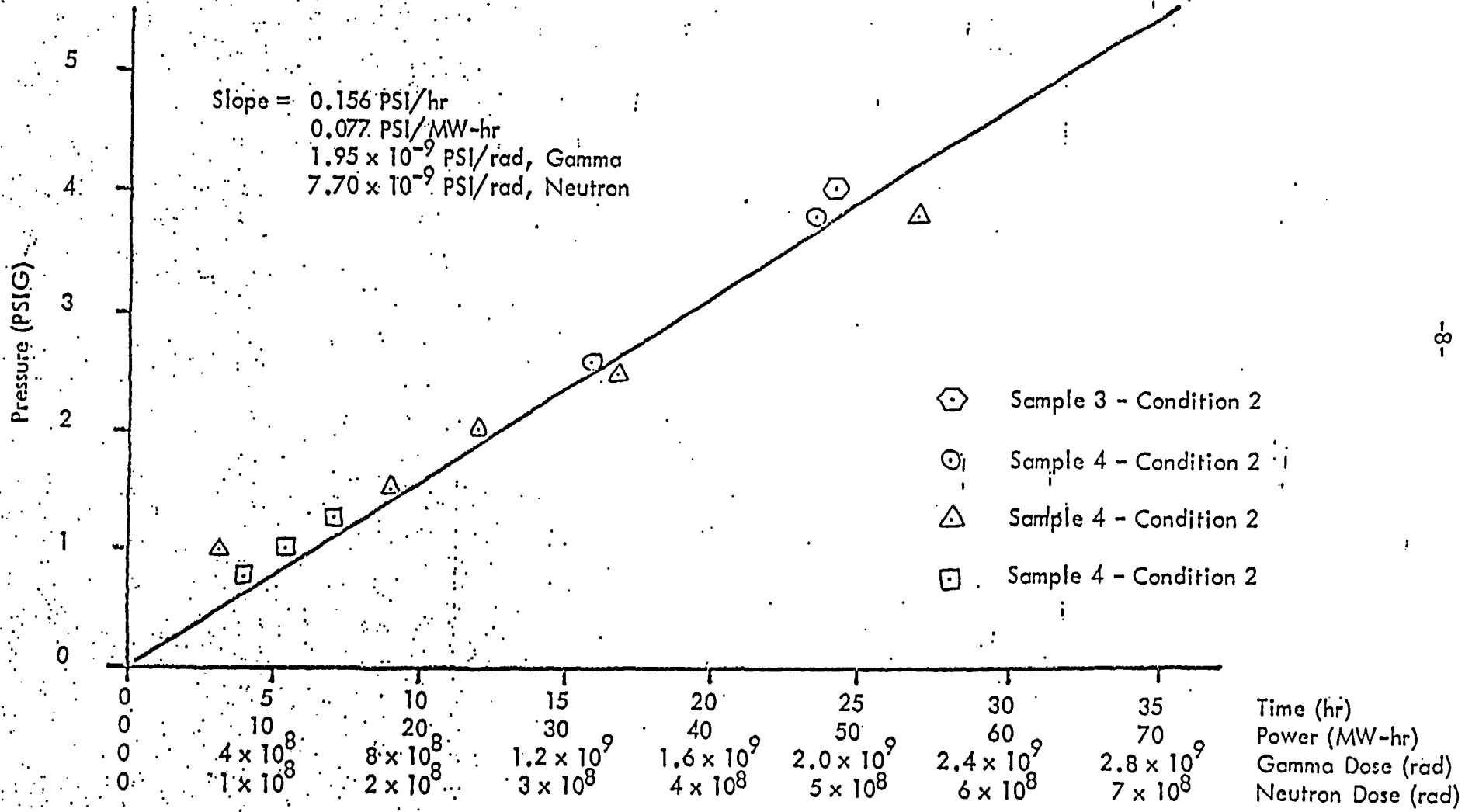


TABLE 2

Page 1 of G.C.# 18 V.S.# 1

ANALYSIS SHEET Van Slyke Apparatus

Rad No. Run No. 1 Vessel No. 10 i.d. Original Sample SAMPLE 2 - DURAL PLATE IN STAINLESS JACKET Sample, as measured Radiation Source/Location CUP 2 - REACTOR Date 1-19-76 Dose Rate 8 - 4 x 10^7 6N^1 - 1 x 10^7 rads/hr Irradiation Time Total Dose rads

Flow Rate 30.3 μ/min Col.#1 10 cc/19.8 sec Col.#2 10 cc/20.0 sec Baragraph 30.15 Humid. 21 % Temp. 74°F V.S. Temp. 22.3°C Vol. 0.823 cc

Pi 474.0 mm 473.0 mm 472.7 mm 3) 1419.7 Pi ave 473.23 mm Po 138.6 mm 138.8 mm 138.7 mm 3) Po ave 138.7 mm PT 334.53 mm

TF2 Closed 2:32 time Loop Loaded time Run Start 2:33 time Total Time 1 MIN.

Integrator Data

1 FILE 3 1196 ID 40 20 10 PW 30 30 30 SS 3 3 3 FP 5 5 5 BL 400 200 1 T1 2 T4 70 T5 900 SEC RUN 100 HA 50 PL 50000 HL SP

Table with 4 columns: Sensitivity Factors Used, Summary Sheet, Date, Calc. Press. Rows include H2, O2, N2 with various numerical values and dates.

Table with 2 columns: TIME, AREA. Rows include 124 H2, 249 O2, 415 NOISE, 587 N2.

Table with 2 columns: TIME, CONC. Rows include 124, 249, 415, 587.

COMMENTS:

attest: Reed R Bur 2/12/76

TABLE 3

ANALYSIS SHEET
Van Slyke Apparatus

Rad No. _____

Run No. 1

Vessel No. 2

Original Sample SAMPLE 3 - BORAL PLATE IN STAINLESS JACKET

Sample, as measured _____

Radiation Source/Location CUP 2 - REACTOR Date 1-29-76

Dose Rate $8 - 4 \times 10^7$ $0.1 - 1 \times 10^7$ rads/hr

Irradiation Time _____ Total Dose _____ rads

Flow Rate 300 cc/min Col.#1 10 cc/20.0 sec Col.#2 10 cc/20.0 sec

Barograph 29.95 Humid. 25 % Temp. 73°F

V.S. Temp. 22.4 Vol. 0.823 cc

1st SAMPLE, AFTER 1 PURGE

P_i 522.1 mm

P_o 138.4 mm

522.4 mm

138.6 mm

522.0 mm

138.5 mm

3) 1566.5

3) _____

P_i ave 522.17 mm

P_o ave 138.5 mm

P_o ave 138.5 mm

P_T 383.57 mm

TF2 Closed 2:30 time

Loop Loaded _____ time

Run Start 2:31 time

Total Time 1 MIN

Integrator Data

#	1	FILE	3
			1296 ID
	40	20	10 PM
	30	30	30 SS
	3	3	3 FP
	5	5	5 BL
	400	200	1 T1
			2 T4
			70 T5
			100 NA
			50 PL
			50000 ML
			SP

830 SEC RUN

Sensitivity Summary
Factors Used Sheet Date CALC. PRESS

1 H₂ 1.400×10^{-4} H₂/1-6 5-2-75 146.20 mm = 4.170

2 O₂ 1.408×10^{-3} O₂/1-2 9-8-75 76.77 = 21.6%

3 N₂ 1.704×10^{-3} N₂/1-2 9-10-75 132.59 = 37.3

4 WITHIN 7.3% OF MEASURED = 355.56 mm 100.0%

5 _____

6 _____

7 _____

TIME	AREA
127	H ₂ 1044272
250	O ₂ 54527
587	N ₂ 77613
	1176612

TIME	CONC
127	88.752
250	1.634
587	6.513
	99.999

COMMENTS:

attest: Richard D. Burr
2/12/76

TABLE 4

G.C.# 1B V.S.# 1B

ANALYSIS SHEET
Van Slyke Apparatus

Rad No. _____

Run No. 2

Vessel No. 2

Original Sample SAMPLE 3 - BAPAL PLATE IN STAINLESS JACKET

Sample, as measured _____

Radiation Source/Location CUP 2 - REACTOR Date 1-29-76

Dose Rate $8 - 4 \times 10^7$ $6N' - 1 \times 10^7$ rads/hr

Irradiation Time _____ Total Dose _____ rads

Flow Rate 30.0 cc/min Col.#1 _____ cc/ _____ sec Col.#2 _____ cc/ _____ sec

Baragraph _____ Humid. _____ % Temp. _____

V.S. Temp. 22.7°C Vol. 0.823 cc

Integrator Data

P_i	<u>357.1</u> mm	P_o	<u>138.1</u> mm
	<u>356.6</u> mm		<u>138.1</u> mm
	<u>356.5</u> mm		<u>138.3</u> mm
3)	<u>1070.3</u>	3)	<u>414.5</u>
P_i ave	<u>356.77</u> mm	P_o ave	<u>138.17</u> mm
P_o ave	<u>138.17</u> mm		
P_T	<u>218.6</u> mm		

#	2	FILE	3	
				1295 ID
	40	20	10	PW
	30	30	30	SS
	3	3	3	FP
	5	5	5	BL
	400	200	1	T1
			2	T4
			70	T5
			100	HA
			50	PL
			50000	HL
				SP

TF2 Closed 3:00 PM time

Loop Loaded _____ time

Run Start 3:01 time

Total Time 1 MIN.

840 SEC RUN

Sensitivity Factors Used

Summary Sheet

Date CALC. PRESS

1	H_2	1.600×10^{-4}	$H_2/1-6$	5-2-75	83.55 mm = 41.0%
2	O_2	1.408×10^{-3}	$O_2/1-2$	9-8-75	44.52 = 21.8
3	N_2	1.704×10^{-3}	$N_2/1-2$	9-10-75	75.81 = 37.2
4			WITHIN 0.7% OF MEAS. PRESS.	203.88	100.0%
5					
6					
7					

TIME	AREA
126 H_2	596793
251 O_2	31622
587 N_2	44487
	672902

TIME	CONC
126	88.669
251	4.699
587	6.611
	99.999

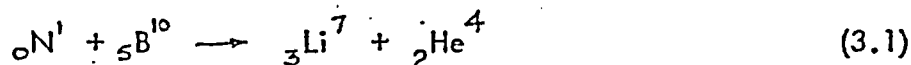
COMMENTS:

Attent: Reed R. Brown
2/12/76

3. CONCLUSIONS:

Under irradiation fluxes and water conditions expected in a power reactor spent fuel pool, the BORAL samples tested exhibited no detectable gas evolution, pressure build-up, or damage due to temperature or other effects.

In the presence of a neutron flux, hydrogen and oxygen gases were generated from the samples containing the 2000 PPM boron solution. Pressure built up in the samples as a linear function of irradiation time and neutron dose. Appendix I has been included because it is a report on a similar phenomenon observed in Ford Nuclear Reactor boron carbide (B_4C) powder filled control rods. A similar linear pressure increase with neutron dose was observed. The tests were terminated at a pressure of 60 PSIG out of concern for rupturing the test device. Radiolysis was attributed to ionization from lithium and helium released by the boron-neutron reaction:



A review of Table 1 shows that radiolysis occurred fairly rapidly in a neutron flux, Condition 2, with 2000 PPM boron solution filled samples, Sample 3 and Sample 4. Sample 2, under the same conditions, exhibited no detectable radiolysis or pressure buildup during the time period of observation. However, in Sample 2, the only boron exposed to water was around the edges of the BORAL plate. Ionizing lithium and helium released within the meat of the plate was stopped by aluminum cladding before reaching the distilled water in the sample.

It is not reasonable to conclude that gas was not generated in the Sample 2 - Condition 2 experiment just because detectable quantities were not observed during the short period of the experiment. It is possible that over an extended period pressure within the jacketed BORAL plate could build up due to radiolysis taking place at a much slower rate.

APPENDIX I
DEFORMATION OF THE FORD NUCLEAR REACTOR
SHIM-SAFETY RODS

Report by:

C. W. Ricker
W. R. Dunbar
J. B. Bullock

Investigations by:

J. B. Bullock
W. R. Dunbar
V. C. Serment
R. H. White

Phoenix Memorial Laboratory
Michigan Memorial Phoenix Project
The University of Michigan

December 1960

Table of Contents

	Page
I. Introduction	1
II. Description of Shim-Safety Rod Incidents	4
III. Investigation	7
IV. Possible Explanations of Deformation	15
V. Recommendations	18
VI. References	23

Plates

I. Photograph of Removal Device	5
II. Radiograph of Typical Shim-Safety Rod	11

Sketches

I. Shim-Safety Rod	2
II. Gas Removal Apparatus	12
III. Rod Sectioning Diagram	13

Tables

I. Shim-Safety Rod Thickness Dimensions	8
II. Shim-Safety Rod Width Dimensions	9

Graph

I. Test Chamber Pressure vs. Megawatt Hours	19
---	----

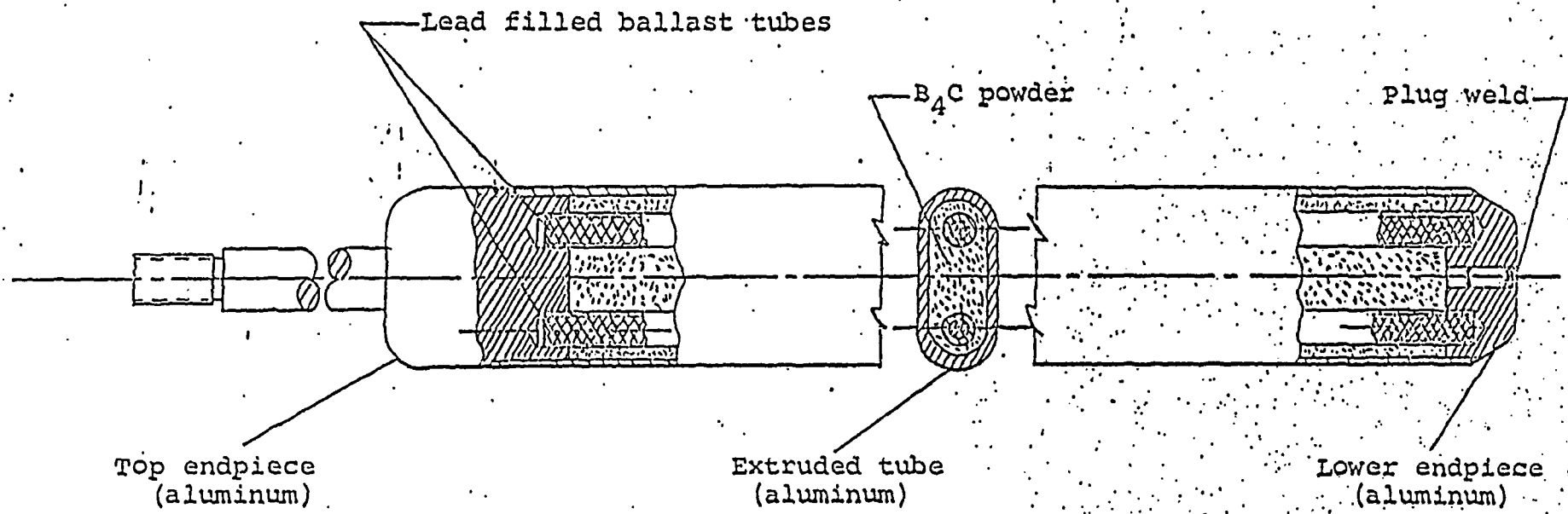
DEFORMATION OF THE FNR SHIM-SAFETY RODS

I. INTRODUCTION

The Ford Nuclear Reactor (FNR), located in the Phoenix Memorial Laboratory on the North Campus of The University of Michigan, is a one megawatt pool type reactor fueled with MTR type fuel elements. Control of the reactor is accomplished by the use of three shim-safety rods and one control rod. These rods move vertically inside special fuel elements in which guide tubes have been inserted in place of the center fuel plates. The shim-safety rods for the FNR, as their name implies, serve the dual function of shim control and safety protection. These rods, worth approximately 3 per cent negative reactivity each, drop into the reactor under the influence of gravity when potentially dangerous conditions exist in the reactor. This results from an interruption of the currents to electromagnets which normally couple the rods to their respective drive mechanisms. A shim-safety rod is constructed from an extruded aluminum tube welded to appropriate endpieces and filled with boron carbide powder (see Sketch I page 2). The powder is loaded through an aperture at the bottom end of the rod. This hole is plugged and welded after the rod is filled.

The FNR was put into operation in September of 1957 and, after initial calibrations, was raised to a power level of 100 kilowatts in February of 1958. Full power operation at one megawatt began in September 1958.

In August of 1960 a potentially hazardous condition arose when one of the shim-safety rods jammed in its special fuel element during a routine start-up of the reactor. There were no operational



-2-

SKETCH I - FNR SHIM-SAFETY ROD

consequences in that the condition was immediately detected and no further attempt was made to start the reactor. All three shim-safety rods were removed and examined. The jammed rod appeared to be deformed. To keep the reactor in operation, three new shim-safety rods were procured, installed and calibrated. The new rods were identical to the original set except for the addition of cadmium liners. The original shim-safety rods are designated as 1-A, 1-B and 1-C, and the new rods as 2-A, 2-B and 2-C. The original set of rods had been in the reactor for 2200 megawatt hours before the jamming incident occurred.

In view of the potentially serious consequences of jammed shim-safety rods, the new rods were removed from the reactor after 320 megawatt hours for an accurate dimensional check. All three rods showed evidence of swelling, and rod 2-C was off-gassing through the bottom plug weld. One of the original rods (1-C) which was in good condition, was substituted for rod 2-C. The shim-safety rods presently installed in the FNR are 2-A, 2-B and 1-C, all of which undergo daily rod-drop tests and are removed from the reactor on a regular schedule and measured dimensionally.

The following sections of this report describe the jamming incident and rod deformations in greater detail, discuss our initial exploratory investigations, and suggest a program of investigation which might establish conclusively the cause of these difficulties. A final report will be distributed after the completion of the program of investigation suggested herein.

II. DESCRIPTION OF SHIM-SAFETY ROD INCIDENTS

A. Incident Involving Rods 1-A, 1-B and 1-C

During reactor start-up on August 11, 1960, the magnet-contact light for shim-safety rod 1-A indicated loss of contact when the rods had been raised about ten inches from their lower limits. This indicated that rod 1-A had become disengaged from the electromagnet which had been pulling the rod out of the reactor core. Withdrawal of the rods was immediately stopped. The staff observer at pool side reported that rod 1-A was still in the raised position even though magnet current was automatically cut off when the magnet-contact light on the operating console indicated the loss of the rod. The special fuel element for rod 1-A was not dislodged from its position in the reactor core:

At this point the currents to the other two electromagnets were manually cut off. The pool side observer reported that rods 1-B and 1-C dropped normally into the core, but rod 1-A remained suspended. The electromagnets were lowered and 1-A magnet-contact light indicated contact as soon as the electromagnet struck the suspended rod. The rod was then successfully driven to its lower limit of travel by its electromagnet and drive mechanism.

The reactor was further secured and fuel was removed from the lattice along with the special control element containing safety rod 1-A. The rod-element assembly was moved to a holder in the center of the reactor pool. A grappling tool pulled the rod about ten inches out of the control element before the rod jammed again. Inspection showed noticeable swelling of the rod.

A special tool was built to remove the rod from the element. Plate No. 1, page 5, is a photograph of this removal device.

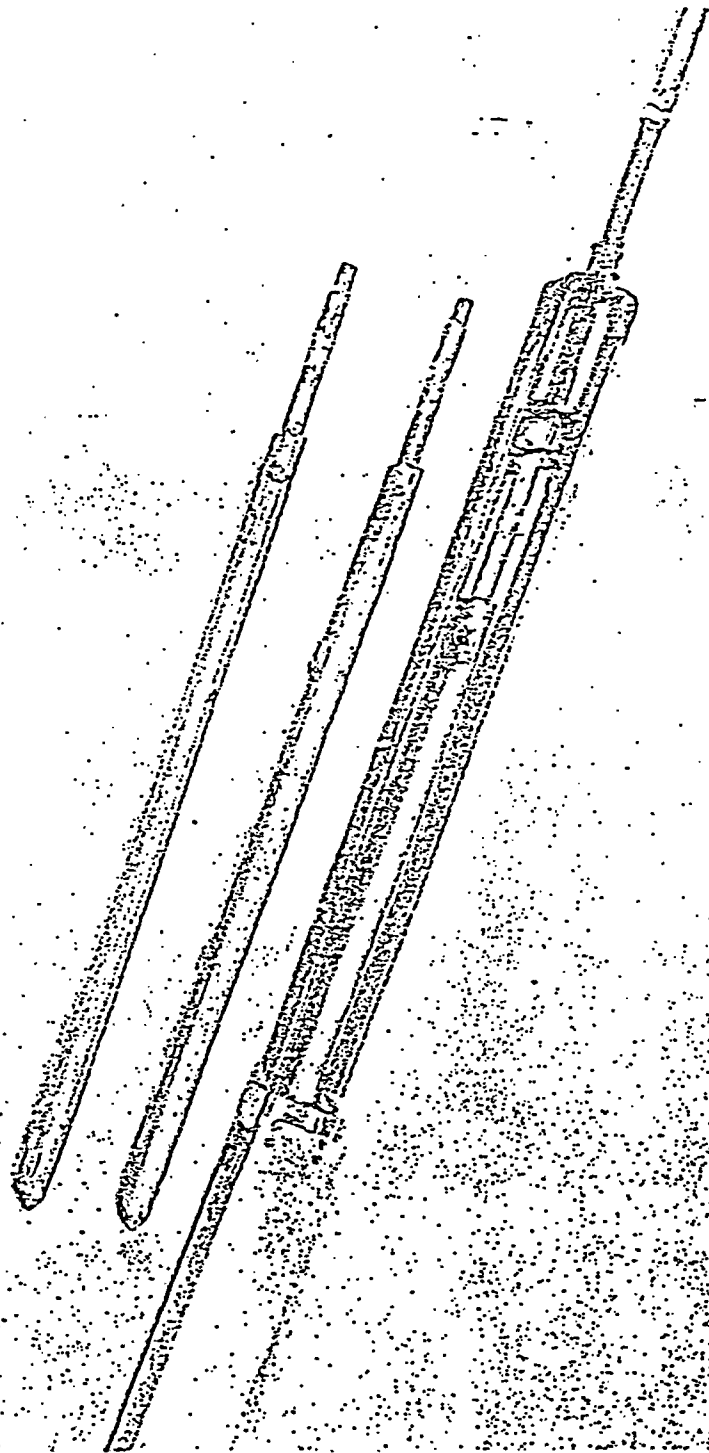


PLATE I -- REMOVAL DEVICE

This device attached to the special fuel element was used to remove shim-safety rod 1-A. Rods 1-B and 1-C are also shown.

During the extraction procedure the fuel element was kept submerged in four feet of water for radiation shielding purposes. There was no serious galling of the rod during the removal procedure, nor was there any off-gassing from the rod. There was no evidence of corrosion or damage to the external surface of the rod. Also, there was no apparent damage to the special fuel element.

The three shim-safety rods had been in the reactor since the beginning of operation in September 1957. The reactor had operated at power levels up to one megawatt for a total of 2200 megawatt-hours. There were no indications prior to the incident that safety rod 1-A was sticking within the guide tube of the special fuel element. The rods on the FNR were inspected on several occasions since 1957 by removing them from the reactor and visually inspecting them under about six feet of water. Also, during that time, frequent rod-magnet release time measurements were made. Further, prior to every start-up rod drop tests are performed. None of these indicated potential jamming.

B. Incident Involving Rods 2-A, 2-B and 2-C

After the above incident a new special fuel element was installed in the lattice and three new replacement shim-safety rods 2-A, 2-B and 2-C were installed and calibrated. On November 25, 1960, these rods were removed from the reactor for observation and dimensional checks. Micrometer measurements showed that all three rods had increased in thickness after only 320 hours at one megawatt. Furthermore, rod 2-C was off-gassing at the bottom plug weld. A water-filled Erlenmeyer flask was held over the submerged rod to collect a sample of the gas for analysis.

The cadmium liners in the new set of rods hindered operations because of the induced radioactivity which gave a 6 roentgens per hour reading at the center of the rods. The bottom ends of the rods read greater than 25 roentgens per hour. In contrast, rods 1-A, 1-B and 1-C, without cadmium liners, read one-third of a roentgen per hour at the lower end.

III. INVESTIGATIONS

A. Dimensional Inspection

After removal from the reactor a complete dimensional inspection was made of rods 1-A, 1-B and 1-C. The thickness and width dimensions are shown in Tables I and II respectively (see pages 8 and 9). The dimensions of the replacement rods 2-A, 2-B and 2-C before installation in the reactor are also shown in these tables. Although no records of the initial dimensions are available for rods 1-A, 1-B and 1-C, a reasonable indication of the degree of swelling which took place can be obtained by an intercomparison of rod dimensions. However, initial and final thickness measurements taken at the middle of the rod are available for rods 2-A, 2-B and 2-C which had been in the reactor for 320 megawatt hours. These measurements are as follows:

<u>Measurement</u>	<u>Shim-Safety Rod</u>		
	<u>2-A</u>	<u>2-B</u>	<u>2-C</u>
Initial	0.922 in.	0.890 in.	0.913 in.
Final	<u>0.928</u>	<u>0.921</u>	<u>0.925</u>
Change	0.006	0.031	0.012

The inside dimensions of the guide tube of the special fuel elements are presented in the last column of Table I.

TABLE I - SHIM-SAFETY ROD THICKNESS DIMENSIONS

Note: The corresponding internal dimensions of the guide tube inside special fuel element 1-A are given in the last column.

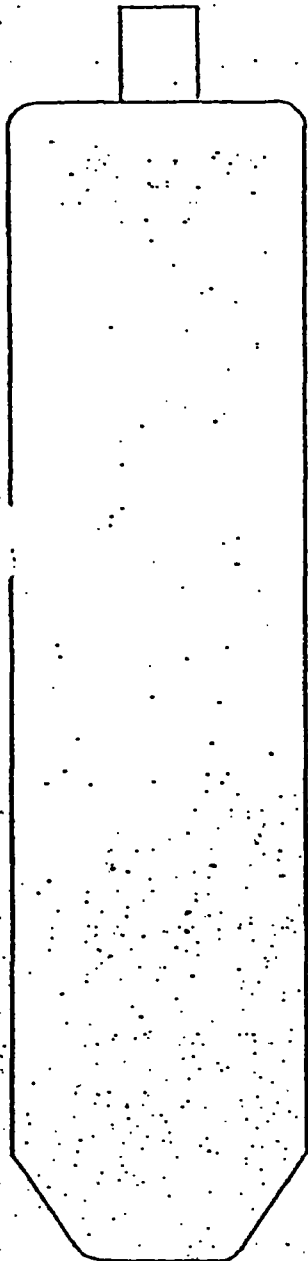
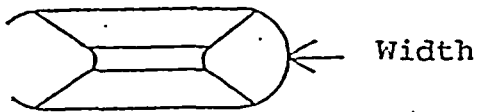


Thickness



	1-A	1-B	1-C	2-A	2-B	2-C	GUIDE TUBE.
	0.882	0.880	0.865	0.875	0.877	0.875	1.100
	0.925	0.920	0.904	0.901	0.883	0.889	1.100
	1.078	0.915	0.905	0.910	0.883	0.909	1.100
	1.107	0.916	0.905	0.915	0.889	0.914	1.100
	1.103	0.912	0.906	0.920	0.892	0.915	1.100
	1.097	0.915	0.908	0.922	0.891	0.914	1.100
	1.093	0.913	0.909	0.922	0.890	0.913	1.100
	1.091	0.913	0.909	0.922	0.890	0.913	1.100
	1.087	0.914	0.909	0.922	0.892	0.913	1.105
	1.088	0.919	0.909	0.923	0.892	0.914	1.105
	1.106	0.920	0.908	0.921	0.892	0.915	1.105
	1.090	0.915	0.909	0.922	0.884	0.915	1.105
	1.057	0.917	0.909	0.917	0.882	0.910	1.105
	1.009	0.886	0.867	0.897	0.872	0.888	1.105
	0.875	0.888	0.890	0.886	---	0.870	1.105

TABLE II - SHIM-SAFETY ROD WIDTH DIMENSIONS



	<u>1-A</u>	<u>1-B</u>	<u>1-C</u>	<u>2-A</u>	<u>2-B</u>	<u>2-C</u>
—	2.242	2.242	2.245	2.251	2.245	2.248
—	2.239	2.249	2.246	2.258	2.245	2.239
—	2.175	2.244	2.249	2.255	2.232	2.227
—	2.187	2.250	2.247	2.255	2.225	2.225
—	2.187	2.247	2.250	2.252	2.225	2.225
—	2.184	2.250	2.250	2.251	2.225	2.225
—	2.187	2.249	2.250	2.250	2.225	2.226
—	2.191	2.248	2.251	2.250	2.225	2.226
—	2.184	2.248	2.253	2.248	2.225	2.226
—	2.183	2.247	2.253	2.251	2.225	2.227
—	2.185	2.247	2.255	2.252	2.225	2.226
—	2.200	2.245	2.255	2.252	2.225	2.226
—	2.227	2.251	2.247	2.255	2.230	2.231
—	2.246	2.250	2.250	2.257	2.245	2.245
—	-----	-----	2.232	2.250	-----	-----

B. Radiographic and Dye Penetrant Studies

Complete radiographs were taken to determine the conditions inside the rods. The most significant finding from these radiographs was the presence of a void above the B_4C powder in the rods. This is shown in Plate II on page 11. Dye penetrant tests indicated pitting on the surface of the rods but no cracks were revealed.

C. Techniques for Collection of Gas and B_4C Powder Samples

The apparatus shown in Sketch II, page 12, was set up to measure any existing pressure and to collect any gas contained in the rod. The apparatus consisted of a self-sealing puncturing device with a pressure-vacuum gauge and an evacuated reservoir for collecting gas samples from the rod. Two rods, 1-A and 1-B, were punctured at the top where the voids were located. After the gas samples were removed, both rods were subjected to internal pressures of 40 psig while immersed in water.

The rods were then opened by cutting out a section on one side of each rod. The section that was removed is shown in Sketch III on page 13. Care was taken to avoid getting aluminum shavings in the B_4C powder. Samples of the powder were removed from different positions along the length of the rod.

D. Analysis of Contents of Shim Rods

Gas Analysis

When pressure measurements were made on the two shim-safety rods, 1-B had a pressure of 20 psig while rod 1-A, the deformed rod, was at atmospheric pressure. The gas samples from 1-A, 1-B and 2-C were analyzed using a mass spectrometer.

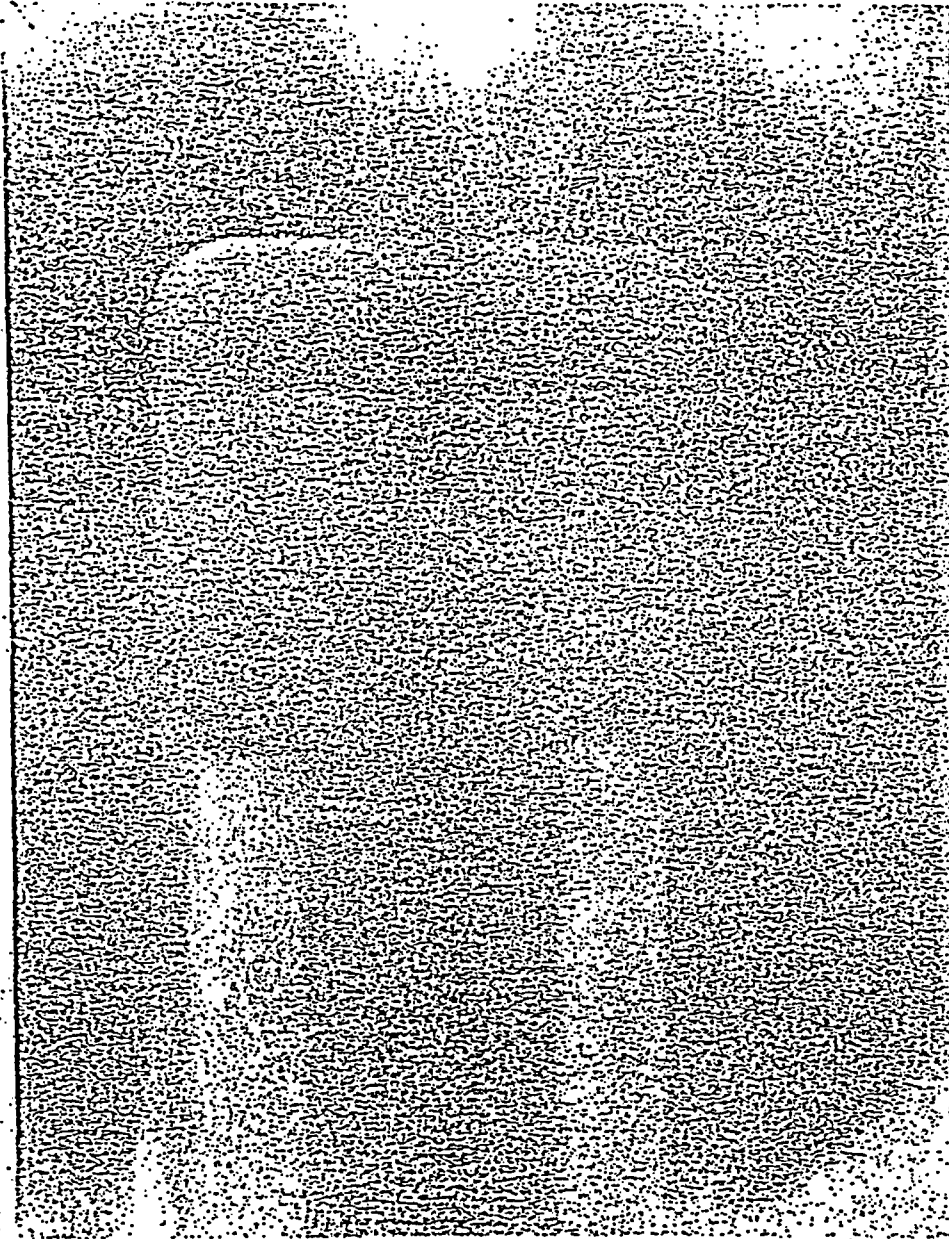
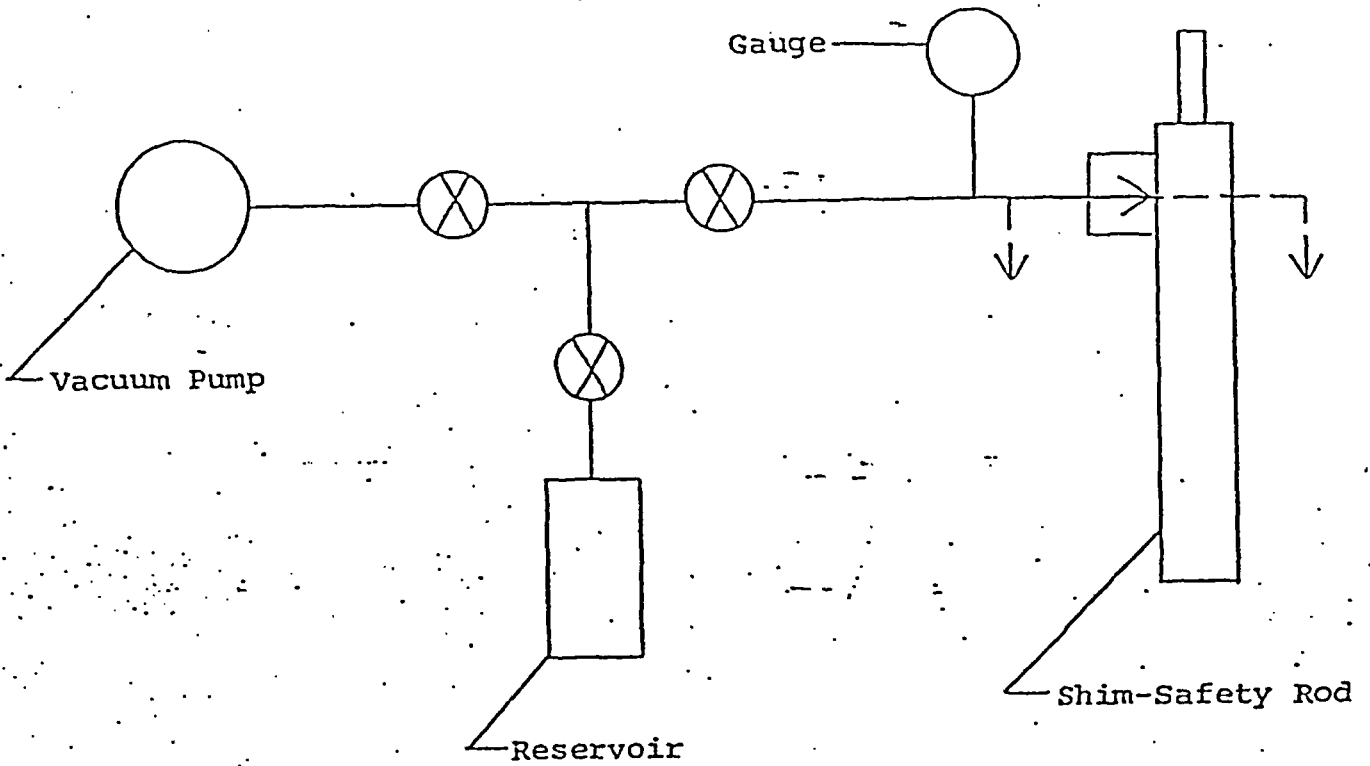
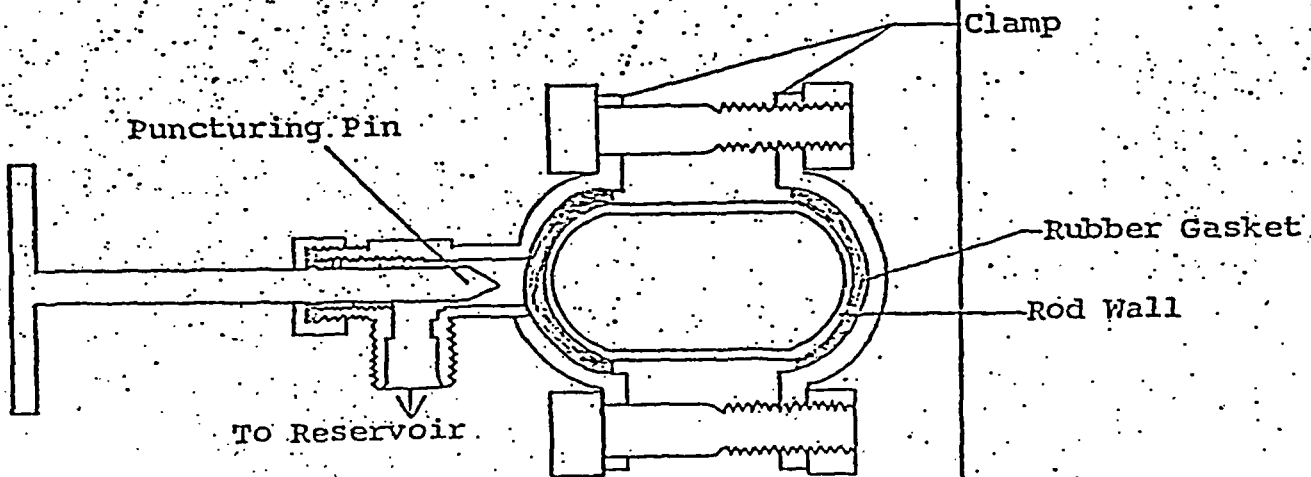


PLATE II - RADIOGRAPH OF THE TOP END OF A SHIM-SAFETY ROD

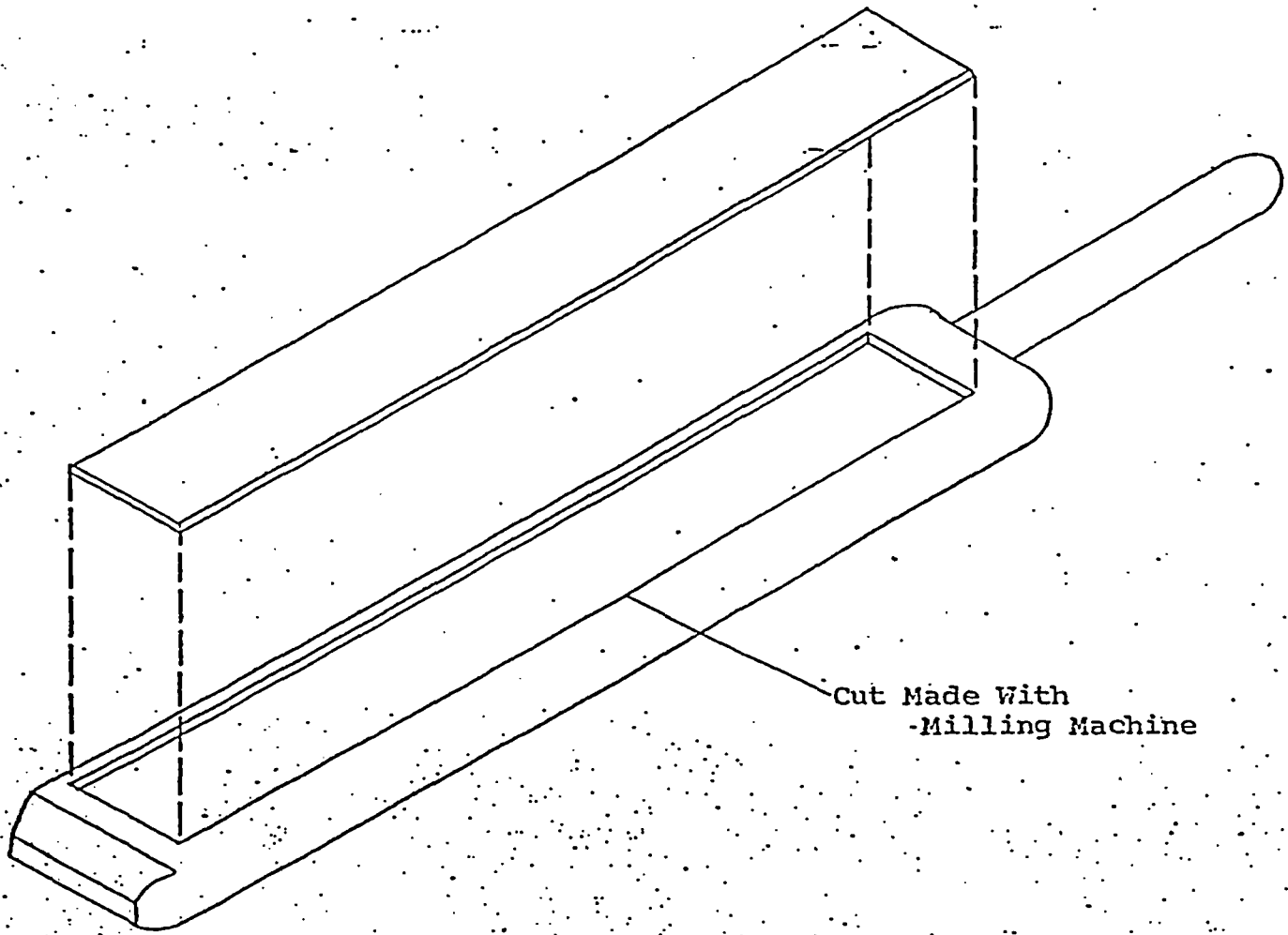
The light vertical rods are lead filled ballast tubes. The darkest area between the two tubes represents the void above the powder.



Section A - A



SKETCH II - GAS REMOVAL APPARATUS



Cut Made With
-Milling Machine

SKETCH III - ROD SECTIONING DIAGRAM

The results are as follows:

Gas Analyses
(in Mole Per Cent)

Rod 1-A Rod which jammed
Rod 1-B "Normal rod"
Rod 2-C Rod which off-gassed

<u>Gas</u>	<u>1-A</u>	<u>1-B</u>	<u>2-C</u>
H ₂	36.42	78.6	39.47
O ₂	36.00	0.4	14.98
N ₂	23.23	15.4	44.54
CO ₂	1.70	4.6	0.15
A	0.29	0.35	0.71
He	0.0	0.7	0.0

Note that the hydrogen-oxygen concentrations observed in 1-A and 2-C are in the detonable range.

Analysis of B₄C Powder and Inspection of Rod Interiors

When rod 1-B was opened, the B₄C powder was dry and lightly packed. The interior walls of the rod were not corroded. The powder removed from the lower portion of the rod was radioactive and had a total beta-gamma activity of about 3 mr/hr/gram on contact. A gamma spectral analysis indicated the presence of Mn⁵⁴, Zn⁶⁵, and Co⁶⁰. Analyses of the B₄C by emission spectroscopy showed the most predominant impurities to be Al, Cu, Fe, Zn and Mn. The supplier of the B₄C powder reports 98.79% B, 1.08% C, 0.10% Si, 0.02% Se and 0.02% N.

The B_4C in rod 1-A, the deformed rod, was found to be in a caked rather than a powdered form as in rod 1-B. The hard layer was concentrated between the ballast rods along the lower six inches of the shim rod. This cake had a grayish appearance unlike the characteristically black color of B_4C powder. The powder removed from the lower portion of rod 1-A was found to contain approximately 5 weight per cent water.

Oxidation was prevalent on the interior walls at the lower end of rod 1-A. A crust of Al_2O_3 surrounded the lead filled aluminum ballast rods.

The water found in rod 1-A indicated a leak had occurred. However, the 40 psig pressure test before sectioning failed to show such a leak. Therefore, another attempt was made to locate a leak in rod 1-A with the powder removed and the inner surface cleaned. This was done by replacing and rewelding the removed section and pressurizing to 40 psig. Under these conditions a 30 cc/hr leak was noted at the top of the rod where the endpiece is welded to the extruded tube. The gas leaked from a very small hole which looked much like the pits revealed by the dye penetrant test.

The leakage rate was reduced drastically by evacuating and then re-pressurizing the rod. It appeared that the leak was capable of a valve-like action which was dependent on the internal pressures of the rod.

IV. POSSIBLE EXPLANATION OF DEFORMATION

Consideration has been given to the possible causes of the swelling of rod 1-A. The deformation of rods 2-A, 2-B and 2-C, although not as great as that of 1-A, was also considered.

The hypotheses are:

- A. Mechanical stresses resulting from expansion of wet B_4C powder.
- B. Internal gas pressure generated by:
 - 1. $B^{10} (n, \alpha) Li^7$ reactions
 - 2. Chemical reactions between B_4C and H_2O
 - 3. Chemical reactions between Li^7 and H_2O
 - 4. Radiolysis of H_2O

Several experiments and calculations have been made to assist in evaluating these hypotheses.

A. The hypothesis that the deformation of the rod was a result of volumetric changes in wetted B_4C powder appears to be without foundation. Radial measurements of a polyethylene bottle containing wetted B_4C at room temperature showed no dimensional changes during an eight week period of observation.

B-1. It has been demonstrated that a pressure of approximately 110 psig is required to obtain the degree of deformation observed for rod 1-A. Calculations indicate that the generation of this pressure by helium as a result of (n, α) reactions on boron is extremely doubtful. Further, the gas analysis of rods 1-A and 1-B showed a relatively low concentration of helium.

B-2. The hypothesis involving a chemical reaction between B_4C and H_2O has been given little consideration since the reaction rate constant is small even at temperatures of $400^\circ C$. (Reference 1)

B-3. Significant pressures from the $Li-H_2O$ reaction are unlikely in view of the low lithium concentrations from the $B^{10} (n, \alpha) Li^7$ reactions.

B-4. Present data strongly indicates that the necessary pressure to cause the observed rod deformation can be generated inside the rod by the radiolytic decomposition of water into gaseous hydrogen and oxygen. To produce free H_2 and O_2 , this reaction requires free radical scavengers which could well be the B_4C powder itself, impurities in the powder, impurities in the water or the component parts of the rod (References 2, -3, -4, 5 and 6). The generation of gases was not the only prerequisite for the rod deformation. In addition, either the hole which allowed water to get into the rod and which allowed gas to escape must have closed off at some time or, the gas generation rate far exceeded the gas leakage rate.

The possibility of having water present at the time the rods were sealed in the fabrication process was considered since a small amount of water is capable of causing rod deformation. This is especially significant since B_4C powder is naturally hygroscopic.

In the case of the deformed rod, the above possibility was discounted in favor of an external leak since the rod was in the reactor for a long period of time before jamming occurred. However, this possibility exists for rods 2-A, 2-B and 2-C. It is therefore imperative that the B_4C powder used in fabricating shim-safety rods be dried and subsequently handled in humidity controlled environments.

In an attempt to demonstrate the feasibility of generating significant quantities of gas in reasonably short periods of time, an experiment was designed which would simulate the conditions that were suspected within the jammed rod. Two

small, aluminum sealed vessels, one containing water and the other water and B_4C powder were installed adjacent to the reactor core in a thermal flux of 5×10^{12} neutrons per square centimeter-second and a gamma field of 5×10^7 roentgens per hour. Pressures in these chambers were monitored over a period of three days during which time the reactor operated at a power level of one megawatt for 50 hours. The pressure in the chamber containing water and B_4C powder increased linearly with respect to reactor operating time at a rate of 1.2 psig per hour. See Graph I, page 19. This test chamber had a volume of 295 cc and contained 10 grams of water and 25 grams of B_4C powder. The pressure in the chamber containing water only was 1.1 psig after 50 hours of reactor operation as compared to 60 psig in the chamber containing both water and B_4C powder.

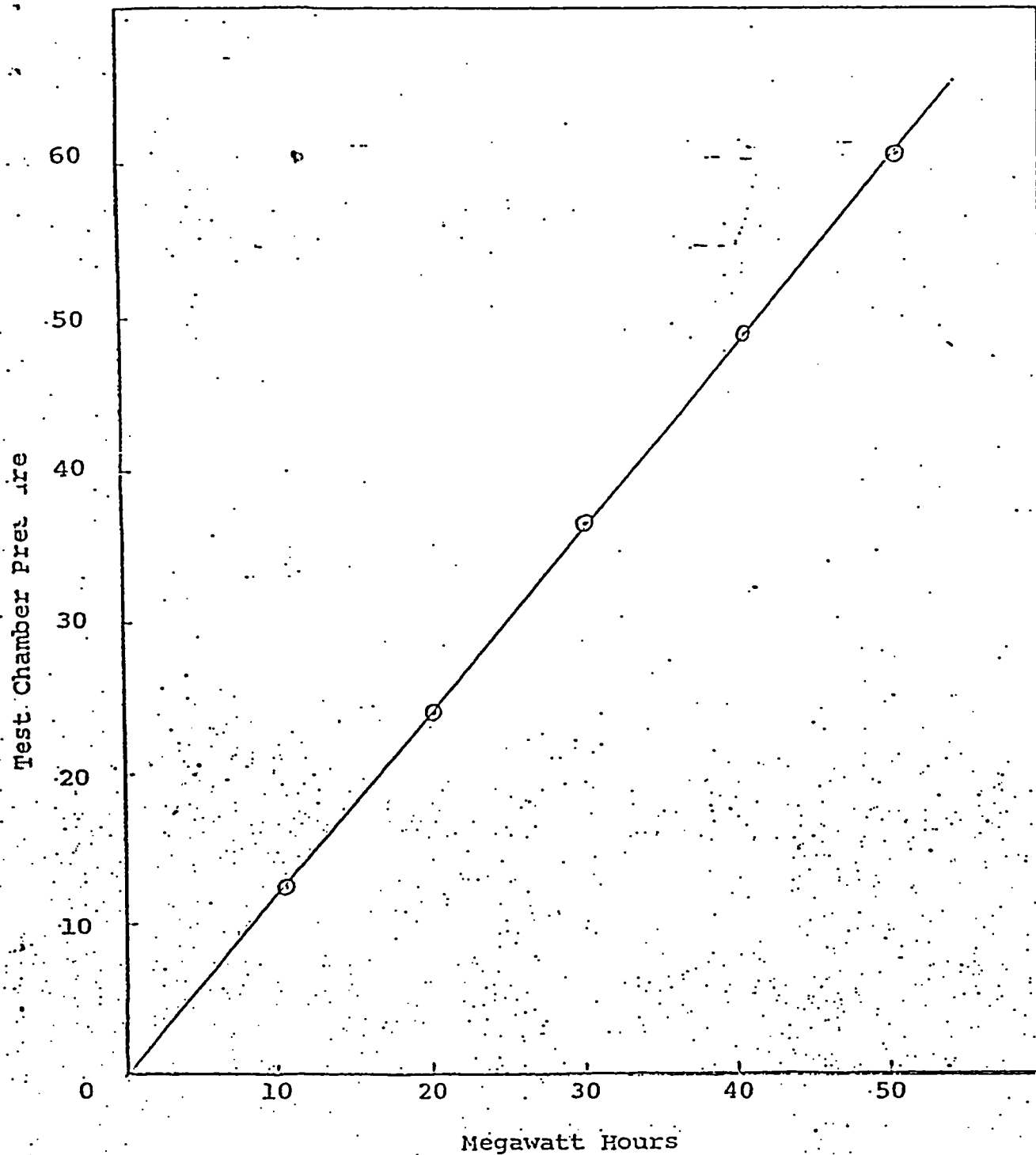
Analysis showed that the gas generated in the water- B_4C chamber contained predominantly a hydrogen-oxygen gas mixture in a 2:1 ratio, similar to the finding for rod 2-C.

V. RECOMMENDATIONS

Deformation of shim-safety rods because of internal pressure could lead to the following dangerous conditions:

1. Withdrawal of a special fuel element during start-up. Any subsequent release and drop of this special fuel element could result in a large and rapid increase in the positive reactivity of the reactor.
2. Jamming of the rods during reactor operation. In such an event, it would not be possible to insert the deformed

GRAPH I - TEST CHAMBER PRESSURE VS MEGAWATT HOURS



rods into the reactor when unsafe conditions exist or even for routine shut down. This is a particularly serious possibility in reactors which operate at power for long periods of time.

3. Detonation of the hydrogen-oxygen gas mixture contained in the shim-safety rods. This could cause damage to the reactor core in addition to rupturing the rod. Although such a detonation appears to be improbable, it is nevertheless a potential hazard that needs further investigation, especially in strong radiation fields.

Operational Recommendations

In view of the important function of shim-safety rods, a detailed inspection should be made of all rods before installation in a reactor. Records of these inspections, especially weights in water and dimensional measurements, should be maintained for reference purposes. A careful survey of the surface conditions of the rods including all welds is extremely important. Radiographs have proved valuable in determining internal conditions of reactor rods.

In addition to the initial tests, shim-safety rods should undergo periodic inspections. The ENR is presently on a schedule calling for rod inspection every 320 megawatt hours of operation. This inspection requires the rods to be removed from the reactor, the dimensions measured directly and the surface observed for corrosion or any other indication of damage, such as off-gassing.

Close attention should also be given to the potential hazards that exist when water containing free-radical scavengers is present in any sealed experiment or device located in a radiation field.

Recommendations for Design and Fabrication

Consideration should be given to the design of new shim-safety rods which would avoid the possibility of the generation of gases leading to high pressures. Further, consideration should be given to the design of the special fuel elements for these rods which would minimize the possibility of jamming. Any arrangement of element and rod which would make dimensional changes easily and readily detectable would be a decided improvement over our present system.

In the fabrication of shim-safety rods similar to those presently used on the FNR, it is extremely important that all substances capable of producing gases in the presence of radiation be held to a minimum. These substances include volatile degreasing agents, water used for rinsing and any water contained in the B_4C powder.

Proposed Investigations

As a result of this investigation of the shim-safety rod incident, it has become evident that the following subjects should be investigated more thoroughly.

1. The internal pressures necessary for shim-safety rod deformation.
2. Gas and pressure generation in shim-safety rods located in a reactor core as a function of water content in B_4C powder.
3. The effect of alpha particles and lithium recoils from B_4C powder on the radiolytic process.
4. The sources of free-radical scavengers which are required in the radiolytic process.

5. Possible sources of ignition energy for the detonation of hydrogen-oxygen gas mixtures.

Recognizing the importance of the above problems, these investigations will be undertaken at the Phoenix Memorial Laboratory. Financial assistance will be required for a thorough investigation of these problems.

From an operational point of view, the removal of shim-safety rods from their special fuel elements and the reactor for dimensional tests is a time consuming and complicated manipulation. In an attempt to simplify these inspections a study of "in situ" rod inspection techniques will be undertaken. Further, the criteria for the frequency and technique of inspection for shim-safety rods will be re-evaluated in light of the results of the aforementioned experimental investigations.

I. REFERENCES

1. F. F. Mikus, Reactor Technology Quarterly Report No. 6 KAPL-2000-3, 48-49 (1958).
2. J. B. Hoag, Nuclear Reactor Experiments, D. Van Nostrand Co., Inc., Princeton, New Jersey 346-347 (1958).
3. E. J. Hart and P. D. Walsh, Proc. 2nd Intern. Conf. Peaceful Uses of Atomic Energy, Geneva 29, p/763 38-42 (1958).
4. A. O. Allen and H. A. Schwarz, Proc. 2nd Intern. Conf. Peaceful Uses of Atomic Energy, Geneva 29, p/1403 30-37 (1958).
5. E. J. Hart, et al, Proc. 2nd Intern. Conf. Peaceful Uses of Atomic Energy, Geneva 7, p/839 593-598 (1955).
6. C. B. Senvar and E. J. Hart, Proc. 2nd Intern. Conf. Peaceful Uses of Atomic Energy, Geneva 29, p/1128 19-23 (1958).

QUANTITATIVE ANALYSIS
OF
BORALtm PANELS

PROGRAM CONDUCTED FOR:

YANKEE ATOMIC ELECTRIC COMPANY
20 Turnpike Road
Westborough, Mass. 01581

PROGRAM CONDUCTED BY:

Brooks & Perkins, Inc.
17515 W. Nine Mile Road
Southfield, Mich. 48075

*Ret'd
5/10*

July 30, 1976



Mr. Leslie Mollon - Director
Nuclear Product Development

TABLE OF CONTENTS

	<u>Page</u>
Title Page	1
Table of Contents	2.
1. Introduction	4
1.1 Purpose	4
1.2 Program	4
1.3 Background	5
1.4 Methods Used	7
1.4.1 Metallographic Technique	7
1.4.2 Ultrasonic Technique	8
1.4.3 Quantitative Chemical Analysis	8
2. Summary	10
2.1 Results	10
2.2 Areas	10
2.3 Panel Lots	10
2.4 Weighted Average	12
2.5 Theory	15
2.5.1 Mean	15.
2.5.2 Standard Deviation	15
2.5.3 Probability	16

Table of Contents (cont'd)

	<u>Page</u>
3. Conclusion	17
Appendix A Panel Lot I	19
Appendix B Panel Lot II	38
Appendix C Panel Lot III	59
Appendix D Panel Lot IV	62
Appendix E Panel Lot V	69
Appendix F Solubility Test	90
Appendix G Core Taper	92
Appendix H Boron in B ₄ C	96
Appendix J B ₄ C Distribution	98
Appendix K BORAL tm Spec.	100
Appendix L BORAL tm Physicals	108

1. INTRODUCTION

1.1 Purpose. This report provides the results of a quantitative analysis program conducted to determine the amount of boron carbide present in the core (inner layer) of BORALtm panels. The information obtained for this program was supplemental to the physical characteristics obtained during the routine quality assurance checks which are performed in accordance with Brooks & Perkins, Inc. Specification BPS-9000-01.

1.2 Program. The program involved the physical measurement of the BORALtm panels by destructive and non-destructive methods in various locations within each panel. A total of 147 panels were analyzed in five different lots. Four of the lots were randomly selected and the other lot consisted of panels having the lowest content of boron carbide by neutron radiographic examination.

The program included 1,833 thickness measurements taken by metallographic techniques, 66 thickness measurements by ultrasonic techniques and 196 quantitative chemical analyses (See Appendix A thru G

The recorded data was statistically analyzed and for each characteristic in each lot a mean and standard deviation was established. The probability that each characteristic will be above a certain minimum value can now be determined from the statistical data.

1.3 Background. BORALtm is a thermal neutron shielding material that can best be described as a sandwich-type panel. The outer layers or "skins" of the panel are 1100 alloy aluminum. The inner layer or "core" of the panel is a mixture of boron carbide and 1100 alloy aluminum. The interface between a skin and the core is not a clearly discernible surface when viewed with a microscope. The interface is in reality an irregular zone that is approximately five thousandths of an inch (.005 in.) in thickness. In this zone there is a linear transition from 100% aluminum and zero % boron carbide in the skin to 65% aluminum and 35% boron carbide particles of various sizes in the core. The appearance of the interface is a series of peaks and valleys. (See Fig. 1

The boron carbide particles is the constituent of the BORALtm panel that absorbs or attenuates the thermal neutrons. The ability of the panel to provide a particular level of neutron attenuation is directly related to the amount of boron carbide contained per unit surface area of the panel.

The BORALtm panel is produced by the rolling of a specially prepared ingot into a sheet ⁽¹⁾ that will yield one or more finished panels⁽¹⁾ that are four feet wide and ten feet long. The finished panels are sheared from the oversized sheets by the removal of the scrap material around the

(1) Note term usage, "sheet" - the untrimmed product of rolling, "panel" 48" x 120" product cut from the original rolled product.

10 X 1931B-64

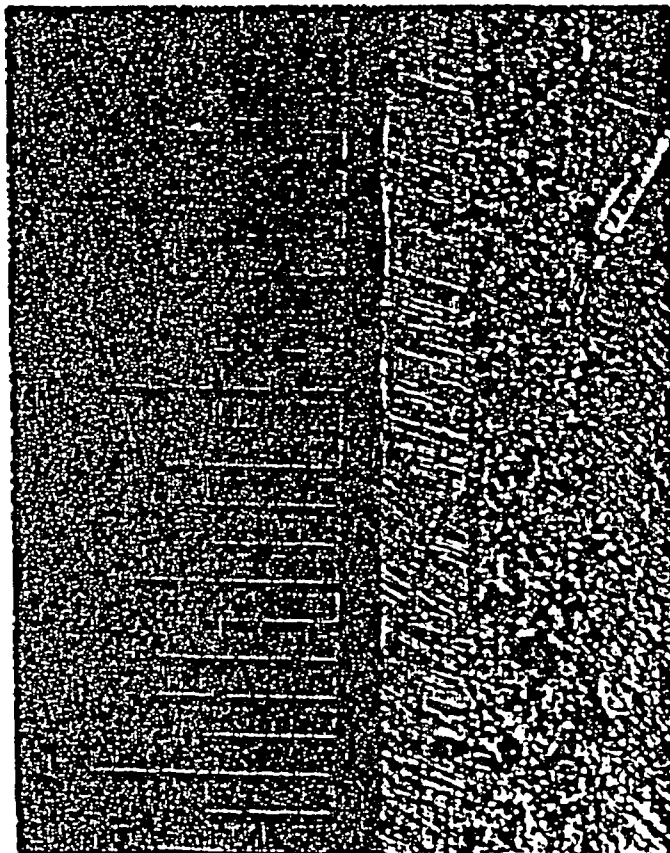


FIGURE 1

MICROSCOPIC VIEW OF THE EDGE
OF BORALTM PANEL NO. 1931-B (10X)

periphery of the oversized sheet. The scrap material contains a core that tapers from zero thickness on the extreme outer edge to a core of full thickness on the edge adjacent to the finished panel. If the shear line is improperly placed on the oversized sheet the finished panels could contain a core thickness along that line that is not of full thickness.

1.4 Methods Used.

1.4.1 Metallographic Technique. The thickness of the core was measured by a 7.5 power optical comparator after the edge of the panel or the retain strip was mechanically and chemically prepared. Approximately one eighth of an inch (.125 in.) was machined away from the edge to remove the material affected by the searing action. The edge was then made smooth by using a sequence of files of decreasing coarseness. The edge was then polished with emery paper before chemically etching it to improve the visual contrast and to remove any minute overlapping of the boron carbide by the aluminum from the mechanical removal operations.

The core thickness measurement was established by averaging the one maximum and the one minimum measurement that could be observed within the visual range of the optical comparator.

1.4.2 Ultrasonic Technique. The thickness of the core was measured by a Sonoray Model 303B Ultrasonic Flow and Thickness Tester using a dual element transducer. The tester was calibrated with a standard block before taking any set of thickness measurements. The tester was also frequently checked during the taking of measurements to assure the instrument remained in calibration.

To take a thickness measurement the tester operator would place the dual element transducer on the surface of the BORALtm panel that had been wetted with a drop of liquid couplant. The operator would adjust the position of the transducer within the spot of couplant until a stable wave pattern was displayed on the scope of the tester. The particular tester used was equipped with a digital readout which eliminated the possibility of human error in reading the grid lines on the scope face of the tester because the displayed number was the actual core thickness at that location.

1.4.3 Quantitative Chemical Analysis. The chemical analysis was performed on samples approximately one inch square which had been removed from a retain strip or the finished BORALtm panel. The samples were marked with a numbering system which identified the BORALtm sheet and the location on the sheet from where the sample was taken. The four edges of the samples were filed smooth and straight to prevent erroneous volumetric readings.

The surface area of each sample was determined by dividing the sample's volume by its thickness. The volume was determined by deducting the weight of the sample in water from the weight of the sample in air and correcting the result for the difference of the water temperature from the standard temperature.

The weight of boron carbide in the sample was determined by weighing the dry residue remaining after dissolving the sample in dilute hydrochloric acid and correcting the result for the soluble portion of the boron carbide. It was determined by actual test that 4.12 percent of boron carbide conforming to Type 2 of ASTM C750-73T is soluble in dilute hydrochloric acid (See Appendix

The content of boron carbide per unit area (commonly referred to as the "grams loading") was determined by dividing the total weight of the boron carbide in the sample in grams by the area of the original sample in square centimeters.

The weight factor or percentage of boron carbide present in the core was determined by dividing the total weight of boron carbide by the total weight of the sample less the calculated weight of the aluminum cladding.

The core compaction factor was determined by dividing the total weight of the sample less the calculated weight of aluminum cladding by the theoretical weight of the core based on the weight factor and core thickness.

The core proportionality was determined by dividing the core thickness by the total thickness of the sample.

2. SUMMARY

2.1 Results. The mean core thickness, the weight factor of boron carbide within the panel core and the standard deviation of each are listed in Table I. These results are listed by panel lot number and by the sheet area where the observations were taken. The averages by area and the overall weighted average is also shown in Table I.

2.2 Areas. The location of each observation taken during this program can be determined by the sample serial number and a map of the panels. The observation results were then segregated by area and listed accordingly. The three main sheet areas are: (1) Retain Strip, which is a portion of the scrap that is trimmed from the edge that is immediately adjacent to the end of a finished panel, (2) Outer Edge, which is the area lying in the one inch border strip on the periphery of the finished panel, (3) Central Portion, which is the area lying internal to the one inch border strip (i.e. - the area that is more than one inch in from the finished panel edge).

2.3 Panel Lots. The BORALtm panels analyzed in this program are listed in Table II by lot number and panel serial number. The lots were established during the progress of the program and can be described as follows:

TECHNICAL ANALYSIS FORM

BY LM DATE _____
 CK. _____ DATE _____
 REV. _____ DATE _____

b+p Brooks & Perkins, Incorporated

ADVANCED STRUCTURES DIVISION

SHEET _____ OF _____

SUBJECT _____

SUMMARY OF STATISTICAL FACTORS

PANEL LOT NO.	RESULTS BY AREA OF SHEET				WEIGHTED AVERAGES
	STA. FAC.	RETAIN STRIP	OUTER EDGE	CENTRAL PORTION	
I	\bar{E}_c	(26) .0800	(48) .0772	(217) .0894	—
	S.D.	.0054	.0071	.0068	
II	$\bar{W.F.}$	(38) .3800	(48) .3821	N/A	—
	S.D.	.0173	.0348		
III	\bar{E}_c	N/A	(150) .0843	(170) .0924	—
	S.D.		.0056	.0025	
IV	$\bar{W.F.}$	(7) .3902	(2) .3858	(1) .3791	—
	S.D.	.0125	.0216	-0-	
V	\bar{E}_c	N/A	(170) .0882	N/A	—
	S.D.		.0031		
VI	\bar{E}_c	(167) .0846	N/A	N/A	—
	S.D.	.0045			
VII	$\bar{W.F.}$	(27) .3962	N/A	N/A	—
	S.D.	.0194			
VIII	\bar{E}_c	(1001) .0894	N/A	N/A	—
	S.D.	.0064			
UNBIASED AVERAGES LOTS I, II, III, IV, V	\bar{E}_c	(1194) .0847	(318) .0832	(387) .0909	—
	S.D.	.0056	.0053	.0047	
UNBIASED AVERAGES LOTS II, III, IV, V	$\bar{W.F.}$	(145) .3886	(50) .3840	(1) .3791	—
	S.D.	.0164	.0282	-0-	
UNBIASED AVERAGES LOTS II, III, IV, V	\bar{E}_c	(1168) .0870	(270) .0863	(170) .0924	(1608) .0921 *
	S.D.	.0055	.0044	.0025	.0027
UNBIASED AVERAGES LOTS II, III, IV, V	$\bar{W.F.}$	(107) .3914	(2) .3858	(1) .3791	(110) .3911 *
	S.D.	.0161	.0282	-0-	.0162

LEGEND — STA. FAC. = STATISTICAL FACTORS, \bar{E}_c = MEAN CORE THICKNESS (INCHES), S.D. = STANDARD DEVIATION, $\bar{W.F.}$ = MEAN WEIGHT-FACTOR, (26) = NO. OF OBSERVATIONS, N/A = NOT AVAILABLE.

* BY AREA RATIOS OF .0576 OUTER, .9424 CENTRAL.

* BY NUMBER RATIOS OF .9727 RETAIN, .0182 OUTER, .0091 CENTRAL

Lot I - The thirteen (13) panels which appeared to have the lowest content of boron carbide by inspection of the neutron radiographs previously provided as a routine quality assurance item;

Lot II - The ten (10) panels picked at random to fulfill an incremental shipment release by the customer;

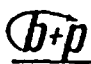
Lot III - The twenty (20) panels picked at random to fulfill a second incremental shipment release by the customer;

Lot IV - The twenty-seven (27) retain strips are from the sheets of previously delivered panels for spent fuel storage racks for Yankee Rowe;

Lot V - The seventy-seven (77) retain strips are from the sheets previously delivered panels for spent fuel racks for Maine Yankee.

2.4 Weighted Average. The "weighted average of the mean core thickness" quoted in Table I, was obtained by multiplying the unbiased average mean core thickness for the outer edge and central portion areas by the percentage factor each area represents of the total finished panel area and then adding the two products. The "weighted average of the mean core

TECHNICAL ANALYSIS FORM

BY <u>LM</u> DATE _____	 Brooks & Perkins, Incorporated ADVANCED STRUCTURES DIVISION	SHEET _____ OF _____
CK. _____ DATE _____		SUBJECT _____
REV. _____ DATE _____		

IDENTIFICATION OF LOTS BY PANEL NO.

LOT NO.	PANEL NUMBER					
I (13) MIN. B+C	1000B	1069B	1338B	1372A	1381A	1394A
	1416A	1426B	1492A	1496B	1533B	1537B
	1568A					
II (10) RANDOM	1266A	1325A	1325B	1352A	1352B	1402B
	1406B	1434A	1462B	1931B		
III (20) RANDOM	2003A	2004A	2004B	2005A	2005B	2006A
	2006B	2007A	2010A	2013A	2015B	2017B
	2019A	2019B	2025B	2028B	2033A	2033B
	2035A	2035B				
IV (27) RETAINS (ROWE)	1531A	1531B	1535A	1535B	1545B	1552A
	1552B	1555A	1555B	1556A	1556B	1558A
	1558B	1565B	1566B	1569A	1569B	1575B
	1581A	1585A	1585B	1589A	1589B	1590A
	1590B	1594A	1594B			
V (77) RETAINS (MAINE ETC.)	1001B	1010A	1012B	1013A	1023A	1025B
	1052A	1055A	1057A	1059B	1064A	1067A
	1072B	1077B	1084B	1086B	1091B	1093B
	1101A	1111A	1112B	1113B	1116A	1118A
	1118B	1124A	1151A	1151B	1152A	1152B
	1155A	1156B	1167A	1182A	1184B	1201A
	1201B	1203A	1203B	1206A	1206B	1207B
	1212A	1222B	1224A	1227A	1228A	1228B
	1233A	1233B	1243A	1243B	1245A	1251B
	1260A	1281A	1302A	1302B	1304A	1307B
	1320A	1323B	1334A	1334B	1335B	1336A
	1336B	1359A	1361B	1364A	1397A	1535B
	1555A	1558A	1590A	1594A	(X)	

thickness" represents the result that will be obtained from a set of observations that are randomly spaced across the entire surface of a panel. The "weighted average of the standard deviation" for the "weighted average of mean core thickness" was also determined by the ratio of areas.

The "weighted average of the mean weight-factor" was determined on the basis of the number of observations in each area because no valid relationship between the value of the weight-factor and the location of the observation was discovered. The number of weight-factor observations taken from the retain strip, outer edge, and central portion areas were 145, 50, and 1 respectively. The number ratios for those areas is therefore .7398, .255, and .0051 respectively. The "weighted average of the mean weight-factor" was determined by multiplying the average weight-factor in each area by the number ratio for that area and then adding the three products. The "weighted average of the mean weight-factor" represents the results that would be obtained from an equal number of observations in each area.

The "weighted average of the standard deviation" for the mean weight-factor was also determined by the ratio of the number of observations. The results from the panels in Lot I were excluded from the averages used to determine all of the weighted averages because the panels

in Lot I do not represent a normal distribution that would be in a randomly selected lot.

2.5 Theory. The statistical factors obtained from the recorded data were determined in the following manners,

2.5.1 Mean. The arithmetic mean for the core thickness and the weight-factor were determined by dividing the summation of those observations separately in each lot by the number of those observations in the lot.

$$\text{mean core thickness} = \bar{t}_c = \frac{\sum t_c}{\text{No. of } t_c \text{ OBSERVATIONS}}$$

$$\text{mean weight-factor} = \bar{W.F.} = \frac{\sum W.F.}{\text{No. of W.F. OBSERVATIONS}}$$

2.5.2 Standard Deviation. The standard deviation for a set of core thickness observations and weight-factor observations were determined by taking the square root of the average squared residual.

$$\text{standard deviation (core thickness)} = S.D. t_c = \sqrt{\frac{\sum t_c^2 - \frac{(\sum t_c)^2}{n}}{n-1}}$$

$$\text{Standard deviation (weight-factor)} = S.D. W.F. = \sqrt{\frac{\sum W.F.^2 - \frac{(\sum W.F.)^2}{n}}{n-1}}$$

2.5.3 Probability. The probability that a deviation of an individual observation from the mean lies between minus x (S.D.) and infinity is determined from the probability integral.

$$P = \frac{1}{\sqrt{2\pi}} \int_{-x(\text{S.D.})}^{\infty} e^{-\frac{x^2}{2}} dx$$

By consulting a table of probability functions such as is found in "Handbook of Mathematical Tables and Formulas" by Burington, it can be determined that a value of 1.65 times the standard deviation will provide a probability of .9505 for a normal distribution of observations.

3. CONCLUSIONS

The boron carbide content per unit area of the BORALtm panels is equal to or greater than 0.203 grams per square centimeter with a probability of .9505. This conclusion was arrived at in the following manner:

$$P = \frac{1}{\sqrt{2\pi}} \int_{-1.65 \text{ S.D.}}^{\infty} e^{-\frac{x^2}{2}} dx = .9505 \quad (\text{SEE PARA. 2.5.3})$$

weighted average of mean core thickness = $\bar{t}_c^w = .0921$ INCHES

weighted average of standard deviation for $t_c = \text{S.D.}_{t_c}^w = .0027$

95% of observation fall between - 1.65 SD and infinity

core thickness at minimum of 95% = $\bar{t}_c^w - 1.65 \text{ S.D.}_{t_c}^w$

$$\text{minimum } t_c = .0921 - .0044 = \underline{\underline{.0877 \text{ in.}}}$$

weighted average of mean weight-factor = $\text{W.F.}^w = .3911$

weighted average of standard deviation for W.F. = $\text{S.D.}_{\text{W.F.}}^w = .0162$

95% of observations fall between - 1.65 SD and infinity

weight-factor at minimum of 95% range = $\text{W.F.}^w - 1.65 \text{ S.D.}_{\text{W.F.}}^w$

$$\text{minimum W.F.} = .3911 - .0267 = \underline{\underline{.3644}}$$

The boron carbide distribution per unit area is directly proportional to the core thickness and the boron carbide content weight factor. The theoretical distribution of boron carbide is 0.1894 grams per square centimeter for a core thickness of 0.085 inches and a weight factor of .3500 (see Appendix L). The actual distribution can be determined from the following relationship:

$$\frac{\text{actual B}_4\text{C distribution}}{\text{theoretical B}_4\text{C distribution}} = \frac{t_c \text{ (actual)}}{t_c \text{ (theor.)}} \times \frac{\text{W.F. (actual)}}{\text{W.F. (theor.)}}$$

$$\text{actual B}_4\text{C distribution} = \frac{.1894}{.0850} \times \frac{.0877}{.3500} = \frac{.3644}{.3500} = \underline{\underline{.2035 \text{ gm/square}}}$$

APPENDIX A

EXPERIMENTAL DATA

PANEL LOT I

PAGES I-1 THRU I-18

	SAMPLE No.	1000 BR-1	1000 BR-2	1000 B-EVEN	1000 B-2
1	λ_a (in./cm.)	.185/.4699	.185/.4699	.172/.4369	.173/.439
2	WT _a (gms.)	6.9252	6.3700	5.3698	6.9181
3	A _a (sq. cm.)	5.6555	5.2139	4.6343	5.9504
4	WT-b (gms.)	1.0378	.9463	.5881	.8839
	G.L. (gms./sq. cm.)	.184	.181	.120	.149
	W.F.	.3614	.3643	.3630	.3550
5	λ_c (in./cm.)	.081/.2057	.080/.2032	.052/.1321	.065/.16
	C.F. / C.P	.9364/.4378	.9303/.4324	.9530/.3024	.9610/.37
	SAMPLE No.	1000 B-000	1000 B-7	1069 BR-1	1069 BR-
	λ_a (in./cm.)	.178/.4521	.179/.4547	.188/.4775	.188/.477
	WT _a (gms.)	6.2887	5.3870	8.1414	7.9152
	A _a (sq. cm.)	5.2866	4.5148	6.5893	6.3590
	WT-b (gms.)	.9446	.7402	1.3822	1.3659
	G.L.	.1787	.1639	.2098	.2147
	W.F.	.3474	.3891	.3790	.3771
	λ_c (in./cm.)	.080/.2032	.067/.1702	.089/.2261	.090/.22
	C.F. / C.P	.9591/.4495	.9412/.3743	.9300/.4735	.9462/.4
	SAMPLE No.	1338 BR-1	1338 BR-2	1338 B-7	1338 B-
	λ_s (in./cm.)	.180/.4572	.183/.4648	.175/.4445	.175/.444
	WT-s (gms.)	6.7924	6.8312	6.3658	6.4657
	A _s (sq. cm.)	5.7478	5.7307	5.4308	5.5524
	WT-b (gms.)	1.1416	1.1492	.9319	.8329
	G.L.	.1986	.2005	.1716	.1500
	W.F.	.3817	.3987	.3603	.3155
	λ_c (in./cm.)	.084/.2134	.083/.2108	.074/.1880	.075/.190
	C.F. / C.P	.9265/.4668	.9078/.4535	.9610/.4229	.9433/.4
	SAMPLE No.	1338 B-8	1338 B-10	1372A-4	1372A-6
	λ_s (in./cm.)	.172/.4369	.170/.4318	.172/.4369	.174/.44
	WT _s (gms.)	5.0311	5.0849	6.4842	6.6420
	A _s (sq. cm.)	4.4477	4.5862	5.6988	5.8131
	WT-b (gms.)	.9006	.8698	1.1717	1.1623
	G.L.	.2025	.1897	.2056	.1999
	W.F.	.4511	.3829	.3869	.3682
	λ_c (in./cm.)	.073/.1854	.081/.2057	.084/.2134	.087/.22

SAMPLE No.	1372A-7	1372A-9	1372AR-1	1372AR-
\bar{x}_a (in./cm.)	.177/.4496	.176/.4470	.182/.4623	.184/.46
WT-a (gms.)	6.9310	6.8497	7.0670	7.1194
A-a (sq. cm.)	5.9144	5.8901	5.7741	5.9125
WT-b (gms.)	1.2253	1.2737	1.0996	1.1318
G.L. (gms./sq. cm.)	.2072	.2162	.1904	.1914
W.F.	.3663	.4371	.3608	.4101
\bar{x}_a (in./cm.)	.089/.2261	.079/.2007	.081/.2057	.077/.19
C.F. / C.P.	.9493/.5029	.9407/.4490	.9733/.4449	.9087/.41
SAMPLE No.	1381AR-1	1381AR-2	1381A-4	1381A-2
\bar{x}_a (in./cm.)	.190/.4826	.190/.4826	.177/.4496	.178/.45
WT-a (gms.)	7.1598	6.2661	7.1400	6.9440
A-a (sq. cm.)	5.7663	4.9560	6.1057	5.9530
WT-b (gms.)	1.0536	.9205	1.1672	.9975
G.L.	.1827	.1857	.1912	.1676
W.F.	.3623	.3478	.3315	.3842
\bar{x}_a (in./cm.)	.083/.2108	.084/.2134	.091/.2311	.072/.18
C.F. / C.P.	.9076/.4368	.9483/.4422	.9443/.5140	.9062/.4
SAMPLE No.	1381A-5	1381A-7	1394AR-1	1394AR-
\bar{x}_s (in./cm.)	.183/.4648	.183/.4648	.185/.4699	.182/.46
WT-s (gms.)	6.2407	5.8232	6.7935	6.9290
A-s (sq. cm.)	5.1461	4.8100	5.5205	5.7570
WT-b (gms.)	1.0076	.9504	.9135	1.0370
G.L.	.1958	.1976	.1655	.1801
W.F.	.4306	.4574	.3719	.4040
\bar{x}_a (in./cm.)	.073/.1854	.070/.1778	.071/.1803	.072/.18
C.F. / C.P.	.9355/.3989	.9287/.3825	.9369/.3837	.9272/.30
SAMPLE No.	1394A-8	1394A-10	1394A-7	1394A-
\bar{x}_s (in./cm.)	.174/.4420	.171/.4343	.173/.4394	.171/.43
WT-s (gms.)	6.6993	6.4895	6.4685	6.1480
A-s (sq. cm.)	5.7867	5.7199	5.6557	5.3690
WT-b (gms.)	1.1563	1.1323	1.0772	.9669
G.L.	.1998	.1980	.1906	.1801
W.F.	.3972	.3849	.3739	.3570
\bar{x}_a (in./cm.)	.079/.2007	.081/.2057	.081/.2057	.078/.19
C.F. / C.P.	.9521/.4541	.9504/.4721	.9109/.4681	.9656/.4

SAMPLE No.	1416AR-1	1416AR-2	1416A-4	1416A-11
\bar{x}_a (in./cm.)	.181/.4597	.181/.4597	.174/.4420	.174/.44
WT-a (gms.)	7.0529	6.7357	6.7885	6.5814
A-a (sq. cm.)	5.8066	5.5308	5.8616	5.6606
WT-b (gms.)	1.0290	.9875	.9601	.9211
G.L. (gms./sq. cm.)	.1772	.1785	.1638	.1627
W.F.	.4064	.3769	.3492	.3488
\bar{x}_r (in./cm.)	.068/.1727	.073/.1854	.074/.1880	.073/.181
C.F. / C.P.	.9612/.3757	.9704/.4033	.9456/.4253	.9536/.4

SAMPLE No.	1416A-1	1416A-3	1426B-8	1426B-11
\bar{x}_a (in./cm.)	.178/.4521	.176/.4470	.177/.4496	.176/.447
WT-a (gms.)	6.4845	6.6940	6.4404	6.6156
A-a (sq. cm.)	5.5564	5.7347	5.9540	5.6400
WT-b (gms.)	1.1340	1.1746	1.0796	1.0344
G.L.	.2041	.2048	.1979	.1834
W.F.	.3929	.3791	.3915	.3900
\bar{x}_r (in./cm.)	.084/.2134	.085/.2159	.079/.2007	.074/.188
C.F. / C.P.	.9257/.4720	.9507/.4830	.9580/.4464	.9512/.42

SAMPLE No.	1426B-3	1426B-5	1426BR-1	1426BR-
\bar{x}_s (in./cm.)	.177/.4496	.178/.4521	.186/.4724	.186/.472
WT-s (gms.)	6.5744	6.8949	6.5092	6.5127
A-s (sq. cm.)	5.5936	5.8660	5.2164	5.2175
WT-b (gms.)	1.0846	1.2233	.8936	.8664
G.L.	.1939	.2085	.1713	.1661
W.F.	.3724	.3852	.3762	.3588
\bar{x}_r (in./cm.)	.082/.2083	.086/.2184	.071/.1803	.072/.18
C.F. / C.P.	.9491/.4633	.9421/.4831	.9593/.3817	.9598/.38

SAMPLE No.	1492AR-1	1492AR-2	1492A-2	1492A-1
\bar{x}_s (in./cm.)	.184/.4674	.186/.4724	.171/.4343	.171/.434
WT-s (gms.)	7.3039	5.8688	6.2767	6.0813
A-s (sq. cm.)	6.0001	4.8289	5.4755	5.4169
WT-b (gms.)	1.1512	.8886	.8614	1.0601
G.L.	.1919	.1840	.1573	.1957
W.F.	.3682	.3742	.2990	.4120
\bar{x}_r (in./cm.)	.083/.2108	.081/.2057	.081/.2057	.077/.19
C.F. / C.P.	.9384/.4510	.9079/.4354	.9656/.4736	.9251/.4

SAMPLE No.	1492A-1	1492A-7	1496BR-1	1496BR-
\bar{x}_a (in./cm.)	.173/.4394	.171/.4343	.198/.4775	.188/.477
WT-a (gms.)	6.7973	5.8282	6.3313	7.6183
A-a (sq. cm.)	5.9627	5.1042	5.1066	6.0847
WT-b (gms.)	.9391	.8548	1.0426	1.2506
G.L. (gms./sq. cm.)	.1575	.1675	.2042	²⁰⁵⁵ .246
W.F.	.3661	.3755	.4007	⁴¹⁶⁰ .3322
\bar{x}_c (in./cm.)	.070/.1778	.070/.1778	.082/.2083	.078/.198
C.F. / C.P.	.9184/.4046	.9526/.4094	.9308/.4362	.4144 / .41 .4502

SAMPLE No.	1496B-6	1496B-8	1496B-7	1496B-6
\bar{x}_a (in./cm.)	.171/.4343	.171/.4343	.173/.4394	.175/.44
WT-a (gms.)	6.5535	6.3439	6.8716	7.0149
A-a (sq. cm.)	5.7437	5.5447	5.9430	5.9675
WT-b (gms.)	1.1143	1.0409	1.2031	1.1606
G.L.	.1940	.1877	.2024	.1945
W.F.	.3989	.4063	.4334	.4055
\bar{x}_c (in./cm.)	.076/.1930	.072/.1829	.073/.1854	.074/.188
C.F. / C.P.	.9588/.4444	.9618/.4211	.9613/.4219	.9712/.4:

SAMPLE No.	1533BR-1	1533BR-2	1533B-4	1533B-
\bar{x}_s (in./cm.)	.185/.4699	.184/.4674	.172/.4369	.172/.43
WT-s (gms.)	7.3265	6.7002	6.8814	6.7066
A-s (sq. cm.)	5.9515	5.4448	5.9989	5.8692
WT-b (gms.)	1.1465	1.0568	1.1140	1.1791
G.L.	.1926	.1941	.1857	.2009
W.F.	.3555	.3679	.3826	.4003
\bar{x}_c (in./cm.)	.085/.2159	.082/.2083	.076/.1930	.079/.201
C.F. / C.P.	.9518/.4595	.9614/.4457	.9557/.4417	.9515/.4

SAMPLE No.	1533B-5	1533B-9	1537BR-1	1537BR.
\bar{x}_s (in./cm.)	.177/.4496	.174/.4420	.182/.4623	.184/.467
WT-s (gms.)	6.7560	6.9483	7.1220	6.6103
A-s (sq. cm.)	5.6822	5.9340	5.9143	5.4669
WT-b (gms.)	1.1003	.7922	1.1177	.9735
G.L.	.1936	.1335	.1890	.1781
W.F.	.3720	.2853	.3484	.3888
\bar{x}_c (in./cm.)	.080/.2032	.072/.1829	.086/.2184	.075/.19
C.F. / C.P.	.9771 / .4522	.9148 / .4124	.9414 / .4704	.9141 / .4

SAMPLE No.	1537B-5	1537B-7	1537B-8	1537B-10
\bar{x}_s (in./cm.)	.183/.4648	.178/.4521	.177/.4496	.174/.442
WT-s (gms.)	6.5621	6.4670	5.6993	6.0034
As (sq. cm.)	5.3637	5.4723	4.9107	5.2483
WT-b (gms.)	1.1830	1.1530	1.0533	1.1292
G.L. (gms./sq. cm.)	.2206	.2107	.2145	.2152
W.F.	.3878	.4105	.4127	.4109
\bar{x}_c (in./cm.)	.088/.2235	.081/.2057	.084/.2134	.084/.213
C.F. / C.P.	.9675/.4809	.9503/.4550	.9278/.4746	.9346/.48
SAMPLE No.	1568AR-1	1568AR-2	1568A-4	1568A-1
\bar{x}_s (in./cm.)	.180/.4572	.181/.4597	.170/.4318	.170/.43
WT-s (gms.)	6.8920	7.1767	6.7992	6.4068
As (sq. cm.)	5.8067	5.9826	5.9639	5.632
WT-b (gms.)	1.1371	1.1779	1.0418	1.0081
G.L.	.1958	.1969	.1747	.1780
W.F.	.3727	.3705	.3874	.3992
\bar{x}_c (in./cm.)	.084/.2134	.084/.2134	.070/.1778	.070/.17
C.F. / C.P.	.9350/.4668	.9453/.4642	.9642/.4118	.9596/.4
SAMPLE No.	1568A-7	1568A-9		
\bar{x}_s (in./cm.)	.175/.4445	.173/.4394		
WT-s (gms.)	6.5474	6.5846		
As (sq. cm.)	5.5921	5.6802		
WT-b (gms.)	1.1398	1.0550		
G.L.	.2038	.1857		
W.F.	.4057	.3401		
\bar{x}_c (in./cm.)	.078/.1981	.084/.2134		
C.F. / C.P.	.9654/.4457	.9692/.4857		
SAMPLE No.	26 RETAINS	MEANS (74 OBSERVATIONS)	STD. DEVIATIONS	48 FROM EDGE STR
\bar{x}_s (in./cm.)				
WT-s (gms.)				
As (sq. cm.)				
WT-b (gms.)				
G.L.		.1875	.0192	
W.F.		.3803	.0301	
\bar{x}_c (in./cm.)		.0782/.1986	.0068/.0173	
C.F. / C.D.	MEAN ^{SD} .0800/.0059	.9450/.4390	.0177/.0369	MEAN .0772/.

LEGEND

- t_s = thickness of sample (in./cm.)
 WT_s = total weight of sample (grams)
 A_s = surface area of sample (sq. centimeters)
 WT_B = weight of boron carbide (grams)
 $G.L.$ = grams loading (distribution of boron carbide per unit area) (gms./sq. cm.)
 $W.F.$ = weight factor (content ratio of boron carbide in core by weight)
 t_c = thickness of core (in./cm.)
 $C.F.$ = compaction factor (ratio of actual density to ideal)
 $C.P.$ = core proportion (ratio of core thickness to sample thickness)

Sheet # 10000A Date _____ Customer _____ Inspector _____

FORM 302

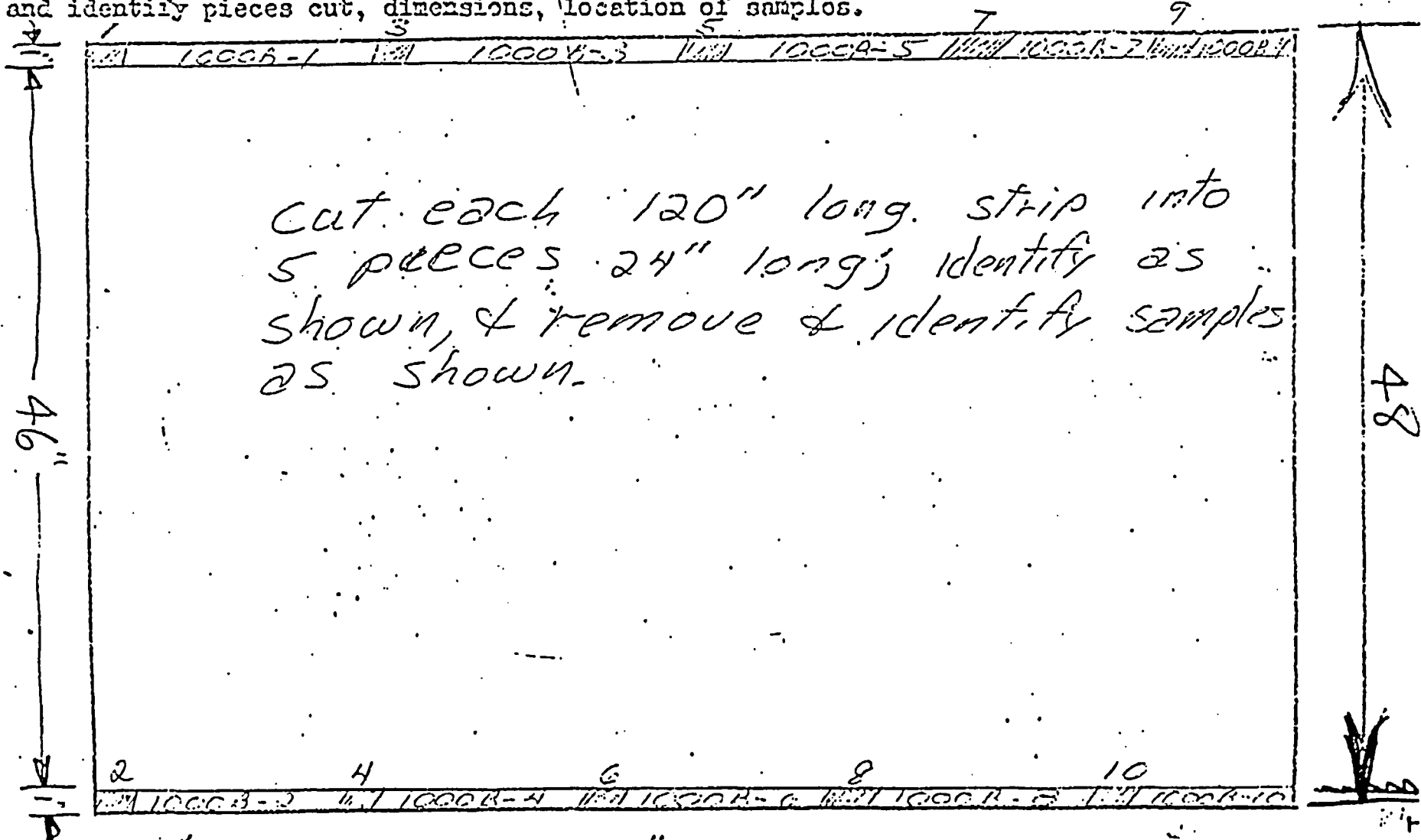
Dimensional inspection (Indicate acceptance or rejection)

Total thickness: _____
Width: _____
Length: _____
Squareness: _____

Workmanship (Indicate acceptance or rejection) _____

Surface Condition (Indicate acceptance or rejection) _____

Diagram and identify pieces cut, dimensions, location of samples.



cut each 120" long strip into
5 pieces 24" long; identify as
shown, & remove & identify samples
as shown.

LATERAL PROFILE

1338B-4

1492A-4

	t_p	t_c	C.P.		t_p	t_c	C.P.
0	.175	.065	.3714		.175	.080	.4571
1	.175	.075	.4286		.177	.085	.4802
2	.175	.080	.4571		.177	.090	.5085
3	.175	.090	.5143		.177	.090	.5085
12	.180	.095	.5278		.185	.095	.5135
24	.182	.095	.5220		.189	.100	.5291
36	.178	.090	.5056		.185	.095	.5135
43	.173	.085	.4913		.178	.090	.5056
44	.173	.080	.4624		.178	.075	.4213
45	.172	.080	.4651		.176	.075	.4261
46	.172	.080	.4651		.176	.070	.3977

1537B-4

0	.179	.085	.4749
1	.179	.085	.4749
2	.179	.085	.4749
3	.179	.085	.4749
12	.188	.100	.5319
24	.189	.100	.5291
36	.185	.100	.5405
43	.178	.090	.5056
44	.178	.085	.4775
45	.176	.080	.4545
46	.176	.085	.4830

Sheet # 1537-B Date 1-2-74 Customer _____ Inspector _____ FORM 70

Dimensional inspection (Indicate acceptance or rejection)

Total thickness: _____

Width: _____

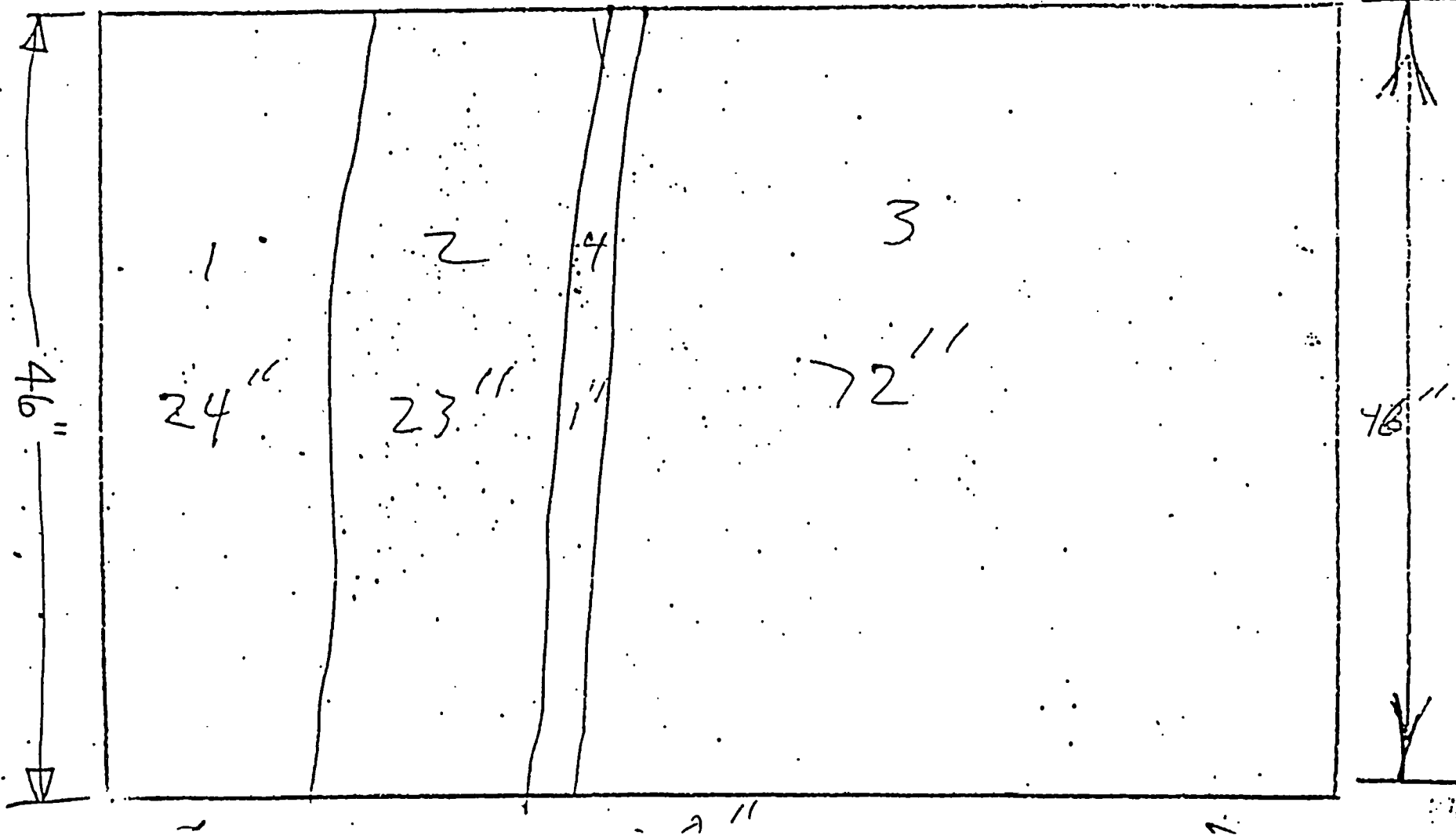
Length: _____

Squareness: _____

Workmanship (Indicate acceptance or rejection) _____

Surface Condition (Indicate acceptance or rejection) _____

Diagram and identify pieces cut, dimensions, location of samples.



Sheet # 1492-A Date 5-2-76 Customer _____ Inspector _____

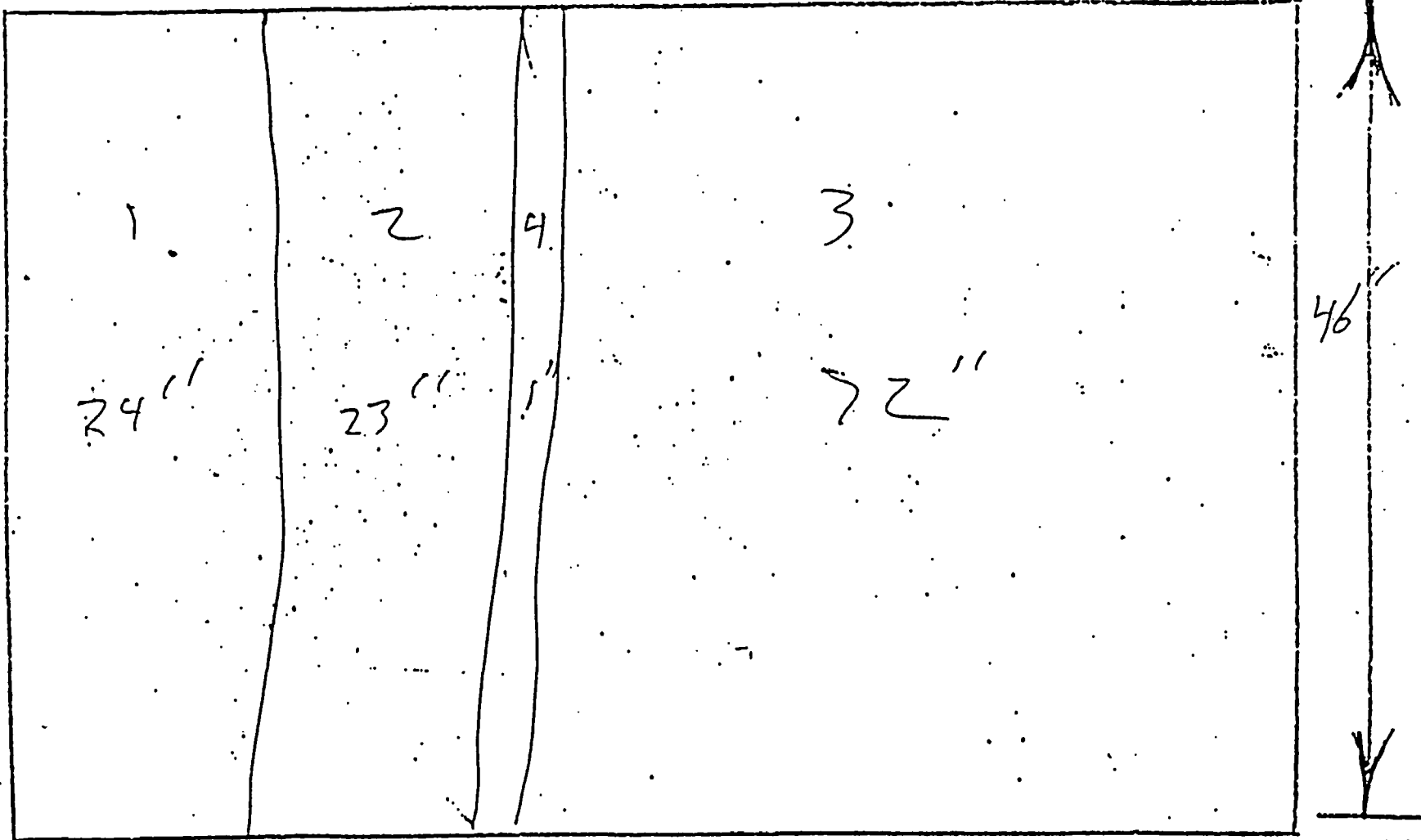
Dimensional inspection (Indicate acceptance or rejection)

Total thickness: _____
Width: _____
Length: _____
Squareness: _____

Workmanship (Indicate acceptance or rejection) _____

Surface Condition (Indicate acceptance or rejection) _____

Diagram and identify pieces cut, dimensions, location of samples.



Sheet # 1000-B Date 5-3-76 Customer _____ Inspector J. Richards FORM 90

Dimensional inspection (Indicate acceptance or rejection)

Total thickness: _____

Width: 46

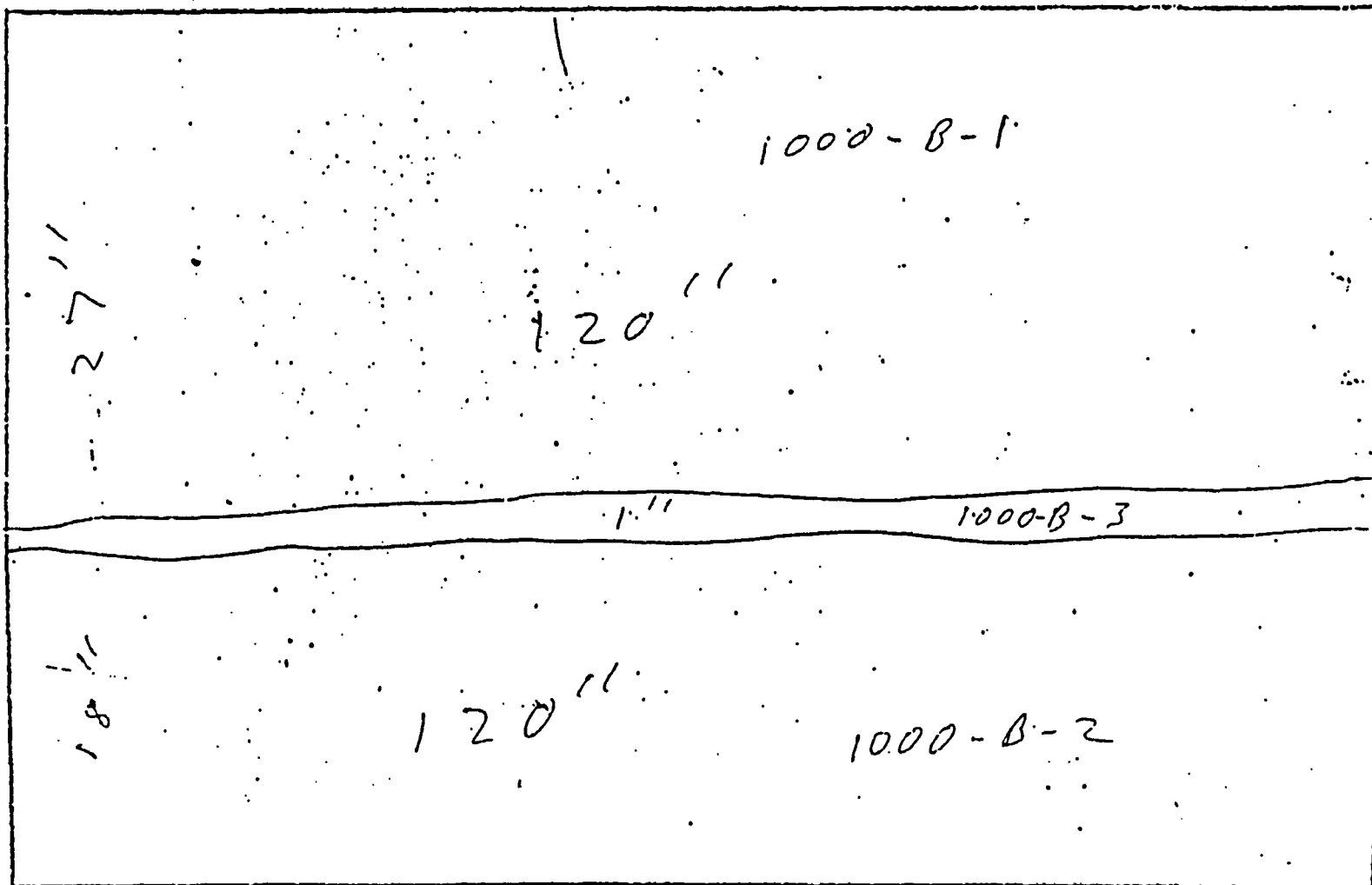
Length: 120

Squareness: _____

Workmanship (Indicate acceptance or rejection) _____

Surface Condition (Indicate acceptance or rejection) _____

Diagram and identify pieces cut, dimensions, location of samples.



Set # 1381-A Date 7-3-76 Customer _____ Inspector _____ FORM 902

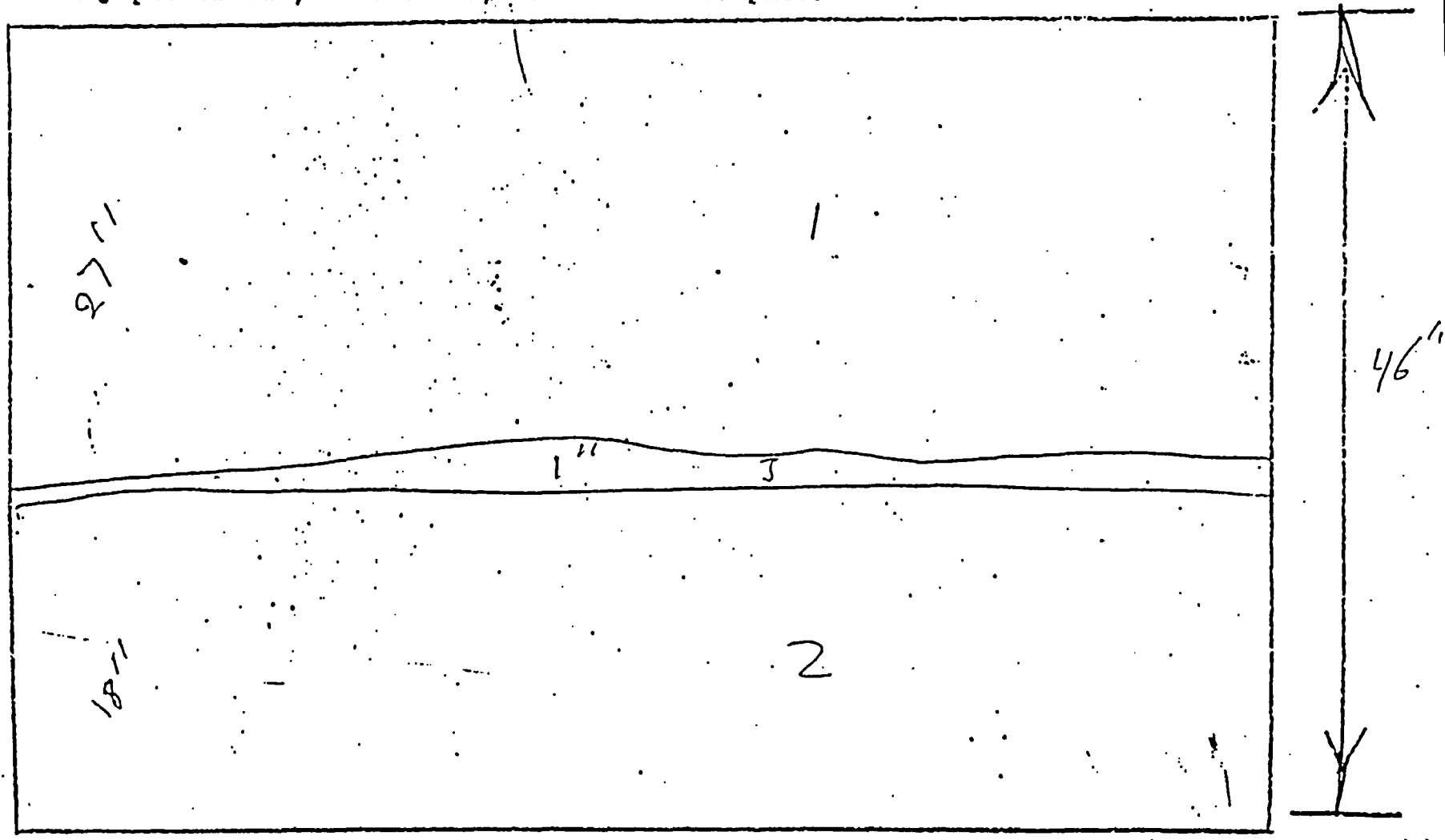
Dimensional inspection (Indicate acceptance or rejection)

Total thickness: _____
Width: _____
Length: _____
Squareness: _____

Workmanship (Indicate acceptance or rejection) _____

Surface Condition (Indicate acceptance or rejection) _____

Diagram and identify pieces cut, dimensions, location of samples.



Dimensional inspection (Indicate acceptance or rejection)

Total thickness: _____

Width: _____

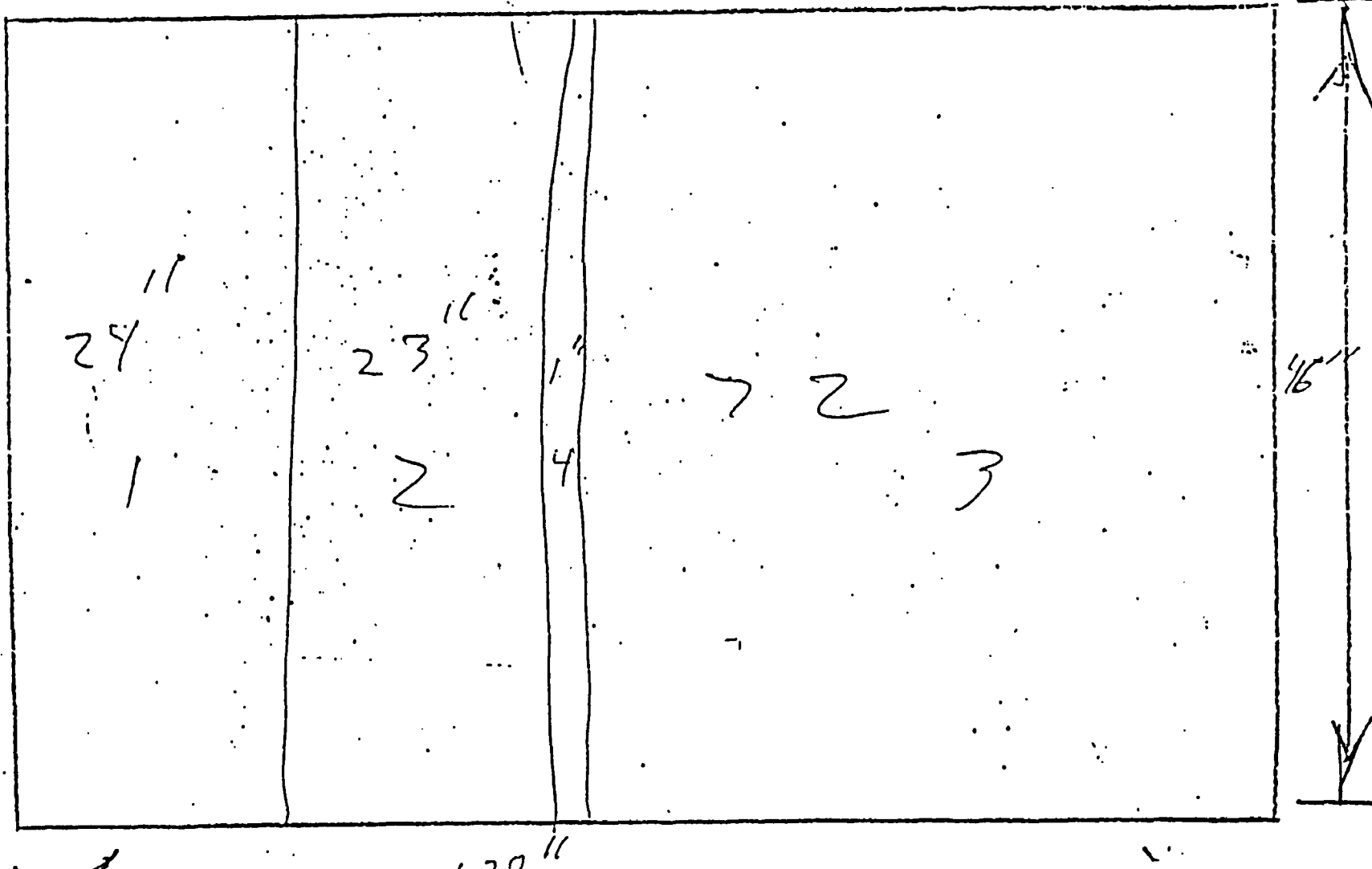
Length: _____

Squareness: _____

Workmanship (Indicate acceptance or rejection) _____

Surface Condition (Indicate acceptance or rejection) _____

Diagram and identify pieces cut, dimensions, location of samples.



5/9/76
LM

LATERAL PROFILE

POSITION	1338 B-4 THICK	CORE	1492 A-4 THICK	CORE	1537-B-4 THICK	CORE
0						
1						
2						
3						
11 1/2						
12						
12 1/2						
23 1/2						
24						
24 1/2						
35 1/2						
36						
36 1/2						
43						
24						
5						
46						

MEAN/STD. DEV. .0865/.0086

.0891/.0092

.0922/.0066

LONGITUDINAL PROFILE

THK.	1000 B-3 CORE	1381 A-3 CORE
1		
12		
24		
36		
48		
60		
72		
84		
96		
108		
19		

.0923/.0052

.0964/.0023

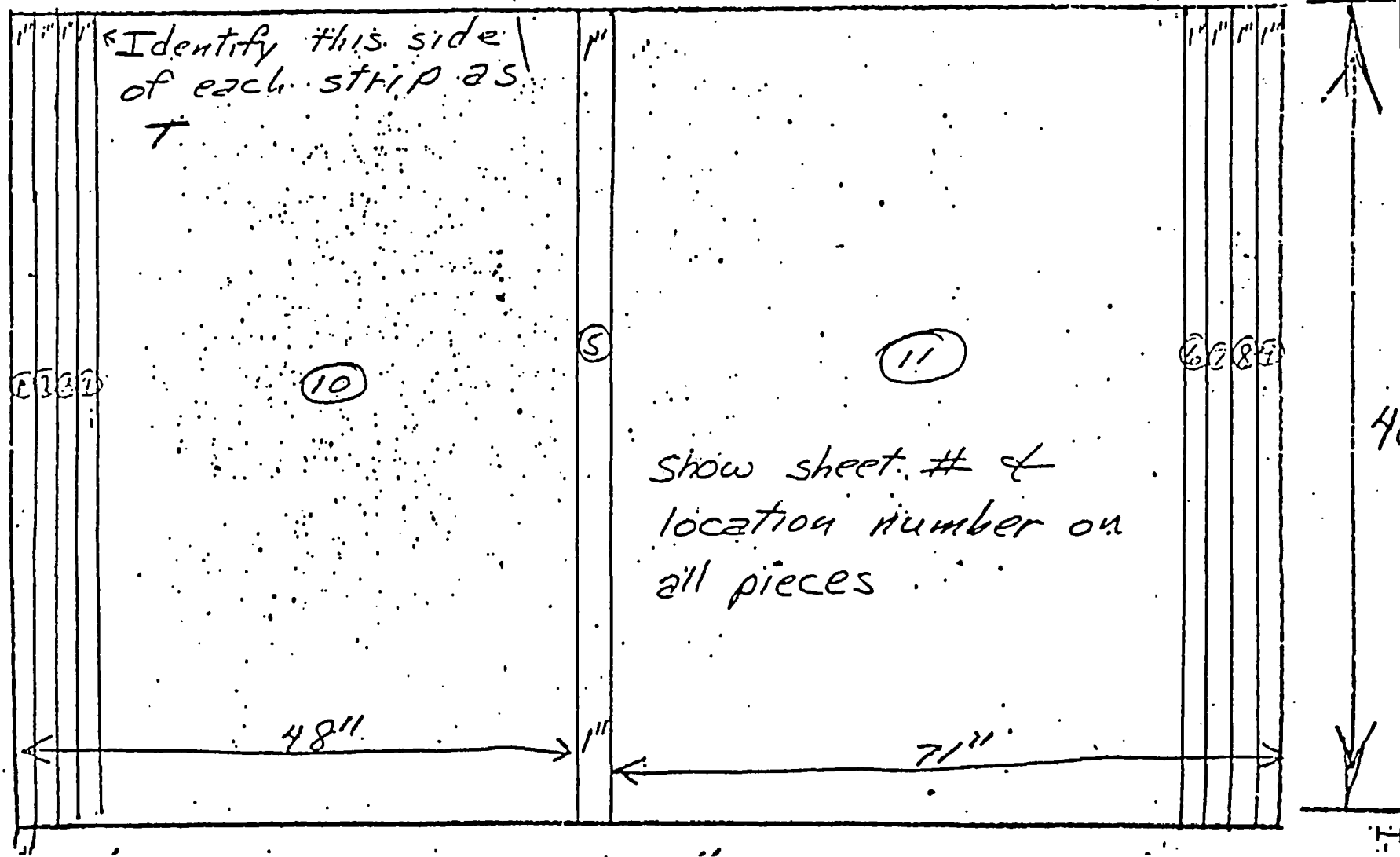
Dimensional inspection (Indicate acceptance or rejection) _____

Total thickness: _____
Width: _____
Length: _____
Squareness: _____

Workmanship (Indicate acceptance or rejection) _____

Surface Condition (Indicate acceptance or rejection) _____

Diagram and identify pieces cut, dimensions, location of samples.



N	T	C
1	.174	.080
2	.175	.085
3	.176	.085
4	.177	
5	.178	
6	.179	
7	.180	
8	.181	
9	.181	
10	.182	
11	.183	.090
12	.183	.085
13	.184	.090
14	.185	.085
15	.185	.090
16	.185	
17	.186	
18	.186	
19	.187	
20	.187	
21	.188	
22	.187	
23	.187	
24	.188	.090
25	.188	.085
26	.188	.085
27	.189	.085
28	.187	
29	.187	
30	.186	
31	.186	
32	.185	
33	.185	
34	.184	
35	.183	.095
36	.183	.095
37	.182	.095
38	.181	.085
39	.180	
40	.180	
41	.179	
42	.177	
43	.176	
44	.175	.085
45	.174	.085
46	.174	.075
47	.173	.075

IN	T	C
0	.181	.085
1	.181	.085
2	.182	.090
3	.183	.090
4	.184	.090
5	.184	
6	.185	
7	.186	
8	.187	
9	.188	
10	.189	.085
11	.190	.085
12	.190	.090
13	.190	
14	.191	
15	.191	
16	.191	
17	.192	
18	.192	
19	.192	
20	.192	
21	.193	.095
22	.193	.090
23	.193	.085
24	.192	.090
25	.192	
26	.192	
27	.192	
28	.191	
29	.191	
30	.191	
31	.191	
32	.190	
33	.190	
34	.189	.090
35	.189	.095
36	.188	.090
37	.185	.090
38	.185	
39	.184	
40	.183	
41	.181	
42	.180	
43	.180	.085
44	.179	.085
45	.177	.080
46	.177	.075

IN	T	C
0	.180	.085
1	.181	.085
2	.182	.090
3	.183	.090
4	.184	.090
5	.185	
6	.186	
7	.186	
8	.187	
9	.188	
10	.189	.095
11	.190	.090
12	.191	.090
13	.191	
14	.192	
15	.192	
16	.192	
17	.192	
18	.194	
19	.193	
20	.194	
21	.194	
22	.194	.095
23	.194	.095
24	.193	.095
25	.193	.100
26	.193	
27	.193	
28	.192	
29	.192	
30	.192	
31	.192	
32	.191	
33	.191	
34	.190	.095
35	.189	.095
36	.188	.090
37	.187	.085
38	.185	
39	.184	
40	.183	
41	.182	
42	.181	.085
43	.180	.085
44	.178	.080
45	.178	.075
46	.177	.070

IN	T	C
0	.177	.080
1	.150	.085
2	.151	.090
3	.182	
4	.183	
5	.184	
6	.186	
7	.186	
8	.187	
9	.187	
10	.188	
11	.189	.100
12	.190	.095
13	.190	.090
14	.191	
15	.191	
16	.192	
17	.192	
18	.193	
19	.193	
20	.193	
21	.194	
22	.193	
23	.193	.100
24	.193	.095
25	.192	.100
26	.192	
27	.192	
28	.192	
29	.191	
30	.191	
31	.190	
32	.190	
33	.190	
34	.187	
35	.188	.095
36	.188	.090
37	.185	.100
38	.184	
39	.183	
40	.182	
41	.181	
42	.180	
43	.179	
44	.178	.095
45	.177	.090
46	.177	.085

MEAN	.0869	.0894	.0888	.0909
STD. DEV	.0056	.0078	.0074	.0078

N	T	C
1	.175	.085
2	.177	.085
3	.178	.085
4	.178	.090
5	.179	.090
6	.180	
7	.181	
8	.182	
9	.183	
10	.184	.085
11	.185	.090
12	.185	.111
13	.186	.095
14	.186	
15	.187	
16	.187	
17	.187	
18	.188	
19	.188	
20	.188	
21	.188	
22	.188	.085
23	.189	.090
24	.189	.075
25	.189	.095
26	.189	
27	.188	
28	.187	
29	.187	
30	.187	
31	.186	
32	.185	
33	.185	.085
34	.189	.090
35	.184	.085
36	.189	.100
37	.183	.075
38	.182	.100
39	.181	
40	.181	
41	.180	
42	.179	
43	.179	
44	.178	
45	.177	.085
46	.176	.085
47	.176	.1085
48	.175	.085
49	.175	.085
50	.174	.085

IN	T	C
0	.174	
1	.175	.075
2	.176	.080
3	.177	.065
4	.178	.085
5	.179	.085
6	.180	
7	.181	
8	.181	
9	.182	
10	.183	.085
11	.184	.090
12	.184	.085
13	.185	
14	.186	
15	.186	
16	.187	
17	.187	
18	.187	
19	.188	
20	.188	
21	.188	
22	.188	.085
23	.189	.080
24	.189	.075
25	.189	.095
26	.189	
27	.188	
28	.187	
29	.187	
30	.187	
31	.186	
32	.185	
33	.185	.085
34	.189	.090
35	.184	.085
36	.183	.100
37	.182	.075
38	.181	.100
39	.180	
40	.179	
41	.179	
42	.178	
43	.177	
44	.176	.090
45	.175	.1085
46	.174	.075
47	.174	.085

IN	T	C
0	.181	
1	.181	.100
2	.182	.095
3	.184	.085
4	.184	.090
5	.185	.095
6	.186	.100
7	.187	.100
8	.188	.100
9	.189	.095
10	.190	.100
11	.190	.095
12	.191	.100
13	.191	.095
14	.191	.095
15	.192	
16	.192	
17	.193	
18	.193	
19	.193	
20	.193	
21	.194	
22	.194	.105
23	.193	.100
24	.193	.100
25	.193	.100
26	.193	
27	.193	
28	.192	
29	.192	
30	.192	
31	.192	
32	.191	
33	.190	
34	.189	.070
35	.188	.075
36	.188	.085
37	.187	
38	.185	
39	.185	
40	.183	
41	.182	
42	.181	
43	.180	.100
44	.179	.095
45	.178	.085
46	.178	.075
47	.178	.100
48	.178	.090

IN	T	C
0	.173	.095
1	.175	.100
2	.175	.095
3	.175	.095
4	.177	.095
5	.178	
6	.179	
7	.180	
8	.181	
9	.181	.100
10	.182	.100
11	.183	.095
12	.184	.100
13	.184	.095
14	.185	
15	.185	
16	.185	
17	.186	
18	.186	
19	.186	
20	.186	
21	.187	.105
22	.187	.100
23	.187	.100
24	.187	.100
25	.187	.100
26	.187	
27	.186	
28	.186	
29	.186	
30	.185	
31	.185	
32	.184	
33	.184	.070
34	.183	.075
35	.182	.085
36	.182	
37	.181	
38	.180	
39	.179	
40	.178	
41	.177	
42	.176	
43	.175	.085
44	.174	.075
45	.173	.080
46	.173	.075
47	.173	.075

MEAN	.0887	.0843	.0947	.0818
STD. DEV.	.0048	.0081	.0067	.0099

N	T	C	IN	T	C	IN	T	C	IN	T	C
	.177	.090	0	.170	.080						
	.179	.085	1	.172	.085						
	.79	.095	2	.172	.090						
	.180		3	.174							
	.181		4	.175							
	.182		5	.175							
	.183		6	.176							
	.184		7	.177							
	.184		8	.178							
	.184		9	.180							
	.185		10	.181							
	.186		11	.182	.085						
	.187		12	.182	.090						
	.187	.090	13	.183	.095						
	.187	.095	14	.183							
	.188	.100	15	.184							
	.188	.095	16	.185							
	.189		17	.185							
	.190		18	.185							
	.190		19	.186							
	.190		20	.187							
	.190		21	.187							
	.190		22	.187							
	.190		23	.187	.090						
	.190		24	.187	.095						
	.191		25	.188							
	.191		26	.188							
	.191		27	.188							
	.191	.095	28	.185							
	.191	.095	29	.185							
	.190	.090	30	.184							
	.190		31	.183							
	.190		32	.182							
	.190		33	.181							
	.189		34	.180							
	.189		35	.179							
	.188		36	.178	.085						
	.187		37	.176	.095						
	.186	.085			.090						
	.186	.090									
	.185	.095									
	.184	.095									
	.183										
	.182										
	.181										
	.180										
	.179										
	.178	.095									
	.177	.090									
	.175	.085									
	.175										
	.175										
	MEAN	.0900			.0891						
	STD. DEV.	.0048			.0049						

APPENDIX B

EXPERIMENTAL DATA

PANEL LOT. II

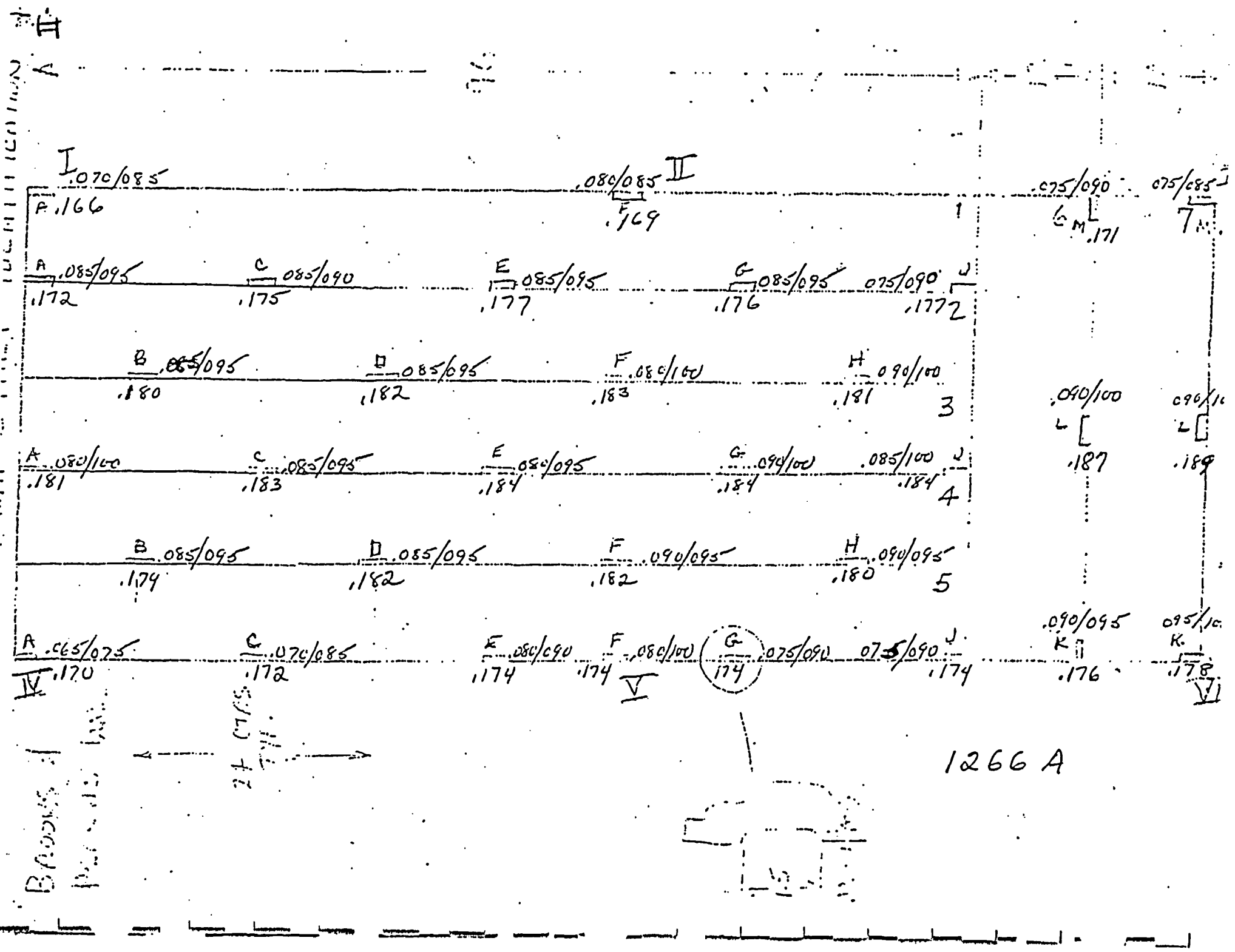
PAGES II-1 THRU II-20

THICKNESS MEASUREMENTS FOR

II-7

BORAL SHEET NO. 1266A

LOCATION	CORE THICKNESS			PANEL THICKNESS	
	MIN.	MAX.	AVG.		
I	.070	.085	.0775	.166	
II	.080	.085	.0825	.169	
6M	.075	.090	.0825	.171	
III	.075	.085	.080	.173	
1A	.085	.095	.090	.172	
1C	.085	.090	.0875	.175	
1E	.085	.095	.090	.177	
1G	.085	.095	.090	.176	
1J	.075	.090	.0825	.177	
2B	.085	.095	.090	.180	
2D	.085	.095	.090	.182	
2F	.080	.100	.090	.183	
2H	.090	.100	.095	.181	
6L	.090	.100	.095	.187	
7L	.090	.100	.095	.189	
3A	.080	.100	.090	.181	
3C	.085	.095	.090	.183	
3E	.080	.095	.0875	.184	
3G	.090	.100	.095	.184	
3J	.085	.100	.0925	.184	
4B	.085	.095	.090	.179	
4D	.085	.095	.090	.182	
4F	.090	.095	.0925	.182	
4H	.090	.095	.0925	.180	
IV	.065	.075	.070	.170	
5C	.070	.085	.0775	.172	
5E	.080	.090	.085	.174	
V	.080	.100	.090	.174	
5G	.075	.090	.0825	.174	
5J	.075	.090	.0825	.174	
6K	.090	.095	.0925	.176	
VI	.095	.100	.0975	.178	
		MEAN	.0879	.0906	.0850
		STD. DEVIATION	.0061	.0031	.0074
			COMBINED	CENTRAL	PERIPHERY



EUM... ..

BROADS... ..

V

1266 A

THICKNESS MEASUREMENTS FOR BORAL SHEET NO. 1325-A

II-3

LOCATION	CORE THICKNESS			PANEL THICKNESS
	MIN.	MAX.	AVG.	
I	.075	.090	.0825	
II	.075	.085	.080	.169
6M	.080	.085	.0825	.173
III	.075	.085	.080	.174
IA	.085	.090	.0875	.175
IC	.085	.100	.0925	.174
IE	.085	.095	.090	.177
IG	.090	.095	.0925	.180
IJ	.085	.095	.090	.178
2B	.085	.095	.090	.178
2D	.090	.100	.095	.180
2F	.090	.100	.095	.182
2H	.090	.100	.095	.183
6L	.080	.100	.090	.180
7L	.095	.100	.0975	.184
3A	.080	.090	.085	.186
3C	.085	.100	.0925	.177
3E	.085	.100	.0925	.180
3G	.085	.100	.0925	.182
3J	.085	.100	.0925	.180
4B	.085	.100	.0925	.180
4D	.085	.100	.0925	.180
4F	.085	.100	.0925	.176
4H	.085	.095	.090	.177
IV	.075	.100	.0925	.178
5C	.080	.080	.0775	.176
5E	.080	.085	.0825	.166
V	.080	.085	.0825	.169
5G	.080	.090	.085	.172
5J	.080	.085	.0825	.172
6K	.075	.085	.0825	.170
VI	.090	.100	.0825	.170
			.095	.172
			.0883	.175
			.0054	.0919
				.0020
				.0843
				.0053

MEAN
STD. DEVIATION

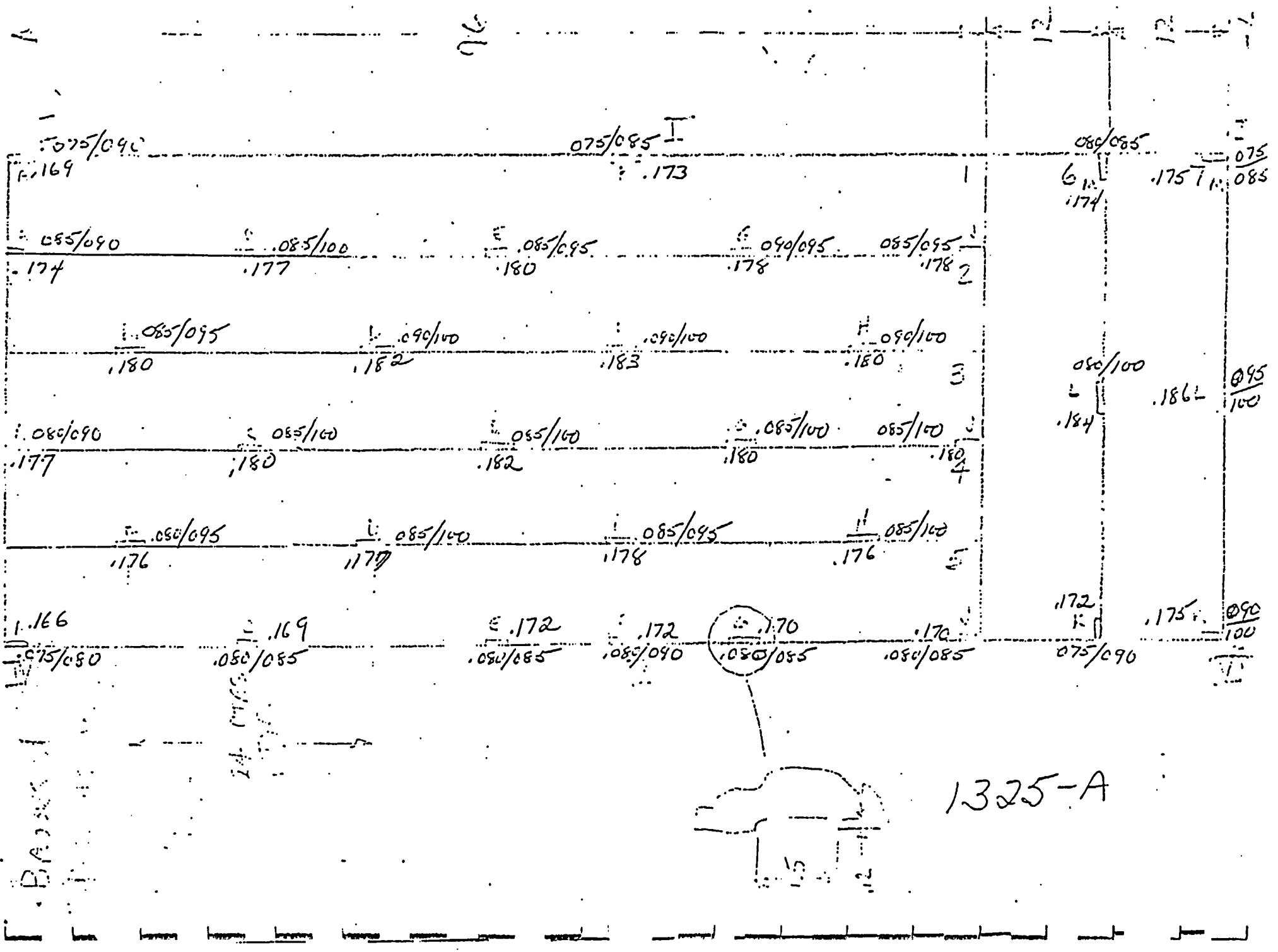
COMBINED

CENTRAL

PERIPHERY

E

76



1325-A

THICKNESS MEASUREMENTS FOR

BORAL SHEET NO. 1325-B

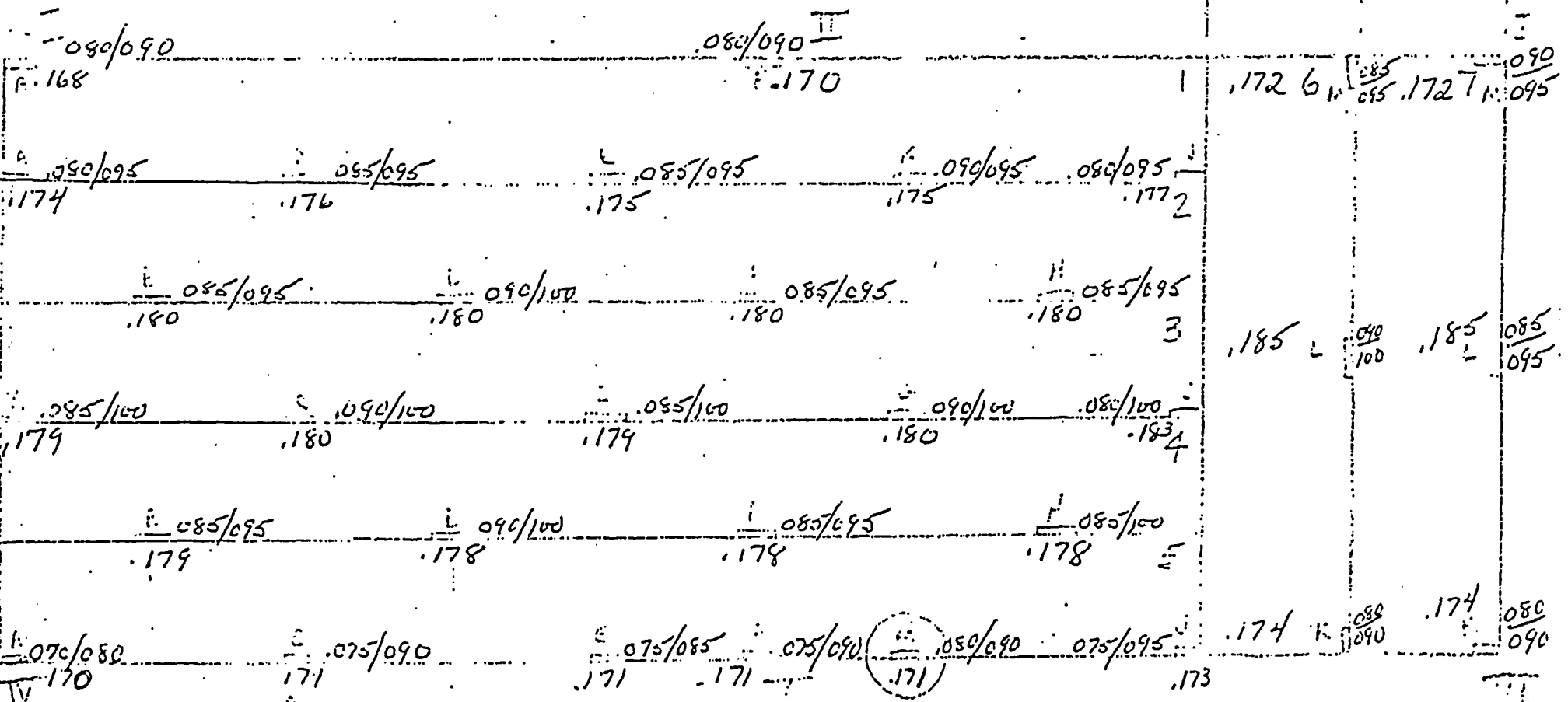
LOCATION	CORE THICKNESS			PANEL THICKNESS	
	MIN.	MAX.	AVG.		
I	.080	.090	.085	.168	
II	.080	.090	.085	.170	
6M	.085	.095	.090	.172	
III	.090	.095	.0925	.172	
IA	.080	.095	.0875	.174	
IC	.085	.095	.090	.176	
IE	.085	.095	.090	.175	
IG	.090	.095	.0925	.175	
IJ	.080	.095	.0875	.177	
2B	.085	.095	.090	.180	
2D	.090	.100	.095	.180	
2F	.085	.095	.090	.180	
2H	.085	.095	.090	.180	
6L	.090	.100	.095	.185	
7L	.085	.095	.090	.185	
3A	.085	.100	.0925	.179	
3C	.090	.100	.095	.180	
3E	.085	.100	.0925	.179	
3G	.090	.100	.095	.180	
3J	.080	.100	.090	.183	
4B	.085	.095	.090	.179	
4D	.090	.100	.095	.178	
4F	.085	.095	.090	.178	
4H	.085	.100	.0925	.178	
IV	.070	.080	.075	.170	
5C	.075	.090	.0825	.171	
5E	.075	.085	.080	.171	
V	.075	.090	.0825	.171	
5G	.080	.090	.085	.171	
5J	.075	.095	.085	.173	
6K	.080	.090	.085	.174	
VI	.080	.090	.085	.174	
MEAN			.0888	.0917	.0855
STD. DEVIATION			.0047	.0024	.0046

APPROVED DATE PERIOD

II

916

12



070/080
170

075/090
171

075/085
171

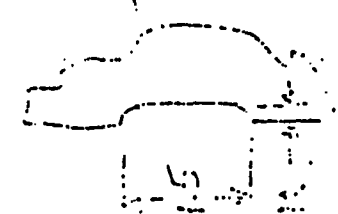
075/090
171

080/090
171

075/095
173

080/090
174

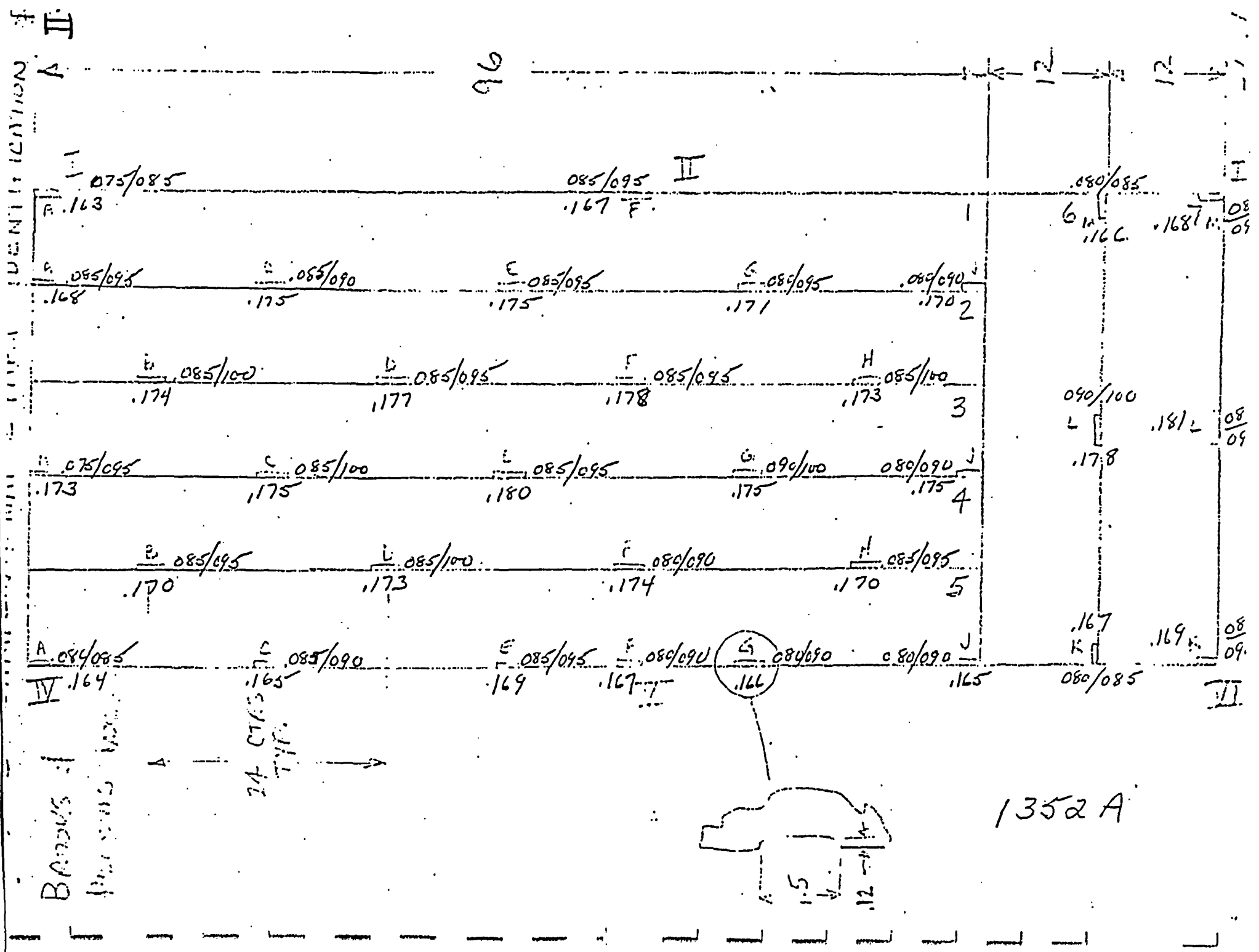
080/090
174



1325 B-

THICKNESS MEASUREMENTS FOR BORAL SHEET NO. 1352-A

LOCATION	CORE THICKNESS			PANEL THICKNESS	
	MIN.	MAX.	AVG.		
I	.075	.085	.080	.163	
II	.085	.095	.090	.167	
6M	.080	.085	.0825	.166	
III	.085	.090	.0875	.168	
1A	.085	.095	.090	.168	
1C	.085	.090	.0875	.175	
1E	.085	.095	.090	.175	
1G	.080	.095	.0875	.171	
1J	.080	.090	.085	.170	
2B	.085	.100	.0925	.174	
2D	.085	.095	.090	.177	
2F	.085	.095	.090	.178	
2H	.085	.100	.0925	.173	
6L	.090	.100	.095	.178	
7L	.085	.090	.0875	.181	
3A	.075	.095	.085	.173	
3C	.085	.100	.0925	.175	
3E	.085	.095	.090	.180	
3G	.090	.100	.095	.175	
3J	.080	.090	.085	.175	
4B	.085	.095	.090	.170	
4D	.085	.100	.0925	.173	
4F	.080	.090	.085	.174	
4H	.085	.095	.090	.170	
IV	.080	.085	.0825	.164	
5C	.085	.090	.0875	.165	
5E	.085	.095	.090	.169	
V	.080	.090	.085	.167	
5G	.080	.090	.085	.166	
5J	.080	.090	.085	.165	
6K	.080	.085	.0825	.167	
VI	.085	.090	.0875	.169	
MEAN			.0880	.0900	.0858
STD. DEVIATION			.0037	.0032	.0031
				CENTRAL	PERIPHERY



96

12

12

I
A 075/085

B 085/095 II

C 080/085

.163

.167

.166

.168

II
A 085/095

B 085/090

C 085/095

D 080/095

E 080/090

.168

.175

.175

.171

.170

III
A 085/100

B 085/095

C 085/095

D 085/100

.174

.177

.178

.173

090/100

.181

IV
A 075/095

B 085/100

C 085/095

D 090/100

E 080/090

.173

.175

.180

.175

.175

.178

V
A 085/095

B 085/100

C 080/090

D 085/095

.170

.173

.174

.170

.167

.169

VI
A 080/085

B 085/090

C 085/095

D 080/090

E 080/090

J 080/090

.164

.165

.169

.167

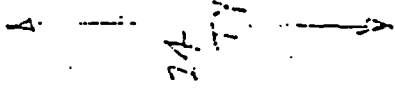
.166

.165

080/085

.169

BRASS
PULVERIZED



1352 A

III

THICKNESS MEASUREMENTS FOR

II-9

BORAL SHEET NO. 1352-B

LOCATION	CORE THICKNESS			PANEL THICKNESS
	MIN.	MAX.	AVG.	
I	.075	.085	.080	.173
II	.085	.095	.090	.175
6M	.080	.090	.085	.175
III	.085	.090	.0875	.176
IA	.080	.090	.085	.179
IC	.090	.100	.095	.179
IE	.085	.100	.0925	.181
IG	.090	.100	.095	.182
IJ	.090	.100	.095	.183
2B	.080	.095	.0875	.184
2D	.085	.095	.090	.183
2F	.090	.100	.095	.186
2H	.090	.100	.095	.187
6L	.085	.095	.090	.187
7L	.095	.100	.0975	.189
3A	.075	.085	.080	.183
3C	.085	.095	.090	.184
3E	.090	.100	.095	.185
3G	.090	.100	.095	.188
3J	.085	.100	.0925	.187
4B	.080	.090	.085	.180
4D	.085	.095	.090	.179
4F	.090	.100	.095	.182
4H	.090	.100	.095	.183
IV	.070	.080	.075	.172
5C	.075	.080	.0775	.172
5E	.085	.095	.090	.174
V	.085	.090	.0875	.175
5G	.085	.095	.090	.176
5J	.085	.095	.090	.175
6K	.080	.095	.0875	.175
VI	.085	.090	.0875	.176
	MEAN		.0894	.0925
	STD. DEVIATION		.0055	.0031
			COMBINED	CENTRAL
				PERIPHERY

.0860
.0058

A II

96

12

12

12

.075/085

.085/095

.080/090

.085/095

.173

.175

.175

.176

.176

.080/090

.090/100

.085/100

.090/100

.090/100

.179

.179

.181

.182

.183

.080/095

.085/095

.090/100

.090/100

.184

.183

.186

.187

.085/095

.189

.095/100

.075/085

.085/095

.090/100

.090/100

.085/100

.183

.184

.185

.188

.187

.187

.080/090

.085/095

.090/100

.090/100

.180

.179

.182

.183

.175

.176

.085/090

.070/080

.075/080

.085/095

.085/090

.085/095

.085/095

.172

.172

.174

.175

.176

.175

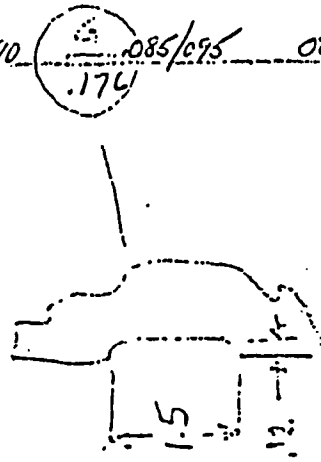
.080/095

.176

.176

Records of
Records

77 0765
77 0765
77 0765



1352-B

THICKNESS MEASUREMENTS FOR

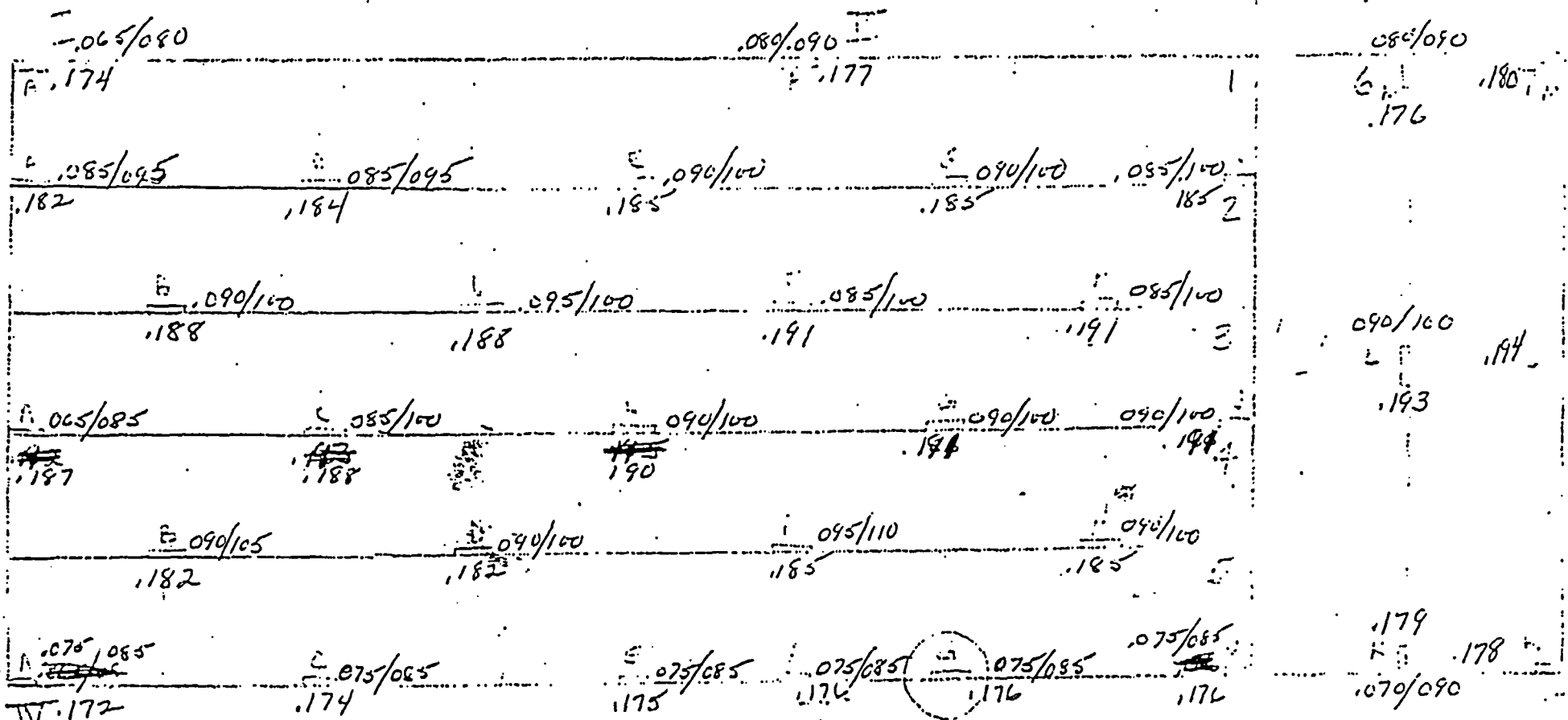
II-11

BORAL SHEET NO. 1402-B

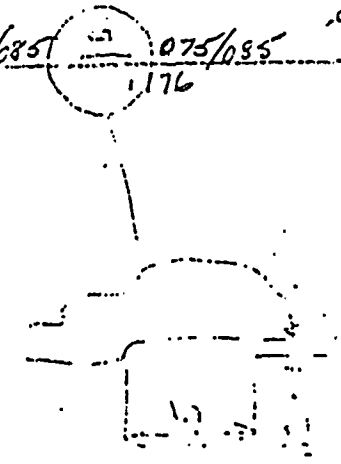
LOCATION	CORE THICKNESS			PANEL THICKNESS	
	MIN.	MAX.	AVG.		
I	.065	.080	.0725	.174	
# II	.080	.090	.085	.177	
6 M	.080	.090	.085	.176	
III	.090	.100	.095	.180	
1 A	.085	.095	.090	.182	
1 C	.085	.095	.090	.184	
1 E	.090	.100	.095	.185	
1 G	.090	.100	.095	.185	
1 J	.085	.100	.0925	.185	
2 B	.090	.100	.095	.188	
2 D	.095	.100	.0975	.188	
2 F	.085	.100	.0925	.191	
2 H	.085	.100	.0925	.191	
6 L	.090	.100	.095	.193	
7 L	.090	.100	.095	.194	
3 A	.065	.085	.075	.187	
3 C	.085	.100	.0925	.188	
3 E	.090	.100	.095	.190	
3 G	.090	.100	.095	.191	
3 J	.090	.100	.095	.191	
4 B	.090	.105	.0975	.182	
4 D	.090	.100	.095	.182	
4 F	.095	.110	.1025	.185	
4 H	.090	.100	.095	.185	
IV	.075	.085	.080	.172	
5 C	.075	.085	.080	.174	
5 E	.075	.085	.080	.175	
V	.075	.085	.080	.176	
5 G	.075	.085	.080	.176	
5 J	.075	.085	.080	.176	
6 K	.070	.090	.080	.179	
VI	.075	.090	.0825	.178	
		MEAN	.0891	.0948	.0826
		STD. DEVIATION	.0077	.0027	.0064
			COMBINED	CENTRAL	PERIPHERY

IDENTIFICATION PL II
MAP & PART
BLOCKS

76



1402-B



THICKNESS MEASUREMENTS FOR

4-11

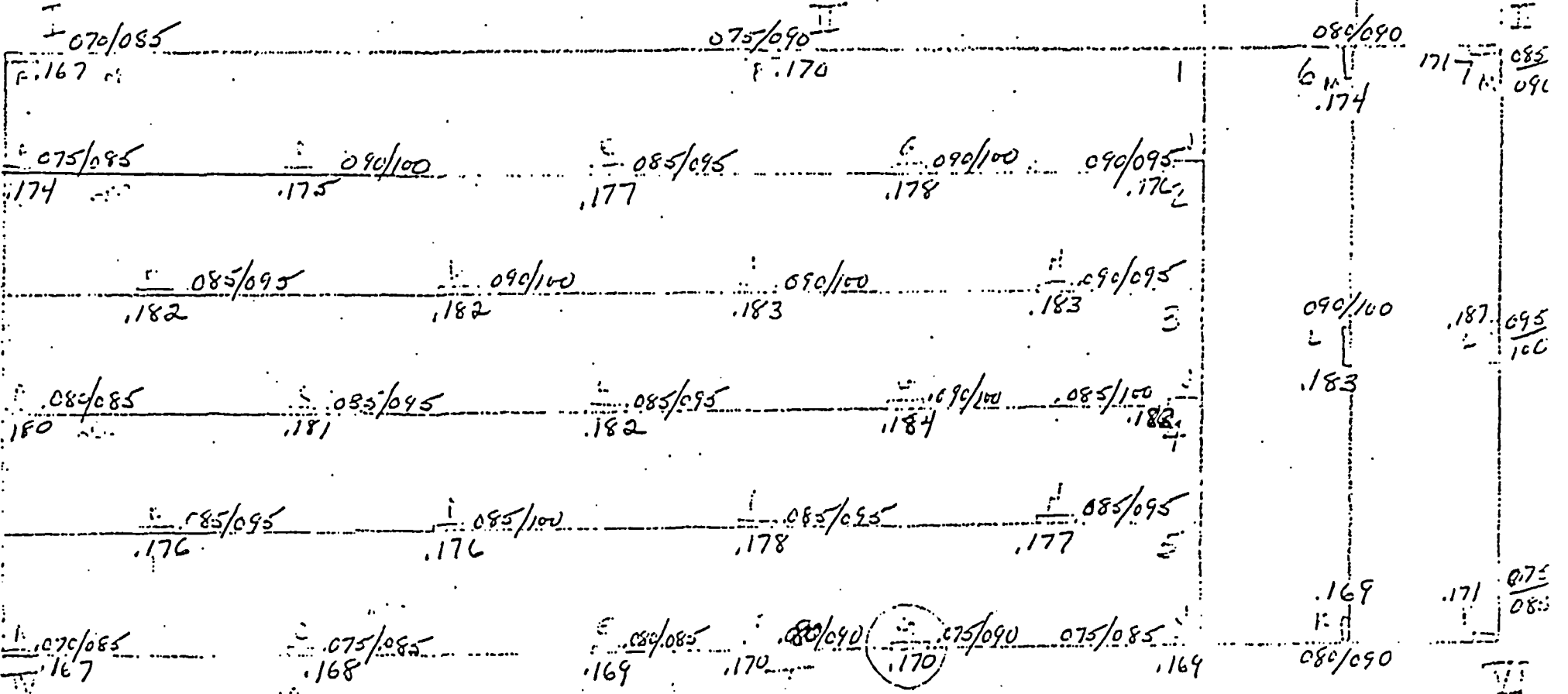
BORAL SHEET NO. 1406-B

LOCATION	CORE THICKNESS			PANEL THICKNESS	
	MIN.	MAX.	AVG.		
I	.070	.085	.0775	.167	
II	.075	.090	.0825	.170	
6M	.080	.090	.0850	.174	
III	.085	.090	.0875	.171	
IA	.075	.085	.0800	.174	
IC	.090	.100	.095	.175	
IE	.085	.095	.090	.177	
IG	.090	.100	.095	.178	
IJ	.090	.095	.0925	.176	
2B	.085	.095	.090	.182	
2D	.090	.100	.095	.182	
2F	.090	.100	.095	.183	
2H	.090	.095	.0925	.183	
6L	.090	.100	.095	.183	
7L	.095	.100	.0975	.187	
3A	.080	.085	.0825	.180	
3C	.085	.095	.090	.181	
3E	.085	.095	.090	.182	
3G	.090	.100	.095	.184	
3J	.085	.100	.0925	.183	
4B	.085	.095	.090	.176	
4D	.085	.100	.0925	.176	
4F	.085	.095	.090	.178	
4H	.085	.095	.090	.177	
IV	.070	.085	.0775	.167	
5C	.075	.085	.080	.168	
5E	.080	.085	.0825	.169	
V	.080	.090	.085	.170	
5G	.075	.090	.0825	.170	
5J	.075	.085	.080	.169	
6K	.080	.090	.085	.169	
VI	.075	.085	.080	.171	
		MEAN	.0879	.0923	.0830
		STD. DEVIATION	.0060	.0022	.0049
			COMBINED	CENTRAL	PERIPHERY

TH
A

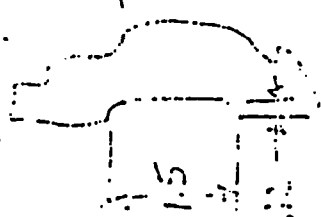
76

12



1406-B

74
→



THICKNESS MEASUREMENTS FOR

4-10

BORAL SHEET NO. 1434-A

LOCATION	CORE THICKNESS			PANEL THICKNESS	
	MIN.	MAX.	AVG.		
I	.075	.085	.080	.173	
II	.080	.100	.090	.176	
6M	.075	.095	.085	.173	
III	.075	.085	.080	.174	
IA	.085	.100	.0925	.181	
IC	.090	.100	.095	.179	
IE	.090	.100	.095	.180	
IG	.090	.100	.095	.183	
IJ	.085	.100	.0925	.180	
2B	.085	.100	.0925	.184	
2D	.090	.100	.095	.183	
2F	.090	.100	.095	.187	
2H	.090	.100	.095	.185	
6L	.095	.100	.0975	.184	
7L	.090	.100	.095	.185	
3A	.085	.095	.090	.183	
3C	.090	.100	.095	.182	
3E	.085	.100	.0925	.183	
3G	.085	.100	.0925	.185	
3J	.085	.095	.090	.183	
4B	.085	.095	.090	.177	
4D	.090	.100	.095	.176	
4F	.090	.100	.095	.180	
4H	.085	.095	.090	.179	
IV	.075	.085	.080	.169	
5C	.075	.085	.080	.169	
5E	.075	.090	.0825	.170	
V	.080	.090	.085	.171	
5G	.080	.095	.0875	.171	
5J	.080	.095	.0875	.169	
6K	.075	.085	.080	.174	
VI	.080	.090	.085	.170	
MEAN			.0897	.0937	.0853
STD. DEVIATION			.0056	.0022	.0040
			COMBINED	PERIPHERY CENTRAL	PERIPHERY

IDENTIFICATION

PART

DATE

BRAND

96

12

12

.075/.085

.080/.100 II

.173

.177C

.173
075
095

1747

.085/.100

.090/.100

.090/.100

.090/.100

.085/.100

.181

.179

.180

.183

.1802

.085/.100

.090/.100

.090/.100

.090/.100

.184

.183

.187

.185

3

.185
095
100

1852

.085/.095

.090/.100

.085/.100

.085/.100

.085/.095

.183

.182

.183

.185

.183

4

.085/.095

.090/.100

.090/.100

.085/.095

.177

.176

.180

.179

5

.075
085

.075/.085

.070/.085

.075/.090

.080/.090

.080/.095

.080/.095

.169

.169

.170

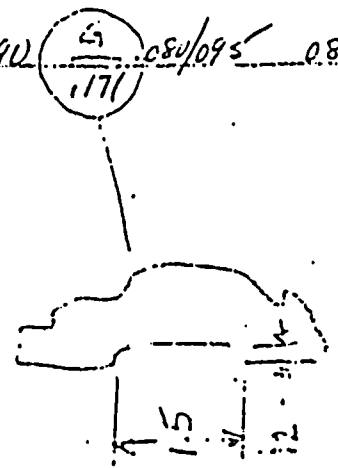
.171

.171

.169

.174K

.170



1434-A

14 CT/CS
TYP.

THICKNESS MEASUREMENTS FOR

II-17

BORAL SHEET NO. 1462-B

LOCATION	CORE THICKNESS			PANEL THICKNESS	
	MIN.	MAX.	AVG.		
I	.075	.085	.080	.168	
II	.075	.085	.080	.167	
6M	.075	.085	.080	.165	
III	.060	.080	.070	.165	
IA	.090	.100	.095	.176	
IC	.090	.100	.095	.176	
IE	.085	.090	.0875	.175	
IG	.085	.095	.090	.174	
IJ	.085	.100	.0925	.175	
2B	.090	.100	.095	.181	
2D	.090	.100	.095	.182	
2F	.085	.100	.0925	.180	
2H	.080	.100	.090	.180	
6L	.090	.100	.095	.182	
7L	.075	.090	.0825	.180	
3A	.090	.100	.095	.183	
3C	.090	.100	.095	.183	
3E	.085	.100	.0925	.183	
3G	.090	.100	.095	.182	
3J	.085	.100	.0925	.182	
4B	.085	.100	.0925	.180	
4D	.085	.100	.0925	.180	
4F	.090	.100	.095	.179	
4H	.090	.100	.095	.179	
IV	.085	.100	.0925	.171	
5C	.085	.095	.090	.172	
5E	.080	.090	.085	.171	
V	.080	.100	.090	.171	
5G	.085	.095	.090	.171	
5J	.080	.095	.0875	.171	
6K	.080	.095	.0875	.170	
VI	.070	.085	.0775	.170	
MEAN			.0895	.0930	.0855
STD. DEVIATION			.0063	.0022	.0070
			COMBINED	CENTRAL	PERIPHERY

IDENTIFICATION

916

.075/085
P. 168

.075/085
.167

.075/085
.165 .165

.090/100
.176

.090/100
.176

.085/090
.175

.085/095
.174

.085/100
.175

.090/100
.181

.090/100
.182

.085/100
.180

.080/100
.180

.090/100
.182 .180

.090/100
.183

.090/100
.183

.085/100
.183

.090/100
.182

.085/100
.182

.085/100
.180

.085/100
.180

.090/100
.179

.090/100
.179

.085/100
.171

.085/095
.172

.080/090
.171

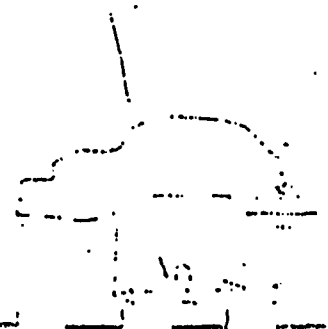
.080/100
.171

.055/095
.171

.080/095
.171

.170 .170
.080/095

1462-B

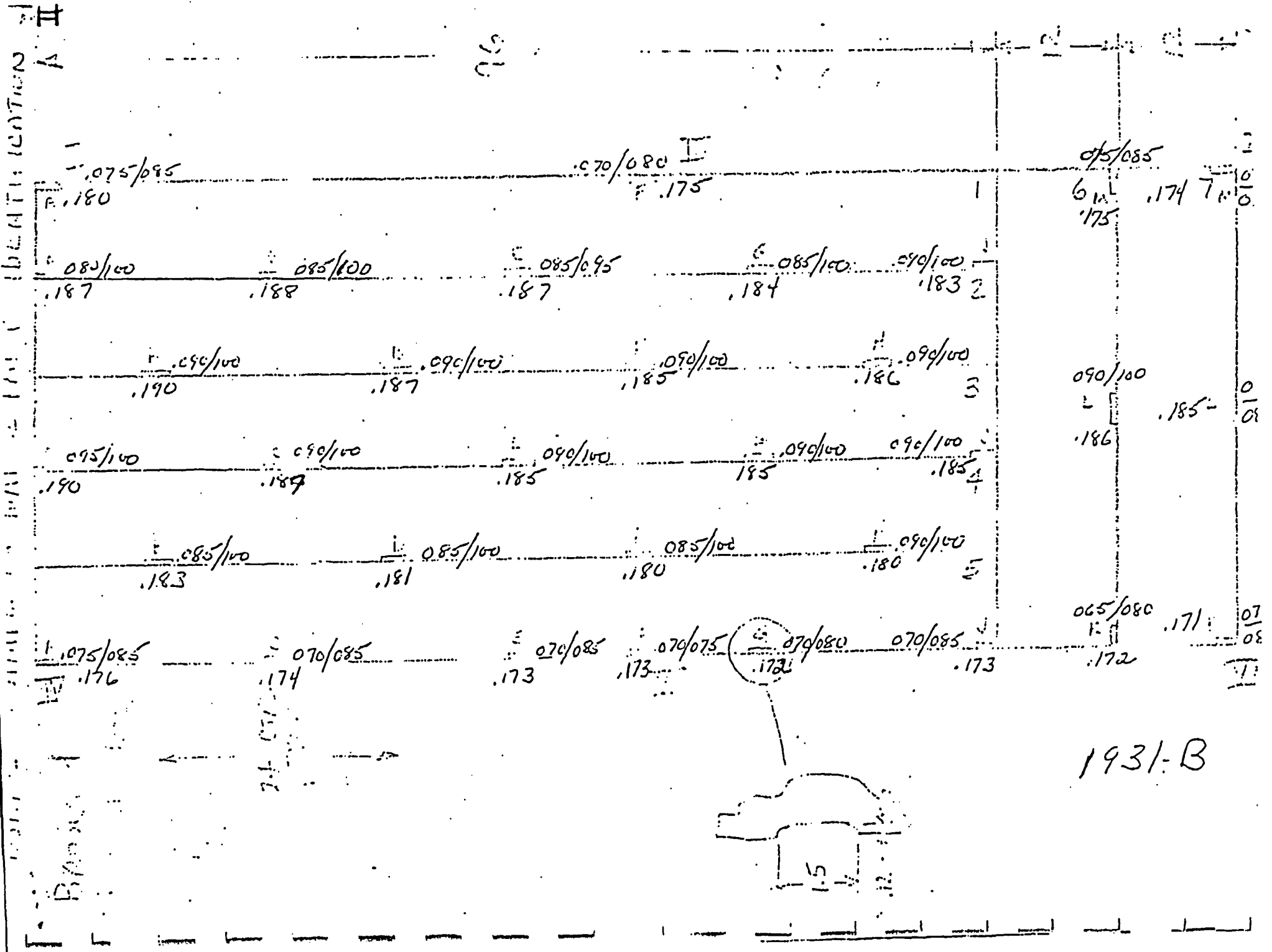


THICKNESS MEASUREMENTS FOR

II-14

BORAL SHEET NO. 1931-B

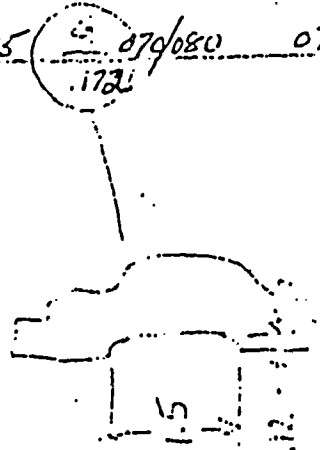
LOCATION	CORE THICKNESS			PANEL THICKNESS	
	MIN.	MAX.	AVG.		
I	.075	.085	.080	.180	
II	.070	.080	.075	.175	
6M	.075	.085	.080	.175	.201 gms/cm ²
III	.075	.080	.0775	.174	
IA	.080	.100	.090	.187	
IC	.085	.100	.0925	.188	
IE	.085	.095	.090	.187	
IG	.085	.100	.0925	.184	
IJ	.090	.100	.095	.183	
2B	.090	.100	.095	.190	
2D	.090	.100	.095	.187	
2F	.090	.100	.095	.185	
2H	.090	.100	.095	.186	
6L	.090	.100	.095	.186	.230 gms/cm ²
7L	.080	.085	.0825	.185	
3A	.095	.100	.0975	.190	
3C	.090	.100	.095	.187	
3E	.090	.100	.095	.185	
3G	.090	.100	.095	.185	
3J	.090	.100	.095	.185	
4B	.085	.100	.0925	.183	
4D	.085	.100	.0925	.181	
4F	.085	.100	.0925	.180	
4H	.090	.100	.095	.180	
IV	.075	.085	.080	.176	
5C	.070	.085	.0775	.174	
5E	.070	.085	.0775	.173	
V	.070	.075	.0725	.173	
5G	.070	.080	.075	.172	
5J	.070	.085	.0775	.173	
6K	.065	.080	.0725	.172	.177 gms/cm ²
VI	.075	.085	.080	.171	
		MEAN	.0872	.0939	.0796
		STD. DEVIATION	.0085	.0015	.0065
			COMBINED	CENTRAL	PERIPHERY



SECTION

976

1931-B



075/085
.180

070/080
.175

075/085
.175
.174
.170

080/100
.187

085/100
.188

085/095
.187

085/100
.184

090/100
.183

090/100
.190

090/100
.187

090/100
.185

090/100
.186

090/100
.185
.186
.185
.180

095/100
.190

090/100
.189

090/100
.185

090/100
.185

090/100
.185

085/100
.183

085/100
.181

085/100
.180

090/100
.180

075/085
.176

070/085
.174

070/085
.173

070/075
.173

070/080
.172

070/085
.173

065/080
.172
.171
.170

APPENDIX C

EXPERIMENTAL DATA

PANEL LOT III

PAGES III-1 THRU III-2

July 1, 1976^{III}
 GAGNON
 ROSLER
 MOLLON
 (PAR)

ET No.		I	II	III	IV	V	VI
2007-A	t _c	.085	.090	.090	.085	.085	.085
	t _s	.168	.169	.172	.165	.168	.170
2019-A	t _c	.085	.085	.085	.090	.085	.085
	t _s	.175	.170	.170	.172	.167	.172
2019-B	t _c	.085	.085	.085	.085	.085	.085
	t _s	.172	.166	.165	.171	.167	.177
2025-B	t _c	.085	.085	.085	.085	.075	.085
	t _s	.176	.168	.168	.166	.168	.174
2005-A	t _c	.085	.085	.085	.085	.090	.085
	t _s	.171	.167	.167	.174	.180	.167
15-B	t _c	.085	.085	.085	.085	.095	.085
	t _s	.177	.175	.181	.174	.173	.175
2013-A	t _c	.085	.085	.085	.085	.085	.085
	t _s	.172	.171	.173	.168	.170	.171
2035-A	t _c	.085	.085	.085	.085	.090	.085
	t _s	.175	.176	.175	.169	.173	.173
2035-B	t _c	.085	.085	.085	.085	.085	.085
	t _s	.174	.173	.176	.169	.170	.171
CAP. PARTIC. PAR V.T.							
2003-A	t _c	.095	.085	.090	.095	.095	.095
	t _s	.170	.168	.172	.166	.173	.170
2005-B	t _c	.085	.085	.090	.085	.085	.095
	t _s	.165	.167	.171	.166	.174	.173
17-B	t _c	.085	.100	.085	.090	.085	
	t _s	.167	.168	.169	.167	.168	.170

SHEET No.	I	II	III	IV	V	VI
2004-A	t_c .090 t_s .165	.090 .168	.095 .172	.090 .168	.095 .170	.090 .174
2004-B	t_c .085 t_s .168	.090 .170	.085 .170	.095 .168	.085 .170	.090 .172
2010-A	t_c .090 t_s .174	.095 .177	.095 .180	.095 .170	.095 .173	.095 .180
2033-B	t_c .085 t_s .166	.090 .168	.085 .173	.085 .170	.080 .166	.085 .165
2033-A	t_c .090 t_s .167	.090 .170	.090 .174	.080 .170	.090 .168	.090 .166
2006-B	t_c .095 t_s .168	.095 .171	.090 .175	.095 .170	.090 .173	.095 .176
2006-A	t_c .095 t_s .169	.095 .172	.095 .177	.100 .172	.090 .172	.095 .178
2028-B	t_c .095 t_s .168	.095 .168	.095 .171	.090 .168	.085 .169	.085 .172

t_s = total thickness of BORAL sheet - all measurements provided verbally by CAD (taken by micrometer)

t_c = thickness of BORAL core - first nine sheets measurements provided verbally by CAD. (taken by optical comparator) - last eleven sheets measured by Krautkramer-Branson USM 2MT Ultrasonic Flaw Detector with Z-103 DUFP transducer (5.0 MHz - 1/4" DIA.)

APPENDIX D

EXPERIMENTAL DATA

PANEL LOT IV

PAGES IV-1 THRU IV-6

T
1552-A

C

1555-A

.174		0	.190	
1 .175	.085	1	.190	.100
2 .176	.085	2	.170	.100
3 .177	.080	3	.190	
4 .178		4	.190	
5 .179		12	.189	
10 .184		13	.190	
11 .185		14	.190	
12 .184		15	.188	.070
13 .185	.085	16	.188	.070
14 .186	.085	17	.187	
15 .186		18	.187	
.187		27	.177	
17 .187		28	.177	
26 .189		29	.175	
27 .189		30	.175	
28 .189		31	.173	.080
29 .189	.095			.080
30 .189	.085			
31 .189	.085			

M	.0843		.0900	M
SD	.0019		.0089	SD

Σ 2.2946

AVERAGE OF 27	
.0846	MEAN
.0045	STD. DE

.122

1558-A		
T	C	
.171		
.171	.060	
.171	.065	
.171		
.172		
.179		
.180		
.180		
.181	.075	
.181	.075	
.181		
.181		
.183		
.183		
.183		
.183	.075	
.183	.075	
.183		
.183		
.183		
.183		
.183		
.183		

1558-B		
IN"	T	C
0	.170	
1	.169	.075
2	.170	.075
3	.170	
4	.171	
5	.172	
16	.178	
17	.178	
18	.178	
19	.178	.085
20	.179	.085
21	.179	
22	.179	
27	.179	
28	.179	
29	.179	
30	.179	
31	.179	.085
32	.179	.085

1559-B		
IN"	T	C
1	.172	.080
2	.172	.075
3	.173	
4	.177	
5	.174	
16	.184	
17	.184	
18	.184	.085
19	.184	.085
20	.184	
21	.184	
29	.184	
29	.184	
30	.182	
31	.182	.085
32	.182	.080
33	.184	

15698		
IN"	T	C
0	.170	
1	.172	
2	.173	
7	.174	.075
4	.174	.080
5	.174	
6	.175	
12	.177	
13	.178	
14	.177	.075
15	.177	.075
16	.178	
17	.178	
28	.178	
29	.178	
30	.179	
30	.177	.080
31	.177	.080
32	.177	
33	.176	

.83 M
 .191 SD
.0708
.0066

.0817	.0817	.0775 M
.0052	.0041	.0027 SD

1581-A		
T	C	
.172		
.173		
.173	.070	
.174	.075	
.175		
.176		
.177		
.184		
.184		
.184		
.184	.085	
.184	.090	
.184		
.185		
.185		
.183		
.184		
.184		
.184	.085	
.183	.090	
.182		

1575-B		
No.	T	C
0	.170	
1	.172	.085
2	.175	.085
3	.179	
9	.175	
5	.176	
6	.177	
14	.183	
15	.183	
16	.183	
17	.183	.080
18	.183	.075
19	.183	
20	.183	
21	.183	
22	.184	
27	.182	
28	.181	
29	.182	.100
30	.182	.090
31	.182	.085
32	.180	.0

1556-B		
No.	T	C
0	.173	
1	.173	
2	.179	.085
3	.179	.085
4	.175	
5	.177	
6	.178	
9	.180	
10	.181	
11	.182	
12	.183	.085
13	.189	.090
14	.189	
15	.185	
16	.185	
17	.185	
25	.186	
26	.185	
27	.185	.090
28	.189	.090
29	.189	.090
30	.184	.090
31	.186	
32	.183	

1589-A		
No.	T	C
0	.172	
1	.171	
2	.172	.085
3	.172	.085
4	.173	
5	.174	
6	.175	
16	.183	
17	.184	
18	.185	
19	.185	.085
20	.189	.090
21	.184	
22	.189	
23	.184	
28	.184	
29	.183	
30	.183	
31	.182	.085
32	.183	.085
33	.183	

.0825	.0857	.0875	.0858	M
-------	-------	-------	-------	---

IN" T	C	IN" T	C	IN" T	C	IN" T	C	
.171		0 .172		0 .171		0 .170		
.171		1 .173		1 .172	.085	1 .171		
.172	.085	2 .173	.090	2 .172	.095	2 .171	.055	
.172	.090	3 .174	.085	3 .173		3 .172	.090	
.173		4 .175		4 .174		4 .173		
.174		5 .177		5 .175		5 .174		
.175		6 .177		13 .182		6 .175		
.183		11 .182		14 .183		16 .184		
.184		12 .183		15 .183		17 .184		
.184		13 .183		16 .184	.090	18 .184		
.184		14 .183		17 .184	.090	19 .184		
.184		15 .183		18 .185		20 .185	.085	
.184	.085	16 .184	.085	19 .185		21 .185	.090	
.184	.085	17 .184	.080	20 .184		22 .185	.100	
.184		18 .185		21 .185		23 .184	.085	
.184		19 .185		26 .184		24 .184		
.184		28 .184		27 .184		28 .183		
.183		29 .184		28 .184		29 .183		
.183		30 .184		29 .183	.100	30 .183	.085	
.182	.085	31 .181	.090	30 .183	.095	31 .183		
.182	.085	32 .181	.085	31 .184		32 .182		
.182						33 .183		
M	.0858		.0842		.0925		.0886	M
SD	.0020		.0038		.0052		.0056	SD

1566-B	C	1569-A	C	1571-B	C	1590-B	C
.165	.080	0 .165	.085	0 .172		0 .171	
.165	.095	1 .167	.085	1 .172	.085	1 .172	.080
.166		2 .171		2 .173	.085	2 .172	.085
.167		3 .171		3 .174		3 .173	.085
.168		4 .172		4 .175		4 .174	
.169		5 .173		5 .176		5 .175	
.174		6 .174		6 .177		6 .176	
.175		13 .179		13 .183			
.175		14 .180		14 .184			
.176		15 .180		15 .183		12 .182	
.176		16 .181		16 .185		13 .181	
.177	.085	17 .181	.085	17 .184	.085	14 .182	
.177	.090	18 .181	.085	18 .184	.090	15 .182	
.177	.100	19 .182		19 .184		16 .182	.085
.177		20 .182		20 .184		17 .183	.090
.177		21 .183		21 .184		18 .183	.085
.177		22 .183		25 .184		19 .183	
.180		26 .183		26 .183		20 .183	
.178		27 .187		27 .183		26 .182	
.178		28 .183		28 .183	.085	27 .182	
.178	.085	29 .183	.085	29 .183	.085	28 .181	
.177	.090	30 .182	.095	30 .183		29 .181	.090
.177		31 .182		31 .183		30 .181	.090
.177						31 .181	.085
.177						32 .181	
M	.0879		.0867		.0858		.0883
SD	.0064		.0041		.0020		.0050

1552-B

1535-A

1594-B

1 .193
 1 .183
 2 .185
 1 .186
 1 .197
 1 .193
 2 .193
 13 .193
 7 .194
 5 .196
 16 .196
 7 .195
 5 .195
 26 .192
 27 .192
 28 .191
 29 .192
 30 .192

.080
.100

.100
.100

.100
.100

0 .168
 1 .168
 2 .171
 3 .171
 4 .170
 16 .140
 17 .180
 18 .181
 19 .181
 20 .181
 21 .181
 22 .181
 28 .180
 29 .180
 30 .180
 31 .178
 32 .178
 33 .178

.065
.080
.075

.090
.090

.080
.085

1 .177
 1 .177
 2 .177
 3 .178
 4 .179
 5 .180
 9 .183
 10 .183
 11 .185
 12 .184
 13 .184
 14 .184
 15 .184
 24 .183
 25 ~~.183~~
 26 .183
 27 .181
 28 .182
 29 .181
 30 .182

~~.085~~
.085

.085
.085

M
SD

.0983
.0041

.0807
.0087

.0850
0

M
S.D.

1535-B

1531-A

1555-B

	T	C	T	C	T	C	M	SD
1	.173		0 .172		0 .171			
2	.171		1 .172	.085	1 .173	.075		
3	.174	.085	2 .175	.085	2 .174	.075		
4	.172		3 .174		3 .174			
5	.172		4 .176		4 .174			
6	.173		5 .177		5 .175			
7	.174		6 .178		6 .176			
8	.179		16 .184		15 .185			
9	.181		17 .184		16 .186			
10			18 .184		17 .185			
11			19 .184		19 .186			
12	.180		20 .184	.090	19 .185			
13	.181		21 .185	.085	20 .186	.080		
14	.181		22 .185		21 .186	.080		
15		.085	23 .185		22 .187			
16	.183	.085	28 .184		23 .186			
17	.183		29 .193		27 .187			
18	.183		30 .182		28 .186			
19			31 .182	.085	27 .186			
20			32 .192	.085	30 .185			
21			33 .182		31 .185	.085		
22		.085			32 .185	.085		
23		.085			33 .183			
24	.183							
25	.184							
26	.182							
27	.182							
28	.182							
29	.182							
30	.182							
31	.182							
32	.182							
33	.182							
M	.0850			.0858		.0800	M	
SD	0			.0020		.0045	SD	

1594-A		1545-B		1500-A	
T	C	T	C	T	C
0 .173		0 .189		0 .172	
1 .172		1 .170		1 .173	.075
2 .173		2 .170	.055	2 .172	.080
3 .173	.085	3 .171	.060	3 .173	
4 .173	.095	4 .171		4 .174	
5 .174		5 .173		5 .177	
11 .180		16 .180		14 .182	
12 .181		17 .180		15 .184	
13 .182		18 .181		16 .188	
14 .183	.055	19 .186	.085	17 .187	.080
15 .185	.085	20 .188	.085	18 .191	.085
16 .189		21 .190		19 .190	
17 .183		22 .197		20 .188	
28 .183		23 .186		21 .184	
29 .182		28 .180		28 .190	
30 .182	0.085	29 .180		29 .189	
31 .182	0.085	30 .179		30 .189	
32 .183		31 .178	.085	31 .187	.085
		32 .178	.085	32 .182	
		33 .180		33 .182	
M	.0850		.0758		.0817
SD	0		.0143		.0041

APPENDIX E

EXPERIMENTAL DATA

PANEL LOT VI

PAGES VI-1 THRU VI-20

IN"	T		IN"	T		IN"	T		IN"	T	
	T	C		T	C		T	C		T	C
0	.168	.075	0	.173	0	0	.170		0	.170	
1	.169	.075	1	.173	.075	1	.170	.085	1	.170	.085
2	.170	.085	2	.173	.075	2	.171	.090	2	.171	.090
3	.170	.095	3	.174	.085	3	.174	.100	3	.174	.100
4			4	.175		4			4		
5			5			5			5		
10			10	.181		10			10		
11	.175		11	.182	.090	11	.183	.100	11	.183	.100
12	.176	.090	12	.182	.090	12	.184	.100	12	.184	.100
13	.176	.090	13	.183		13	.184	.095	13	.184	.095
14	.177	.085	14			14			14	.180	.090
15			15			15			15	.180	.095
22			22	.185		22			22		
23	.179	.085	23	.185	.095	23	.187	.095	23	.181	
24	.178	.085	24	.186	.085	24	.185	.105	24	.182	.100
25	.179	.095	25	.185		25	.187	.100	25	.182	.100
26	.179		26			26			26	.183	
27			27			27			27		
MEAN	.0833		MEAN	.0862		MEAN	.0941		MEAN	.0893	
STD Dev	.0086		STD Dev	.0065		STD Dev	.0096		STD Dev	.0102	
34			34	.182	.090	34			34		
35	.175	.085	35	.182	.085	35	.184	.100	35	.177	
36	.174	.090	36	.181	.095	36	.183	.115	36	.176	.095
37	.174	.085	37			37	.182	.095	37	.175	.095
38			38			38			38	.175	.090
44			44	.172		44	.175	.085	44	.169	
45	.168	.075	45	.172	.090	45	.175	.090	45	.167	.015
46	.161	.075	46	.171	.085	46	.174	.090	46	.167	.080
47	.167	.065	47	.170	.080	47	.174	.075	47	.166	.065
48	.166		48			48			48	.166	
49	.166		49			49			49	.166	

1086-15

1025-15

1025-17

1010-A

V-
ck
Corr

T	C
170	.090
171	.095
172	.090
173	.095
181	.095
181	.095
183	.085
188	.100
189	.100
189	.105
190	.105
187	.100
180	
179	.095
178	.090
176	.085

MAN
S.D.

.0944
.0066

IN"	T	C
1	170	.075
2	171	.075
3	172	.075
4	173	
10	178	.085
11	179	.085
12	180	.095
13	181	
22	184	
23	184	.095
24	185	.095
25	185	
34	184	.095
35	183	.095
36	183	
37	184	
38	182	
39	181	.095
40	180	.085
41	180	.090

.0871
.0084

IN"	T	C
1	185	.095
2	186	.100
3	186	.090
4	187	
11	190	
12	191	.100
13	192	.095
14	192	
23	190	
24	191	.085
25	190	.100
34	182	
35	181	.090
36	182	.085
37	181	.055
38	181	.090
39	178	.090
40	178	.085

.0921
.0061

IN"	T	C
0	165	.060
1	165	.075
2	167	.085
3	168	.085
4	170	
14	176	
15	176	.100
16	176	.085
17	177	
26	179	
27	179	.100
28	178	.085
29	178	
36	176	
37	176	.100
38	176	.090
39	175	.090

.0868
.0119

1175 - 17			1182 - 17			1192 - N			1191 - 17		
T	C	IN"	T	C	IN"	T	C	IN"	T	C	
171	085	0	.168	.085	0	.174	085	0	.185	080	
171	085	1	.169	.075	1	.175	085	1	.178	075	
171	095	2	.170	.075	2	.176	085	2	.176	080	
172	095	3	.171	.075	3	.176	085	3	.177	085	
173		4	.172		4	.177		4	.177		
180					11	.183	090	11	.183	.090	
180	.100	13	.178	.085	12	.184	095	12	.184	.100	
181	.095	14	.179	.085	13	.185	095	13	.185	.160	
181		15	.179	.085							
M	.0910			.0833			.0890			.0885	
SD	.0063			.0056			.0069			.0084	
184	.095	24	.180		23	.189	080	23	.187	.100	
184	.095	25	.180	.090	24	.190	095	24	.188	.085	
184	.100	26	.179	.090	25	.189		25	.187	095	
		27									
183					34	.187	095	34	.183		
182	090	36	.174	090	35	.186	095	35	.182	095	
180	095	37	.174	085	36	.186	100	36	.181	095	
		38	.174	085				37	.181	095	
174					43	.179	085				
173	085	45	.167		44	.178	085	44	.174		
172	.085	46	.167	095	45	.176	090	45	.173	085	
171	085	47	.166	085	46	.176	085	46	.172	085	
171	080	48	.166	085	47	.175	075	47	.171	085	
		49	.166		48			48	.170	075	

II
at
Cor'

1229-A

1243-A

1281-A

1281-A

V.
ck
Core
Thk

IN	T	C	IN	T	C	IN	T	C	IN	T	C
0	.179	.095	0	.175	.085	0	.182	.090	0	.182	.095
1	.176	.095	1	.175	.085	1	.182	.095	1	.181	.095
2	.176	.095	2	.179	.085	2	.181	.085	2	.181	.100
3	.176	.090	3	.179	.090	3	.181	.100	3	.181	.105
4	.175		4	.173		4	.181		4	.181	
11	.176	.090	11	.172		11	.180		11	.180	
12	.176	.090	12	.172	.085	12	.179	.090	12	.180	.190
13	.176	.090	13	.171	.080	13	.179	.090	13	.179	.100
14	.176		14	.171		14	.180		14	.179	
22	.177		22	.172		23	.180		23	.180	
23	.176	.085	23	.172		24	.180	.090	24	.180	.090
24	.175	.090	24	.172	.090	25	.180	.085	25	.180	.085
25	.175		25	.172	.085	26	.180		26	.180	
26			26	.173		26	.181				
32	.175					32	.182		32	.182	
33	.175	.090	33	.173		33	.182	.090	33	.182	.090
34	.175	.085	34	.174	.080	34	.182		34	.183	.085
35	.175	.085	35	.179	.085	35	.183		35	.183	.090
36	.175	.085	36	.175	.085	36	.183		36	.183	.090

.0896
.0038

.0850
.0032

.0906
.0046

1201-0 ✓

IN"	T	C
181	.090	
181	.095	
181	.085	
181	.090	
181		
180		
12	180	.090
11	180	.100
19	179	
23	179	
21	178	.100
27	178	.100
26	178	
33	179	
30	180	.100
31	180	.100
35	180	.085
34	181	.090

.0938
.0061

1200-17 ✓

IN"	T	C
0	186	.095
1	186	.100
2	186	.100
3	186	.090
9	186	
11	189	
12	189	.085
13	189	.100
19	189	
25	183	
29	182	.085
25	182	.085
26	182	
32	182	
33	182	
34	182	.080
35	182	.085
36	183	.085

.0900
.0074

1201-17 ✓

IN"	T	C
0	179	.090
1	179	.095
2	179	.095
3	179	.095
4	179	
11	179	
12	180	.085
13	180	.090
19	180	
22	180	
23	180	
29	180	.090
25	180	.085
26	180	
32	181	
33	182	.100
34	182	.100
35	182	.090
36	183	

.0923
.0052

IN"	T	C
-----	---	---

✓
ok
Cor
1.

1091-B

1072-B

1093-B

VI

at

col

IN"	T	C
	170	.080
	169	.090
	170	.090
	171	
	.178	.090
	.179	
	.182	.090
		.0871
		.0033
	184	
	184	.090
	185	.085
	184	
	.183	.085
	.182	.085
	.184	
	.178	
	.176	.090
	.176	.085
	.175	.085

IN"	T	C
1	177	.085
2	173	.085
3	172	.090
4	174	
	179	
12	180	.090
13	181	.100
		.0877
		.0075
23	184	
24	185	.095
25	184	.095
	181	.085
35	181	.095
36	180	.095
37	179	
	172	
45	172	.085
46	171	.085
47	171	.075
48	170	.075

IN"	T	C
1	166	.060
2	168	.075
3	169	.080
4	169	
	174	
12	175	.085
13	176	.085
		.0815
		.0072
23	181	
24	180	.085
25	181	.085
	179	
35	178	.085
36	178	.085
37	178	
	172	
45	171	.085
46	170	.085
47	170	.085

IN"	T	C
-----	---	---

1251-B ✓

IN	T	C
1	.178	.090
2	.177	.100
3	.179	.100
4	.179	
5	.180	
6	.181	
7		
8	.183	
9	.184	.090
10	.184	.100
11	.184	
12	.185	
13		
14		
15		
16		
17		
18		
19		
20		
21	.189	
22	.187	.090
23	.187	.100
24	.187	
25	.187	
26		
27		
28		
29		
30		
31	.184	
32	.183	.100
33	.182	.090
34	.182	
35	.182	
36		
37		
38		
39		
40	.176	
41	.175	.095
42	.176	.095
43	.177	.090
44		
45		
46		
47		

.0950
.0048

✓

IN	T	C
1	.180	.085
2	.178	.100
3	.178	.100
4	.180	.100
5	.180	
6		
7		
8		
9		
10	.186	.100
11	.186	.102
12	.187	
13	.187	
14		
15		
16		
17		
18		
19		
20		
21	.189	
22	.191	.100
23	.190	.100
24	.190	
25	.189	
26		
27		
28		
29		
30		
31		
32		
33	.189	
34	.186	.100
35	.185	.100
36	.184	.100
37	.183	
38		
39		
40		
41		
42		
43	.176	
44	.175	.095
45	.175	.085
46	.173	.085
47	.172	.085

.0958
.0069

1251-17 ✓

IN	T	C
1	.167	.085
2	.167	.090
3	.170	.090
4	.171	
5		
6		
7		
8		
9		
10	.178	
11	.178	.090
12	.180	.095
13	.182	.100
14	.181	
15		
16		
17		
18		
19		
20		
21		
22	.186	
23	.187	.100
24	.186	.090
25	.186	.090
26	.187	
27		
28		
29		
30		
31		
32		
33		
34	.186	
35	.185	.095
36	.184	.095
37	.184	.100
38		
39		
40		
41		
42		
43	.177	
44	.176	.100
45	.175	.095
46	.174	.085
47	.174	.085

.0928
.0055

✓

IN	T	C
1	.180	.090
2	.180	.085
3	.181	.095
4	.182	
5		
6		
7		
8		
9	.187	
10	.187	
11	.188	.100
12	.189	.100
13	.190	
14		
15		
16		
17		
18		
19		
20		
21		
22	.192	.110
23	.191	.105
24	.191	.100
25		
26		
27		
28		
29		
30		
31		
32		
33		
34	.186	
35	.185	.095
36	.185	.100
37	.183	
38		
39		
40		
41		
42		
43	.178	
44	.177	
45	.175	.095
46	.175	.100
47	.176	.085

.0969
.0072

✓

1124 - H			12067 H			1233 - H			* 1228 - B		
T	C	IN"	T	C	IN"	T	C	IN"	T	C	
.170	.065	0	.085	.100	0	.180		0	.182	.095	
.172	.075	1	.084	.095	1	.180	.085	1	.182	.095	
.173	.080	2	.084	.100	2	.180	.090	2	.182	.085	
.174	.085	3	.084	.095	3	.180	.090	3	.182		
.174		4	.084	-	4	.180		4	.182		
		11	.085		11	.180		11	.181	.100	
.182	.090	12	.085	.095	12	.180	.085	12	.182		
.182	.085	13	.084	.095	13	.180	.090	13	.181	.095	
.182	.095	14	.085		14	.181		14	.181		
		23	.085	.100	23	.182		23	.183	.090	
.184	.100	24	.186	.095	24	.182	.095	24	.182	.100	
.183	.085	25	.186	.100	25	.183	.085	25	.182	.085	
.183	.090	26	.187		26	.182		26	.182		
		29	.186								
.179	.090	30	.186	.095	31	.183		31	.182		
.178	.090	31	.186	.090	32	.183	.095	32	.183	.100	
.178	.085	32	.185	.085	33	.183	.100	33	.182	.100	
.176		33	.185	.085	34	.183	.085	34	.182	.095	
					35	.183	.085	35	.182	.095	
.171											
.170	.085										
.170	.085										
.169	.075										
.169	.075										

.0844
.0085

.0946
.0052

.0895
.0052

.0946
.0054

1064-#

1013-#

1055-#

1052-#

ck
co

T	C
.172	.090
.171	.085
.173	.080
.174	
.181	.100
.182	.100
.183	.095
.183	
.186	.090
.186	.100
.186	.100
.184	
.183	.090
.182	.090
.181	.090
.180	.085
.179	.100
.177	.090

.0923
.0065

IN"	T	C
1	.181	.080
2	.183	.095
3	.184	.085
4	.184	
11	.191	.090
12	.191	.090
13	.192	.100
14	.193	
23	.194	.100
24	.194	.105
25	.194	.100
35	.190	
36	.189	.100
37	.188	.100
45	.180	
46	.179	.085
47	.178	.085

.0935
.0080

IN"	T	C
1	.176	
2	.177	.085
3	.177	.095
4	.178	.095
5	.178	
12	.184	
13	.184	.100
14	.185	.100
24	.188	
25	.188	.085
26	.187	.085
		.090
36	.186	.095
37	.183	.095
38	.183	.095
45	.178	
46	.176	.090
47	.175	.090
47	.175	.080

.0910
.0060

IN"	T	C
1	.183	.100
2	.183	.100
3	.185	.100
4	.195	
5		
10	.191	
11	.191	.100
12	.191	.105
22	.192	
23	.192	.105
24	.192	.100
25	.192	
34	.188	
35	.187	.095
36	.186	.100
37	.185	
43	.178	
44	.179	.090
45	.177	.085
46	.176	.085
47	.176	.075

.0954
.0090

1150-11			1151-11			1156-B			1151-10			V		
T	C	IN*	T	C	IN"	T	C	IN"	T	C	IN"	T	C	IN"
.175	.100	0	.171	.085	0	.176	.090	0	.176	.075	0	.176	.075	0
.175	.095	1	.172	.085	1	.176	.085	1	.177	.075	1	.177	.075	1
.176	.095	2	.172	.085	2	.177	.085	2	.177	.085	2	.177	.085	2
.177	.090	3	.173	.095	3	.177	.090	3	.178	.085	3	.178	.085	3
.177		4	.174		4	.178		4	.181		4	.181		4
.184	.095	12	.182	.100	11	.183	.095	11	.187	.085	11	.187	.085	11
.185	.095	13	.183	.100	12	.189	.100	12	.187	.095	12	.187	.095	12
.185	.095	14	.183	.095	13	.185	.100	13	.189	.075	13	.189	.075	13
	.0947			.0925			.0910			.0924			.0924	
	.0048			.0071			.0060			.0092			.0092	
.190		23	.188		22	.187		22	.187		23	.194	.100	23
.189	.095	24	.188	.100	23	.187	.085	23	.187	.085	24	.195	.100	24
.189	.105	25	.188	.095	24	.187	.100	24	.187	.100	25	.195	.105	25
.189		26	.188		25	.187		25	.187					
.186	.100	34	.187		33	.184		33	.184		35	.194	.100	35
.186	.095	35	.186	.100	34	.189	.095	34	.189	.095	36	.193	.100	36
.185	.095	36	.186	.100	35	.183	.095	35	.183	.095	37	.193	.100	37
		37	.186	.100	36	.182		36	.182					
.177		44	.179	.085	43	.176		43	.176		44	.186		44
.177	.090	45	.178	.085	44	.175	.095	44	.175	.095	45	.186	.100	45
.176	.090	46	.177	.085	45	.175	.085	45	.175	.085	46	.189	.090	46
.175	.085	47	.176	.085	46	.174	.095	46	.174	.095	47	.183	.085	47
.175		48	.175		47	.174	.090	47	.174	.090	48	.182	.085	48

11017-A

1157-A

1157-B

1184-B

V

	T	C	IN ^M	T	C	IN ["]	T	C	IN ["]	T	C
	.168	.075	0	174		0	.168	.085	0	.178	
	.169	.085	1	174	.085	1	.168	.090	1	.179	.085
2	.169	.085	2	175	.085	2	.170	.085	2	180	.090
	.170	.085	3	177	.085	3	.171	.085	3	.181	.095
4	.171		4	178	.085	4	.172		4	.182	105
			5	179							
10	.176	.090									
	.177	.090	11	184		11	.178				
12	.177	.100	12	184	.100	12	.178	.100	12	.190	
			13	.185	.105	13	.179	.085	13	.190	.100
3	.178		14	185		14	.179		14	.191	.095
									15	.191	
		.0894			.0886			.0863		.086	.0932
		.0075			.0072			.0079			.0071
2	.181	.100									
23	.181	.100	23	186		23	.180	.100			
4	.182	.090	24	186	.095	24	.179	.090	24	.193	.100
25	.182		25	186	.095	25	.180	.085	25	.193	.100
			26	185		26	.179		26	.193	.100
2	.180	.100	35	180		34	.174				
	.180	.090	36	179	.085	35	.174	.085	36	.189	.085
3	.178	.095	37	179	.085	36	.172	.090	37	.189	.100
						37	.172	.085	38	.187	.095
74	.172		44	171		44	.165		44	.181	.090
75	.171	.085	45	171	.085	45	.166	.085	75	.180	.090
76	.170	.085	46	170	.085	46	.163	.085	76	.180	.090
		.080	47	169	.080	47	.162	.080	47	.178	.085

1233-B

1207-B

1228-B

1555-A

T	C	IN"	T	C	IN"	T	C	IN"	T	C
.178	.090	0	.182	.085	0	.180	.090			
.178	.095	1	.182	.085	1	.180	.090	0		.085
.178	.095	2	.182	.085	2	.180	.090	1		.085
.178	.100	3	.182	.085	3	.180	.085	2		.090
.178		4	.183		4	.180				
		9								
.178		11	.183		11	.179				
.178	.090	12	.183	.090	12	.179	.095			
.179	.095	13	.183	.095	13	.179	.090			
.179		14	.183		14	.179		15	.100	.100
								16	.100	.100
								17		.100
.180		23	.185		23	.178				
.180	.095	24	.185	.100	24	.178	.095			
.180	.100	25	.185	.100	25	.178	.095			
.180		26	.185							
								29		.100
.181		30	.185		30	.179		30		.100
.181	.090	31	.187	.090	31	.178	.085			
.182	.090	32	.186	.090	32	.178	.090			
.182	.085	33	.186	.100	33	.178	.095			
.182	.090	34	.186	.100	34	.178	.090			

.0929
.0045

.0921
.0066

.0908
.0036

.0950
.0071

ok
C.

IN"	T	C	IN"	T	C	IN"	T	C	IN"	T	C
0	.181	.085	0	.183	.090	0	.186	.100	0	.192	
1	.181	.085	1	.183	.090	1	.185	.095	1	.192	.090
2	.181	.085	2	.183	.090	2	.185	.100	2	.192	.100
3	.181	.090	3	.183	.095	3	.185	.095	3	.192	.100
4	.181		4	3	-	4	.185		4	.192	
			10	.184		11	.185		11	.192	
	.182		11	.184	.100	12	.186	.095	12	.192	.100
12	.181	.090	12	.184	.090	13	.184	.095	13	.192	.095
	.181	.095	13	.184	.100	14	.183		14	.192	
14	.181		14	.184							
			22	.183		23	.183		23	.194	
3	.182		23	.183		24	.184	.095	24	.195	.085
24	.181	.095	24	.182	.095	25	.183	.095	25	.195	.100
	.181	.095	25	.183	.095	26	.183		26	.195	
26	.181		26	.182							
			30	.181		30	.184		31	.195	
29	.181		31	.180	.100	31	.184	.095	32	.195	.095
31	.181	.085	32	.180	.100	32	.184	.095	33	.195	.095
2	.181	.090	33	.180	.095	33	.183	.090	34	.195	.100
38	.181	.085	34	.180	.095	34	.184	.100			
39	.181	.090									

.0892
.0042

.0950
.0041

.0958
.0029

.0970
.0035

✓

✓

✓

✓

✓

<u>1227-A</u>		<u>1222-B</u>			<u>1260-A</u>			<u>1295-A</u>		
T	C	IN ⁿ	T	C	IN ⁿ	T	C	IN ⁿ	T	C
176	.085	0	.184	.090	0	.175	.090	0	.180	.095
177	.090	1	.184	.090	1	.175	.085	1	.180	.090
178	.090	2	.183	.090	2	.179	.090	2	.180	.090
177	.090	3	.183	.085	3	.179	.095	3	.180	.085
177		4	.183		4	.179		4	.180	
11	.178	11	.182		11	.175		11	.181	
12	.090	12	.182	.100	12	.175	.100	12	.181	.100
13	.095	13	.182	.095	13	.175	.100	13	.180	.100
19	.178	19	.182		19	.175		19	.180	
								15	.180	
23	.178	23	.184		23	.177		23	.180	
24	.085	24	.184	.090	24	.177	.095	24	.180	.090
	.090	25	.184	.090	25	.177	.095	25	.180	.090
26	.178	26	.184		26	.177		26	.180	
32	.180	32	.186					31	.180	
33	.095	33	.187	.090	33	.177		32	.180	
35	.085	39	.187	.095	34	.177	.090	33	.180	.095
36	.085	35	.187	.090	35	.177	.085	34	.180	.095
					36	.176	.085	35	.179	.095
								36	.179	

.0891
.0038

.0914
.0039

.0918
.0056

.0932
.0046

1339-B

1339-A

1336-A

?

V.

ok
Core
Tilt

T	C	IN"	T	C	IN"	T	C	IN"	T	C
.169	.085	0	.173	.085	0	.169	.075	0	.173	.070
.170	.085	1	.170	.085	1	.169	.075	1	.173	.075
.170	.090	2	.170	.090	2	.170	.075	2	.173	.085
.171	.085	3	.171	.090	3	.171	.085	3	.173	.085
.172		4	.172		4	.172		4	.179	
.176	.090	11	.177		7	.179		11	.176	
.177	.090	12	.178	.090	8	.175	.090	12	.179	.095
.179	.085	13	.178	.090	9	.176	.090	13	.179	.095
.178		14	.179		10	.177		14	.180	
.181		23	.182		19	.182		23	.182	
.181	.090	24	.183	.090	20	.182	.085	24	.182	.095
.181	.090	25	.182	.095	21	.182	.090	25	.181	.095
.181		26	.183		22	.189		26	.181	
.180		28	.182		29	.183	.085	29	.181	
.180	.090	29	.182	.090	30	.183	.085	30	.180	.095
.180	.090	30	.182	.090	31	.183	.090	31	.180	.090
.180	.090	31	.182	.095	32	.183		32	.180	.095
.180	.085	32	.182	.090	33	.183				
.180	.085	33	.182							
.179										

.0877
.0026

.0900
.0030

.0841
.0063

.0886
.0090

IN"	T	C
.170		.085
.171		.085
.172		.085
.173		.095
.174		.090
.175		

.180		
.181		.095
.182		.090
.182		

.183		
.183		.090
.183		.090
.184		

.183		.085
.182		.090
.182		.090
.182		.090
.182		.090

.181		
------	--	--

.0892
.0034

IN"	T	C
0 .173		.085
1 .174		.080
2 .175		.085
3 .175		.085
4 .176		

11 .180		.095
12 .181		.095
13 .182		.095

23 .183		
24 .183		.085
25 .183		.090
26 .184		

27 .182		
28 .182		.090
29 .183		.085
30 .183		.085
31 .182		.085
32 .182		.090

.0879
.0047

IN"	T	C
0 .170		.075
1 .171		.075
2 .171		.080
3 .172		.085
4 .173		

11 .178		.095
12 .179		.090
13 .179		.090
14 .179		

23 .182		
24 .182		.085
25 .182		.085
26 .183		

28 .183		
29 .182		.090
30 .182		.090
31 .182		.085
32 .182		.090
33 .182		

.0858
.0061

IN"	T	C
0 .175		.085
1 .176		.085
2 .177		.090
3 .177		.090
4 .178		

11 .182		
12 .183		.090
13 .184		.095
14 .183		

23 .184		
24 .184		.085
25 .183		.090
26 .183		

28 .183		.095
29 .182		.090
30 .182		.090
31 .183		.085
32 .179		.100
33 .179		.085

.0896
.0046

Cor
Thi
Gr
V

1397-A

1336-B

1323-D

1307-D

IN"	T	C	IN"	T	C	IN"	T	C	IN"	T	C
	.069	.085	0	.179	.085	0	.174	.080	0	.174	.055
	.170	.080	1	.180	.085	1	.175	.090	1	.175	.065
	.171	.085	2	.180	.080	2	.177	.090	2	.176	.075
	.171	.085	3	.180	.090	3	.178	.090	3	.177	.075
	.172		4	.181		4	.178		4	.178	
	.173		5								
									6	.180	
									7	.181	.085
12	.180		11	.183		11	.184		8	.182	.095
13	.181	.085	12	.182	.090	12	.185	.095	9	.182	
14	.181	.090	13	.182	.085	13	.186	.095			
15	.182		14	.182							
									18	.188	
									19	.188	.095
24	.182		23	.180		23	.190		20	.188	.095
25	.184	.090	24	.179	.085	24	.190	.095	21	.188	
26	.183	.090	25	.178	.085	25	.190	.095			
27	.183		26			26	.191				
						27	.190				
						28	.190	.095			
						29	.191	.095	29	.190	
30	.182	.090	29	.175		30	.191	.095	30	.190	.085
31	.182	.090	30	.174	.080				31	.189	.085
32	.181	.085	31	.173	.085				32	.189	.085
33	.180		32	.173	.075						

.0868
.0034

.0841
.0044

.0923
.0047

.0814
.0129

1361-D

1335-B

1320-A

1392-A

V

	T	C	IN ^{''}	T	C	IN ^{''}	T	C	IN ^{''}	T	C
	.181	.090	0	.172	.080	0	.188	.090	0	.171	.080
	.181	.085	1	.173	.080	1	.180	.085	1	.172	.085
2	.181	.095	2	.174	.085	2	.181	.085	2	.172	.085
	.181	.090	3	.175	.090	3	.182	.095	3	.172	.090
4	.181	.090	4	.175		4	.183		4	.173	
	.181	.085									
			6	.177							
			7	.178	.090						
			8	.178	.090	11	.189		11	.179	
	.179		9	.179		12	.189	.095	12	.179	.095
	.179	.090				13	.190	.095	13	.180	.095
	.178	.085				14	.190		14	.180	
	.178										
			18	.185							
			19	.186	.090	23	.193		23	.183	
			20	.186	.095	24	.193	.100	24	.183	.095
26	.173		21	.186		25	.193	.100	25	.183	.095
	.173	.085				26	.193		26	.183	
28	.172	.085				27	.193				
	.172	.080				28	.192	.100			
			28	.187		29	.192	.100	29	.183	.090
			29	.187		30	.192	.105	30	.183	.090
			30	.187	.075				31	.182	.090
			31	.186	.075				32	.182	
			32	.187	.095				33	.182	

.0864
.0032

.0841
.0058

.0955
.0065

.0900
.0050

1594-B

1535-B

1590-A

1558-A

1594-B		1535-B		1590-A		1558-A	
T	C	IN"	T	C	IN"	T	C
	.085						
	.090	1		.075	1		.060
	.085	2		.085	2		.075
		3		.085	3		.065
	.085						
	.075						
	.060	16		.085			
		17		.085	17		.090
		18		.090	18		.095
					19		.085
	.050						
	.050	30		.080	30		.085
	.055	31		.085	31		.085
		32		.085	32		.080
							.075

V
air
Thin
Grey
V-

.0706
.0167

.0839
.0042

.0844
.0058

.0761
.0086

$\Sigma = 6.8874 \div$
 $.0894$
 $\Sigma = .4899 \div 77$
 $.0064$

APPENDIX F

EXPERIMENTAL DATA

SOLUBILITY TESTS OF

BORON CARBIDE IN DILUTE

HYDROCHLORIC ACID

PAGE VI - 1

BY _____	DATE _____	<i>Brooks & Perkins, Incorporated</i> ADVANCED STRUCTURES DIVISION	SHEET _____	OF _____
CK. _____	DATE _____		SUBJECT _____	_____
REV. _____	DATE _____		_____	_____

SOLUBILITY OF B₄C IN DILUTE HCL

TEST METHOD - PARA. 4.3 OF BPS-9000-01
 BORON CARBIDE - TYPE 2 OF ASTM C750-73T
 WEIGHT IN GRAMS

ITEM	TEST NUMBER			AVERAGE OF THREE TESTS
	1	2	3	
WEIGHT OF WET SAMPLE	2.0683	2.0402	2.4373	
WEIGHT OF DRY SAMP & CRUC.	29.3333	29.4627	29.7916	
WEIGHT OF CRUCIBLE	27.2885	27.4476	27.3832	
WEIGHT OF DRY SAMPLE	2.0448	2.0151	2.4084	2.1561
% LOSS OF MOISTURE	1.1362	1.2303	1.1857	
WEIGHT DRY RESIDUE & CRUC.	19.8131	19.6797	24.5031	
WEIGHT OF CRUCIBLE	17.8547	17.7504	22.1893	
WEIGHT OF DRY RESIDUE	1.9584	1.9293	2.3138	2.0672
WEIGHT LOSS OF B ₄ C	.0864	.0858	.0946	.0889
% LOSS OF B ₄ C	4.2254	4.2579	3.9279	4.12

APPENDIX G


EXPERIMENTAL DATA

CORE TAPER IN

SCRAP AREA OF

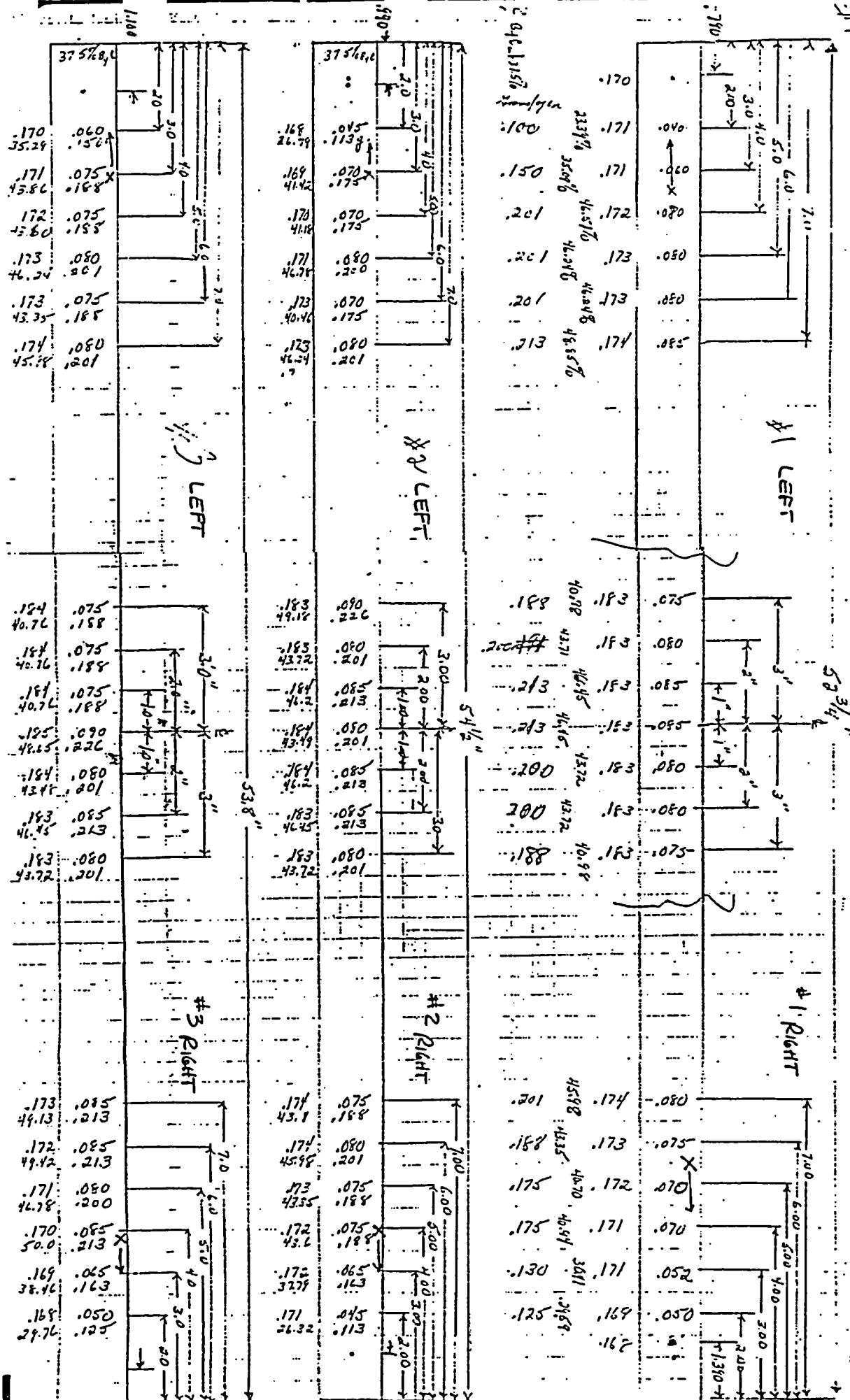
PANEL

PAGES VII-1 THRU VII-3

BY _____	DATE _____	 <i>Brooks & Perkins, Incorporated</i> ADVANCED STRUCTURES DIVISION	SHEET _____ OF _____
CK. _____	DATE _____		SUBJECT _____
REV. _____	DATE _____		

CORE TAPER IN SCRAP AREA OF PANEL

SCRAP SAMPLE TAPERING ZONE	CORE THICKNESS AT TRANSITION POINT	TAPER LENGTH FROM ZERO CORE TO TRANSITION PT.	CORE TAPER (INCHES PER INCH)
#1 LEFT	.080	2.71	.0295
#2 LEFT	.070	2.01	.0348
#3 LEFT	.075	1.90	.0395
#1 RIGHT	.075	4.11	.0182
#2 RIGHT	.075	3.00	.0250
#3 RIGHT	.085	3.30	.0258
<u>AVERAGE CORE TAPER</u>			.0288



Column #1 LEFT

170	.060
35.24	.156
171	.075
43.86	.188
172	.075
45.60	.185
173	.080
46.24	.201
173	.075
43.35	.185
174	.080
45.28	.201

Column #1 RIGHT

184	.075
40.76	.188
184	.075
40.76	.188
184	.075
40.76	.188
185	.090
42.65	.226
184	.080
43.45	.201
183	.085
46.45	.213
183	.080
43.72	.201

Column #3

173	.085
49.13	.213
172	.085
49.42	.213
171	.080
46.78	.200
170	.085
50.0	.213
169	.065
38.46	.163
168	.050
29.72	.125

Column #2 LEFT

168	.045
26.79	.113
169	.070
41.42	.175
170	.070
41.18	.175
171	.080
46.78	.200
173	.070
40.46	.175
173	.080
46.24	.201
173	.080
46.24	.201

Column #2 RIGHT

183	.090
49.12	.226
183	.080
43.72	.201
184	.085
46.2	.213
184	.080
43.45	.201
184	.085
46.2	.213
183	.085
46.45	.213
183	.080
43.72	.201

Column #2

174	.075
43.1	.188
174	.080
45.88	.201
173	.075
43.55	.188
172	.075
43.6	.188
172	.065
32.79	.123
171	.045
26.32	.113

Column #1 LEFT

170	.100
150	.150
201	.201
201	.201
201	.201
213	.213

Column #1 RIGHT

188	.188
201	.201
213	.213
213	.213
200	.200
200	.200
188	.188

Column #1

174	.174
188	.188
175	.175
175	.175
130	.130
125	.125

Column #1 LEFT

170	.040
171	.060
172	.080
173	.080
173	.080
174	.085

Column #1 RIGHT

183	.075
183	.080
183	.085
183	.085
183	.080
183	.080
183	.075

Column #1

174	.080
188	.173
175	.172
175	.171
130	.171
125	.169
125	.162

APPENDIX H

SUPPLEMENTAL DATA

TOTAL BORON CONTENT

IN

BORON CARBIDE

PAGE VIII-1

BORON CARBIDE

LOT OR ORDER NO.	(LBS) AMOUNT	% TOTAL (1) BORON
01-123-312 7/73	2250	71.84
01-336-005 1/75 ITEM 1	5000	74.63
585-35-3 2/75	5000	73.64
585-35-7 4/75	7000	74.13
585-35-9 5/75	7000 8	73.26
585-34-11 6/75	3500 8	74.02
585-35-10 6/75	3500	74.81
585-36-1 8/75	7000 8	75.37
585-36-2 9/75	7000	73.82
585-36-4 10/75	7000	73.28
585-36-6 11/75	7000	71.30
585-36-11 1/76	7000	73.73
585-36-12 1/76	7000	74.25
585-37-1 2/76	7000	73.94

82,250 LBS

73.72
1.08

MEAN
STD. DEV.

(1) PER VENDOR CERTIFICATIONS

75.37

HIGH

APPENDIX J

SUPPLEMENTAL DATA

BORON CARBIDE DISTRIBUTION

VERSUS

CORE THICKNESS & B₄C CONTENT RATIO

PAGE IX-1

WEIGHT OF B₄C PER SQ.
CENTIMETER OF SURFACE
AREA IN GRAMS VERSUS
CORE THICKNESS IN INCHES
FOR DIFFERENT B₄C
CONTENT RATIOS

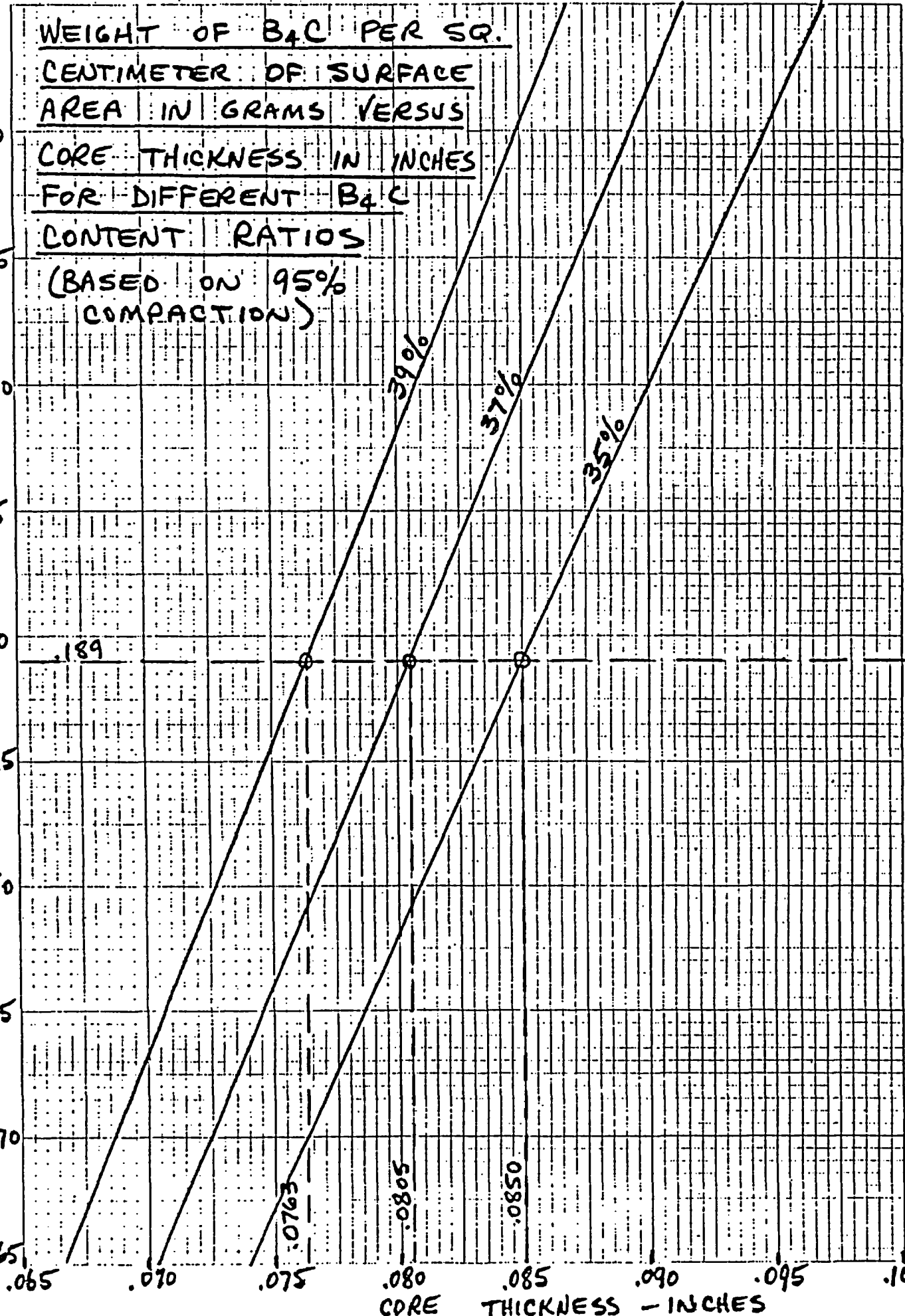
(BASED ON 95%
COMPACTION)

40R-1
ET20
10 X 10 PER INCH
B₄C LOADING
GMS/CM²

MADE IN U. S. A.

40R-1
ET20
10 X 10 PER INCH
B₄C LOADING
GMS/CM²

40R-1
ET20
10 X 10 PER INCH
B₄C LOADING
GMS/CM²



CORE THICKNESS - INCHES

APPENDIX K

SUPPLEMENTAL DATA

ITEM SPECIFICATION FOR BORAL™

BPS-9000-01

PAGES 1 THRU 7

BROOKS & PERKINS, INCORPORATED

Specification Number

BPS-9000-01

Date of original issue: March 19, 1975

Date of revision: May 18, 1977

Date of revision: July 18, 1980
Jan. 6, 1981

Item Specification for BORALtm
A Neutron Shielding Material

1.0 GENERAL

1.1 Description: BORALtm is a sandwich material having exterior faces of an aluminum alloy and a core composed of aluminum and boron carbide. This sandwich material has a unique ability to absorb thermal neutrons without producing hard gamma radiation.

1.2 Scope: This specification establishes the standard for the manufacture, quality assurance, certification documentation, marking, packaging and preparation for shipment for BORALtm sheet and plate material. This specification shall form a part of all purchase orders, agreements and contracts for BORALtm and shall take precedence over any and all conflicting requirements unless specifically and mutually agreed upon to the contrary in writing by Brooks & Perkins, Inc. and the customer.

1.3 Classification: The BORALtm sandwich material will be manufactured with a boron carbide content that will provide the minimum weight of total boron per unit area as specified in Paragraph 3.4.

2.0 APPLICABLE DOCUMENTS: The following specifications and standards of the issue in effect on the date of the purchase agreement shall form a part of this specification.

2.1 Specifications:

ASTM B209

B&P Nuclear Quality Assurance Program Manual, Sections
BP-1000 QA through BP-18000 QA

1 of 7

QA Approval <i>W. Ferguson</i>	Engn. Approval <i>F. Miller</i>	Supercedes Issue May 18, 1977	Document No. BPS-9000-01
-----------------------------------	------------------------------------	----------------------------------	-----------------------------

3.0 REQUIREMENTS: The finished product BORALtm and the components from which it is produced will conform to the following requirements.

3.1 Cladding: The exterior faces or cladding of the sandwich panel will be the 1100 series aluminum in accordance with ASTM B209.

3.2 Boron Carbide Powder: The boron carbide powder contained in the core of the sandwich material will contain a minimum total boron content of 70.0% minimum by weight. Boric oxide will not exceed 3.0% maximum and iron will not exceed 2.0% maximum. The B¹⁰ isotopic content of the boron shall be that which is found in nature.

3.3 Boron Carbide Content (in-process): The core ingredients will be prepared such that any random sample taken from an in-process batch will contain by chemical analysis the minimum weight percentage of boron carbide required to meet Paragraphs 1.3 and 3.4.

3.4 Total Boron Content (sandwich): The minimum weight of total boron per unit area of sandwich material for the overall thickness will be as follows:

<u>Sandwich Material Overall Thickness</u>		<u>Minimum Weight of Total Boron/Unit Area</u>	
in.	(cm.)	oz./sq.in.	(gm./sq.cm.)
.177	(.450)	.029	(.126)
.265	(.673)	.059	(.251)

3.5 Tolerances: The dimensions of the Boraltm sandwich material will be as specified within the following tolerances:

<u>Dimension</u>	<u>Tolerance (plus or minus)</u>	
(1) thickness, .177 in (.450 cm)	0.012 inch	(.0305 cm)
(1) thickness, .265 in (.673 cm)	0.015 inch	(.0381 cm)
width	3/16 inch	(.4763 cm)
length	5/32 inch	(.3969 cm)
(2) squareness	5/16 inch	(.7938 cm)
(3) flatness	1/2 inch	(1.27 cm)

QA Approval <i>W.B. Ferguson</i>	Engrs Approval <i>J. Mollon</i>	Supersedes Issue May 18, 1977	Document No. BPS-9000-01
-------------------------------------	------------------------------------	----------------------------------	-----------------------------

- (1) total thickness of sandwich including core and two faces.
- (2) maximum difference between diagonals of panel.
- (3) rise from flat surface within 36 inches from where hand pressure (not exceeding 25 lbs.) is applied.

3.6 Workmanship: The workmanship provided during the manufacture of the BORALtm sandwich material in accordance with this specification will be of a high level to insure the requirements established herein have been met.

3.6.1 Surface Condition: The surface condition of the BORALtm sandwich material will conform to the requirements of the Aluminum Association for mill products in the "as-rolled" condition.

3.7 Marking: The BORALtm sandwich material will be spot marked for identification purposes with the following information on both the product and on the shipping container. The size of marking characters will be commensurate with the size of the product provided.

3.7.1 Trademark and Identification: The trademark and manufacturer's identification will be shown on a decal attached to the shipping container.

3.7.2 Serial Number: The serialized batch number will be permanently marked on each sheet or plate.

3.8 Packaging: The BORALtm sandwich material will be packaged in accordance with the following:

3.8.1 Lay two (2) thicknesses of polyethylene sheet into box, allowing to drop over sides and ends. Box is a general usage box to be used for BORALtm that will fit within its envelope. Number of pieces that can be shipped in this box will vary with BORALtm thickness, width, length and flatness.

3.8.2 Line bottom and sides of box with corrugated fiber-board sheets.

QA Approval <i>W. H. Ferguson</i>	Engr. Approval <i>L. Mollon</i>	Supersedes Issue May 18, 1977	Document No. BPS-9000-01
--------------------------------------	------------------------------------	----------------------------------	-----------------------------

3.8.3 Load BORALtm into box stacking tight to one side and end of box. Boral shall be separated from each other by corrugated fiberboard sheet.

3.8.4 Block and brace BORALtm with suitable lumber to prevent any shifting within box.

3.8.5 Lay corrugated fiberboard sheet over BORALtm stack. Fold polyethylene sheet over top of BORALtm and tape in place.

3.8.6 Secure box top with lag screws and metal band box four (4) places around girth of box and two (2) places around length of box.

3.9 Preparation for Shipment: The exterior of the shipping container will be suitably marked with the following information:

Customer:

Shipping Destination:

Name and Address of Shipper:

4.0 QUALITY ASSURANCE PROVISIONS: Unless otherwise specified in the purchase agreement, Brooks & Perkins, Inc. will perform the following examinations to assure and certify the BORALtm furnished to the customer complies with the requirements specified herein in regards to materials, workmanship, boron content, marking, packaging and preparation for shipment.

4.1 Cladding: Each lot of raw material will be inspected for certification of compliance from the supplier and any additional tests required to assure the material conforms to the requirements of 3.1.

4.2 Boron Carbide: Each lot of raw material will be inspected for certification of compliance from the supplier and any additional tests required to assure the material conforms to the requirements of 3.2. A sample from each lot of raw material will be subjected to the quantitative analysis described in Paragraph 4.3.1 through 4.3.6 to determine the percentage of raw material remaining after analysis.

QA Approval <i>W. Sweeney</i>	Engr. Approval <i>L. Mollon</i>	Supercedes Issue May 18, 1977	Document No. BPS-9000-01
----------------------------------	------------------------------------	----------------------------------	-----------------------------

4.3 Boron Carbide Content (in-process): Each batch of blended core ingredients will have a minimum of one (1) sample retained for quantitative analysis to assure the material conforms to the requirements of Paragraph 3.3. Each sample will be identified with the serialized batch number. The percentage content of boron carbide in the sample will be determined as follows:

4.3.1 Heat sample in oven at 600°F (316°C) for 30 minutes and cool in a dessicator.

4.3.2 Record net weight of dry samples (gms).

4.3.3 Place the sample in hot dilute hydrochloric acid until the chemical action (bubbling) stops.

4.3.4 Filter the residue out of the solution.

4.3.5 Heat the residue in oven at 600°F (316°C) for one hour and cool in a dessicator.

4.3.6 Record the net weight of the dry residue (gms).

4.3.7 Divide the dry residue weight by the percentage of raw material remaining after analysis determined in Paragraph 4.2 for the particular lot of material.

4.3.8 Compute the percentage content in the sample dry weight (Paragraph 4.3.2) of the residue dry weight divided by the percentage of raw material remaining after analysis (Paragraph 4.3.7).

4.3.9 Compute the percentage content by weight of the total boron by multiplying the percentage determined in Paragraph 4.3.8 by the total boron percentage content stated on raw material certification.

4.4 Boron Carbide Content (sandwich): Each finished sheet or plate of BORAL[™] sandwich material will have a minimum of one (1) sample retained from the trim material cut from the short edges for quantitative analysis to assure the material conforms to the requirements of Paragraph 3.4. The remaining portion of the sample will be retained by Brooks & Perkins Inc. for a period of one year and then will be disposed of unless instructed otherwise. Each sample will be identified with the serialized batch number. The percentage content of boron carbide and total boron in the samples will be determined as follows:

5 of 7

QA Approval <i>W. B. Ferguson</i>	Engr. Approval <i>J. M. Miller</i>	Supercedes Issue May 18, 1977	Document No. BPS-9000-01
--------------------------------------	---------------------------------------	----------------------------------	-----------------------------

- 4.4.1 Record the overall thickness (cms) of the sample, including the cladding and core thickness.
- 4.4.2 Heat sample in oven at 600°F (316°C) for one hour and cool in dessicator.
- 4.4.3 Record the net dry weight (gms) of the sample in air and also in distilled water, and determine the difference between the two, which is the volume in cubic centimeters.
- 4.4.4 Compute the density of the sample by dividing the net dry weight in air by the volume of the sample determined in Paragraph 4.4.3 (gms/cc).
- 4.4.5 Place the sample in hot dilute hydrochloric acid until the chemical action (bubbling) stops.
- 4.4.6 Filter the residue out of the solution.
- 4.4.7 Wash the residue at least three times in hot dilute hydrochloric acid, followed each time by a rinse in distilled water.
- 4.4.8 Filter the residue through a Gooch crucible.
- 4.4.9 Heat the residue in oven at 600°F (316°C) for one hour and cool in a dessicator.
- 4.4.10 Record the net weight of dry residue (gms).
- 4.4.11 Divide the dry residue weight by the percentage of raw material remaining after analysis determined in Paragraph 4.2 for the particular lot of material.
- 4.4.12 Compute the boron carbide weight per unit area (gms/sq. cm.) by multiplying the corrected residue weight from Paragraph 4.4.11 by the sample thickness from Paragraph 4.4.1 and dividing by the volume from Paragraph 4.4.3.
- 4.4.13 Compute the total boron per unit area (gms/sq. cm.) by multiplying the boron carbide weight per unit area from Paragraph 4.4.12 by the total boron percentage content stated on raw material certification.

QA Approval <i>W. Juegen</i>	Engr. Approval <i>L. Miller</i>	Supercedes Issue May 18, 1977	Document No. BPS-9000-01
---------------------------------	------------------------------------	----------------------------------	-----------------------------

4.5 Visual Examination: Each finished sheet or plate of BORALtm sandwich material will be visually examined to assure the material conforms to the requirements of Paragraphs 3.5, 3.6, 3.7, 3.8 and 3.9.

4.6 X-Ray Radiographic Examination: When specifically required by the purchase order, the following additional testing will be performed. X-Ray radiographs will be taken in accordance with MIL-STD-00453 or the ASME Boiler and Pressure Vessel Code, Section 5, Subsection A, Article 2. The quantity and location of radiographs to be taken will be in accordance with the purchase order requirements. The radiograph film will be examined visually to determine the presence of any of the following defects which are unacceptable.

- (a) Cracks or fractures in the aluminum cladding.
- (b) Internal inclusions, discontinuities or voids in the core.
- (c) Inclusions in the cladding that cannot be removed without destroying the integrity of the cladding.

4.7 Neutron Radiographic Examination: When specifically required by the purchase order, the following additional testing will be performed. Required additional samples will be retained from the trim material obtained in Paragraph 4.4 for neutron radiograph examination to assure the uniform dispersion of the boron. Each sample will be identified with the serialized batch number. The neutron radiograph will be taken in accordance with BP-9004QAP. The radiograph film will be examined visually or with a MacBeth Densitometer or equivalent for areas not having comparable density to the standard for the boron content requirement of Paragraph 1.3.

5.0 CERTIFICATION DOCUMENTATION: Documentation will be issued to the purchaser to certify that the material supplied hereunder has been inspected and tested and has been found to meet the requirements specified herein, including any additional testing that has been mutually agreed upon and so stated in the purchase order.

QA Approval <i>W.R. Suezgane</i>	Eng' Approval <i>L. Mollon</i>	Supercedes Issue May 18, 1977	Document No. BPS-9000-01
-------------------------------------	-----------------------------------	----------------------------------	-----------------------------

APPENDIX L

SUPPLEMENTAL DATA

BORAL™ THEORETICAL PHYSICAL
CHARACTERISTICS

PAGES X-1 & X-2

BORAL THEORETICAL WEIGHT FACTORS

DENSITIES


ALUM. (1100) = .098 LBS/IN³ = 2.713 GM/CC
 BORON CARBIDE (B₄C) = 2.510 GM/CC

<u>BORAL CORE</u>	<u>35%</u>	<u>50%</u>
ALUM. 6.5 gm	2.3959 cc	1.8430
B ₄ C 3.5 gm	1.3944 cc	1.9920
10.0 gm	3.7903 cc	3.8350 cc
<u>10 gm</u>	<u>3.7903 cc</u>	<u>2.6076 gm/cc</u>
	<u>= 2.6383 gm/cc</u>	

PANEL THICKNESSES CM. (INCHES)

<u>.178</u>	<u>MIN.</u>	<u>NOM.</u>	<u>MAX.</u>
CLAD	.1016 (.0400)	.1090 (.0429)	.1163 (.0458)
CORE	.2159 (.0850)	.2316 (.0912)	.2474 (.0974)
CLAD	.1016 (.0400)	.1090 (.0429)	.1163 (.0458)
<u>TOTAL</u>	<u>.4191 (.1650)</u>	<u>.4496 (.1770)</u>	<u>.4800 (.1890)</u>

<u>.265</u>	<u>MIN.</u>	<u>NOM.</u>	<u>MAX.</u>
CLAD	.1016 (.0400)	.1077 (.0424)	.1138 (.0448)
CORE	.4318 (.1700)	.4577 (.1802)	.4836 (.1904)
CLAD	.1016 (.0400)	.1077 (.0424)	.1138 (.0448)
<u>TOTAL</u>	<u>.6350 (.2500)</u>	<u>.6731 (.2650)</u>	<u>.7112 (.2800)</u>

BY <u>LM</u> DATE _____	 Brooks & Perkins, Incorporated ADVANCED STRUCTURES DIVISION	SHEET _____ OF _____
CK. _____ DATE _____		SUBJECT _____
REV. _____ DATE _____		

BORAL CORE - MINIMUM CONTENTS (THEOR.)

CORE THICKNESS INCHES/CM.	% OF THEOR. DENSITY	% OF B ₄ C W CORE	<div style="display: flex; justify-content: space-around;"> ① ② ③ </div>		
			DISTRIBUTION OF B ₄ C GMS/SQ. CM.	DISTRIBUTION OF TOTAL BORON GMS/SQ. CM.	DISTRIBUTION OF B ¹⁰ ISOTOPES GMS/SQ. CM.
.085/.2159	100 (IDEAL)	35	.1994	.1396	.0251
.085/.2159	95 (MEAN)	35	.1894	.1326	.0239
.085/.2159	90 (MIN.)	35	.1795	.1256	.0226
.170/.4318	100 (IDEAL)	35	.3987	.2791	.0503
.170/.4318	95 (MEAN)	35	.3788	.2651	.0477
.170/.4318	90 (MIN.)	35	.3588	.2512	.0452

① B₄C PER ASTM C750-73T - TYPE 2
 ② 70.0 % MINIMUM - BY WEIGHT
 ③ 19.75 ± 0.30 ATOM % = 18.29 ± .28 % BY WEIGHT

ACR
DGW
RCK
FILE

THE UNIVERSITY OF MICHIGAN
PHOENIX MEMORIAL LABORATORY
FORD NUCLEAR REACTOR
ANN ARBOR, MICHIGAN 48105

December 2, 1976

Mr. Les Mollon
Brooks and Perkins, Inc.
P. O. Box 2067
Livonia, Michigan 48151

Dear Les:

Enclosed are data and rough graphs per our telephone conversation. The three data sheets are for the 115 crystal plane which affords the least higher order neutron interference.

Figure 1 shows the transmission versus B4C mesh size. Each plot is for a different energy. As you can see transmission drops drastically down to 50-60 mesh, but not so much from that point on. We could use several in between size samples to verify this figure.

Figure 2 provides experimental transmission versus energy. Figure 3 shows the experimental transmission constant versus energy.

Figures 4, 5, and 6 show the individual experimental plots from Figure 3 with the theoretical plot imposed for comparison.

Very truly yours,

Reed R. Burn

Reed R. Burn
Reactor Manager
Ford Nuclear Reactor

RRB:dmz

cc: J. Lee

Enclosures

RECEIVED

DEC - 2 1976

BROOKS & PERKINS, INC.

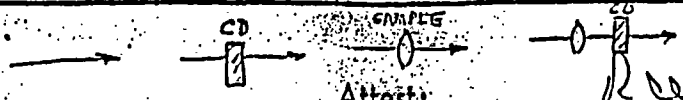
DATE: 11-24-76

SPECTROMETER DATA SHEET

TITLE: BROOKS AND PERKINS BORAL SAMPLES

E, Neutron Energy, eV	Sample Identification	Counting Time, Seconds	I ₀ , Beam Intensity, Counts	B ₀ , Beam Background, Counts	I, Transmitted Intensity, Counts	B, Transmitted Background, Counts	T, Transmission, $(I-B)/(I_0-B_0)$	t, Thickness, Inches	C, Transmission Constant $(\sqrt{E}/t) \ln(1/T)$
<u>115</u>	<u>Crystal</u>	<u>P-Count</u>							
0.100	25/30-1	100	29878	461	3484	359	.1062	.087	8.15
0.125	25/30-1	100	30149	612	3733	459	.1108	.087	8.94
0.150	25/30-1	100	44502	730	6254	541	.1305	.087	9.06
0.175	25/30-1	100	46833	748	5889	553	.1331	.087	9.70
0.200	25/30-1	100	30715	809	5521	680	.1619	.087	9.36
0.250	25/30-1	100	33538	1346	6677	434	.1784	.087	9.91
0.300	25/30-1	100	23130	1632	5002	1168	.1783	.087	10.85

Comments:



Attest:

Red R. Brown

Signature

DATE: 11-24-76

SPECTROMETER DATA SHEET

TITLE: BROOKS AND PERKINS BDEAL SAMPLES

E, Neutron Energy, eV	Sample Identification	Counting Time, Seconds	I ₀ , Beam Intensity, Counts	B ₀ , Beam Background, Counts	I, Transmitted Intensity, Counts	B, Transmitted Background, Counts	T, Transmission, $(I-B)/(I_0-B_0)$	t, Thickness, Inches	C, Transmission Constant $(\sqrt{E}/t) \ln (1/T)$
<u>115</u>	<u>Crystal</u>	<u>A. Lane</u>							
<u>0.100</u>	<u>50/60-1</u>	<u>100</u>	<u>29878</u>	<u>461</u>	<u>1864</u>	<u>373</u>	<u>.0487</u>	<u>.087</u>	<u>10.99</u>
<u>0.125</u>	<u>50/60-1</u>	<u>100</u>	<u>30149</u>	<u>612</u>	<u>1953</u>	<u>423</u>	<u>.0518</u>	<u>.087</u>	<u>12.03</u>
<u>0.150</u>	<u>50/60-1</u>	<u>100</u>	<u>44502</u>	<u>730</u>	<u>3941</u>	<u>516</u>	<u>.0684</u>	<u>.087</u>	<u>11.94</u>
<u>0.175</u>	<u>50/60-1</u>	<u>100</u>	<u>40833</u>	<u>748</u>	<u>3350</u>	<u>524</u>	<u>.0705</u>	<u>.087</u>	<u>12.75</u>
<u>0.200</u>	<u>50/60-1</u>	<u>100</u>	<u>30715</u>	<u>809</u>	<u>3433</u>	<u>631</u>	<u>.0937</u>	<u>.087</u>	<u>12.17</u>
<u>0.250</u>	<u>50/60-1</u>	<u>100</u>	<u>33538</u>	<u>1346</u>	<u>4327</u>	<u>840</u>	<u>.1083</u>	<u>.087</u>	<u>12.77</u>
<u>0.300</u>	<u>50/60-1</u>	<u>100</u>	<u>23103</u>	<u>1632</u>	<u>3773</u>	<u>1047</u>	<u>.1268</u>	<u>.087</u>	<u>13.00</u>

Comments:

Attest:

R. W. R. Perkins
Signature

DATE: 11-24-76

SPECTROMETER DATA SHEET

TITLE: BROOKS AND PERKINS BARAL SAMPLES

E, Neutron Energy, eV	Sample Identification	Counting Time, Seconds	I_0 , Beam Intensity, Counts	B_0 , Beam Background, Counts	I , Transmitted Intensity, Counts	B , Transmitted Background, Counts	T, Transmission, $I-B/I_0-B_0$	t, Thickness, Inches	C, Transmission Constant $(\sqrt{E}/t)\ln(1/T)$
<u>115</u>	<u>Crystal</u>	<u>Plane</u>							
0.100	170-1	100	29878	461	1467	368	.0374	.087	11.95
0.125	170-1	100	30149	612	1713	458	.0425	.087	12.84
0.150	170-1	100	44562	730	2978	548	.0555	.087	12.87
0.175	170-1	100	40833	748	3017	547	.0616	.087	13.40
0.200	170-1	100	30715	809	3016	632	.0797	.087	13.00
0.250	170-1	100	33538	1346	4067	887	.0988	.087	13.30
0.300	170-1	100	23130	1632	3672	1049	.1220	.087	13.24

Comments:

Attest:

Reed R. Burns

Signature

FIGURE 1

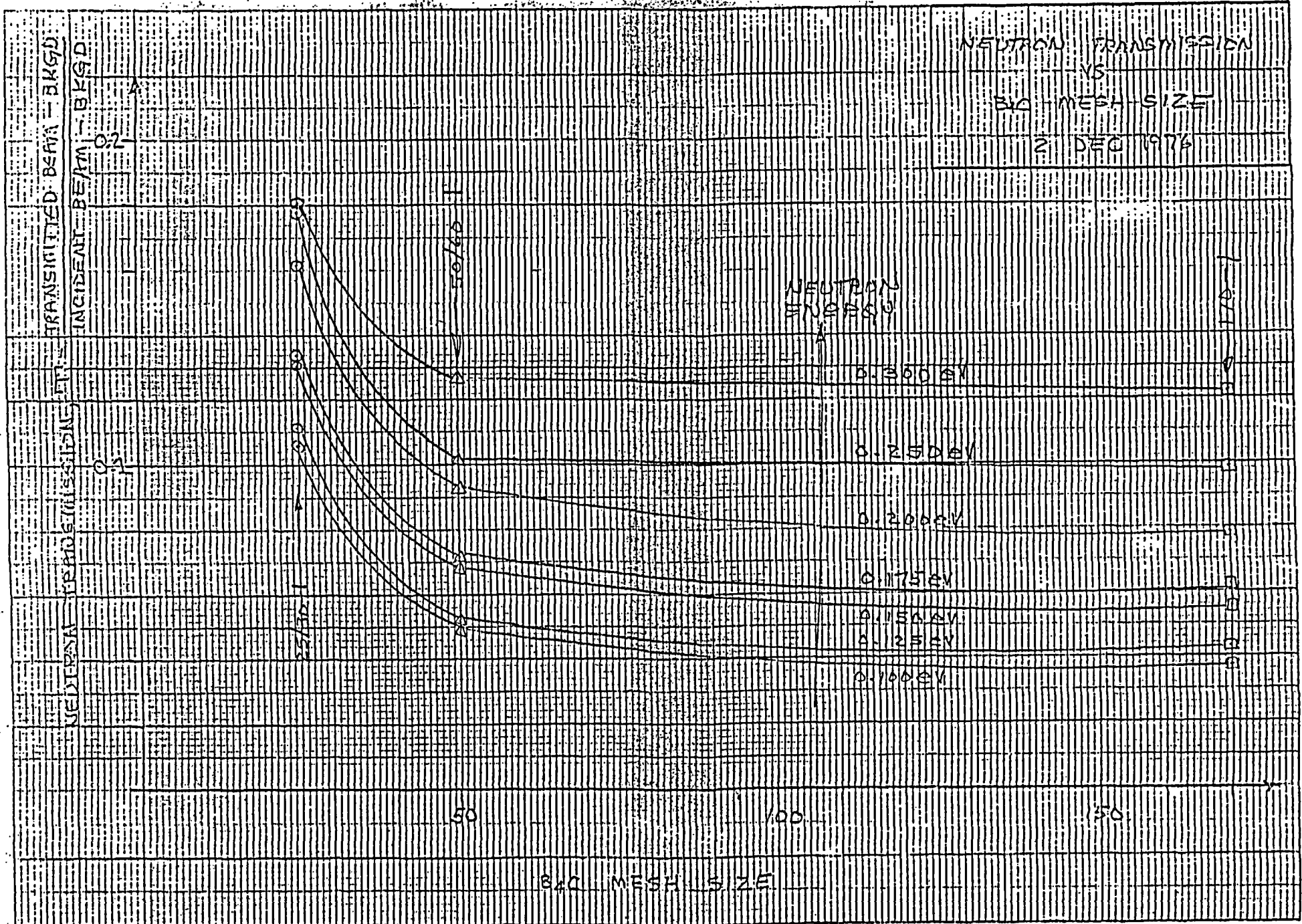


FIGURE 2

NEUTRON TRANSMISSION
VS
NEUTRON ENERGY
Zr/Sr, 50/60, 170 MESH
2 DEC 1976

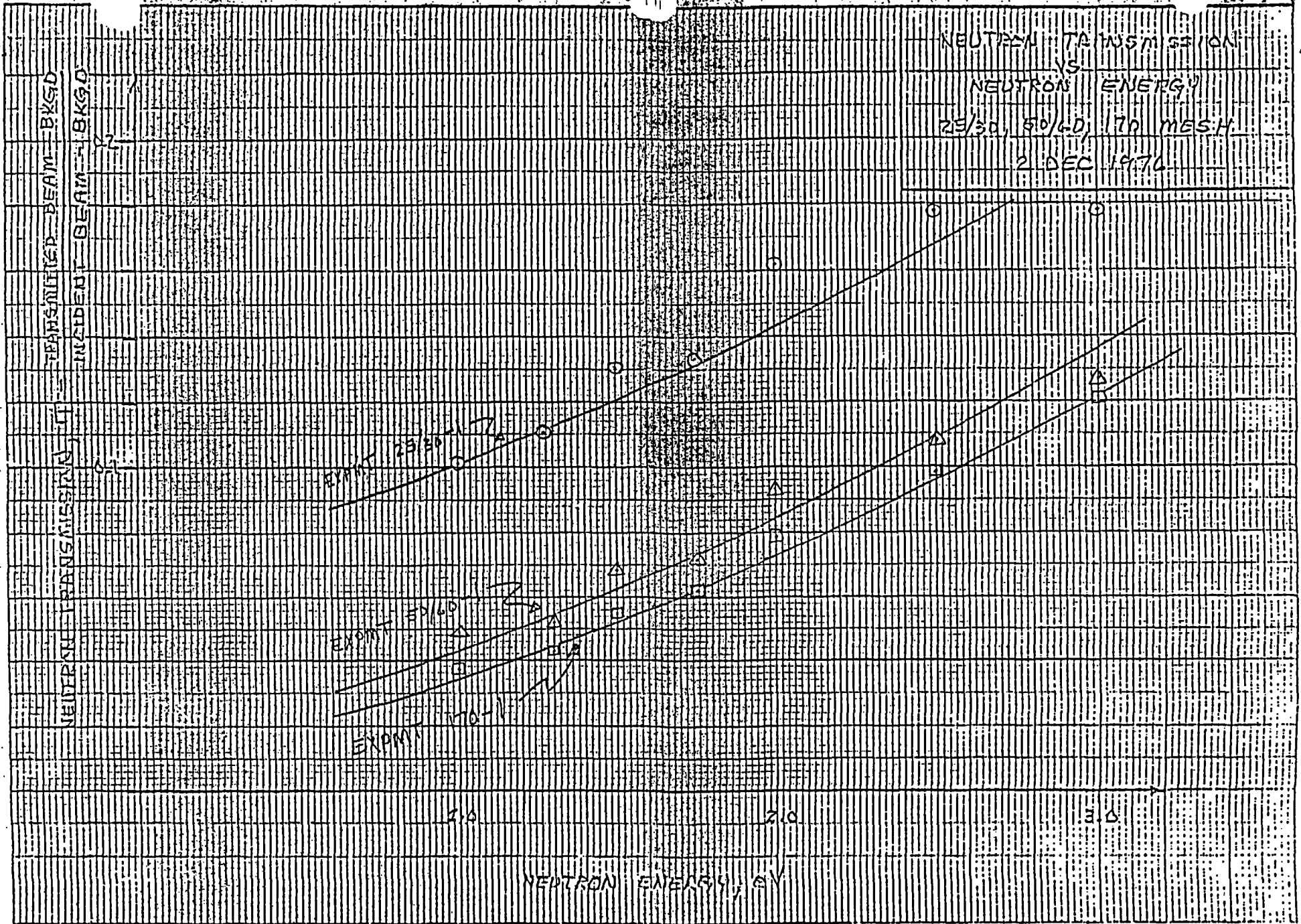


FIGURE 3

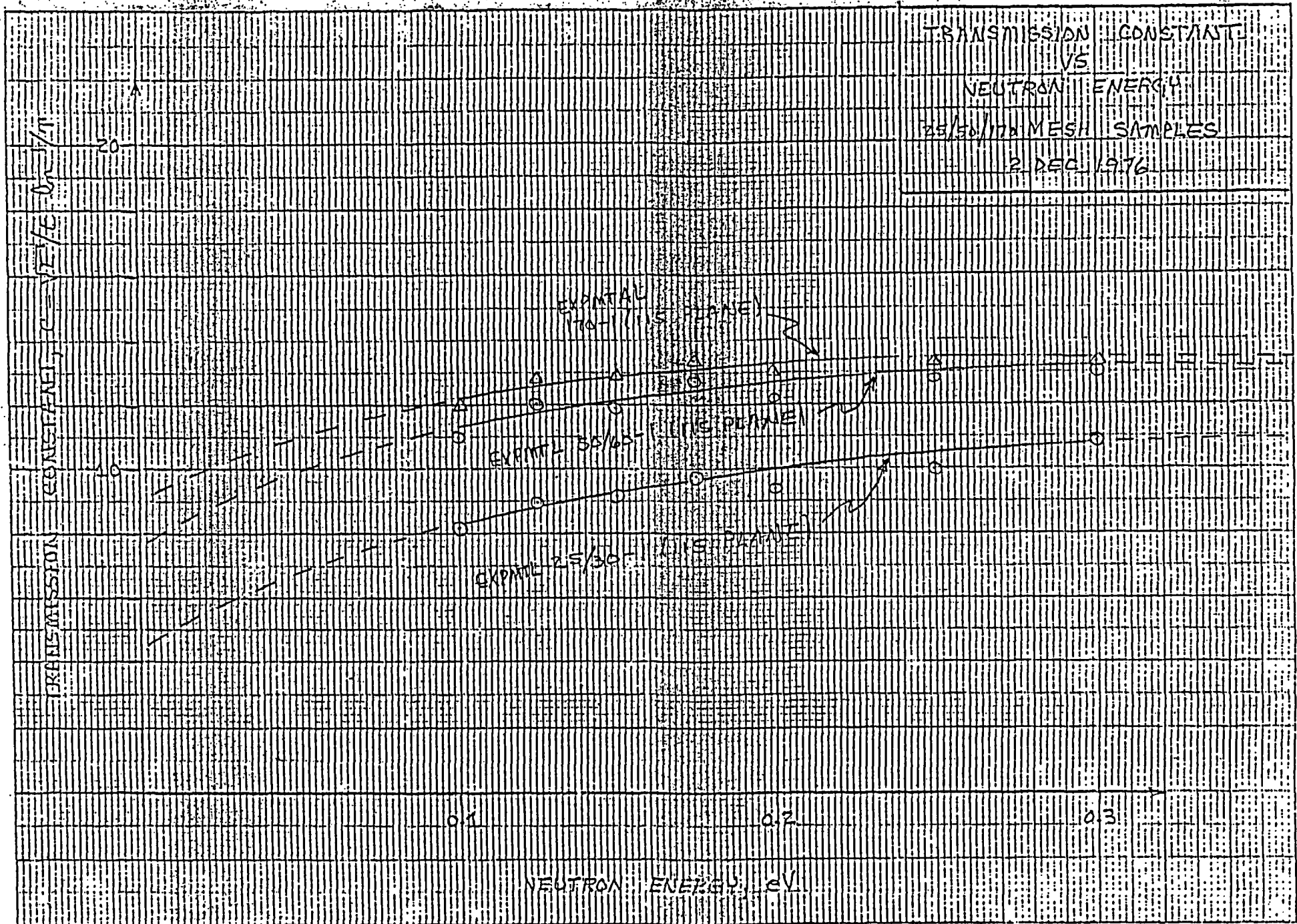


FIGURE 4

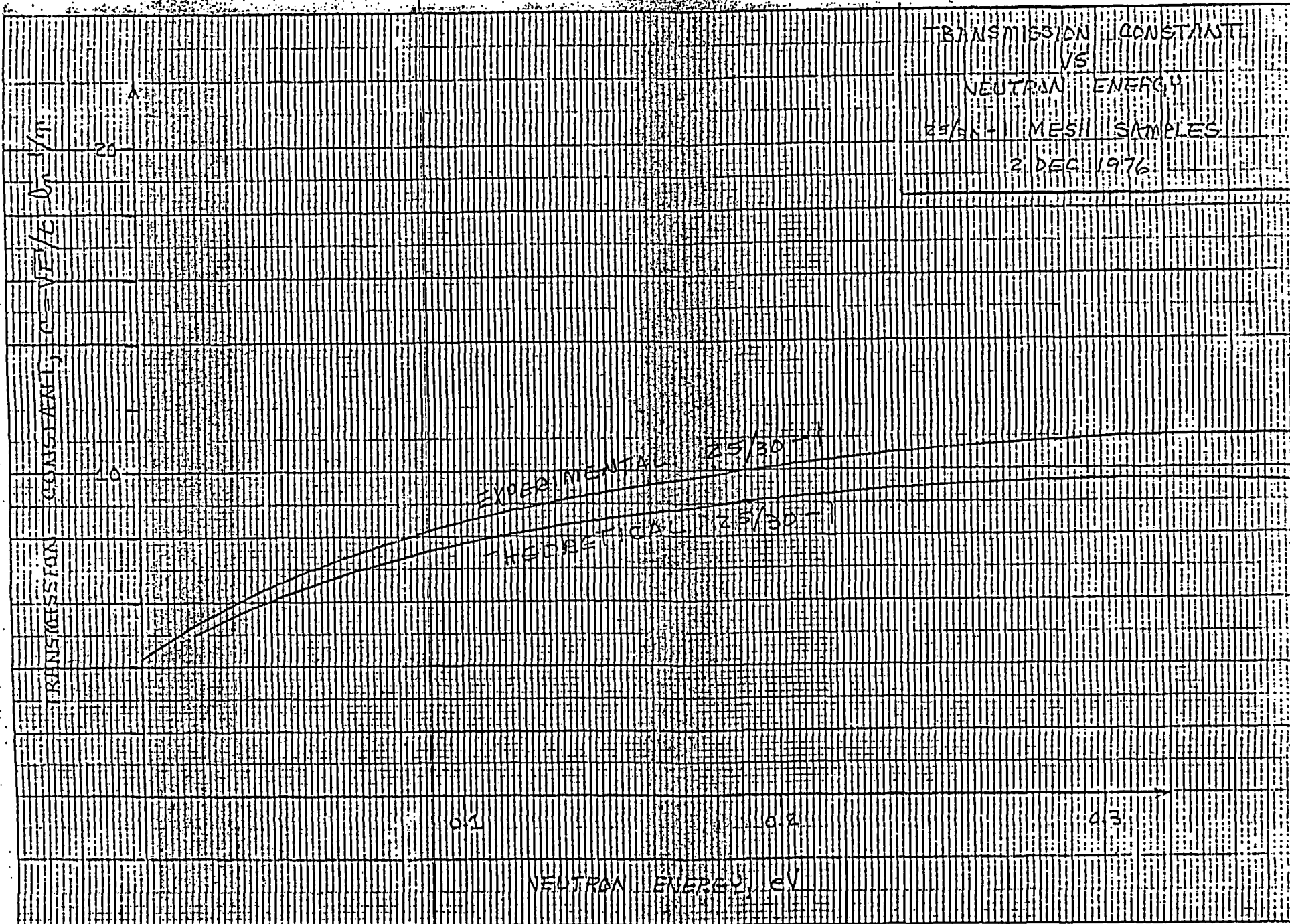


FIGURE 5

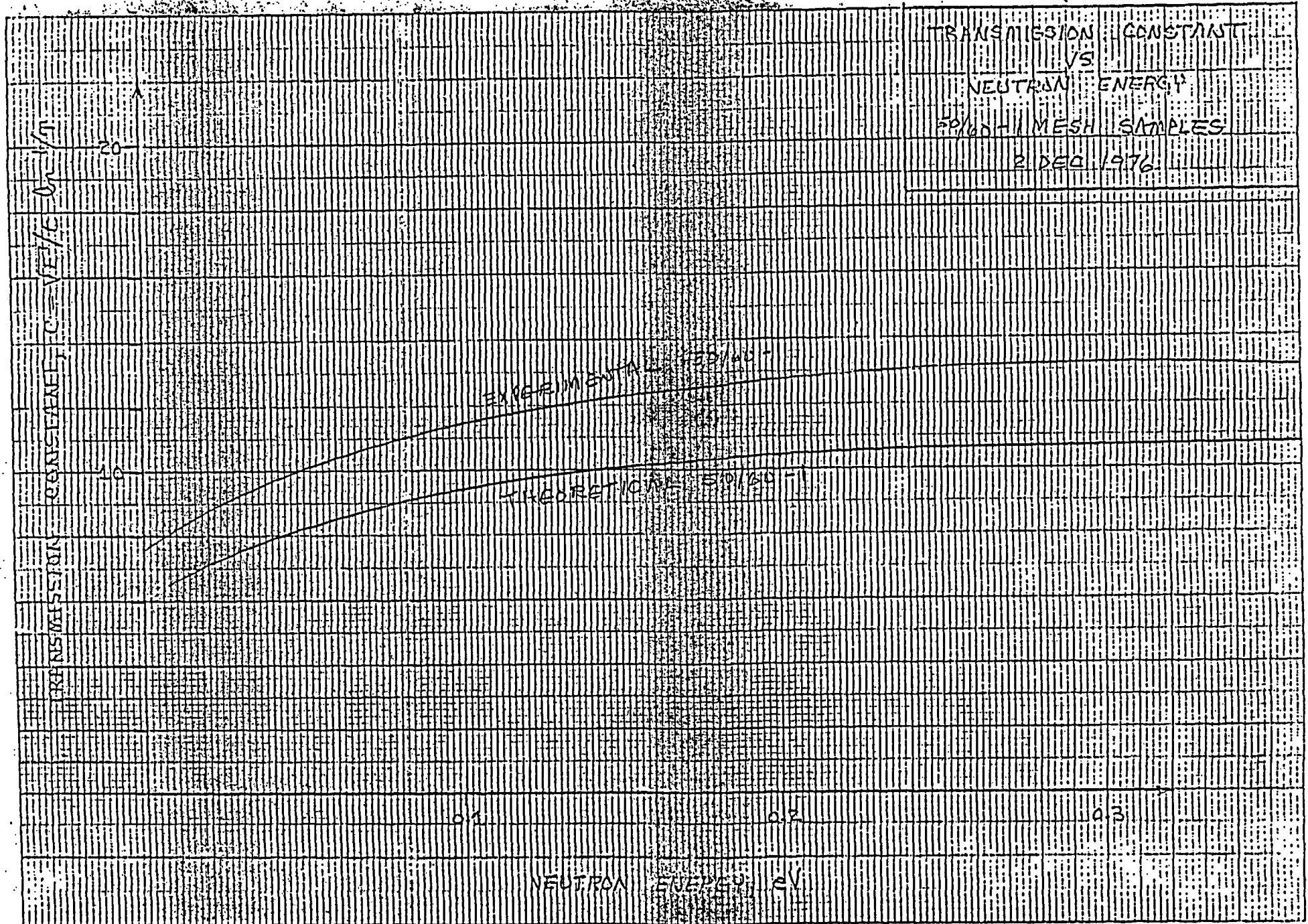
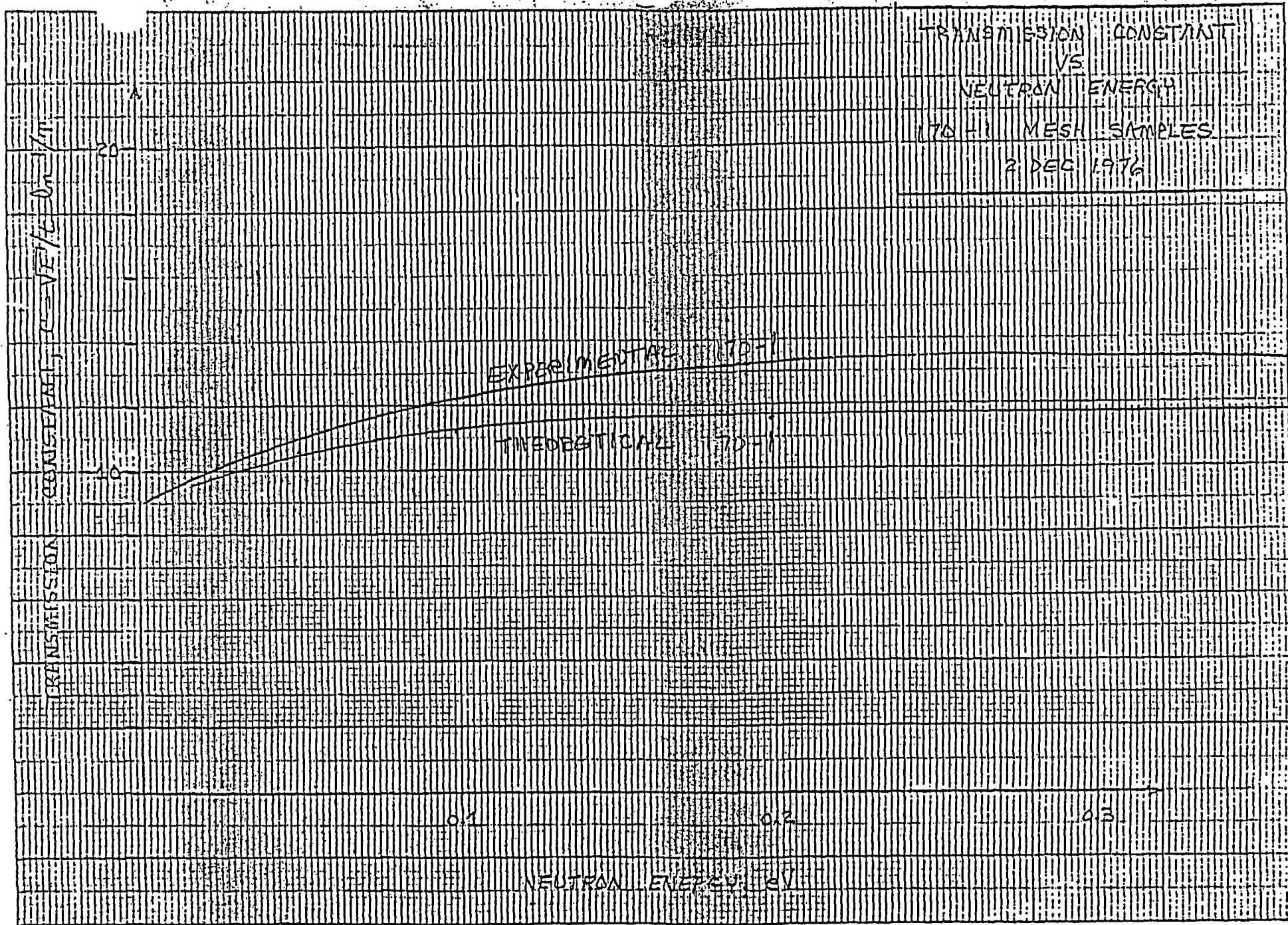


FIGURE 6 -

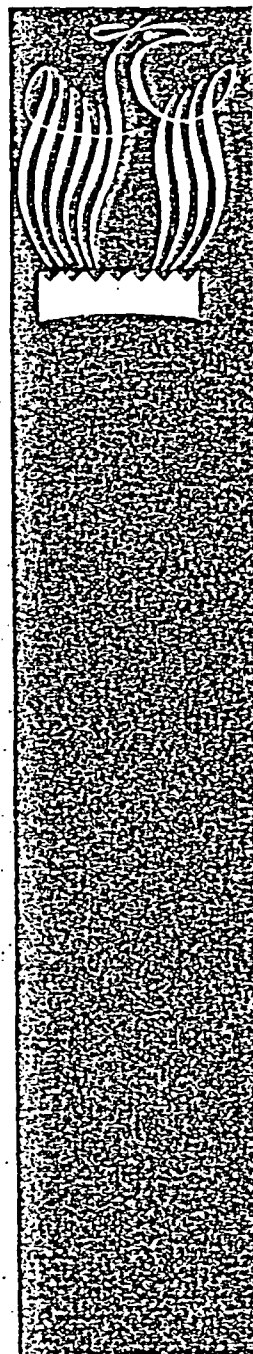


**MICHIGAN MEMORIAL PHOENIX PROJECT
THE UNIVERSITY OF MICHIGAN**

NEUTRON TRANSMISSION
THROUGH BORAL SHIELDING MATERIAL

January, 1978

Prepared For
Brooks and Perkins, Incorporated
12633 Inkster Road
Livonia, Michigan 48150



This report provides neutron transmission information for Brooks and Perkins BORAL shielding material.

Combinations of boron-10 loading (gm/cm^2) and core thickness (in) for nine BORAL case evaluations are listed in TABLE 1. Boron-10 loading ranges from 0.01 gm/cm^2 to 0.03 gm/cm^2 . Core thickness varies linearly with boron-10 loading. The BORAL core is a compaction of aluminum and boron carbide (B_4C). Boron carbide core volume fraction is the volume fraction of the core compaction that is boron carbide. Because of the linear relationship between boron-10 loading and core thickness, volume fraction is essentially constant.

Boron carbide particle sizes are expressed in terms of Tyler screen mesh numbers. Screen mesh openings correspond to particle diameters under the assumption that the particles are spherical. The mesh number range for boron carbide in the BORAL core is 60-200. TABLE 2 shows the actual sizes and percentage distributions of core particles.

BORAL neutron transmission versus neutron energy is presented in TABLE 3 for the various boron-10 loading-core thickness cases listed in TABLE 1. Transmission values are based upon a collimated beam theory developed at the University of Michigan which has been verified by transmission measurement experiments.¹

FIGURE 1 is a linear plot of neutron transmission versus neutron energy over the energy range 0 - 0.55 eV. FIGURE 2 is a similar logarithmic plot over the narrower energy range 0 - 0.1 eV.

Integrated transmission shown on FIGURE 1 represents the integral of (Source Flux (E) X Neutron Transmission (E)) divided by the integral of (Source Flux (E)) over the energy range 0 - 0.55 eV. Source flux is assumed to be the Maxwell-Boltzmann flux distribution.

¹ J. W. Bryson, J. C. Lee, and R. R. Burn, "Neutron Transmission Through BORAL Shielding Material: Theoretical Model and Experimental Comparison", Department of Nuclear Engineering, Michigan Memorial-Phoenix Project, The University of Michigan, November, 1977.

TABLE 1

BORAL PARAMETRIC COMBINATIONS FOR CASE EVALUATIONS

<u>Case</u>	<u>Boron-10 Loading (gm/cm²)</u>	<u>Core Thickness (in)</u>	<u>Boron Carbide Particle Size (Mesh Number)</u>	<u>Boron Carbide Core Volume Fraction</u>
1	.0100	.0274	60 - 200	.4468
2	.0125	.0336	60 - 200	.4557
3	.0150	.0402	60 - 200	.4569
4	.0175	.0463	60 - 200	.4628
5	.0200	.0533	60 - 200	.4594
6	.0225	.0598	60 - 200	.4607
7	.0250	.0662	60 - 200	.4625
8	.0275	.0728	60 - 200	.4625
9	.0300	.0796	60 - 200	.4614

TABLE 2

60 - 200 BORON CARBIDE PARTICLE SIZE DISTRIBUTION FOR CASE EVALUATIONS

<u>Particle Size (Mesh Number)</u>	<u>Mesh Opening Particle Diameter (in)</u>	<u>Particle Radius (cm)</u>	<u>Particle Percentage (%)</u>
70	.0077	.0098	11.5
90	.0063	.0080	39.7
130	.0046	.0058	38.6
170	.0035	.0044	8.6
200	.0029	.0037	1.6
Average		.0070	100.0

TABLE 3

BORAL NEUTRON TRANSMISSION VERSUS NEUTRON ENERGY (eV)For Parametric Combinations of
Boron-10 Loading (B, gm/cm²) and Core Thickness (T, in)

Neutron Energy	1.	2.	3.	4.	5.	6.	7.	8.	9.
	B .0100 T .0274	B .0125 T .0336	B .0150 T .0402	B .0175 T .0463	B .0200 T .0533	B .0225 T .0598	B .0250 T .0662	B .0275 T .0728	B .0300 T .0796
0.01	.0530	.0249	.0119	.0056	.0027	.0013	.0006	.0003	.0001
0.02	.1077	.0610	.0348	.0197	.0113	.0064	.0037	.0021	.0012
0.03	.1533	.0952	.0594	.0368	.0231	.0144	.0090	.0056	.0035
0.04	.1915	.1260	.0831	.0546	.0362	.0239	.0157	.0104	.0069
0.05	.2240	.1534	.1054	.0721	.0496	.0341	.0234	.0161	.0110
0.06	.2522	.1780	.1260	.0889	.0630	.0446	.0315	.0223	.0158
0.07	.2770	.2002	.1451	.1048	.0761	.0551	.0399	.0289	.0210
0.08	.2990	.2204	.1628	.1200	.0888	.0655	.0484	.0357	.0264
0.09	.3188	.2389	.1793	.1343	.1010	.0757	.0568	.0427	.0320
0.10	.3367	.2558	.1947	.1479	.1127	.0857	.0652	.0496	.0378
0.15	.4065	.3241	.2586	.2061	.1646	.1313	.1048	.0836	.0668
0.20	.4560	.3743	.3074	.2522	.2073	.1703	.1398	.1149	.0944
0.25	.4937	.4134	.3464	.2900	.2432	.2037	.1707	.1430	.1199
0.30	.5238	.4452	.3786	.3218	.2738	.2328	.1980	.1684	.1432
0.35	.5486	.4718	.4059	.3491	.3004	.2584	.2224	.1913	.1646
0.40	.5696	.4945	.4295	.3728	.3239	.2813	.2443	.2122	.1843
0.45	.5876	.5142	.4501	.3938	.3448	.3018	.2642	.2313	.2025
0.50	.6034	.5316	.4684	.4126	.3637	.3204	.2823	.2488	.2193
0.55	.6174	.5470	.4848	.4295	.3807	.3374	.2990	.2650	.2349
Integrated Transmission	.1810	.1240	.0863	.0606	.0431	.0307	.0222	.0161	.0018

FIGURE 1 BORON-10 NEUTRON TRANSMISSION VERSUS NEUTRON ENERGY

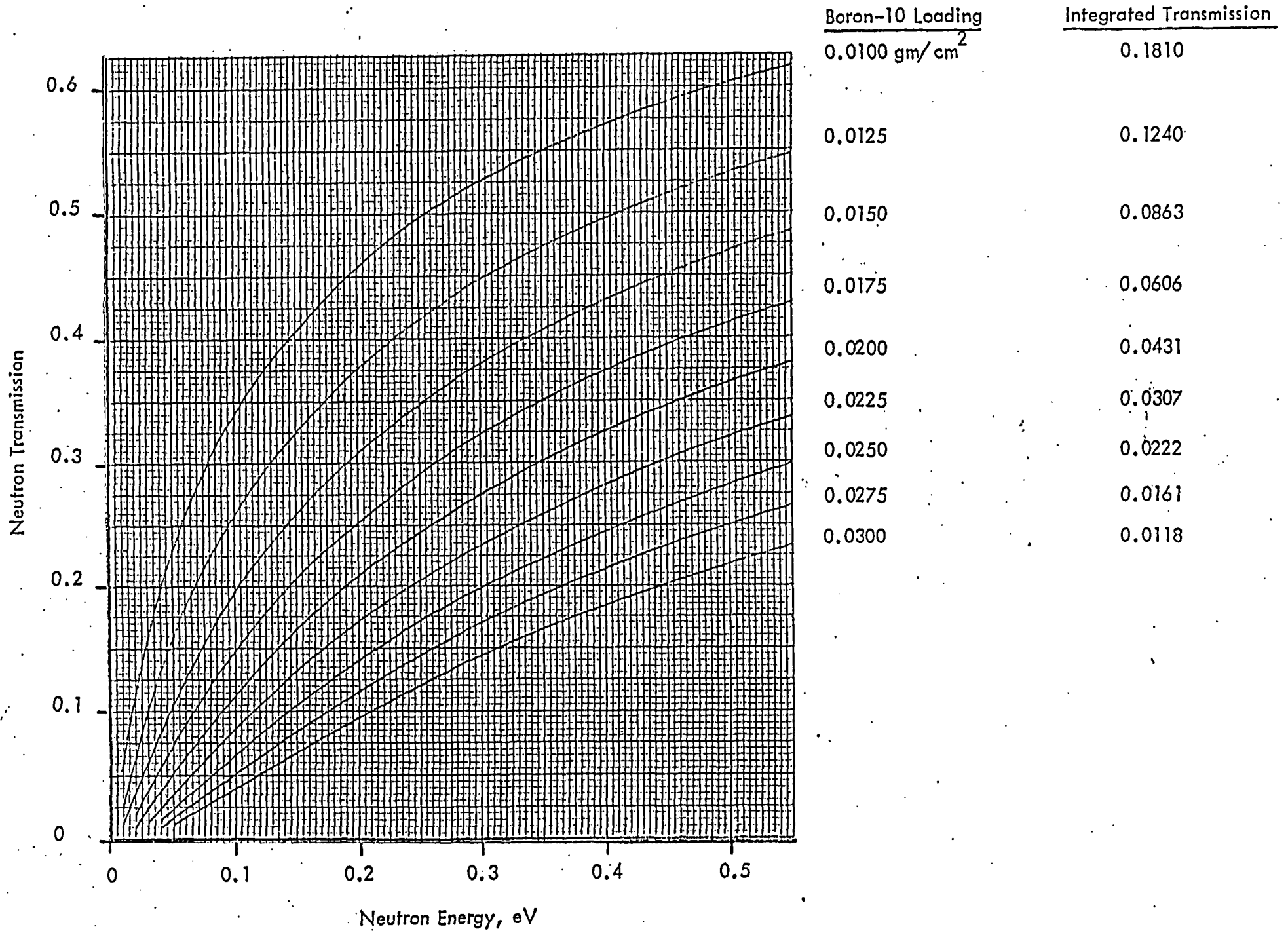


FIGURE 2

BORAL NEUTRON TRANSMISSION VERSUS NEUTRON ENERGY

